UNIVERSITY OF CALIFORNIA,
IRVINE

Non-image forming vision: an integration of multiple photoreceptor systems on the circadian/arousal neural circuit of Drosophila melanogaster

DISSERTATION

submitted in partial satisfaction of the requirements
for the degree of

DOCTOR OF PHIILOSOPHY

in Biomedical Sciences

by

David Au

Dissertation Committee:
Professor Todd C. Holmes, Chair
Associate Professor Francesco Tombola
Assistant Professor Kevin Beier
Associate Professor Brian Zoltowski

2023

DEDICATION

To my parents, who sacrificed so much so that their children could have the opportunities to pursue the American Dream, and to my siblings, who have been unrelenting role models for me to follow since I was a child, I wouldn't have found what gives my life meaning if not for them.

To all the kids who started at the bottom and kept climbing the ladder towards a better tomorrow, the road will get lonelier the higher you go, but be proud that you have paved a way for others to follow.

To the hundreds of thousands of flies (probably millions) – I hope this work was worth it.

And to my newborn niece, Baby Emma:

I'm glad you didn't poop on me at any time before my defense. Thanks for that. I will try to be the best uncle I can be for you, because you mean so much more than you will ever know to us.

TABLE OF CONTENTS

LIST OF FIGURES

LIST OF ACRONYMS

AeCRY1	Aedes aegypti Cryptochrome1
AgCRY1	Anopheles gambiae Cryptochrome1
aME	Accessory Medulla
CaCl2	Calcium Chloride
CO2	Carbon Dioxide
CTT	C-Terminal Tail
CRY	Cryptochrome
DD	Constant Dark
DmCRY	Drosophila Cryptochrome
DN	Dorsal Neuron
DNA	Deoxyribonucleic Acid
DPI	Diphenyleneiodonium
eGFP	enhanced Green Fluorescent Protein
EGTA	Egtazic Acid
FAD	Flavin Adenine Dinucleotide
FDR	False Discovery Rate
FF	Firing Frequency
Gl60j	glass60j
Gq	G protein
HB	Hofbauer-Buchner
HEPES	4-(2-hydroxyethyl)-1-piperazineethanesulfonic acid
HK	Hyperkinetic
Hr	Hour(s)
Hz	Hertz, 1/s
IR	Infrared
KCl	Potassium Chloride
Kvβ	Voltage-gated Potassium Beta
LD	Light:Dark
LED	Light Emitting Diode
LL	Constant Light
LNv	Lateral Ventral Neuron
l-LNv	Large Lateral Ventral Neuron
LNd	Lateral Dorsal Neuron
LOF	Loss-of-Function
MgCl2	Magnesium Chloride
Min	Minute(s)
NaCL	Sodium Chloride
nm	nanometer
Osm	osmols
PBS	Phosphate Buffered Saline
PDF	Pigment Dispersing Factor
PER	Period
PFA	Paraformaldehyde

PI	Pars Intercerebralis
PLC	Phospholipase C
Rh1	Rhodopsin 1
Rh2	Rhodopsin 2
Rh3	Rhodopsin 3
Rh4	Rhodopsin 4
Rh5	Rhodopsin 5
Rh6	Rhodopsin 6
Rh7	Rhodopsin 7
RMP/MP	Resting Membrane Potential/Membrane Potential
Sec	Second(s)
SEM	Standard Error Mean
s-LNv	Small Lateral Ventral Neuron
TIM	Timeless
Trp	Tryptophan
TTL	Transistor-Transistor-Logic
Tyr	Tyrosine
UAS	Upstream Activating Sequence
UV	UltraViolet
WHO	World Health Organization
WT	Wild Type
ZT	Zeitgeber Time

LIST OF SYMBOLS

μ	micro
τ	tau, period length
Δ	delta, difference
K+	Potassium Ion

ACKNOWLEDGMENTS

First and foremost, I cannot not mention the hundreds of thousands (if not millions) of flies that had given up their lives for the sake of this research and the completion of this dissertation. Regardless of what spectrum of life something is on, I still consider it to be a precious thing to be able to be born and experience this thing we call life in this crazy world and its impossibly unprobabilistic odds of existing. Our understanding of nature and her complexities is improved just incrementally more with the completion of this dissertation, and I hope it helps lead to a future that makes these sacrifices worth it in the end.

To my advisor, Todd C. Holmes, who from the start has been a role model for the way I conduct science and navigate this field, I want to truly thank you for giving me this opportunity to thrive in your lab. While it may have been a bumpy start on this road during my rotation, I'm glad you gave me that second chance that ignited my desire to excel. As a poor first-generation student who did not have the luxury of being able to follow the footsteps of my family or peers in my community and thus grew up with a lot of self-doubt and lack of confidence in what I do now, I count myself extremely fortunate to have had such an understanding and patient mentor who helped me realize my greater potential for success. You helped me accomplish goals that I thought I could only dream about. Though I may never be able to fully verbally express it, I hope this acknowledgement will at least partly convey the deep gratitude I hold for your fantastic mentorship. I will carry on the lessons I have learned from you for the rest of my career.

I would be remiss if I did not acknowledge the other graduate students in the lab that set my foundation in the Holmes Lab, so to Ceazar Nave and Lisa Baik, thank you. As a naïve and bright-eyed first year graduate student, of course I would look up to you both as my older peers, almost like cool, older siblings, and want to fit in, both scientifically and personally. I appreciate the lessons you both allowed me to experience, through good times and bad, and hope that even though our paths have separated, we can still look back on the times we shared as the Holmes Lab Trio with fondness. And an extra recognition to Lisa, whom was my direct mentor before transitioning out, thank you for being an incredible role model for me and leaving behind giant shoes for me to follow your footsteps in. I hope you can be proud of the influence you left on me and what I was able to accomplish in my graduate career because of it.

As is the way information has been preserved throughout history since the dawn of man, mentors pass down ideas and knowledge to their students who in turn become mentors that pass down their own ideas and built knowledge to their students and on and on the cycle goes. This mechanism raises the proverbial "giants" whom we stand on the shoulders of today, allowing us to see further than any other generation has before our time. I am grateful for the amazing students and trainees that I have had the esteemed pleasure of mentoring during my time in graduate school. Without them, my dissertation would not even remotely be close to what it is at present, and I would have surely sunk. I must pay special acknowledgement to my three trainees who were with me the longest: Alex, Soo Jee, and Jenny. To my first trainee in the Holmes Lab, Alex Foden, I could not be prouder of you and all that you have accomplished. It has been an incredible privilege watching you grow into the person you are today, and I hope you keep moving up in life representing us and all that you stand for. I expect incredible things from you and your

contributions to our world. To Soo Jee Park, you helped make the lab such a fun environment to be in and clearly made me feel my old age much of the time. You have such a strong drive and tenacity for success, and I know that whatever you set your sights on you will achieve in strides. I look forward to hearing all about the successes you find in whatever direction you choose to pursue next. And to Jenny Liu, who could not have joined my team at a better time, you've impressed me with every day that we have been in the lab. As an undergraduate, you hit the ground running and very quickly got to a level of what I would expect first-year graduate students to be performing at. A student like you only comes around once in a blue moon, and it is my privilege to have been able to work with someone so hardworking, dedicated, and reliable. You are a superstar in the making and I truly believe that you have the potential to accomplish amazing things in life. And to the rest of my trainees that I do not have enough space here to individually acknowledge, your contributions to this work has been absolutely essential and I would not be the incredibly fortunate mentor that I am today without you lot: Wendy Enrriquez-Villalva, Mary Tran, Mia Dimalanta, Angelica Armesto, Tony Bui, Thanh Nguyen, Jessica Lin, Lauren Otsuka, Olga Jaime, and our many work-study students.

I appreciate the guidance and encouragement from my thesis committee members, Professors Francesco Tombola and Kevin Beier at UCI, and Brian Zoltowski at SMU, and their commitment to providing their valuable time and effort in order to ensure that I had a successful doctoral experience.

To my family, this Ph.D. really would not have been possible if not for the love and support I received from you all. To my parents, I cannot imagine taking such a high risk gamble that wagered everything you built in Vietnam in exchange for some miracle opportunity overseas that would give your children the freedom of opportunity to pursue anything. More than 29 years later, I hope you can rest assured it paid off – I will be the only member in our entire family's history to obtain a Ph.D. and it is thanks to you both. I have found something that I truly believe is worth spending the rest of my life pursuing for the betterment of this world. I can only reflect on the struggles we had as a family of refugees with appreciation and gratitude that allow me to navigate my life now with an unrelenting determination and humbleness to provide these same freedoms of opportunity to other disadvantaged families around our world. Thank you, ma and ba, for planting the roots of me and my siblings here and nourishing us to blossom. Much like us, our future generations will get to live in a much better world that you both helped pave for us.

Thank you to the National Institute of Health and the National Institute of General Medical Sciences for providing my Ruth L. Kirschstein-NRSA F31-Diversity Fellowship (NIH F31 GM140592 awarded to DA), Office of Inclusive Excellence for providing my Inclusive Excellence Fellowship, Graduate Division for providing my Distinguished Public Impact and Graduate Dean's Dissertation Fellowships for supporting my dissertation projects. This work was also funded by NIH R35 GM127102 awarded to TCH. The text of parts of Chapter 1 of this dissertation is a reprint of the material as it appears in Baik, L. S. *et al.* CRYPTOCHROME mediates behavioral executive choice in response to UV light. *Proc. Natl. Acad. Sci.* **114**, 776–781 (2017) and Wang, J., Du, X., Pan, W., Wang, X. & Wu, W. Photoactivation of the cryptochrome/photolyase superfamily. *J. Photochem. Photobiol. C Photochem. Rev.* **22**, 84–102 (2015), used with permission from PNAS and Elsevier, respectively. The co-authors listed in the 2017 PNAS manuscript are Lisa S. Baik, Keri J. Fogle, Logan Roberts, Alexis M. Galschiodt,

Joshua A. Chevez, Yocelyn Recinos, Vinh Nguy, and Todd C. Holmes. The co-authors listed in the J. Photochem. Photobiol. C Photochem. Rev manuscript are Jing Wang, Xianli Du, Weisong Pan, Xiaojie Wang, and Wenjian Wu.

VITA

EDUCATION

Ph.D. in Biomedical Sciences, University of California, Irvine, Irvine, CA 2023
B.S. in Biomedical Engineering w/ Minor in Physics, University of Utah, SLC, UT 2016

EMPLOYMENT

R&D Engineer at Carterra, Inc. 1/2015 – 9/2017
Salt Lake City, UT
Part-time, 29 hours/week

- Led quality control testing of microfluidic devices.
- Designed dextran-surface functionalization protocol for Surface Plasmon Resonance (SPR) biosensors.

EXPERIENCE

Graduate Researcher at Holmes Lab 4/2018 – present
University of California, Irvine, Department of Physiology and Biophysics, Irvine, CA
Full-time, 50 hours/week

- PCR mutagenesis, transgenic fly generation, neural electrophysiology, behavioral assays, immunocytochemistry, confocal microscopy, and programming/circuit building for tool-development.
- Tested phototransduction potential of CRY structural mutants and mosquito CRY1 in *Drosophila* transgenics using electrophysiological, behavioral, immunostaining techniques.
- Demonstrated successful whole-cell light-evoked current-clamping of *Drosophila* lateral ventral neurons.

Teaching Assistant (Physio 232 – *Physiology of Ion Channels*) 5/2021 – 7/2021
University of California, Irvine, Department of Physiology and Biophysics, Irvine, CA
Part-time, 10 hours/week

- Evaluated student performance using various metrics for grading (assignments, presentations, reports, etc.)

Graduate Rotation at Tombola Lab 4/2018 – 6/2018
University of California, Irvine, Department of Physiology and Biophysics, Irvine, CA
Full-time, 50 hours/week

- Performed PCR mutagenesis to develop point mutant constructs of the proton-gated ion channel, Hv1.
- DNA/RNA amplification/purification and RNA injection into *Xenopus* oocytes for protein expression.
- Demonstrated successful whole-cell and inside-out patch-clamping of *Xenopus* oocytes.

Graduate Rotation at Pathak Lab 9/2017 – 12/2017
University of California, Irvine, Department of Physiology and Biophysics, Irvine, CA
Full-time, 40 hours/week

- Designed and developed several GCaMP6f-modified hPiezo1 sensors for calcium imaging.

- Performed QC tests (DNA amplification, restriction digest, western blot) to verify plasmid constructs.
- Developed skills with HEK293A cell transfection and total internal reflection fluorescence microscopy.

Undergraduate Researcher at Grainger/Brooks Lab 9/2011 – 12/2014
University of Utah, Department of Bioengineering and Department of Pharmaceutics, SLC, UT
Part-time, 12 hours/week

- Developed skills in laboratory maintenance, sterile technique, cell-culturing, and microfluidic cell-printing.
- Assisted with proving new instrumentation capabilities for the submission of two research grant proposals.
- Led a research project on cell-printing macrophages and fibroblasts to mimic biomaterial-induced fibrosis.

HONORS AND AWARDS

Center for Circadian Biology Network Award (2023)
NIH NRSA F31-Diversity Fellowship (funded by NIGMS) (2021-2023)
Society for Neuroscience Trainee Professional Development Award (TPDA) (2022)
Honorary Graduate Student UROP Fellow (2022)
UCI Inclusive Excellence Fellowship (2022)
UCI Graduate Dean's Dissertation Fellowship (2022)
Society for Research in Biological Rhythms Emmett Chappell Award (2022)
UCI Distinguished Public Impact Fellowship (2021)
UCI School of Medicine Grad Day Outstanding Elevator Talk (2021)
Outstanding Diverse Educational Community and Doctoral Experience (DECADE) Representative Award (2021)
Activate-to-Captivate Public Speaking Certificate of Achievement (2021)
Mentoring Excellence Certificate of Achievement (2021)
Inclusive Excellence Certificate of Achievement (2021)
Behrens Research Excellence Award (2021)
UCI School of Medicine Grad Day Outstanding Poster Talk (2020)
Society for Research in Biological Rhythms Merit Travel Award (2020)
Center for Circadian Biology Outstanding Poster Award (2019)
Undergraduate Research Scholar Designation (2016)
Larry H. and Gail Miller Enrichment Scholarship (full tuition, room/board, stipend) (2011-2016)
Mathematics Engineering Science Achievement (MESA) Scholarship (2011)

LIST OF PUBLICATIONS

1. **Au, D.,** Liu, J., Nguyen, T.H., Dimalanta, M., Park, SJ., Foden, A., and Holmes, T. Light-evoked membrane potential of Drosophila primary arousal neurons indicate electrophysiological photoreceptor convergence, (*manuscript in preparation*)
2. **Au, D.,** Liu, J., Park, SJ., Nguyen, T.H., Dimalanta, M., Foden, A., and Holmes, T. Drosophila phototransduction occurs in arousal/circadian neurons via color-specific external and internal photoreceptors, (*manuscript in submission*)

3. **Au, D.**, Liu, J., Nguyen, T., Foden, A., Park, SJ., Dimalanta, M., Yu, Z., and Holmes, T. Nocturnal mosquito Cryptochrome1 mediates greater electrophysiological and behavioral responses to blue light relative to diurnal mosquito Cryptochrome1. Frontiers in Neuroscience, (2022)
4. **Au, D.**, Foden, A., Park, SJ., Tran, M., Nguyen, T., Liu, J., Jaime, OG., Yu, Z., and Holmes, T. Mosquito Cryptochromes expressed in *Drosophila* are functionally active and confer species-specific behavioral light responses. Current Biology, (2022).
5. Baik, L., Nave, C., **Au D.**, Guda, T., Chevez, J., Ray, A., and Holmes, T. Circadian regulation of light-evoked attraction/avoidance in day- vs. night-biting mosquitoes. Current Biology, (2020)
6. Baik, L., **Au, D.**, Nave, C., Foden, A., Enrriquez-Villalva, W. and Holmes, T. Distinct mechanisms of Drosophila CRYPTOCHROME-mediated light-evoked membrane depolarization and in vivo clock resetting. Proceedings of the National Academy of Sciences. (2019)
7. Baik, L., Recinos, Y., Chevez, J., **Au, D.**, and Holmes, T. Multiple Phototransduction Inputs Integrate to Mediate UV Light–evoked Avoidance/Attraction Behavior in Drosophila. J. Biol. Rhym. (2019)
8. **Au, D**+, Davidoff, S.N.+, Gale, B., Brooks, B., Brooks, A. (+: equal contribution). Maximizing Fibroblast Adhesion on Protein-Coated Surfaces Using Microfluidic Cell Printing. RSC Adv, (2015)
9. Davidoff, S.N., **Au, D.**, Smith, S., Brooks, A., and Brooks, B. Comparison of submerged and unsubmerged printing of ovarian cancer cells. Biomed Sci Instrum, (2015)

ABSTRACT PUBLICATIONS AND PRESENTATIONS

1. **Au, D.**, Liu, J., Nguyen, T., Park, SJ., Foden, A., Dimalanta, M., Yu, Z., and Holmes, T. Drosophila phototransduction occurs in arousal/circadian neurons via color-specific external and internal photoreceptors. (2022)
   - Data Blitz and Poster Presentations, Advancing Sleep & Circadian Science (ASCS), Clearwater Beach, FL (2023).
   - Poster Presentation, Society for Neuroscience, San Diego, CA (2022).
2. **Au, D.**, Foden, A., Park, SJ., Tran, M., Jaime, O., and Holmes, T. Mosquito cryptochrome is a well-conserved key photoreceptor for light-mediated behaviors in flies. (2021)
   - Oral Presentation, UCI Progress in Neuroscience (PiN) Seminar, Irvine, CA (2022).
   - Oral Presentation, Society for Research in Biological Rhythms, Amelia Island, FL (2022).
   - Poster Presentation, Society for Neuroscience, Zoom Virtual (2021).
   - Oral and Poster Presentations, Center for Circadian Biology Workshop, Zoom Virtual (2021).
   - Oral Presentation, CSHL – Drosophila Neurobiology Symposium, Zoom Virtual (2021).
3. Baik, L., **Au, D.**, Nave, C., Foden, A., Enrriquez-Villalva, W. and Holmes, T. Elucidating the Mechanistic Distinction of Drosophila CRYPTOCHROME's Role in Clock Resetting and Light-Evoked Potential. (2019)
   - Poster Presentation, Society for Research in Biological Rhythms, Zoom Virtual (2019).
   - Poster Presentation, Center for Circadian Biology, UCSD, San Diego, CA (2020).
   - Poster Presentation, CSHL – Drosophila Neurobiology Symposium, Cold Spring Harbor, NY (2020).

4. Baik, L., Recinos, Y., Chevez, J., **Au, D.**, and Holmes, T. Phototransduction processes to UV light stimuli relay avoidance/attraction behavior in Drosophila melanogaster. (2018)
    - Poster Presentation, Center for Circadian Biology, UCSD, San Diego, CA (2019).

OTHER EXPERIENCES AND PROFESSIONAL MEMBERSHIPS

Invited Speaker, Graduate Dean's Leadership Council Event (2022)
Peer-reviewer, NIH Fellowship Success Writing Course at UCI (2022)
Mentor, UROP Research Discovery Program (2022)
Member, Stanford Postdoctoral Recruitment Initiative in Sciences and Medicine (PRISM) (2022)
Councilmember, UCI School of Medicine (SOM) Student Council (2020-present)
Representative, Diverse Educational Community and Doctoral Experience (DECADE) (2018-present)
Recruiter, NIH Graduate & Professional School at UCI (2020, 2021, 2022)
Recruiter, SACNAS at UCI (2020, 2021)
Member, Society for Neuroscience (SfN) (2021, 2022)
Member, Society for Research in Biological Rhythms (SRBR) (2020, 2022)
Mentor, UCI Cellular and Molecular Bioscience (CMB) Program (2020-2021)
Participant, Bench-to-Bedside Competition at University of Utah (2015-2016)
Participant, Undergraduate Research Opportunities Program (UROP) (2011-2013)

ABSTRACT OF THE DISSERTATION

Non-image forming vision: an integration of multiple photoreceptor systems on the circadian/arousal neural circuit of *Drosophila melanogaster*

By

David Au

Doctor of Philosophy in Biomedical Sciences

University of California, Irvine, 2023

Professor Todd. C. Holmes, Chair

Mosquito disease vector control relies mostly on toxic insecticides. A more environmentally friendly alternative is to make use of light-based behavioral manipulation to attract pests to traps and repel pests away from human habitation. The present technology is based on the assumption that mosquito UV light detection occurs solely through opsin-based photoreception in the eyes. The Holmes Lab has recently found additional UV and short wavelength photoreceptive elements expressed in central brain neurons that strongly modulate complex insect behavioral responses to light. *Therefore, there is a need to incorporate these additional elements in disease vector control designs for improved efficiency.* Namely, CRYPTOCHROME (CRY), which is classically associated with its role in circadian clock resetting, activates with blue- and UV- light and increases the electrical excitability of circadian/arousal neurons. I hypothesized that CRY and other photoreceptor systems mediate photic input to the circadian/arousal circuit of flies in order to mediate specific light-based behavioral responses. To test this, I modified and adapted light-evoked electrophysiology

protocols to test the photoexcitability of primary arousal neurons in response to different stimuli of light using several photoreceptor mutants that lack one of three photoreceptor systems, as well as transgenic flies expressing mosquito CRY1 from a diurnal and nocturnal species. I also modified and adapted several behavioral assays to determine light attraction/avoidance as well as light-pulse arousal behavioral response to these different mutants. These modifications involved developing a new light emitting apparatus that improved on intensity control and spatiotemporal light exposure with a finer tuned spectral emission for UV, violet, blue, and red light. In this dissertation, I found that CRY coordinates with other photoreceptors to mediate light-induced electrical excitability of neurons, which underlie complex sleep/wake and light arousal behaviors. Furthermore, I found that CRY phototransduction persists across species in an intensity-dependent and species-specific manner, controlling light behavioral phototaxis across diurnal and nocturnal mosquito CRY1 profiles. I conclude with non-image forming as an amalgamation of multiple photoreceptor system contributions over a broad spectral range that affect downstream behavioral processes, including CRY as a primary short-wavelength photoreceptor for flies and mosquitos.

CHAPTER 1: Introduction

1.1 Significance

Short-wavelength light (UV, violet, blue) evokes diverse behaviors in insects, including arousal, phototaxis/photoavoidance, circadian entrainment, and others. Until very recently, it was widely assumed that all behavioral responses to short wavelength light are mediated by opsin-based photoreception in insect eyes. My thesis lab, the Holmes Lab, has discovered that many of these light-regulated behaviors are strongly modulated by two internal photoreceptors: CRYPTOCHROME (CRY) [1] and Rhodopsin 7 (Rh7) [2]. CRY is a UV and blue light-sensing flavin-based photopigment expressed in a small number of central brain circadian neurons (and external photoreceptors). CRY photoactivation evokes rapid and very long-lasting (30-40 sec) neuronal depolarization in large ventral lateral neurons (lLNv)r [1,3]. This leads to increased action potential firing rates that depend on electron transfer between the photo-reduced CRY cofactor Flavin Adenine Dinucleotide (FAD) and multiple tryptophan residues which form a chain between FAD buried within the CRY protein and the protein surface [3–5]. CRY's photoactivated redox state change couples to the voltage-gated potassium channel beta subunit (Kvβ) Hyperkinetic (Hk) that mediates membrane depolarization by modulating the activity of co-assembled ion conducting (K+) potassium subunits [6]. Rh7 is an atypical rhodopsin with partial overlapping expression with CRY in fly brain circadian neurons that couples to a Gq/PLC signaling pathway [2]. Rh7's spectral absorbance peak corresponds to violet light just below 400 nm as a bistable pigment with a broad range between 350-500 nm [2,7]. All three phototransduction pathways (CRY, Rh7 and external UV sensitive opsins) coordinately regulate fly circadian entrainment [2] and avoidance/attraction

behavioral responses to short wavelength light [8]. The CRY/Hk pathway in lLNvs underlie UV avoidance/attraction in flies [8,9].

Numerous insect species are dangerous to humans due to their ability to transmit diseases, including malaria, Zika virus fever, yellow fever, dengue fever, West Nile fever, Chagas disease, leishmaniasis, and many others. The World Health Organization (WHO) estimates 17% of all infectious diseases are vector-borne and propagate in tropical and subtropical areas. The recent spread of diseases like West Nile Disease has become a major concern and increases the need to maintain the spread of mosquito transmitted diseases. Current front-line mosquito control strategies require the use of toxic pesticides that can have harmful effects on humans and damage the environment. Insect control strategies that use light to attract or repel insects are becoming an increasingly appealing alternative, as light has such modest environmental impact. Much of my proposed work will extend our mechanistic understanding of how light attracts or repels insects in a species-specific manner at different times of day. Light-based insect control is manifested by "bug zapper" devices that attract insects to a UV light source, followed by trapping or a high voltage shock that eradicates the pest. Reciprocally, we should be able to translate our findings on how different light spectra repels insects by developing outside lighting around where humans live to keep harmful insects away. Current technology is limited by the outdated notion that UV light detection occurs solely through UV sensitive ocular photoreceptors. My work has very high potential significance due to the enormous scale of vector borne disease. Recent discoveries in the Holmes Lab identify additional UV and short wavelength photoreceptive elements that are expressed directly in central brain neurons. CRY and Rh7 strongly modulate complex insect behavioral responses to light. My goal is to combine and extend my previous training in engineering and biomedical sciences to characterize the detailed mechanisms of novel short

wavelength photoreceptors of *Drosophila* and mosquitoes towards making more effective and species-specific light control devices.

Light intensity, spectral composition, circadian timing, and different light input channels all contribute to light-modulated behaviors. CRY's conservation between *Drosophila melanogaster* and mosquitoes is 58% identity for day biting *Aedes aegypti* and 61% identity for night biting *Anopheles gambiae*. Purified CRY from *Drosophila* and *Anopheles gambiae* share light absorption peaks around the UV and blue light range in the base oxidized state. Rh7 also shows some conservation between *Drosophila melanogaster* and mosquitoes, with 49% identity for *Aedes aegypti* and 52% identity for *Anopheles gambiae*. Non-conserved protein features of CRY and Rh7 likely confer species-specific functions. Our very recent work using an evoked potential electrophysiological analysis of CRY expressing circadian/arousal *Drosophila* neurons shows surprisingly that CRY mediates a very long-lasting depolarizing photo-response that lasts nearly a minute, and also mediates a red-light response as well [3]. While image forming opsin-based phototransduction exhibits very rapid on/off kinetic responses, CRY's non-image forming vision is extraordinarily long lasting for 10s of seconds even following the cessation of light and thus may act as an irradiance detector tuned to short wavelength light. Together, I hypothesize that CRY coordinates with other photoreceptors to mediate light-induced electrical excitability of neurons, which underlie complex sleep/wake and circadian modulated attraction/avoidance behaviors. Implementing these findings into the development of novel light devices will likely improve the control efficiency of disease-spreading insects.

1.2 Innovation

The Holmes research group at UC Irvine recently identified CRY and Rh7 in *Drosophila* as two novel electrical photoreceptors that contribute to time-of-day modulated arousal and avoidance/attraction behavioral responses to short-wavelength light activation [8–10]. Previously, CRY was well characterized for contributing to the light-induced resetting of the *Drosophila* circadian molecular clock [11,12]. Our recent publications and my preliminary data show that CRY works in an integrated fashion with external opsin-based photoreceptors and Rh7 for light-modulated behavior, but how this integration occurs remains unclear. I will examine the molecular phototransduction mechanism and photo-response of transgenic *Drosophila* that express day- versus night-biting mosquito CRYs in **Chapters 2 and 3.** Next, I will measure the relative contribution of different photoreceptor inputs that mediate the electrophysiological photoresponse in circadian/arousal neurons in **Chapters 4 and 5**. My research will be useful for developing innovative LED devices for species-specific harmful insect control in the ongoing fight against vector-borne diseases.

1.3 Background and Preliminary Data

CRY, a blue- and UV- light-sensitive photoreceptor found in roughly half of the circadian neurons, including lLNv which act dually as light activated arousal neurons [13–15]. CRY regulates the circadian rhythm by light induced degradation of the TIMELESS (TIM) clock protein upon C-Terminal Tail (CTT) translocation, which subsequently leads to the degradation of co-complexed clock protein, PERIOD (PER). We found recently that CRY also modulates other light responsive

behaviors in animals, including avoidance/attraction to short wavelength light. Light-activated CRY underlies rapid membrane depolarization and increased action potential firing in circadian neurons via a redox based mechanism based on photoreduction of CRY's FAD (**Figure 1-1, A-C**) [10]. The exact biological redox mechanism underlying FAD photoreduction in CRY is unclear, but recent studies suggest multiple mechanisms utilize electron transfer pathways to facilitate FAD conversion to its anionic radical state, FAD^{-}. Also, reactive oxygen species (ROS) accumulation generated by CRY appear to be important [1,6,16,17].

Recently, my colleagues and I generated transgenic flies expressing partial loss-of-function (LOF) tryptophan-to-tyrosine mutant CRYs in the Trp triad; a highly conserved chain of tryptophan residues thought to mediate photoreduction of the FAD cofactor from its fully oxidized state to an anionic semiquinone ($FAD^{\bullet-}$) state via electron transport. Partial LOF mutants are more interpretable than more severe mutations that can cause non-specific protein folding defects. After generation of the mutant flies, we used electrophysiological techniques to measure the light-

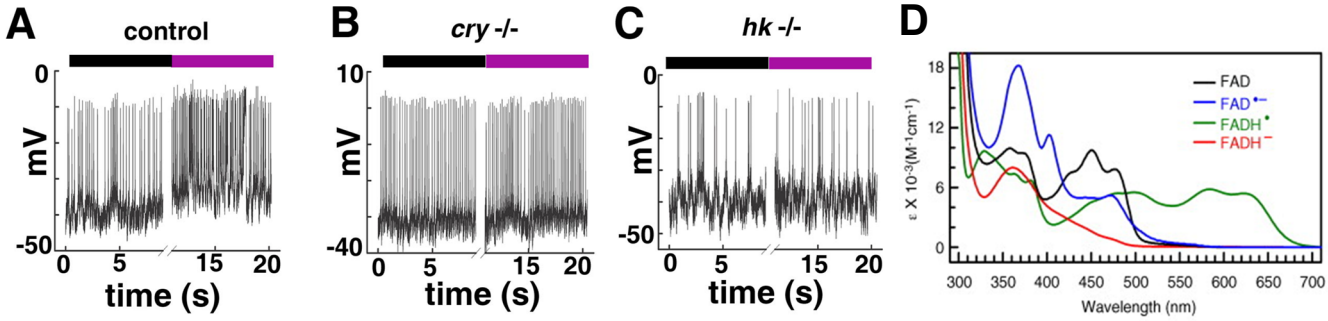

Figure 1-1. lLNv UV light-evoked response is dependent on CRY and HK.

(A) Representative trace of UV light evoked increase in firing frequency of lLNvs in control flies. **(B-C)** Representative traces showing attenuation of UV light evoked firing frequency response of lLNvs null for **(B)** CRY ($cry^{-/-}$) and **(C)** Hk ($hk^{-/-}$). **(D)** Absorbance spectra and extinction coefficients of purified AgCRY1 shows blue light (450 nm) peak for oxidized FAD (black), UV light (365 nm) peak for hemi-reduced FAD (blue line). **Baseline firing rate for each trace is within normal range and baselines do not vary significantly.** Green and red lines correspond to plant CRY excitation states and don't pertain to this proposal.

evoked potential from *ex vivo* brain preparations, as well as behavioral assays to measure the *in vivo* circadian clock resetting response to light. Mutating the tryptophan residue that sits closest to the FAD interaction site of CRY with a partial LOF tyrosine (W420Y) showed an attenuation of the blue and UV light evoked electrophysiological response in comparison to wild type CRY, identifying the importance of only this residue for CRY's interaction with Kvβ Hk, which leads to neuronal excitation. Additionally, mutating the furthest tryptophan in the triad from the FAD interaction site (W342Y) failed to appropriately reset the circadian clock, indicating a crucial role of this residue in the circadian clock resetting response to light, while the other tryptophan play a lesser role [9]. **These findings show that CRY photoactivation leads to very long-lasting neuronal excitation and circadian clock resetting via distinct phototransduction mechanistic pathways.**

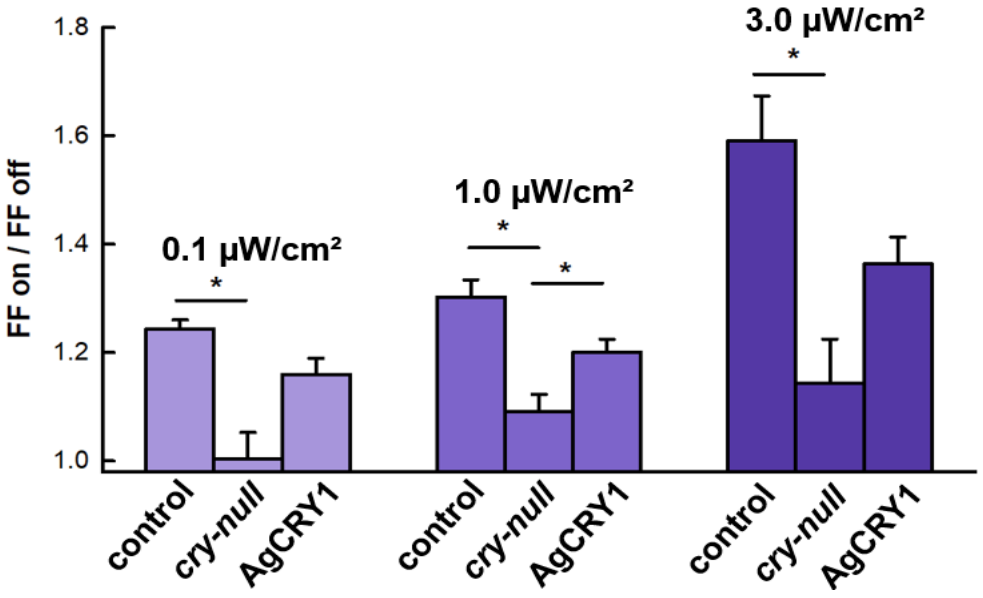

Figure 1-2. AgCRY1 exhibits partial rescue of Drosophila cry-null.

Transgenic flies expressing AgCRY1 with pdfGAL4 driver on *cry-null* background shows partial rescue of UV light lLNv excitation with intensity-dependent increase of FF compared to *cry-null* flies. (Au, Baik, unpublished)

Similar to *Drosophila* CRY (dCRY), absorbance spectra and extinction coefficients of purified mosquito CRY protein from *Anopheles gambiae* (Ag) shows a high peak of sensitivity for the oxidized resting state of FAD for blue light, and a high peak of sensitivity for the hemi-reduced FAD for UV light (**Figure 1-1, D**) [18]. We have generated *Drosophila* transgenic lines using the UAS/GAL4 system to drive expression of AgCRY1-eGFP in Pigment Dispersing Factor positive (PDF+) neurons over a *cry-null* background. Electrophysiological recordings of the lLNvs under UV light stimulation show an increase of firing frequency (FF) (reported as the ratio of FF lights on/ FF lights off) in *Drosophila* transgenic lines expressing AgCRY1 compared to *cry-null* flies. As the positive control group, dCRY is expressed using the UAS/GAL4 system on a *cry-null* background (dCRY rescue) and shows no statistical significance from conventional wild-type CRY expression and UV FF (data not shown). The firing frequency light-response is also intensity dependent, as higher intensity UV light (3.0 $\mu W/m^2$) has a greater increase of FF compared to lower intensity UV light (0.1 $\mu W/m^2$) (**Figure 1-2**, Au, Baik, unpublished). *Cry-null* recordings exhibit minor UV light responsiveness in the lLNvs, indicating that other photic inputs may converge on circadian/arousal neurons, as rhodopsins are the only other known UV photoreceptors expressed in *Drosophila*. These preliminary results indicate AgCRY1 partially rescues the function of *Drosophila* CRY photoreception. The relatively greater UV light response by *Drosophila* CRY compared to AgCRY1 may reflect the fact that *Drosophila* is a more day active species while *Anopheles gambiae* is night active. This data is consistent with the idea of some shared features of CRY-mediated neuronal excitation in *Anopheles gambiae* and *Drosophila* species. Our recent findings show that the nighttime active *Anopheles gambiae* circadian clock exhibits antiphasic PER expression levels in PDF+ neurons compared to daytime active *Aedes aegypti* mosquitos [19] and *Drosophila*. This may further account for reduced light sensitivity to

nighttime active species and may explain the partial rescue of AgCRY1 and suggest mechanisms of the mosquito molecular clock that create such differences in photic input that have yet to be discovered.

Reprinted with permission from:

Baik, L. S. *et al.* CRYPTOCHROME mediates behavioral executive choice in response to UV light. *Proc. Natl. Acad. Sci.* **114**, 776–781 (2017).

Wang, J., Du, X., Pan, W., Wang, X. & Wu, W. Photoactivation of the cryptochrome/photolyase superfamily. *J. Photochem. Photobiol. C Photochem. Rev.* **22**, 84–102 (2015).

CHAPTER 2: Mosquito Cryptochromes expressed in *Drosophila* are functionally active and confer species-specific behavioral light responses

2.1 Introduction

Mosquitoes are lethal disease vectors that threaten humans and account for millions of human deaths and hundreds of millions of infections each year [20]. Female mosquitoes seeking blood meals for reproductive energy hunt using an arsenal of finely tuned sensors for smell, taste, temperature, and sight [21–26]. The predominant current mosquito control strategies use environmentally damaging toxic pesticides [27–29]. Short-wavelength light (UV, violet, blue) evokes diverse behaviors in insects, including arousal, phototaxis/photoavoidance, circadian entrainment, and others [6,9,13,30–33]. Until recently, it was widely assumed that all behavioral responses to short wavelength light are mediated by opsin-based image forming photoreception in insect eyes [33–36]. However, many light-regulated behaviors have been found recently to be regulated by the non-opsin photoreceptor CRYPTOCHROME (CRY) [1,3,6,10]. CRY is a light-sensing flavin-based photopigment that detects UV and blue light in its FAD oxidized and FAD•- anionic semiquinone semi-reduced states and red light in its FADH• neutral radical state [4,5,37–39]. *Drosophila* CRY is expressed in a small number of central brain arousal and circadian neurons (and external photoreceptors) [1,11,13,40,41]. In contrast to the rapid on/off electrophysiological light responses mediated by image forming opsins, CRY photoactivation evokes rapid and very long-lasting (30-40 sec) neuronal depolarization and increased action potential firing in large ventral lateral neurons (l-LNvs) [1,3,9,10]. CRY phototransduction in LNvs mediates UV light avoidance behavior in flies [8–10]. Recent findings show *An. gambiae* mosquitoes are behaviorally photophobic to UV light, while

Ae. aegypti mosquitoes exhibit phototaxis to UV light [19]. We hypothesize that mosquito species-specific light response behaviors are mediated by species-specific CRY isoforms, considering that light intensity, spectral composition, circadian timing, and different light input channels may also contribute to light-modulated behaviors. We are interested in understanding the basis for these poorly understood light response behaviors for better control of harmful disease-spreading insects.

2.2 Materials and Methods

2.2.1 Experimental Animals

We created synthetic DNA constructs (Genscript) using a pJFRC7 vector containing the full *Drosophila* cryptochrome sequence, in frame with eGFP (Addgene). Generation of constructs containing cryptochrome 1 from *An. gambiae* (Ag) and *Ae. aegypti* (Ae) in frame with eGFP were also performed this way. DmCRY-eGFP, AgCRY1-eGFP, and AeCRY1-eGFP constructs using the pJFRC7 vector allow for a controlled insertion into the same genomic location via a specific PhiC31 genomic site. The synthetic DNA constructs containing each cryptochrome-eGFP variant were injected into fly embryos, reared, then screened for eye color as evidence of successful transgenesis. Resultant transgenic flies were isogenized by backcrossing with w1118 flies for a minimum of 6 generations. The following primers were designed to genotype-verify successful transgene insertion: AeCRY1 Forward: CGA GAA AGT GCA GGC CAA CAA TC, AeCRY1 Reverse: GT TCT TCA ACT CCG GCA GAT ATC, AgCRY1 Forward: CAG CCA GTT CAA GTA TCC GG, and AgCRY1 Reverse: CGG TTC GTG CAC AAA CTG TG. For quality control, DNA constructs were sequenced before embryonic insertion and gDNA from transgenic flies after

embryonic insertion (GeneWiz). All vectors were injected into *Drosophila* embryos (BestGene) to generate the UAS-eGFP-DmCRY, UAS-eGFP-AgCRY1, and UAS-eGFP-AeCRY1 transgenic flies. Each transgenic fly line was crossed into a *cry-null* background (obtained from Jeff Hall, Brandeis University) and again with a *pdfGAL4* or *crypGAL4-24* flies to generate the final transgenic mutant lines expressing DmCRY or mosquito CRY1 under a pdf- or cry-driver in a *cry-null* background.

2.2.2 Immunocytochemistry

Flies were entrained at 12:12 hr LD conditions for 3-5 days before males were separated and CO2 anesthetized for dissection. Dissections began approximately 1 hour before each respective ZT timepoint (ZT5, 11, 17, 23). To minimize introducing variance by circadian timing or experimental differences, all flies were entrained and dissected at the same time and days. Dissections were carried out at the same time for all genotypes tested and were repeated over 3 total experimental repeats. Brains were dissected in chilled 1X PBS, fixed in 4% paraformaldehyde (PFA) for 30min, washed 3X 10min in PBS-Triton-X 1%, incubated in blocking buffer (10% Horse Serum-PBS-Triton-X 0.5%) at room temperature before incubation with rabbit α-TIM, polyclonal (1:1,000) antibodies overnight in 4°C. Brains were washed 3X 10min in PBS-Triton-X 0.5% then incubated in goat α-rabbit-Alexa- 594 (1:1,000) secondary antibodies in blocking buffer overnight in 4°C. Brains were washed 5X 15min in PBS-Triton-X 0.5% before mounting in Vectashield mounting media (Vector Laboratories). Microscopy was performed using a Leica SP8 confocal microscope.

2.2.3 Locomotor Activity Behavior Assay

For our constant light behavior experiments, we used an adapted fly locomotor activity protocol [42,43]. Adult male flies were selected at 2-4 days post-eclosion then loaded in individual locomotor activity tubes. Locomotor activity of individual flies was measured using the TriKinetics Locomotor Activity Monitoring System via infrared beam-crossing recording total crosses in 30 min bins. Flies were initially entrained in 12:12 hr light:dark (LD) condition for 7 days, then they were exposed to 7 days of constant light (LL) conditions. Actograms were generated using Clocklab software. Average activity eduction graphs and its statistics were measured using FaasX software, then graphed using Microsoft Excel. Within FaasX, the CycleP analysis toolkit was used to calculate tau (τ), rhythm power, and period width via periodogram analysis with the following scoring criteria for flies in LL: minimum power ≥ 20, minimum width (h) ≥ 2, Chi-square significance ≥ 0.05. Data are reported as approximations of means.

2.2.4 Light-Evoked Neuronal Electrophysiology

Electrophysiology whole-cell current-clamp recordings were carried out from previously established and adapted protocols[3]. Adult male (3-5 days post-eclosion) fly brains were dissected in external recording solution. l-LNvs were subjected to whole-cell current-clamp with external solution: 122mM NaCl, 3mM KCl, 1.8mM CaCl2, 0.8mM MgCl2, 5mM glucose, 10mM HEPES, 7.2 pH, and 250-255mOsm; internal solution: 102mM Kgluconate, 17mM NaCl, 0.085mM CaCl2, 1.7mM MgCl2 (hexahydrate), 8.5mM HEPES, 0.94mM EGTA, 7.2pH, and 232-235mOsm. Custom-ordered multichannel LED source (Prizmatix/Stanford Photonics, Palo Alto, CA) fitted to the Olympus BX51 WI microscope was used for all optics using electrophysiology recordings. LED peak wavelengths are as follows: UV (365 nm) blue (450 nm), and red (635 nm), and all

exposures were set to intensity of 200 μW/cm2. Lower light intensities (20, 2, 0.2 μW/cm2) were adjusted using GamColor CineFilter 1516 .6 neutral density filters placed against the light source. Light intensities were determined by a Newport 842-PE Power/Energy meter. Each LED was triggered on and off for each sweep with TTL pulses programmed by pClamp (Molecular Dynamics) data acquisition software. Each color pulse was 5 seconds long. Each light pulse was preceded by minimum 50 second pre-pulse dark baseline, and there was 95 second inter-pulse intervals between each light exposure from there on, with 5-10 times of each color exposed per cell. All sweeps containing each light exposure recordings were averaged, and baseline was adjusted to pre-pulse signal. Furthermore, Gaussian and Butterworth filters were applied to the averaged signals using the ClampFit 10 software (Molecular Dynamics). The light evoked potential protocol collects individual baseline pre-stimulus recordings of membrane potential in current clamp mode and during the 5 second LED light stimulus, followed by 45-90 seconds of post light stimulus recording of membrane potential. The light pulse is repeated multiple times and all individual recordings for a given genotype and light stimulus are time locked to the light pulse duration, then averaged to capture averaged light evoked changes in membrane potential measured in millivolts [20,22], thus providing a kinetically robust light evoked potential.

2.2.5 UV Light Attraction/Avoidance Behavior Assay

Standard LD light choice assays were conducted from previously established and adapted protocols [10]. The locomotor activity of individual flies was measured using the TriKinetics Locomotor Activity Monitoring System via infrared beam-crossing, recording total crosses in 1-min bins. Percentage activity and statistics were measured using Microsoft Excel. Philips TL-D

Blacklight UV source with a narrow peak wavelength of 365 nm and intensity of 400 μW/cm2 was used for high intensity, and 10 μW/cm2 was used for low intensity by using neutral-density filters.

2.2.6 Confocal Microscopy and Image Processing

Brains were imaged with Leica SP8 confocal microscope. Images were quantified with ImageJ by selecting all regions of CRY-expressing/GFP-positive neurons for *crypGAL4-24* driven transgenic flies, or PDF-expressing/GFP-positive neurons for *pdfGAL4* driven transgenic flies. Maximum intensity projections were created using the Z stack tool between the image slices corresponding to the brain. Fluorescence from each brain were calculated by normalizing the mean intensities of the neurons against the background region of the brain. Only TIM fluorescence was quantified for the *cry-null* negative control flies, because there was no clear GFP expression to be able to identify those neurons. All images are adjusted for clarity with +40% Brightness and -20% Contrast from the original images.

2.2.7 Protein Sequence Alignment

Protein BLAST comparison in Figure 2-1 was generated by using FASTA sequences obtained from NCBI Protein Database for DmCRY (Accession: NP_732407), AgCRY1 (Accession: ABB29886), and AeCRY1 (Accession: Q17DK5). Sequences were aligned using a third party T-coffee multiple alignment tool (https://tcoffee.crg.eu/apps/tcoffee/do:regular) and color formatted using a BoxShade toolkit (https://www.ch.embnet.org/software/BOX_form.html).

2.2.8 Quantification and Statistical Analysis

Data are presented as mean ± SEM. Values of n refer to the total number of tested flies. In all cases, the n values were obtained from at least three separate experiments. Firing frequency data are reported as a ratio of spike events occurring during the 5 seconds of lights on/average spike events in the preceding 50 seconds binned in 10 second increments. Light-evoked increases of FF are significantly greater than the baseline FF ratio of 1. This was done to normalize across individual preparations. Statistical tests were performed using Minitab, Matlab, and Microsoft Excel software. Data were established as normally distributed through Anderson-Darling normality tests. For pairwise comparisons: F-tests were used to determine equal or unequal variance for normally distributed data, and one-tailed T-tests were used to determine significance between groups. Otherwise, for nonparametric data Mann-Whitney U-tests were run to determine significance between groups. For multi-group comparison: Barlett's test was used on normally distributed data and the Brown-Forsythe test was used on nonnormally distributed data to determine equivalence of variance. Significance within normally distributed data having equal variance was determined with one-way ANOVA and post-hoc Tukey test analysis, whereas Games-Howell was run for post-hoc analysis on data with unequal variance. Nonparametric tests to determine significance for data with equal and unequal variance was determined with Kruskal-Wallis one-way analysis of variance and post-hoc analysis using Dunn's test. Firing frequency analysis on electrophysiological recordings were performed using a custom Matlab script. To ensure Type I errors, i.e., false positives, are not inflated by the multiple comparisons, we computed the adjusted p-values based on an approach that controls the false discovery rate (FDR [44]). A commonly used threshold 0.1 indicates that among the ones reported significant, the expected proportion of false positives is no greater than 10%. Membrane potential statistical

analysis was simplified by binning each timepoint into 1 second average signal responses, then performing the appropriate statistical tests/post-hoc analyses based on normal distribution and equivalence of variance for each individual timepoint. These calculations were streamlined using custom Matlab scripts and excel spreadsheet.

2.3 Results

2.3.1 AeCRY1 and AgCRY1 expression does not determine diurnal/nocturnal behavior or the time-of-day peak of the circadian clock in transgenic flies

Drosophila CRY (DmCRY) mediates light-induced degradation of TIM, which subsequently resets the circadian clock and circadian regulated rhythms in flies [11,45]. Diurnal *Ae. aegypti* mosquitoes and nocturnal *An. gambiae* mosquitoes show opposite phases of sleep/wake activity cycles and 12 hr differences in their circadian clock phase [19]. To determine whether CRY expression of day versus night active mosquitoes is sufficient to set the circadian clock to peak either in the late evening or shifted 12 hrs to late day, we employ an established "empty neuron system" approach for interspecific transformation for studying species-specific effects [46–48], including olfaction [49,50]. The l-LNvs do not drive circadian behavior on their own as shown by mosaic analysis [51]. We tested the effects of mosquito AeCRY1 and AgCRY1 expression in *Drosophila* by generating transgenic UAS-flies to express CRY1 over a *cry-null* mutant fly background from *Ae. aegypti* (AeCRY1) or *An. gambiae* (AgCRY1) using the *crypGAL4-24* driver to express in all cells that ordinarily express CRY [52]. The amino acid sequence comparison of DmCRY (positive control), AgCRY1 and AeCRY1 is shown in Figure 2-1. The N-terminal fusion

of eGFP verifies protein expression levels and shows all three CRYs with levels of expression less than an order of magnitude difference (Figure 2-2).

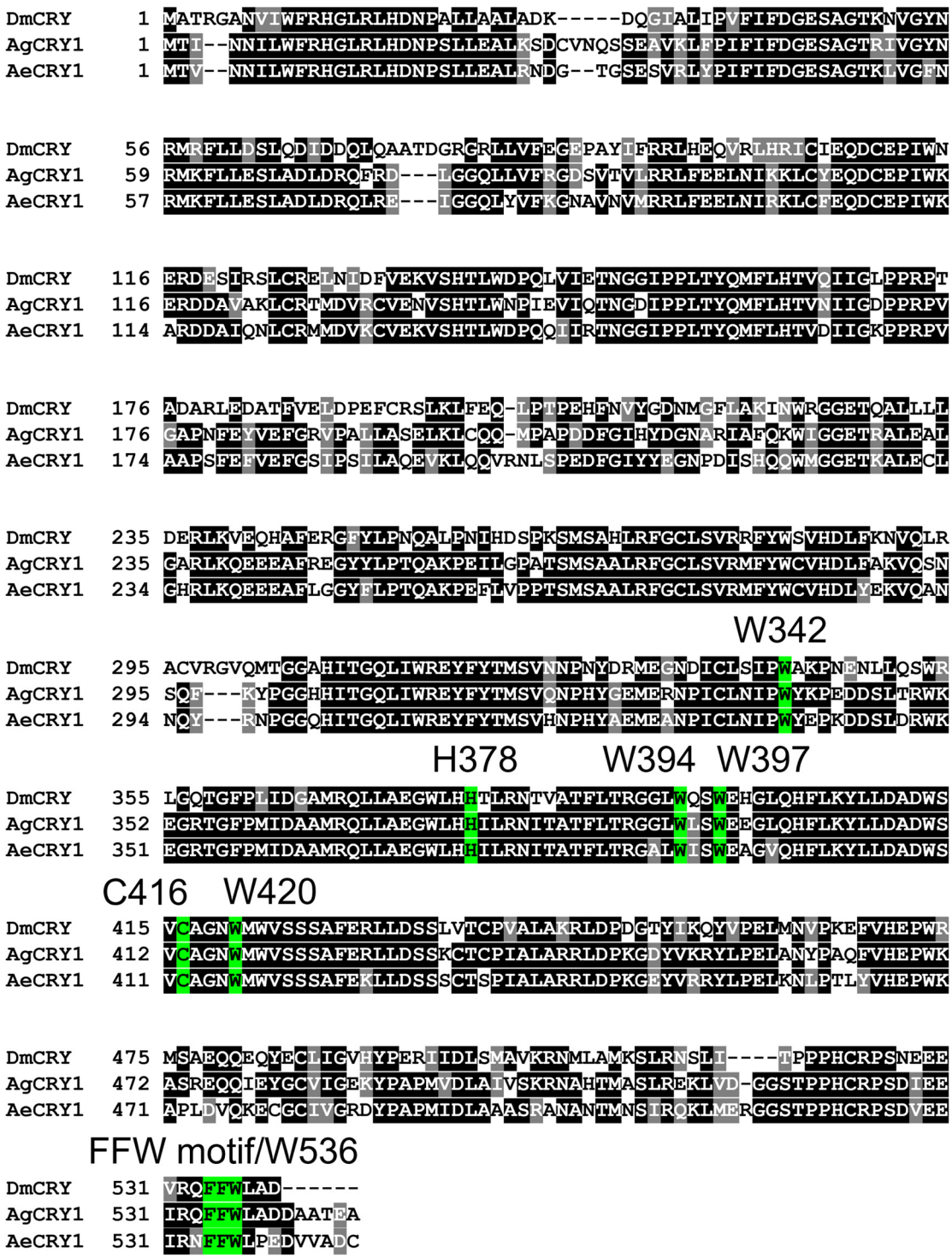

Figure 2-1. Protein BLAST comparison of DmCRY, AgCRY1, and AeCRY1 sequence

Protein BLAST comparison of sequences from DmCRY, AgCRY1, and AeCRY1 (see STAR Methods) show approximately 58% identity between *Drosophila melanogaster* CRY and diurnal *Aedes aegypti* CRY1, and 61% identity between *Drosophila melanogaster* CRY and nocturnal *Anopheles gambiae* CRY1. Regions highlighted in green show key amino acids conserved across the different species' CRY, such as the tryptophan tetrad (W342, W394, W397, W420), H378, C416, and c-terminal tail motif and back-door tryptophan (FFW and W536, respectively).

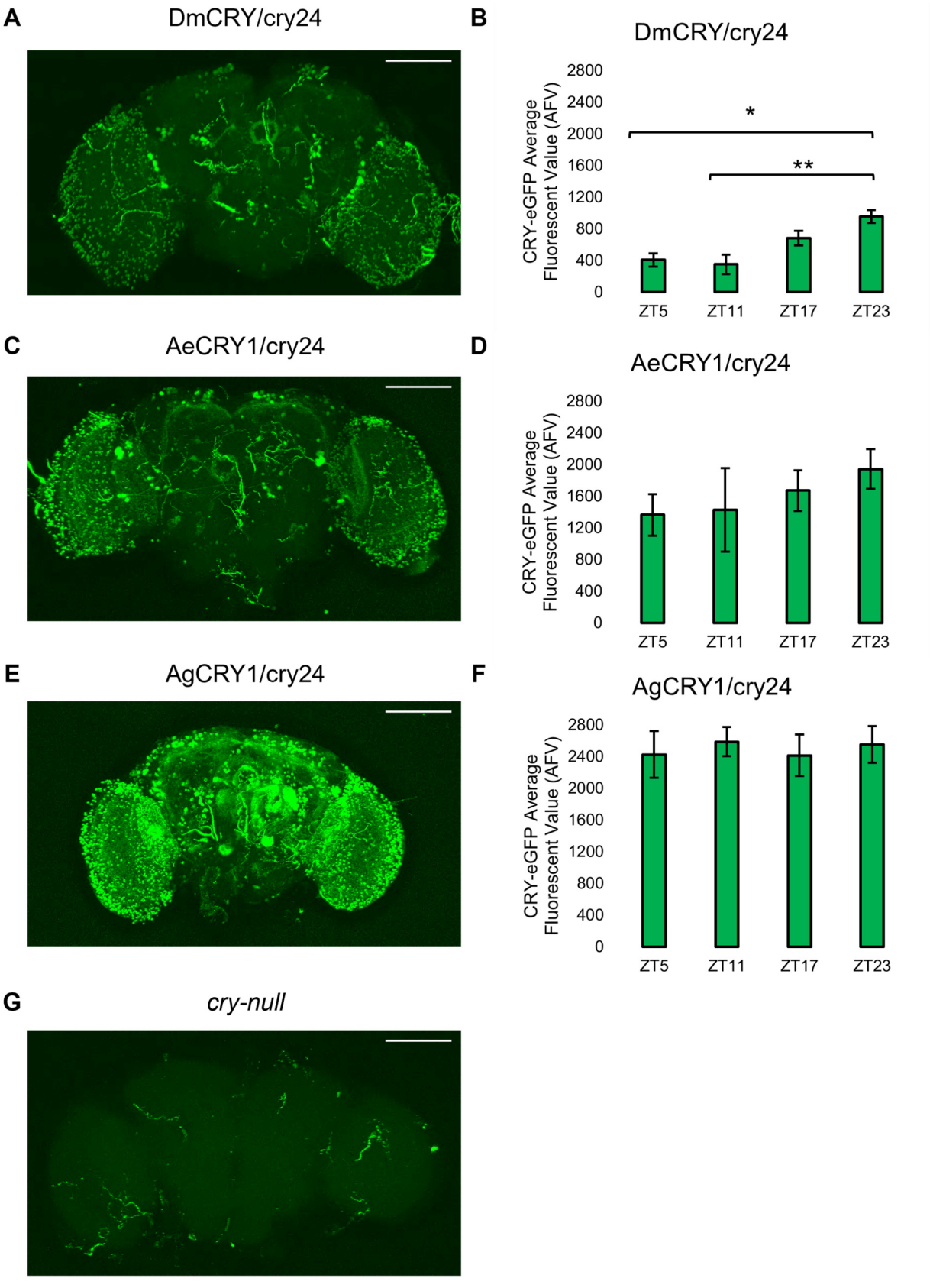
A
DmCRY/cry24
B
DmCRY/cry24
CRY-eGFP Average Fluorescent Value (AFV)
2800
2400
2000
1600
1200
800
400
0
*
**
ZT5
ZT11
ZT17
ZT23
C
AeCRY1/cry24
D
AeCRY1/cry24
E
AgCRY1/cry24
F
AgCRY1/cry24
G
cry-null

Figure 2-2. All transgenic flies show similar expression of CRY-eGFP

Immunocytochemistry average fluorescent value of CRY-eGFP expression over 12:12 hr LD at ZT 5, 11, 17, and 23 timepoints in LNvs expressing **(A, B)** DmCRY with representative image, **(C, D)** AeCRY1 with representative image, **(E, F)** AgCRY1 with representative image over *cry-null* background, and **(G)** representative image of negative control *cry-null*. Quantification chart for *cry-null* not shown because of absence of signal. All representative images are at ZT 23, have a 100-micron scale bar for reference, and have been modified for clarity with 40% brightness and -20% contrast. Data are represented as mean ± SEM. One significance symbol; $p \leq 0.05$, two significance symbols; $p \leq 0.005$, three significance symbols; $p \leq 0.001$.

To test whether mosquito CRY1s determine the circadian clock peak, anti-TIM polyclonal antibodies followed by confocal imaging semi-quantified TIM levels at time points ZT5, ZT11, ZT17, and ZT23 were measured in the lateral ventral neuron (LNv) subgroup after at least three days of 12:12 hr Light:Dark (LD) entrainment, and showed peak signal at ZT23 and lowest signal at ZT5 and ZT11 for control DmCRY, AeCRY1, and AgCRY1 expressing transgenic flies (Figure 2-3A, B, C, D, E, F, G). AeCRY1 TIM values are almost two times higher than AgCRY1 flies, suggesting that AeCRY1 from the day-active mosquito is less light sensitive than nocturnal AgCRY1. Negative control *cry-null* flies lacking CRY expression show a similar pattern of TIM cycling in the LNvs (Figure 2-3H). CRY variant and TIM expression in the number of LNvs in the brain is shown in Figure 2-4. Thus, AeCRY1 and AgCRY1 expression in flies does not disrupt the circadian clock or determine the timing of the TIM peak.

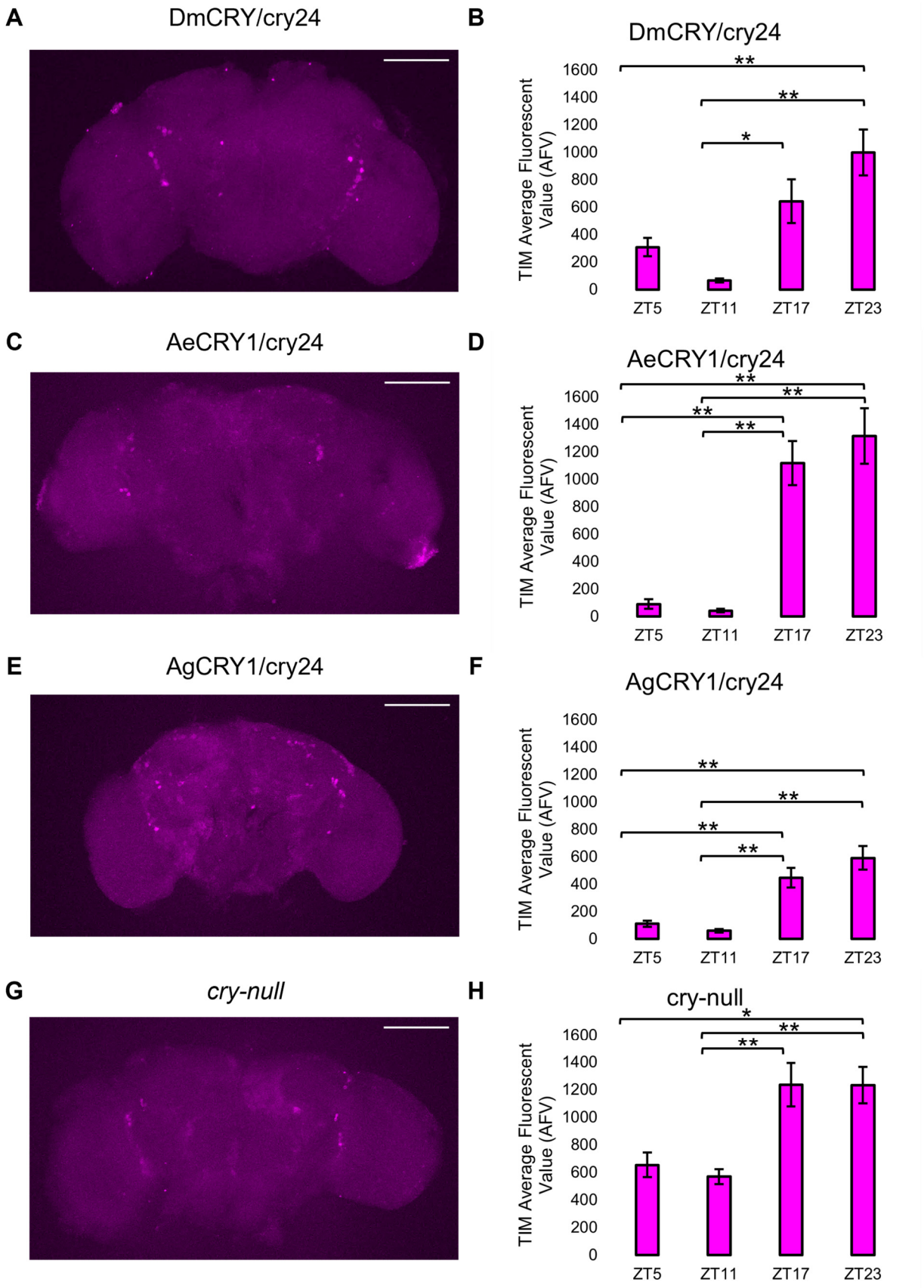
A
DmCRY/cry24
B
DmCRY/cry24
TIM Average Fluorescent Value (AFV)
1600
1400
1200
1000
800
600
400
200
0
**
**
*
ZT5
ZT11
ZT17
ZT23
C
AeCRY1/cry24
D
AeCRY1/cry24
TIM Average Fluorescent Value (AFV)
**
**
**
**
ZT5
ZT11
ZT17
ZT23
E
AgCRY1/cry24
F
AgCRY1/cry24
TIM Average Fluorescent Value (AFV)
**
**
**
**
ZT5
ZT11
ZT17
ZT23
G
cry-null
H
cry-null
TIM Average Fluorescent Value (AFV)
*
**
**
ZT5
ZT11
ZT17
ZT23

Figure 2-3. AeCRY1 and AgCRY1 expression does not disrupt the phase of the circadian clock in transgenic flies

Immunocytochemistry average fluorescent value of TIM expression over 12:12 hr LD at ZT 5, 11, 17, and 23 timepoints in LNvs expressing **(A, B)** DmCRY with representative image, **(C, D)** AeCRY1 with representative image, **(E, F)** AgCRY1 with representative image over *cry-null* background, and **(G, H)** negative control *cry-null*. All representative images are at ZT 23, have a 100-micron scale bar for reference, and have been modified for clarity with 40% brightness and -20% contrast. Data are represented as mean ± SEM. One significance symbol; $p \leq 0.05$, two significance symbols; $p \leq 0.005$, three significance symbols; $p \leq 0.001$.

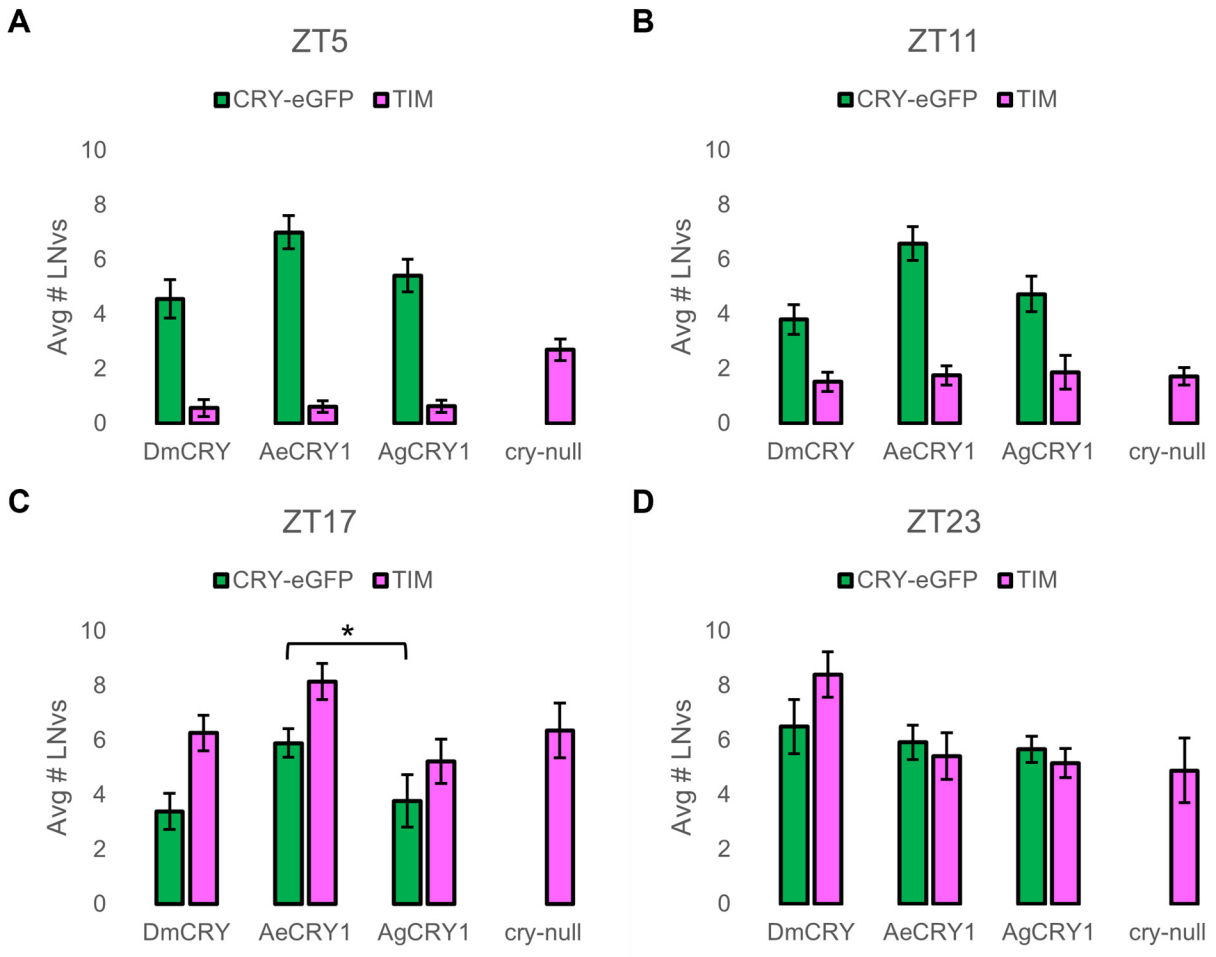

Figure 2-4. The number of lateral ventral neurons that express TIM or CRY-eGFP across the DmCRY/cry24, AgCRY1/cry24, AeCRY1/cry24 groups, except for AeCRY1/cry24 versus AgCRY1/cry24 at ZT17

Average number of LNvs that indicate DmCRY, AeCRY1, or AgCRY1 expression via eGFP (green columns) and TIM (pink columns) signal presence at **(A)** ZT 5, **(B)** ZT 11, **(C)** ZT 17, and **(D)** ZT 23. Data are represented as mean ± SEM. One significance symbol; $p \leq 0.05$, two significance symbols; $p \leq 0.005$, three significance symbols; $p \leq 0.001$.

2.3.2 AgCRY1 expressing flies show greater intensity-dependent light sensitivity than AeCRY1 expressing flies based on their comparative degree of arrhythmicity in an LL assay

Constant light (LL) evokes behavioral arrhythmicity while flies lacking functional CRY maintain greater rhythmicity under LL [3,53]. To determine the relative light sensitivities of mosquito CRY1s, we tested locomotor rhythmicity after subjecting transgenic flies and *cry-null* control flies to at least five days of intensity-tuned 12:12 hr LD entrainment, followed by at least five days of LL white light at high (1000 lux) or low (1 lux) intensity. DmCRY expressing flies become highly arrhythmic in high intensity LL (Figure 2-5A) and negative control *cry-null* flies maintain a high level of rhythmicity in all LL light conditions, confirming the absence of functional CRY (Figure 2-5D, Figure 2-6D). AeCRY1 expressing flies are partially arrhythmic in high and low intensity LL, showing higher rhythmicity than DmCRY expressing flies, but significantly less rhythmicity than *cry-null* flies, suggesting AeCRY1 is functional but less light sensitive by this measure (Figure 2-5B, Figure 2-6B). AgCRY1 flies exhibit significantly less rhythmicity in high intensity LL relative to AeCRY1 flies, showing greater light sensitivity of AgCRY1 compared to AeCRY1 (Figure 2-5C, E). AgCRY1 expressing flies exhibit arrhythmicity in response to high intensity LL that is indistinguishable to DmCRY expressing flies (Figure 2-5E) but maintain detectable rhythmicity in low intensity LL (Figure 2-6C).

Unexpectedly, both AgCRY1 and AeCRY1 flies die in progressively greater numbers when exposed to prolonged high intensity 1000 lux white light LL compared to DmCRY and *cry-null* groups. AgCRY1 shows the highest mortality after seven days of LL (Figures 2-5F-H). At low intensity 1 lux LL, AgCRY1 and AeCRY1 flies also exhibit higher mortality after prolonged LL exposure (Figures 2-6F-H). AgCRY1 flies show significantly higher mortality in 1000 lux LL at day 7 relative to 1 lux LL at day 7, showing that LL mortality is a function of light intensity (Figure 2-5H, Figure 2-6H). This phenomenon may be related to CRY mediated modulation of lifespan in aged flies[54]. AeCRY1 (day-active) expressing flies are less light sensitive than AgCRY1 (night-active) expressing flies by the LL mortality assay. Thus, the relative light sensitivities of mosquito CRY1s may contribute to the very strong light avoidance seen in nocturnal mosquitoes[19].

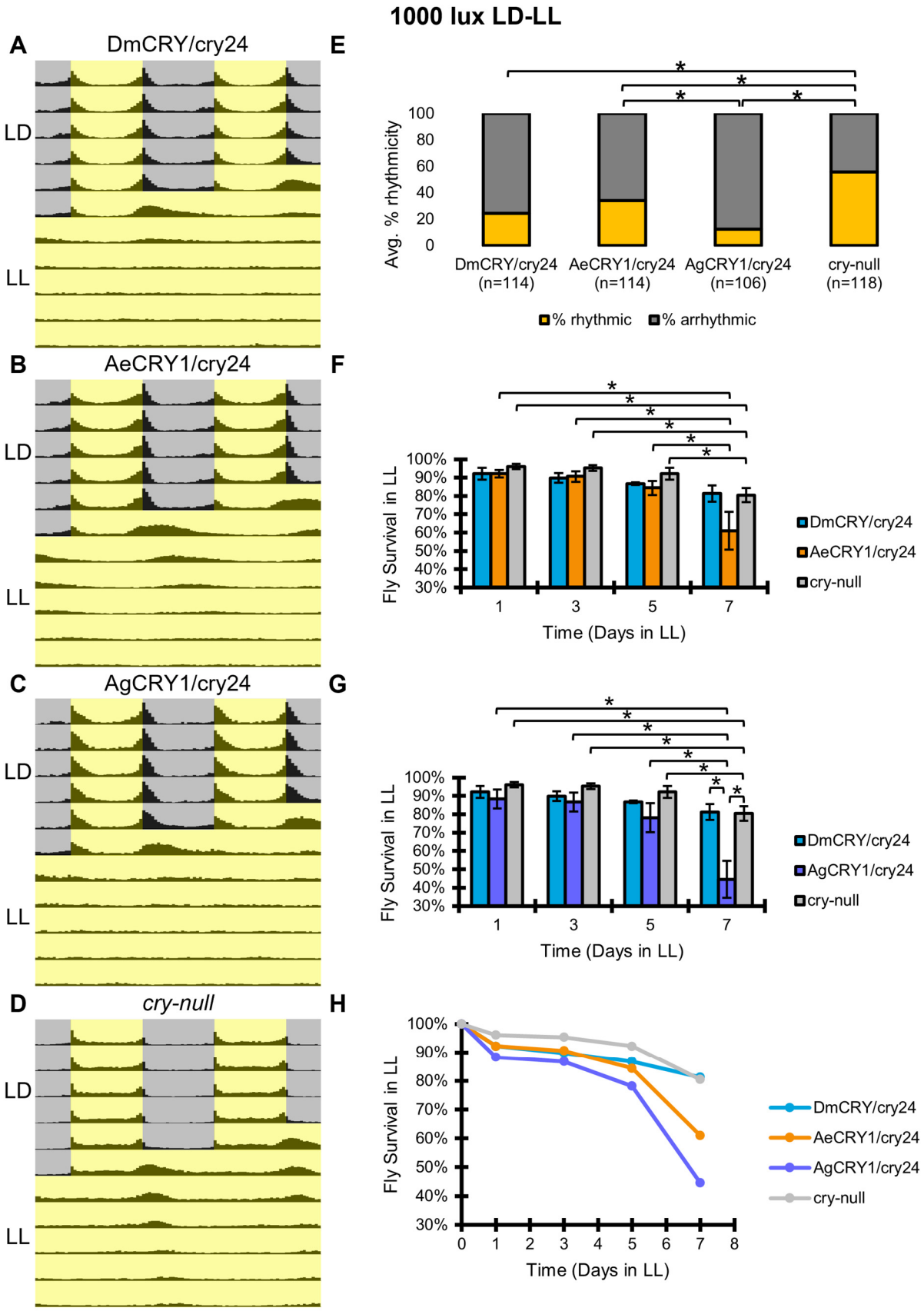
1000 lux LD-LL
A
DmCRY/cry24
LD
LL
B
AeCRY1/cry24
LD
LL
C
AgCRY1/cry24
LD
LL
D
cry-null
LD
LL
E
Avg. % rhythmicity
100
80
60
40
20
0
DmCRY/cry24 (n=114)
AeCRY1/cry24 (n=114)
AgCRY1/cry24 (n=106)
cry-null (n=118)
% rhythmic
% arrhythmic
F
Fly Survival in LL
100%
90%
80%
70%
60%
50%
40%
30%
1
3
5
7
Time (Days in LL)
DmCRY/cry24
AeCRY1/cry24
cry-null
G
Fly Survival in LL
Time (Days in LL)
DmCRY/cry24
AgCRY1/cry24
cry-null
H
Fly Survival in LL
0
1
2
3
4
5
6
7
8
Time (Days in LL)
DmCRY/cry24
AeCRY1/cry24
AgCRY1/cry24
cry-null

Figure 2-5. AgCRY1 and control DmCRY expressing flies are arrhythmic in high intensity constant light (1000 lux LL), AeCRY1 expressing flies are partial arrhythmic and *cry-null* flies remain rhythmic in LL

(A-D) Actograms plots containing 5 days of 12:12 hr LD entrainment followed by 5 days of high intensity constant light (1000 lux LL) conditions for flies expressing: **(A)** DmCRY (n=114; τ_{avg}≈25.2, $power_{avg}$≈51.0, $width_{avg}$≈3.4), **(B)** AeCRY1 (n=114; τ_{avg}≈25.4, $power_{avg}$≈47.6, $width_{avg}$≈4.2), **(C)** AgCRY1 (n=106; τ_{avg}≈25.1, $power_{avg}$≈34.4, $width_{avg}$≈2.4), **(D)** *cry-null* (n=118; τ_{avg}≈25.1, $power_{avg}$≈67.4, $width_{avg}$≈3.6). **(E)** Quantification of fly rhythmicity (orange) to arrhythmicity (grey) in LL. **(F-H)** Fly survival plots over an extended 7-day period of high intensity LL exposure: **(F)** Bar charts of the average survival percentage at days 1, 3, 5, and 7 in LL of DmCRY (blue) vs AeCRY1 (orange) vs *cry-null* (grey) groups. **(G)** Bar charts of the average survival percentage at days 1, 3, 5, and 7 in LL of DmCRY vs AgCRY1 (purple) vs *cry-null* groups. **(H)** Line plot summary of LL survivability for both AeCRY1 and AgCRY1 groups compared with DmCRY and *cry-null*. Data are represented as mean ± SEM. One significance symbol; $p \leq 0.05$, two significance symbols; $p \leq 0.005$, three significance symbols; $p \leq 0.001$.

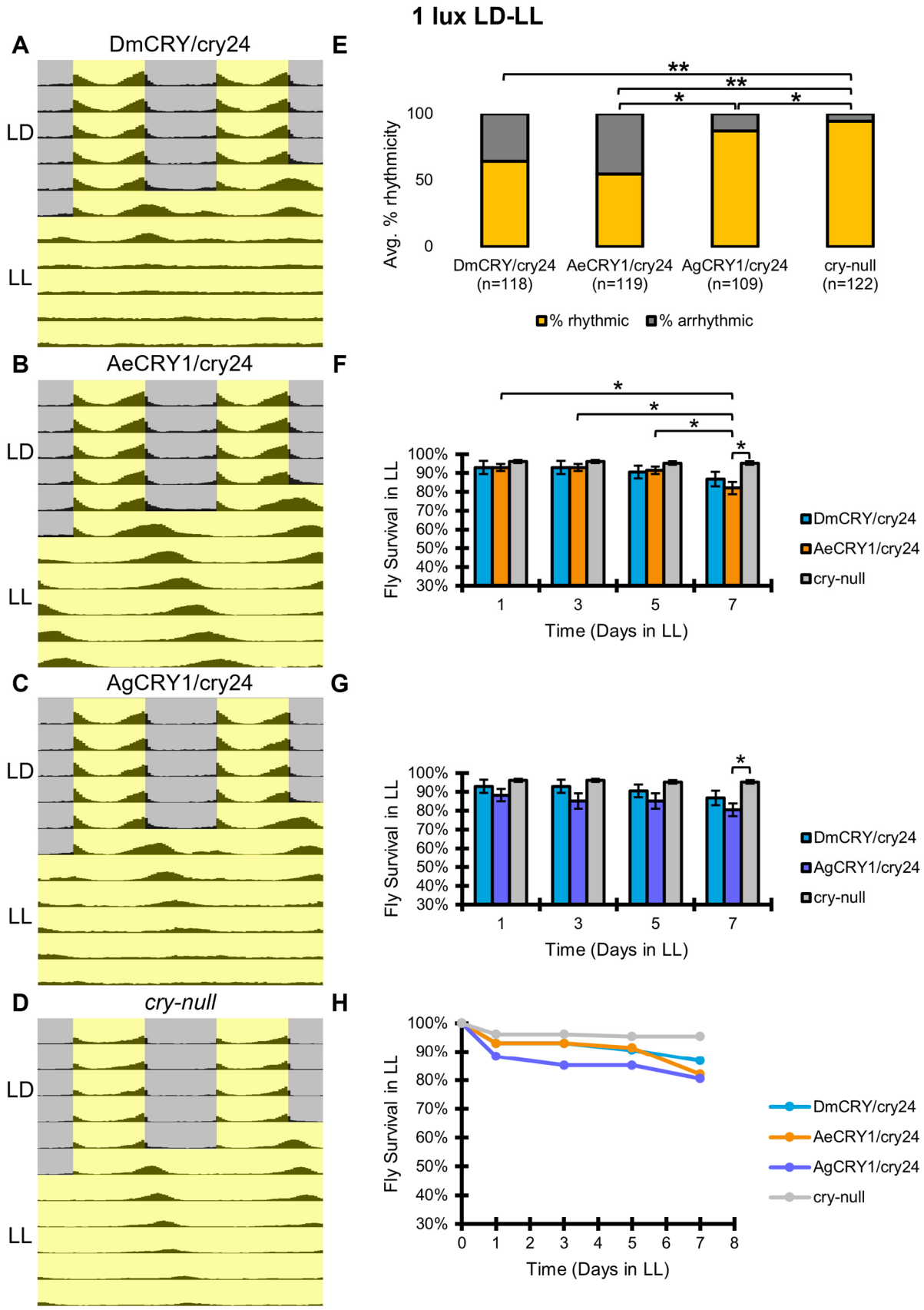
A
DmCRY/cry24
LD
LL
B
AeCRY1/cry24
LD
LL
C
AgCRY1/cry24
LD
LL
D
cry-null
LD
LL
E
1 lux LD-LL
Avg. % rhythmicity
100
50
0
**
**
*
*
DmCRY/cry24 (n=118)
AeCRY1/cry24 (n=119)
AgCRY1/cry24 (n=109)
cry-null (n=122)
% rhythmic
% arrhythmic
F
Fly Survival in LL
100%
90%
80%
70%
60%
50%
40%
30%
1
3
5
7
Time (Days in LL)
DmCRY/cry24
AeCRY1/cry24
cry-null
G
Fly Survival in LL
Time (Days in LL)
DmCRY/cry24
AgCRY1/cry24
cry-null
H
Fly Survival in LL
0
1
2
3
4
5
6
7
8
Time (Days in LL)
DmCRY/cry24
AeCRY1/cry24
AgCRY1/cry24
cry-null

Figure 2-6. AeCRY1 and control DmCRY expressing flies are partial arrhythmic in low intensity constant light (1 lux LL), AgCRY1 and *cry-null* flies remain highly rhythmic in LL

(A-D) Actograms plots containing 5 days of 12:12 hr LD entrainment followed by 5 days of low intensity constant light (1 lux LL) conditions for flies expressing: **(A)** DmCRY (n=118; τ_{avg}≈24.9, $power_{avg}$≈62.5, $width_{avg}$≈3.2), **(B)** AeCRY1 (n=119; τ_{avg}≈26.0, $power_{avg}$≈118.0, $width_{avg}$≈5.6), **(C)** AgCRY1 (n=109; τ_{avg}≈26.0, $power_{avg}$≈68.0, $width_{avg}$≈4.3), **(D)** *cry-null* (n=122; τ_{avg}≈25.2, $power_{avg}$≈109.8, $width_{avg}$≈5.2). **(E)** Quantification of fly rhythmicity (orange) to arrhythmicity (grey) in LL. **(F-H)** Fly survival plots over an extended 7-day period of low intensity LL exposure: **(F)** Bar charts of the average survival percentage at days 1, 3, 5, and 7 in LL of DmCRY (blue) vs AeCRY1 (orange) vs *cry-null* (gray) groups. **(G)** Bar charts of the average survival percentage at days 1, 3, 5, and 7 in LL of DmCRY vs AgCRY1 (purple) vs *cry-null* groups. **(H)** Line plot summary of LL survivability of both AeCRY1 and AgCRY1 groups compared with DmCRY and *cry-null*. Data are represented as mean ± SEM. One significance symbol; $p \leq 0.05$, two significance symbols; $p \leq 0.005$, three significance symbols; $p \leq 0.001$.

2.3.3 AgCRY1 mediates more robust cell autonomous electrophysiological responses to short-wavelength and red light than AeCRY1

Drosophila LNvs are circadian/arousal neurons that drive CRY-dependent photoavoidance [3,6,8,10,13]. As nocturnal mosquitoes exhibit strong short wavelength photoavoidance [19], we tested the hypothesis that nocturnal mosquito AgCRY1 confers cell autonomous greater electrophysiological responsiveness to 365 nm UV light than diurnal AeCRY1. We expressed AeCRY1, AgCRY1, and control DmCRY in the *cry-null* genetic background flies using the *pdfGAL4* driver line that restricts expression to the LNvs, then compared electrophysiological responses to 365 nm UV light over a four order of magnitude intensity range (200 μW/cm², 20 μW/cm², 2 μW/cm² and 0.2 μW/cm²) measured by whole-cell patch-clamp recordings of l-LNvs in transgenic flies. *Drosophila* eye and head cuticles are >85% and 50% transparent respectively to 365 nm UV light[1]. DmCRY expressing l-LNvs show robust light evoked increases in firing frequency (FF) at 200, 20, 2 and 0.2 μW/cm² light intensities (Figure 2-7A). AgCRY1 UV light evoked FF increases are significantly higher than stimulus intensity matched AeCRY1 UV light

evoked FFs at 200 μW/cm², 2 μW/cm², and 0.2 μW/cm² (Figure 2-7A), thus AgCRY1 consistently exhibits higher electrophysiological light sensitivity relative to AeCRY1. While DmCRY UV light evoked FFs are consistently higher than either mosquito CRY1, comparing the absolute performances of native versus heterologously expressed CRY proteins is interpretationally questionable[39,55,56]. Representative l-LNv patch clamp voltage traces depicting 1-minute raw action potential firing data 10 seconds prior to, during the 5 seconds 365 nm UV light stimulus at 200 μW/cm², 45 seconds post light stimulus are shown in Figure 2-11.

The relationship between light onset and the timing of the first light evoked action potential is not kinetically robust[1]. We developed a kinetically robust CRY mediated light evoked potential method[1,3] using signal averaging of multiple current-clamp recordings. Control DmCRY light evoked responses tend to increase sharply during and immediately after the UV light pulse for all four UV light intensities tested (200 μW/cm², 20 μW/cm², 2 μW/cm², and 0.2 μW/cm²), followed by monotonically decreasing levels of sustained responses over tens of seconds post light stimulus as light intensity decreases (Figure 2-7B, D, F, and H). In contrast, very weak or absent UV light responses are seen for evoked potential recordings from *cry-nulls* at all light intensities tested (Figure 2-7B, D, F, and H). DmCRY recordings show significantly greater UV light evoked increases in membrane potential relative to the *cry-nulls*, particularly during and several seconds after the 5 sec 200 μW/cm² UV light pulse (Figure 2-7B).

AgCRY1 mediates remarkably sustained evoked potentials in response to the 200 μW/cm² 365 nm UV light stimulus, as seen up to 45 seconds after the cessation of the UV light pulse (Figure 2-7C). 200 μW/cm² UV light evoked AgCRY1 potentials show significantly higher magnitude evoked increases in membrane potential than AeCRY1 at nearly all time points after

the light pulse, statistically calculated using FDR adjustment for which $p \leq 0.1$ indicates significance (Figure 2-7C). The 200 μW/cm² UV light evoked AeCRY1 potential after the cessation of light is sustained, but significantly less than that for AgCRY1. Similar results are seen for all lower stimulus intensities: AgCRY1 UV light evoked responses tend to be significantly higher than AeCRY1 recorded following 20 μW/cm², 2 μW/cm², and 0.2 μW/cm² 365 nm UV light stimulus (Figure 2-7E, G and I). Thus, cell autonomous AgCRY1 UV light evoked responses are significantly higher than those of AeCRY1 over a wide range of light intensities. These results indicate that the greater light response of AgCRY1 over AeCRY1 is likely due to intrinsic CRY molecular properties.

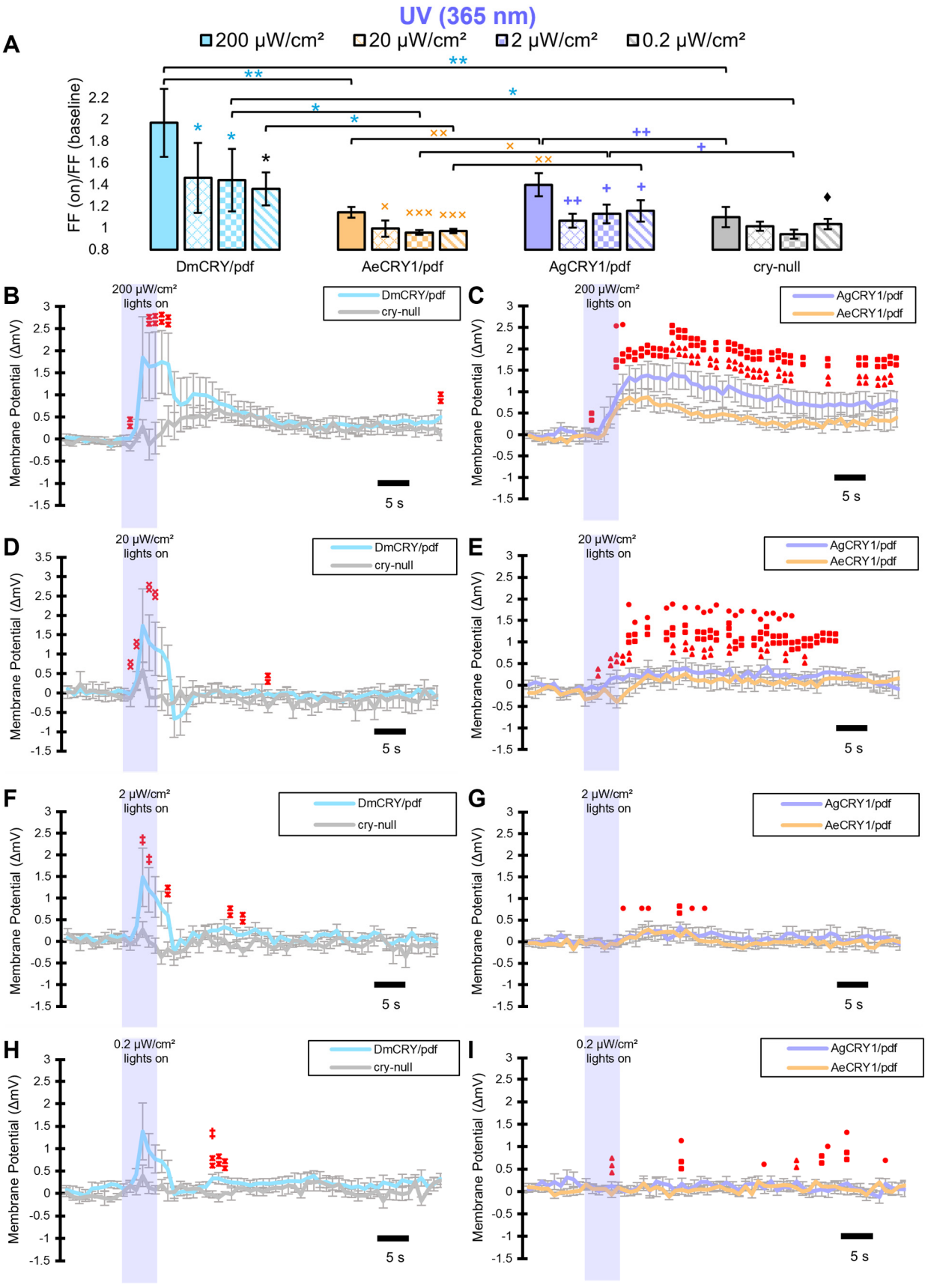
A
UV (365 nm)
200 µW/cm²
20 µW/cm²
2 µW/cm²
0.2 µW/cm²
FF (on)/FF (baseline)
DmCRY/pdf
AeCRY1/pdf
AgCRY1/pdf
cry-null
B
C
D
E
F
G
H
I
Membrane Potential (ΔmV)
lights on
5 s

Figure 2-7. Transgenic PDF+ *Drosophila* neurons expressing either AeCRY1 or AgCRY1 show intensity-dependent light-evoked excitation to UV light

(A) *pdfGAL4* driven DmCRY (light blue) and *cry-null* (grey) comparison of AeCRY1 (light orange) and AgCRY1 (light purple) expressing l-LNvs FF upon five seconds of UV (365 nm) light exposure over 50 seconds of baseline FF at varying intensities light intensities of 200 (solid color), 20 (crisscrossed pattern), 2 (checkered pattern), and 0.2 (diagonally striped pattern) µW/cm². **(B-E)** Light-evoked change in membrane potential at: 200 µW/cm² UV stimulus for **(B)** DmCRY (light blue, n=9) vs *cry-null* (grey, n=6) and **(C)** AeCRY1 (light orange, n=10) vs AgCRY1 (light purple, n=9); 20 µW/cm² UV stimulus for **(D)** DmCRY (n=8) vs *cry-null* (n=6) and **(E)** AeCRY1 (n=10) vs AgCRY1 (n=9); 2 µW/cm² UV stimulus for **(F)** DmCRY (n=8) vs *cry-null* (n=6) and **(G)** AeCRY1 (n=10) vs AgCRY1 (n=8); and 0.2 µW/cm² UV stimulus for **(H)** DmCRY (n=8) vs *cry-null* (n=5) and **(I)** AeCRY1 (n=10) vs AgCRY1 (n=8). Purple bar on membrane potential plots indicates the timing of the 5 seconds of UV-light stimuli and black scale-bar indicates 5 seconds. Traces represent the average last 60 seconds of each recording. **(A)** Black * indicates $p \leq 0.05$ for comparisons against DmCRY/pdf. Black ♦ indicates $p \leq 0.05$ for comparisons against *cry-null*. Light blue * indicates FDR adjusted $p \leq 0.1$ for comparisons against DmCRY/pdf. Light orange x indicates FDR adjusted $p \leq 0.1$ for comparisons against AeCRY1/cry24. Light purple + indicates FDR adjusted $p \leq 0.1$ for comparisons against AgCRY1/cry24. Grey ♦ indicates FDR adjusted $p \leq 0.1$ for comparisons against *cry-null*. **(B-I)** Red * indicates FDR adjusted $p \leq 0.1$ between DmCRY/cry24 and *cry-null*. Red x indicates FDR adjusted $p \leq 0.1$ between AeCRY1/cry24 and DmCRY/cry24. Red + indicates FDR adjusted $p \leq 0.1$ between AgCRY1/cry24 and DmCRY/cry24. Red ▲ indicates FDR adjusted $p \leq 0.1$ between AgCRY1/cry24 and AeCRY1/cry24. Red ■ indicates FDR adjusted $p \leq 0.1$ between AgCRY1/cry24 and *cry-null*. Red ● indicates FDR adjusted $p \leq 0.1$ between AeCRY1/cry24 and *cry-null*. Data are represented as mean ± SEM. For black significance symbols: One symbol; $p \leq 0.05$, two symbols; $p \leq 0.005$, three symbols; $p \leq 0.001$. For colored significance symbols: One symbol; $p \leq 0.1$, two symbols; $p \leq 0.05$, three symbols; $p \leq 0.01$.

The LNv/circadian neural circuit networks in nocturnal *Anopheles coluzzi* and diurnal *Aedes* mosquitoes show similar and species-specific features and share neuroanatomical features with *Drosophila* [19]. To determine whether circuit-wide expression of mosquito CRY1s confer distinguishable electrophysiological differences compared to expression restricted to the LNvs, we used the *crypGAL4-24* driver line that drives expression in all CRY neurons. DmCRY expression via the *crypGAL4-24* driver mediates robust electrophysiological light responses in the l-LNvs that do not differ from endogenous wild type CRY (Figure 2-8).

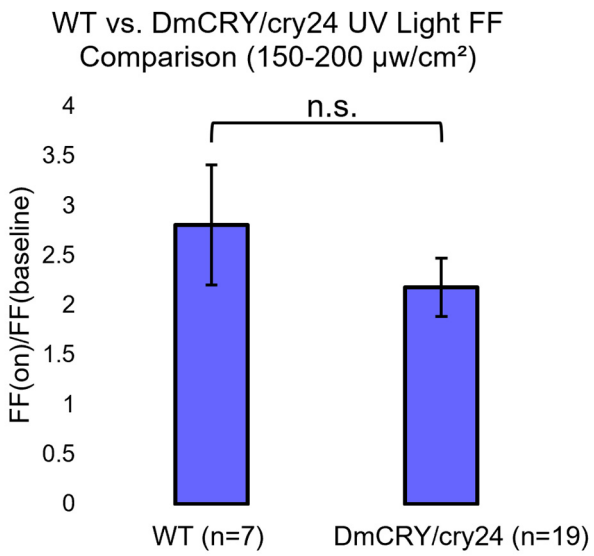

Figure 2-8. UV (365 nm) light-evoked excitation FF between non-UAS/GAL4 Wild-Type l-LNvs and DmCRY rescue Wild-Type are not significantly different

Wild-Type (left, w;*pdfGAL4*-p12c;+, n=7) vs *crypGAL4-24* driven UAS-DmCRY-eGFP (right, n=19) FF response to 5 seconds of UV (365 nm, 150-200 µW/cm²) light stimulus. Data are represented as mean ± SEM. One significance symbol; $p \leq 0.05$, two significance symbols; $p \leq 0.005$, three significance symbols; $p \leq 0.001$.

DmCRY expression driven by the *crypGAL4-24* driver mediates robust and significant increases in FF in the l-LNvs in response to 200 µW/cm² UV light relative to *cry-null* (blue column, Figure 2-9A). DmCRY expression restricted to LNvs also mediates robust and significant increases in FF in the l-LNvs in response to 200 µW/cm² UV light relative to *cry-null* (light blue column, Figure 2-9A). AeCRY1 expression restricted to LNvs mediates little or no change in firing in response to 200 µW/cm² UV light (light orange column, Figure 2-9A) and appears nearly identical to the lack of light response under these conditions to *cry-null* (grey column, Figure 2-9A). Light responses from *crypGAL4-24* driven DmCRY, AeCRY1, and AgCRY1 are significantly greater than *pdfGAL4* driven AeCRY1 (Figure 2-9A). AeCRY1 expressed in all CRY neurons, however, does show a significant light evoked response compared to *cry-null* in response

to 200 μW/cm² UV light (orange column, Figure 2-9A), perhaps due to a compounding effect of CRY1 photoactivation in other clock neurons. In contrast, AgCRY1 expression restricted to LNvs mediates significant increases in firing in response to 200 μW/cm² UV light (light purple column, Figure 2-9A) relative to *cry-null*, but significantly less than the 200 μW/cm² UV light response measured from transgenics that express DmCRY and AgCRY1 driven in all CRY expressing neurons (blue and purple columns, respectively, Figure 2-9A). Comparing the FF ratio during stimulus and several 10-second bins post-stimulus along with their evoked potential profiles (Figure 2-9E, F, G), *crypGAL4-24* driven DmCRY and *pdfGAL4* driven AgCRY1 show a sustained response to UV light (Figure 2-9B, D, E, G), whereas *pdfGAL4* driven DmCRY, *pdfGAL4* and *crypGAL4-24* driven AeCRY1, and *crypGAL4-24* driven AgCRY1 rapidly return to baseline after stimulus (Figure 2-9C, D, F).

The FF ratio for *crypGAL4-24* driven DmCRY is significantly higher than *pdfGAL4* driven DmCRY and *cry-null* up to the 10 second post-stimulus bin (Figure 2-9B). *crypGAL4-24* driven AeCRY1 UV light evoked FF is significantly higher than *pdfGAL4* driven AeCRY1 UV light evoked FF during stimulus and at the 30 second post-stimulus bin, but after FDR adjustment, only shows significance during stimulus (Figure 2-9C). Both *crypGAL4-24* driven AgCRY1 UV light evoked FF and *pdfGAL4* driven AgCRY1 UV light evoked FF are significantly greater than *cry-null* but not relative to each other (Figure 2-9D). Recordings from l-LNvs expressing DmCRY using the *pdfGAL4* or *crypGAL4-24* driver show significantly greater UV light evoked potentials relative to the *cry-null* negative control. The *pdfGAL4* driven DmCRY membrane potential response rapidly returns to baseline after stimulus, while the *crypGAL4-24* driven DmCRY response sustains for approximately 30-40 seconds post-stimulus and remains significant compared to the *cry-null* and the *pdfGAL4* driven DmCRY responses (Figure 2-9E). Both the

pdfGAL4 and *crypGAL4-24* driven AeCRY1 membrane potential UV light responses rapidly return to baseline, but the *crypGAL4-24* driven AeCRY1 shows a greater and slightly more sustained (2 seconds longer) response compared to the *pdfGAL4* driven response (Figure 2-9F). AgCRY1 generates sustained depolarized light responses when expressed by the *pdfGAL4* driver line and a sustained and more rapid response when expressed in all CRY neurons (light purple and purple traces, respectively, Figure 2-9G) as compared to *cry-null* evoked responses (grey trace, Figure 2-9E). AgCRY1 mediates cell-autonomous light responses in the LNvs, while AeCRY1 does not. The sustained AgCRY1 evoked response is another feature of its greater light sensitivity than AeCRY1 (Figure 2-9F, G). All CRYs tested exhibit higher magnitude and more sustained light evoked potentials when expressed broadly using the *crypGAL4-24* driver relative to LNv restricted expression by the *pdfGAL4* driver. Representative 1-minute l-LNv patch clamp voltage traces are shown in Figure 2-10 and 2-11.

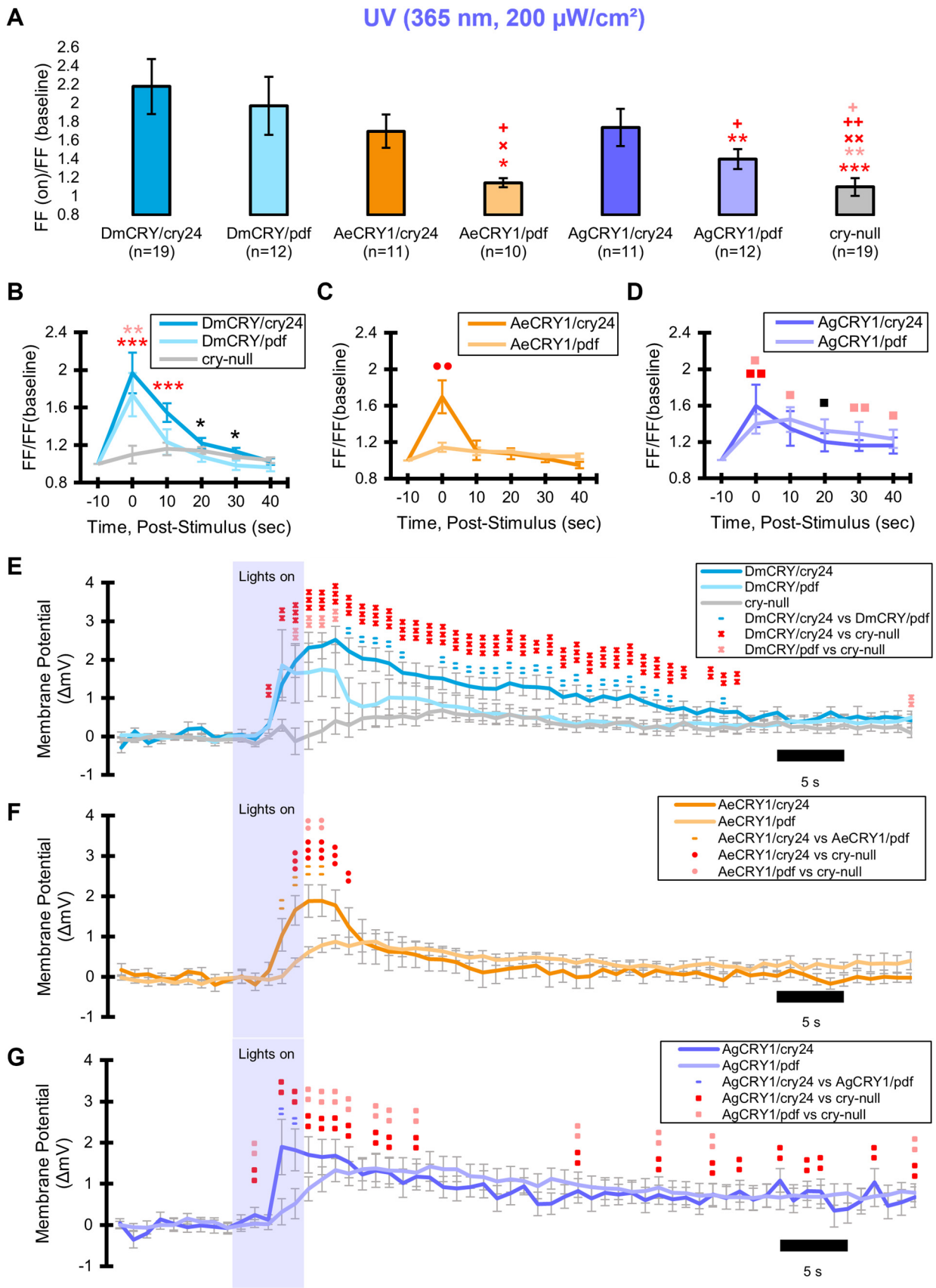
A
UV (365 nm, 200 µW/cm²)
FF (on)/FF (baseline)
DmCRY/cry24 (n=19)
DmCRY/pdf (n=12)
AeCRY1/cry24 (n=11)
AeCRY1/pdf (n=10)
AgCRY1/cry24 (n=11)
AgCRY1/pdf (n=12)
cry-null (n=19)
B
DmCRY/cry24
DmCRY/pdf
cry-null
FF/FF(baseline)
Time, Post-Stimulus (sec)
C
AeCRY1/cry24
AeCRY1/pdf
FF/FF(baseline)
Time, Post-Stimulus (sec)
D
AgCRY1/cry24
AgCRY1/pdf
FF/FF(baseline)
Time, Post-Stimulus (sec)
E
Lights on
Membrane Potential (ΔmV)
DmCRY/cry24
DmCRY/pdf
cry-null
DmCRY/cry24 vs DmCRY/pdf
DmCRY/cry24 vs cry-null
DmCRY/pdf vs cry-null
5 s
F
Lights on
Membrane Potential (ΔmV)
AeCRY1/cry24
AeCRY1/pdf
AeCRY1/cry24 vs AeCRY1/pdf
AeCRY1/cry24 vs cry-null
AeCRY1/pdf vs cry-null
5 s
G
Lights on
Membrane Potential (ΔmV)
AgCRY1/cry24
AgCRY1/pdf
AgCRY1/cry24 vs AgCRY1/pdf
AgCRY1/cry24 vs cry-null
AgCRY1/pdf vs cry-null
5 s

Figure 2-9. AeCRY1 and AgCRY1 mediate electrophysiological responses to short-wavelength UV light

Light-evoked **(A)** FF ratio, **(B-D)** post-stimulus FF, and **(E-G)** membrane potential responses to UV light stimulus (5 seconds, 365 nm, 200 μW/cm²) of l-LNvs expressing: **(A, B, E)** DmCRY (blue, *crypGAL4-24* (n=19); light blue, *pdfGAL4* (n=12); grey, *cry-null* (n=19)), **(A, C, F)** AeCRY1 (orange, *crypGAL4-24* (n=11); light orange, *pdfGAL4* (n=10)), and **(A, D, G)** AgCRY1 (purple, *crypGAL4-24* (n=8); light purple, *pdfGAL4* (n=9)) driven by *crypGAL4-24* versus *pdfGAL4* drivers over a *cry-null* background. **(E-G)** Purple bar on membrane potential plots indicates the timing of the 5 seconds of UV-light stimuli and black scale-bar indicates 5 seconds. Traces represent the average last 60 seconds of each recording. **(A)** Red * indicates FDR adjusted $p \leq 0.1$ compared to DmCRY/cry24. Red x indicates FDR adjusted $p \leq 0.1$ compared against AeCRY1/cry24. Red + indicates FDR adjusted $p \leq 0.1$ compared to AgCRY1/cry24. Light red * indicates FDR adjusted $p \leq 0.1$ compared to DmCRY/pdf. Light red + indicates FDR adjusted $p \leq 0.1$ compared to AgCRY1/pdf. **(B-G)**: Black * indicates $p \leq 0.05$ between DmCRY/cry24 and *cry-null*. Black ■ indicates $p \leq 0.05$ between AgCRY1/cry24 and *cry-null*. Red * indicates FDR adjusted $p \leq 0.1$ between DmCRY/cry24 and *cry-null*. Red ■ indicates FDR adjusted $p \leq 0.1$ between AgCRY1/cry24 and *cry-null*. Red ● indicates FDR adjusted $p \leq 0.1$ between AeCRY1/cry24 and *cry-null*. Light red * indicates FDR adjusted $p \leq 0.1$ between DmCRY/pdf and *cry-null*. Light red ■ indicates FDR adjusted $p \leq 0.1$ between AgCRY1/pdf and *cry-null*. Light red ● indicates FDR adjusted $p \leq 0.1$ between AeCRY1/pdf and *cry-null*. Blue - indicates FDR adjusted $p \leq 0.1$ between DmCRY/cry24 and DmCRY/pdf. Orange - indicates FDR adjusted $p \leq 0.1$ between AeCRY1/cry24 and AeCRY1/pdf. Purple - indicates FDR adjusted $p \leq 0.1$ between AgCRY1/cry24 and AgCRY1/pdf. Data are represented as mean ± SEM. For black significance symbols: One symbol; $p \leq 0.05$, two symbols; $p \leq 0.005$, three symbols; $p \leq 0.001$. For colored significance symbols: One symbol; $p \leq 0.1$, two symbols; $p \leq 0.05$, three symbols; $p \leq 0.01$.

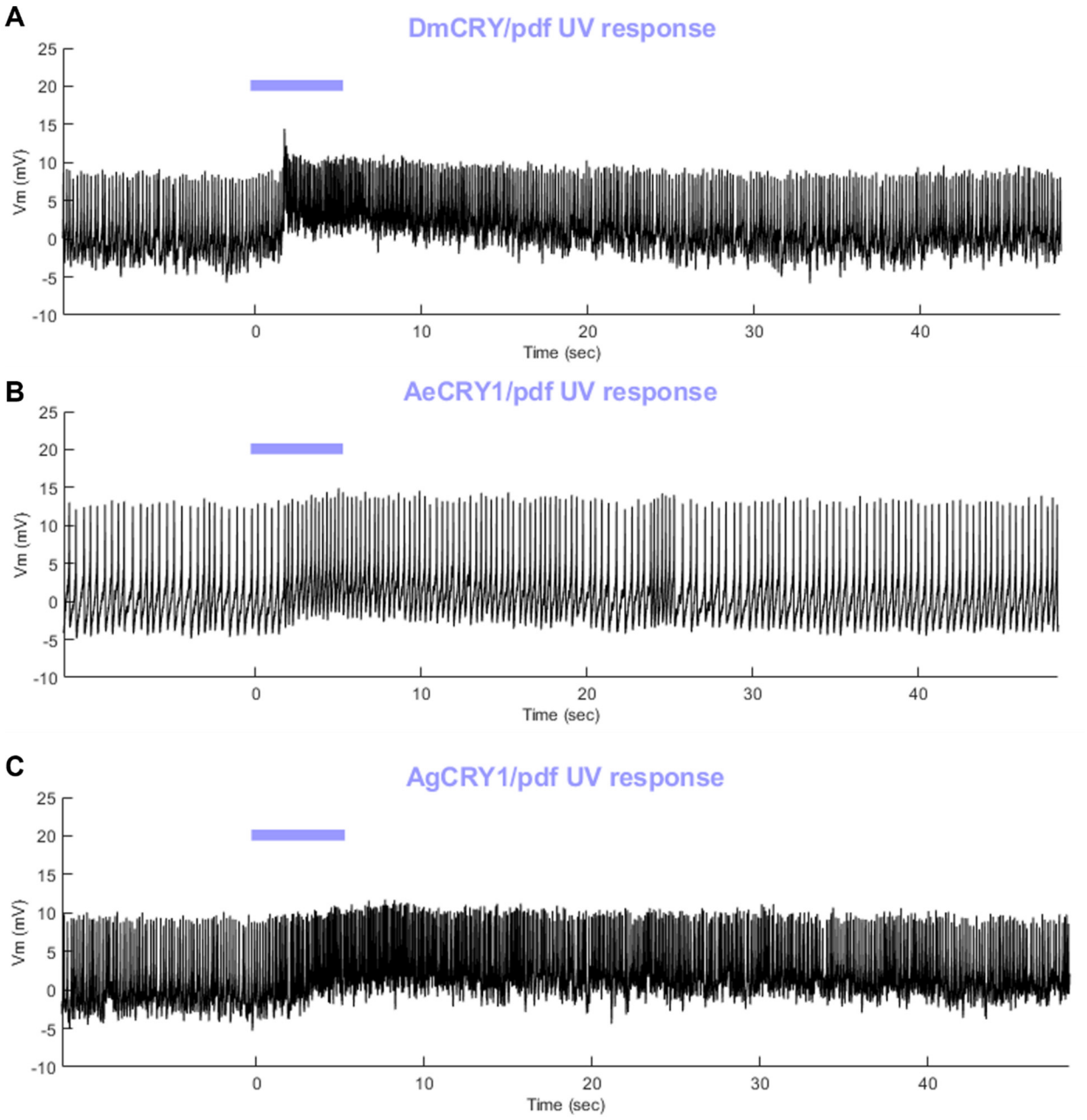

Figure 2-10. Representative voltage traces of l-LNvs electrophysiological response to UV light stimuli shows distinct differences in spike firing and membrane depolarization for all pdfGAL4 driver genotypes

Representative voltage traces of the last 60 seconds of a patch-clamp recording of l-LNvs subjected to 5 seconds of UV light stimuli for **(A)** DmCRY/pdf, **(B)** AeCRY1/pdf, and **(C)** AgCRY1/pdf. Purple bar indicates 5 seconds of 200 µW/cm² UV light stimulus.

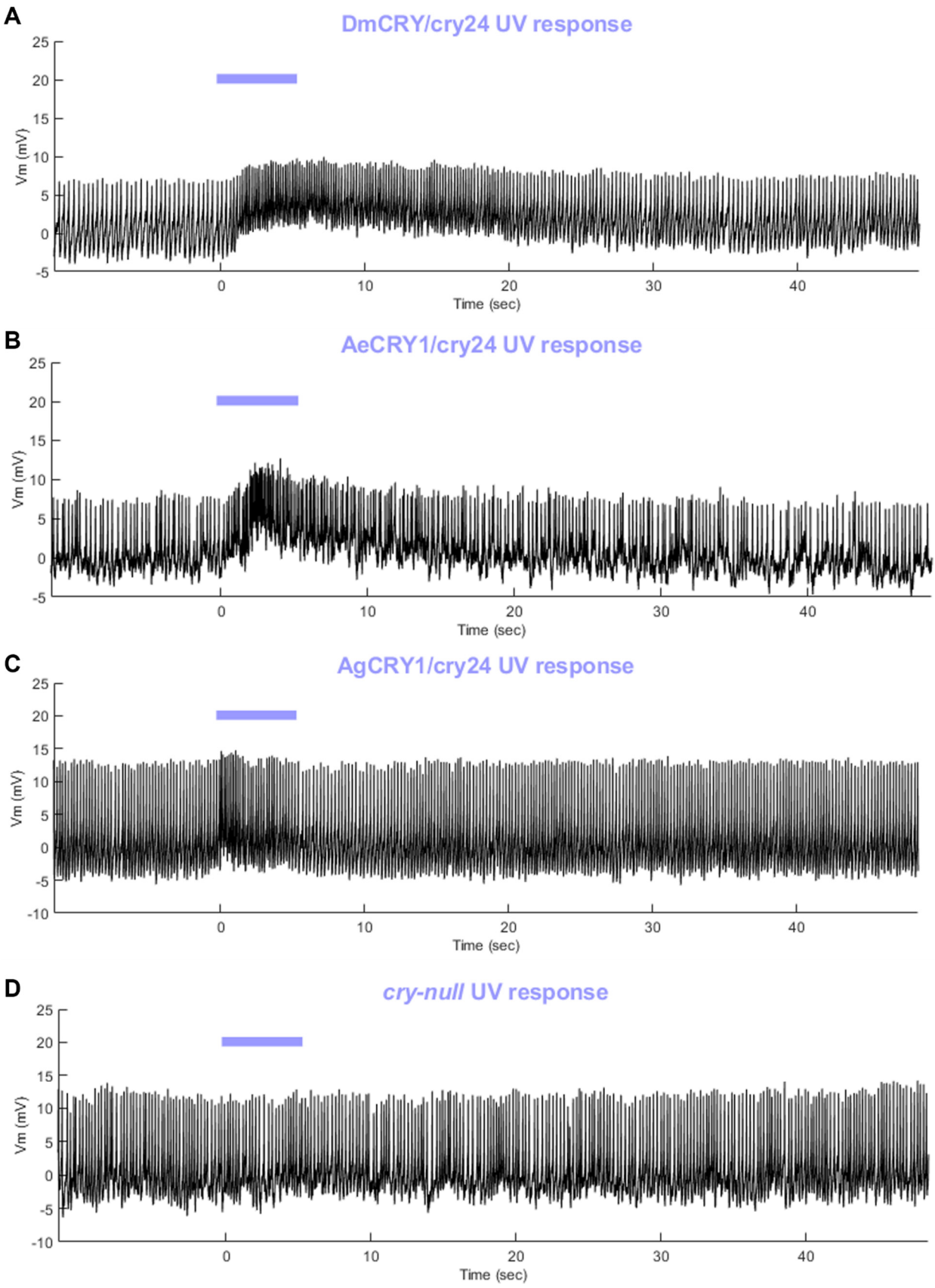
A
DmCRY/cry24 UV response
Vm (mV)
Time (sec)
B
AeCRY1/cry24 UV response
Vm (mV)
Time (sec)
C
AgCRY1/cry24 UV response
Vm (mV)
Time (sec)
D
cry-null UV response
Vm (mV)
Time (sec)

Figure 2-11. Representative voltage traces of l-LNvs electrophysiological response to UV light stimuli shows distinct differences in spike firing and membrane depolarization for all genotypes

Representative voltage traces of the last 60 seconds of a patch-clamp recording of l-LNvs subjected to 5 seconds of UV light stimuli for **(A)** DmCRY/cry24, **(B)** AeCRY1/cry24, **(C)** AgCRY1/cry24, and **(D)** *cry-null* flies. Purple bar indicates 5 seconds of 200 μW/cm² UV light stimulus.

Insects exhibit species-specific light attraction/avoidance behavioral responses over the spectral range between ultraviolet to red [3,8,10,19,26,31,57–61]. Spectral absorption analysis of *in vitro* purified DmCRY in the FAD oxidized and FAD•- anionic semiquinone states exhibit peaks around 365 and 450 nm that correspond to UV and blue [37,62–64]. However, we recently demonstrated in *ex vivo* patch clamp recordings that DmCRY mediates electrophysiological responses to red light (635 nm) that are absent in recordings made from the brains of *cry-null* flies and wild type flies treated with the redox sensitive flavin specific inhibitor diphenyleneiodonium (DPI) [3]. These results suggest that *in situ* DmCRY in its native neuronal environment expresses the further reduced FADH• neutral semiquinone state that exhibits red light absorption and biological activity[39]. Diurnal *Ae. aegypti* female mosquitoes show no differences between UV, blue or red-light attraction behavior during the day, while nocturnal *An. coluzzii* female mosquitoes strongly avoid UV and blue light, but are significantly attracted to red light during the day [19]. *Ae. aegypti* mosquitoes also exhibit strong attraction and image discrimination towards red-colored objects as part of their image-forming vision for prey detection [26]. To test the hypothesis that nocturnal AgCRY1 is red light responsive, but diurnal AeCRY1 is not, we expressed AgCRY1, AeCRY1 and DmCRY using the *crypGAL4-24* driver, along with *cry-null* controls and measured the electrophysiological changes of l-LNvs in response to 200 μW/cm² red light stimulation for all genotypes. Red light evokes significant increases in firing rate in flies expressing AgCRY1 and

flies expressing DmCRY relative to *cry-null* (Figure 2-12A). In contrast, AeCRY1 lacks a red light FF electrophysiological response and is significantly lower relative to AgCRY1 (Figure 2-12A, C). The red light evoked potential response of DmCRY is robust, with a sharp spike in membrane potential at the onset of light that lasts 10 seconds that returns to baseline rapidly (Figure 2-12). Negative control *cry-null* flies completely lack a red light response (Figure 2-12A, B, D). Comparing the FF ratio during stimulus and several 10-second bins post-stimulus along with red light evoked potentials, we observed a rapid decay (<10 seconds) back to baseline for red light with DmCRY and AgCRY1 flies, and a lack of sustained response for AeCRY1 and *cry-null* flies (Figure 2-12B-E). These results confirm and extend findings showing that insect CRY1s *in situ* are capable of biological responses to red light. Representative 1-minute l-LNv patch clamp voltage traces are shown in Figure 2-13. Blue and UV light pulses evoking long duration l-LNvs depolarization mediated by DmCRY are associated with behavioral photoavoidance of UV light in flies and nocturnal mosquitoes, while the much shorter duration red light evoked depolarization mediated by AgCRY1 may code for behavioral phototaxis in *Anopheline* mosquitoes[19].

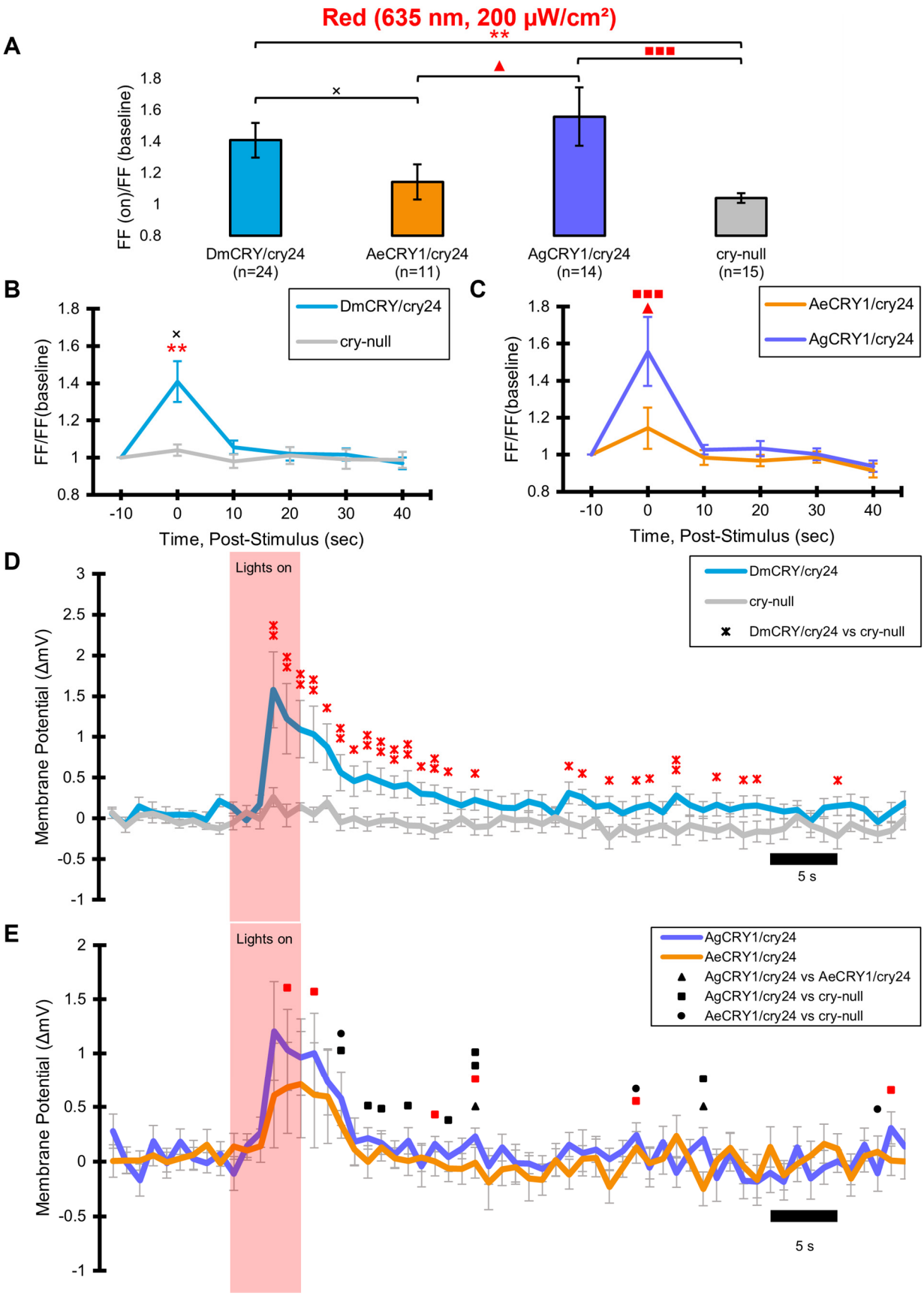
Red (635 nm, 200 μW/cm²)
A
FF (on)/FF (baseline)
DmCRY/cry24 (n=24)
AeCRY1/cry24 (n=11)
AgCRY1/cry24 (n=14)
cry-null (n=15)
B
DmCRY/cry24
cry-null
FF/FF(baseline)
Time, Post-Stimulus (sec)
C
AeCRY1/cry24
AgCRY1/cry24
FF/FF(baseline)
Time, Post-Stimulus (sec)
D
Lights on
DmCRY/cry24
cry-null
DmCRY/cry24 vs cry-null
Membrane Potential (ΔmV)
5 s
E
Lights on
AgCRY1/cry24
AeCRY1/cry24
AgCRY1/cry24 vs AeCRY1/cry24
AgCRY1/cry24 vs cry-null
AeCRY1/cry24 vs cry-null
Membrane Potential (ΔmV)
5 s

Figure 2-12. AgCRY1 elicits a strong and robust red-light response, while AeCRY1 does not

Light-evoked **(A)** FF ratio, **(B, C)** post-stimulus FF, and **(D, E)** membrane potential comparison of red-light (635 nm, 200 μW/cm²) excited l-LNvs expressing: **(A, B, D)** DmCRY (blue, n=24) and negative control *cry-null* (grey, n=15), **(A, C, E)** AeCRY1 (orange, n=11) and AgCRY1 (purple, n=14). **(D, E)** Red bar on membrane potential plots indicates the timing of the 5 seconds of red-light stimuli and black scale-bar indicates 5 seconds. Traces represent the average last 60 seconds of each recording. **(A-E)** Black **x** indicates $p \leq 0.05$ between AeCRY1/cry24 and DmCRY/cry24. Black ▲ indicates $p \leq 0.05$ between AgCRY1/cry24 and AeCRY1/cry24. Black ■ indicates $p \leq 0.05$ between AgCRY1/cry24 and *cry-null*. Black ● indicates $p \leq 0.05$ between AeCRY1/cry24 and *cry-null*. Red * indicates FDR adjusted $p \leq 0.1$ between DmCRY/cry24 and *cry-null*. Red ▲ indicates FDR adjusted $p \leq 0.1$ between AgCRY1/cry24 and AeCRY1/cry24. Red ■ indicates FDR adjusted $p \leq 0.1$ between AgCRY1/cry24 and *cry-null*. Data are represented as mean ± SEM. For black significance symbols: One symbol; $p \leq 0.05$, two symbols; $p \leq 0.005$, three symbols; $p \leq 0.001$. For colored significance symbols: One symbol; $p \leq 0.1$, two symbols; $p \leq 0.05$, three symbols; $p \leq 0.01$.

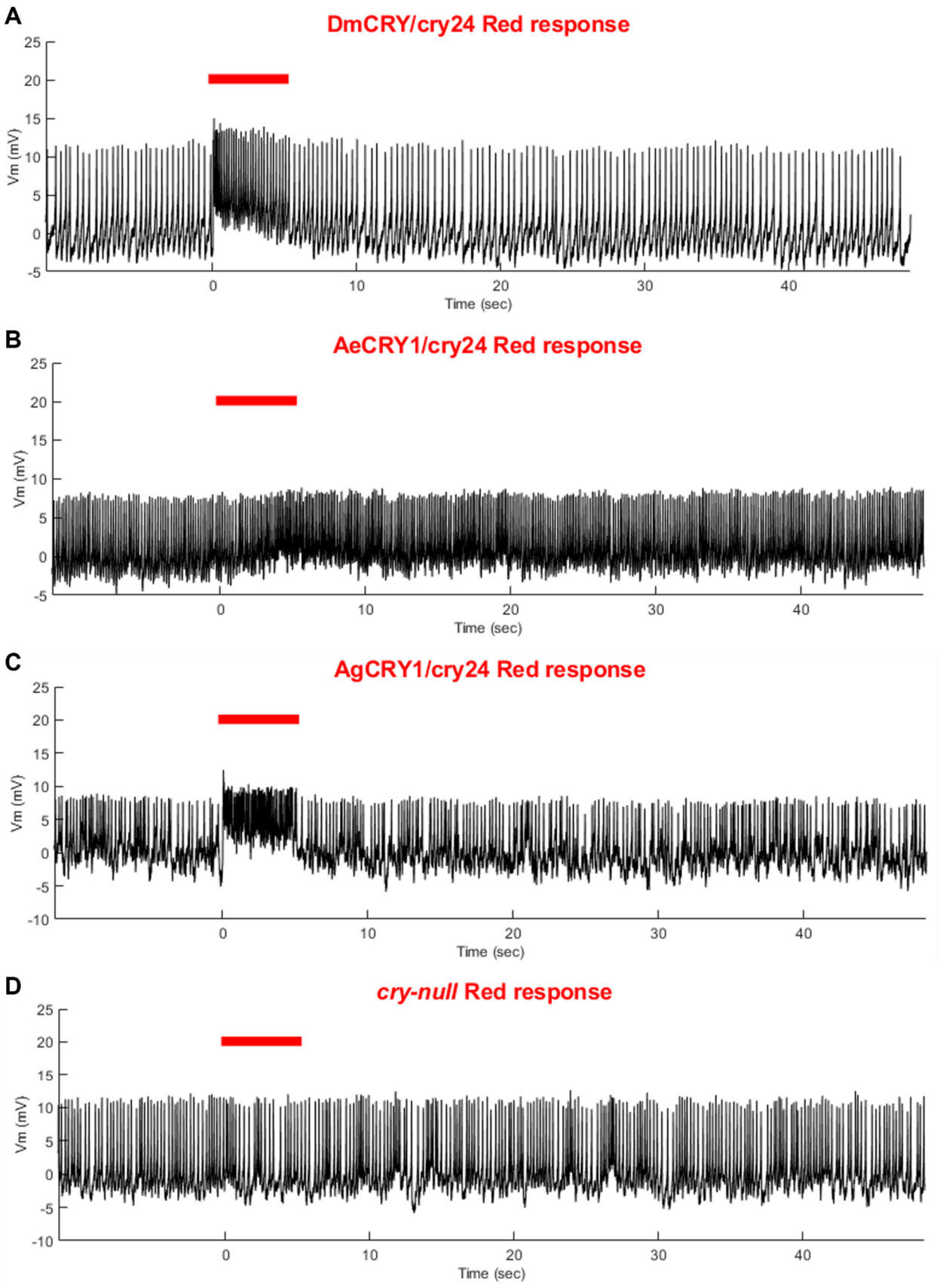
A
DmCRY/cry24 Red response
B
AeCRY1/cry24 Red response
C
AgCRY1/cry24 Red response
D
cry-null Red response
Vm (mV)
Time (sec)

Figure 2-13. Representative voltage traces show of l-LNvs electrophysiological response to red light stimuli shows distinct differences in spike firing and membrane depolarization for all genotypes

Representative voltage traces of the last 60 seconds of a patch-clamp recording of l-LNvs subjected to 5 seconds of red light stimuli for **(A)** DmCRY/cry24, **(B)** AeCRY1/cry24, **(C)** AgCRY1/cry24, and **(D)** *cry-null* flies. Red bar indicates 5 seconds of 200 μW/cm² red light stimulus.

2.3.4 Mosquito CRY1s confer species-specific and intensity-dependent behavioral attraction/avoidance to UV light

Night-active mosquitoes exhibit strong daytime behavioral avoidance of UV light, while diurnal mosquitoes exhibit strong daytime attraction to UV light [19]. To explore CRY1's potential role for conferring day- versus night-active mosquito species-specific light choice behaviors, we performed a UV light choice behavioral assay with flies expressing DmCRY, AgCRY1, AeCRY1 under the *crypGAL4-24* promoter at three different light intensities. At very low intensity 365 nm UV light (1 μW/cm²) during the first 30 minutes of environmental light choice preference, all fly groups show no differences between the genotypes and are attracted to the very low intensity UV light exposed side (Figure 2-14A). At moderately low-intensity UV light (10 μW/cm²), the genotypes begin to diverge: DmCRY and diurnal AeCRY1 expressing flies still prefer the light exposed side and do not differ between each other (Figure 2-14B), but the nocturnal AgCRY1 exhibit significant light avoidance to the moderately low-intensity UV light exposed environment, with approximately 50-60% of flies being in the shaded environment during daytime hours (Figure 2-14B). At high-intensity UV light (400 μW/cm²), AgCRY1 flies increase avoidance to the UV exposed environment and DmCRY flies shift to exhibit light avoidance behaviors (Figure 2-14C). However, the AeCRY1 flies remain significantly attracted to the high intensity UV light environment (Figure 2-14C). These results show a sensitivity threshold for UV light avoidance

response for AgCRY1 flies at 10 μW/cm², compared to the 400 μW/cm² threshold for the UV light avoidance response for DmCRY flies as reported previously [8–10]. These results are not due to differences in the number of LNvs in the brain that express CRY or TIM (Figure 2-4). We integrated all mean activity starting at lights on through 30 minutes, then compared these summed mean activities with paired t-tests and represent the results as additional bar graphs in D, E, F in Figure 2-14, showing significant differences between AgCRY1 and AeCRY1 expressing flies at all light intensities tested. The UV light intensity dependent divergence between AeCRY1 and AgCRY1 expressing flies for the light attraction/avoidance assay is highly consistent with the behavioral results of the same assay testing diurnal and nocturnal mosquitoes and further supports our claim that CRY photoreceptors mediate species-specific physiological and behavioral light responses.

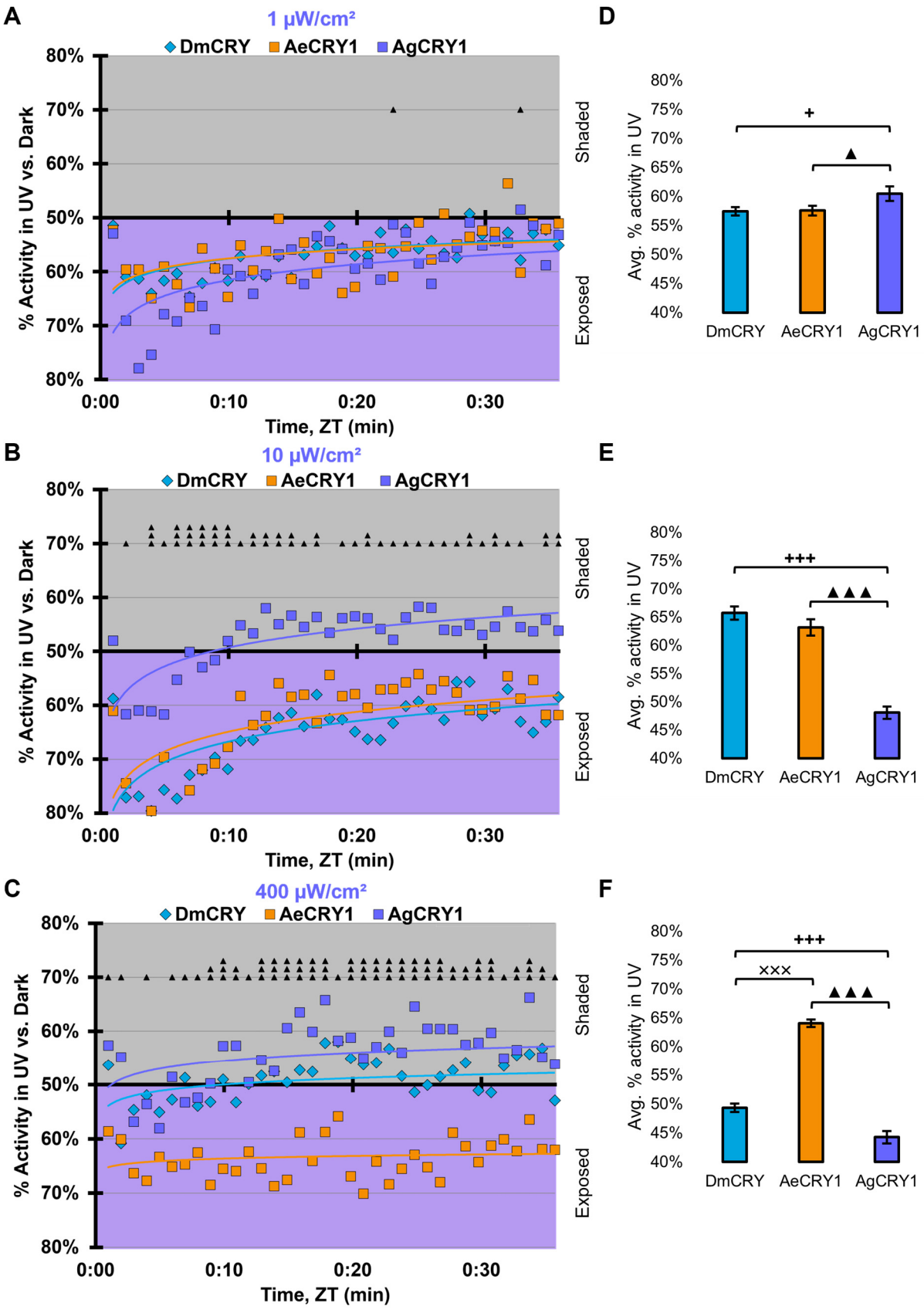
A
1 µW/cm²
DmCRY
AeCRY1
AgCRY1
% Activity in UV vs. Dark
Shaded
Exposed
Time, ZT (min)
B
10 µW/cm²
C
400 µW/cm²
D
E
F
Avg. % activity in UV
+
▲
+++
▲▲▲
×××

Figure 2-14. Mosquito CRY1s confer species-specific and intensity-dependent behavioral attraction and avoidance to UV light

(A-C) UV attraction/avoidance behavior is measured by % activity in a dark shaded environment versus **(A)** very low-intensity (1 μW/cm²), **(B)** moderately low-intensity (10 μW/cm²), and **(C)** high-intensity (400 μW/cm²) UV-exposed environments (365 nm) during the light phase of a standard 12:12 hr LD cycle. Preference is calculated by percentage of activity in each environment over total activity for each time bin. **(A)** DmCRY (blue, n=76) vs. diurnal AeCRY1 (orange, n=65) vs. nocturnal AgCRY1 (purple, n=65) expressing flies show a strong attraction to very low-intensity (1 μW/cm²) UV light in the first 30 minutes of UV light exposure. **(B)** Daytime-active DmCRY (blue, n=76) and AeCRY1 (orange, n=76) flies show a maintained, slightly stronger attraction to low-intensity (10 μW/cm²) UV light in the first 30 minutes of UV light exposure, whereas nocturnal AgCRY1 (purple, n=78) expressing flies show a fast, strong negative phototaxis after a few minutes of UV light exposure. **(C)** DmCRY (blue, n=73) and AgCRY1 (purple, n=72) expressing flies show a strong and very fast negative phototaxis to high-intensity (400 μW/cm²) UV light in the first couple minutes of UV light exposure, whereas diurnal AeCRY1 (orange, n=63) remain strongly attracted to the UV environment. All plots are shown from ZT 0-30 min in 1-min bins. **(D-F)** Quantified mean % activity of flies in UV environment across the first 30 minutes for **(D)** very low-intensity, **(E)** moderately low-intensity, and **(F)** high-intensity UV light environments. Black + indicates $p \leq 0.05$ between AgCRY1/cry24 and DmCRY/cry24. Black **x** indicates $p \leq 0.05$ between AeCRY1/cry24 and DmCRY/cry24. Black ▲ indicates $p \leq 0.05$ between AgCRY1/cry24 and AeCRY1/cry24. Data are represented as mean ± SEM. One significance symbol; $p \leq 0.05$, two significance symbols; $p \leq 0.005$, three significance symbols; $p \leq 0.001$.

2.4 Discussion

These findings highlight CRY as a strong species-specific behavioral regulator of behavioral light responses shown by a wide range of physiological and behavioral assays. *Drosophila* CRY- and diurnal/nocturnal mosquito CRY1- mediated behavioral light responses and electrophysiological responses provide strong support for the idea that CRY mediates light responses by species-specific mechanisms. Species-specific behaviors have evolved to optimize inter-species survival by time-of-day specific feeding, mating, and predatory avoidance behaviors. *Ae. aegypti* and *An. gambiae* mosquitoes are active at 12 hr opposing times of the day [19]. *Ae. aegypti* are diurnal and are aggressive daytime biters, while nocturnal *An. gambiae* are less aggressive and prefer to feed on defenseless prey that sleep during the night. *Ae. aegypti*

mosquitoes are attracted to a wide range of light spectra during the daytime, while *An. gambiae* mosquitoes specifically avoid short-wavelength light during the day but exhibit daytime attraction to red light. We conclude that CRY1 from nocturnal *An. gambiae* exhibits greater light sensitivity than CRY1 from diurnal *Ae. aegypti*, and that these functional differences contribute to their distinct species-specific light responses.

Reprinted with permission from:

Au, D. D. *et al.* Mosquito cryptochromes expressed in Drosophila confer species-specific behavioral light responses. *Curr. Biol.* S0960982222011228 (2022) doi:10.1016/j.cub.2022.07.021.

CHAPTER 3: Nocturnal mosquito Cryptochrome1 mediates greater electrophysiological and behavioral responses to blue light relative to diurnal mosquito Cryptochrome1

3.1 Introduction

Many insect behaviors are modulated by short wavelength light [26,36,65–74]. It has been long assumed that insect behavioral light responses rely on image forming vision through eye photoreceptors that express opsins. However, insects additionally have non-image forming vision mediated by photoreceptors that are expressed directly in brain neurons [1,2].

Insect non-imaging forming visual photoreceptors include ultraviolet, blue, and red-light activated Cryptochrome (CRY) that was first characterized as the primary circadian photoreceptor in *Drosophila* [11,12] and violet-light activated Rhodopsin 7 (Rh7 [2]). Rh7 is an opsin photoreceptor expressed in central brain neurons that couples to G protein signaling pathways and also regulates light-evoked circadian photo-attraction/avoidance behaviors [2,9,75,76]. CRY is a riboflavin-based photoreceptor protein that uses flavin adenine dinucleotide (FAD) as its light sensing chromophore. In *Drosophila*, CRY is expressed in roughly half of all circadian neurons [1,13,40,41,77,78], which include all of the Pigment Dispersing Factor (PDF) expressing ventral lateral neurons (LNvs) that also mediate light-evoked behavioral arousal [6,13–15,79–84]. While *Drosophila* only express light sensitive "type 1" CRYs, other insects also express light insensitive "type 2" CRYs similar to CRYs expressed in vertebrates that function as transcriptional repressors [1,56,85,86]. The best characterized function of CRYs in insects is the light activated initiation of the slow (~1 hr) and irreversible process of circadian clock resetting that has been well characterized by molecular genetic analysis in *Drosophila*. This mechanism occurs by CRY mediated light

activated protein degradation of the heteromultimeric clock protein complex consisting of TIMELESS (TIM), PERIOD (PER) and CRY itself, thus relieving repression of the transcriptional activators CLOCK and CYCLE at E-box promoter sequences upstream from the *tim* and *per* genes [11,12,45,86–88].

CRY photoactivation also evokes rapid and very long-lasting (30-40 sec) neuronal depolarization and increased spontaneous action potential firing in large ventral lateral neurons (l-LNvs) and other CRY expressing neurons [1,3,10,13,89–91]. While light-evoked CRY mediated electrophysiological effects are acute and reversible in contrast to CRY mediated clock resetting, CRY on/off electrophysiological kinetic light responses are not as rapid as those mediated by image-forming opsins. Light-activated CRY couples to electrophysiological depolarization and clock resetting through multiple mechanisms including photoreduction electron transfer events along a chain of CRY tryptophan residues in close proximity to the FAD chromophore and CRY protein conformational changes, including the C terminal tail [3,4,6,37,39,62–64,92–96]. In addition to circadian clock resetting, CRY phototransduction evokes acute behaviors in insects, including arousal [6,13] and short wavelength light attraction/avoidance behavior [8–10,19,91], which is under circadian modulation.

Light-activated CRY evoked behavioral changes are particularly interesting in mosquitoes as mosquito-spread diseases afflict hundreds of millions of people worldwide. Two medically important genera include nocturnal *Anopheline* and diurnal *Aedes* mosquitoes. *Anopheline* mosquitoes are responsible for over 200 million cases of malaria worldwide. *Aedes* mosquitoes are the principal vectors for Dengue virus (over 90 million cases worldwide) and yellow fever, West Nile fever, chikungunya fever, Zika fever, and Japanese encephalitis (WHO website fact

sheet). Insect control methods based on the sensory physiology of mosquitoes is very appealing as chemical pesticides are non-specific and environmentally harmful. The behavior of nocturnal *An. gambiae* (Ag) and diurnal *Ae. aegypti* (Ae) mosquitoes is subject to circadian regulation, thus enforcing their ecologically distinct temporal activity patterns [97,98]. Recently, we found that nocturnal *An. coluzzii* and diurnal *Ae. aegypti* mosquitoes display distinct innate circadian temporal attraction/avoidance behavioral responses to light. Nocturnal *Anopheles* mosquitoes behaviorally avoid short wavelength light during the day, while diurnal *Aedes*, particularly females, are behaviorally attracted to a broad range of light spectra during the day [19]. Attraction/avoidance behavioral responses to light for both species change with time-of-day and show distinct sex differences that are consistent with predation and mate swarming activities of females versus males. These distinct *Anopheles* and *Aedes* mosquito behavioral light responses appear to be mediated by light activated type 1 Cryptochrome signaling shown by disruption of these behaviors by prior exposure to constant light [19]. Further, attraction/avoidance behavioral responses to light are mediated by ventral lateral neurons that are characterized by PDF and PER proteins co-expressed in *Drosophila melanogaster* and other insect species. We recently showed that *Ae. aegypti* and *An. coluzzii* mosquito female adult brains also display characteristics of large- (l-LNvs) and small-ventral lateral neurons (s-LNvs) marked by PDF and PER co-expression with similar morphology and projection patterning [19]. Putative circadian dorsal neurons (DNs) are seen in both *Ae. aegypti* and *An. coluzzii* mosquito female adult brains, again identified by similar morphological projections in common with *Drosophila* [19]. Therefore, we employed an "empty-neuron" model approach using transgenic *Drosophila* on a *cry-null* background to express AgCRY1 and AeCRY1. In that paper we show mosquito CRY electrophysiological and behavioral responses to UV and red-light and find by multiple assays that nocturnal AgCRY1 is significantly

more light sensitive as compared with diurnal AeCRY1. In a previous study [91], we focused on those two light wavelengths because UV light is the most commonly used part of the light spectrum for insect control devices using light ("bug lights") to trap mosquitoes. We earlier characterized nocturnal and diurnal mosquito behavioral responses to UV light [19]. Red light is of interest because we found distinctly different nocturnal and diurnal mosquito behavioral responses to red light [19]. This followed our unexpected findings that insect CRYs functionally respond to red light [3], in contrast to the lack of response of purified insect CRYs to red light for *in vitro* biophysical assays. In addition to CRYs which show spectral absorbance peaks in their base oxidized states to 365 nm UV light and 450 nm blue light, another photoreceptor, Rhodopsin 7 (Rh7) is expressed in the LNv and other brain neurons [2,9,75]. Rh7 exhibits a comparatively broad spectral absorbance that peaks around 405 nm violet light. To compare the potential interactions between mosquito CRYs and Rh7, we tested AgCRY1 and AeCRY1 expressing transgenic flies for their responses to 450 nm blue light and 405 nm violet light.

3.2 Materials and Methods

3.2.1 Experimental Animals

Drosophila melanogaster flies were raised on standard media (yeast, cornmeal, agar) at 25±1 ºC and 40-60% relative humidity in 12:12 hr Light:Dark cycles. All flies used in experiments were first isogenized (backcrossed) to the w1118 genetic background for a minimum of six generations. All behavioral experiments used 3–4-day post-eclosion adult male flies. We generated pJFRC7 vectors containing cryptochrome 1 from *Drosophila melanogaster* (Dm), *An. gambiae*

(Ag) and *Ae. aegypti* (Ae) in frame with eGFP. Use of the pJFRC7 vector allows for a controlled site-specific PhiC31 genomic insertion site. DNA constructs were then sent to the vendor Bestgene for fly embryonic injection and screening for successful transgenesis. Experimental transgenic flies backcrossed to the common wild-type w1118 background for a minimum of 6 generations. Genotyping primers were designed with the following sequences: AeCRY1 Forward: CGA GAA AGT GCA GGC CAA CAA TC, AeCRY1 Reverse: GT TCT TCA ACT CCG GCA GAT ATC, AgCRY1 Forward: CAG CCA GTT CAA GTA TCC GG, and AgCRY1 Reverse: CGG TTC GTG CAC AAA CTG TG. Experimental transgenic flies were crossed with a *cry-null* background (obtained from Jeff Hall, Brandeis University), then with a *crypGAL4-24* driver line for CRY-neuron specific expression of DmCRY or mosquito CRY1.

3.2.2 Locomotor Activity Behavioral Assay

Adaptations to the behavioral assays from [42,43,99] were made for testing constant dark conditions for circadian behavior following 12h:12h light:dark entrainment (LD:DD) tested under two light intensities of l lux and 400 lux white light. Adult male flies (2-4 days post-eclosion) were anesthetized over CO2 and individually loaded into borosilicate activity tubes. The TriKinetics Locomotor Activity Monitoring System was used to track fly behavior over a protocol of: 12:12 hr Light:Dark (LD) entrainment for 7 days, then 7 days of constant dark (DD) conditions. Actograms were generated using Clocklab software. Average activity eduction graphs and its statistics were measured using FaasX software, then graphed using Microsoft Excel. Within FaasX, the CycleP analysis toolkit was used to calculate % rhythmicity from periodogram analysis with the following scoring criteria for flies in DD: minimum power ≥ 20, minimum width (h) ≥ 2, Chi-square significance ≥ 0.05 and calculation of tau. Data are reported as averages ± standard

error mean. Anticipation index measurements during LD were adapted for the entrainment duration from (Harrisingh et al., 2007; Sheeba et al., 2010) taking the average activity in the 3 hours preceding lights on (morning anticipation) or lights off (afternoon/evening anticipation) as a ratio over the average activity in the 6 hours preceding lights on or off for individual flies over 5 days of LD entrainment. The reported values for anticipation index are an average of all the flies over the 5 days of LD entrainment.

3.2.3 Immunocytochemistry

Experimental transgenic flies were dissected for *ex vivo* brain preparations after 3-5 days of 12:12 hr LD entrainment. Dissections began approximately 1 hour before each ZT time point measured (ZT5, 11, 17, 23). Immunocytochemistry (ICC) experiments were performed for all genotypes in a given experiment, then repeated a minimum of 3 times to optimize statistical analysis and minimize experimental error. Dissected brains were placed in chilled 1X PBS, fixed in 4% paraformaldehyde (PFA) for 30min, washed 3X 10min in PBS-Triton-X 1%, incubated in blocking buffer (10% Horse Serum-PBS-Triton-X 0.5%) at room temperature before incubation with rabbit α-TIM, polyclonal (1:1,000) antibodies overnight in 4°C. 3 rinse steps were performed at 10min intervals with PBS-Triton-X 0.5% then incubated in goat α-rabbit-Alexa- 594 (1:1,000) secondary antibodies in blocking buffer overnight in 4°C. Brains were then rinsed 5 times at 15min intervals in PBS-Triton-X 0.5% before mounting in Vectashield mounting media (Vector Laboratories). Sample slides were imaged using a Leica SP8 confocal microscope. We reproduced the TIM and CRY-GFP experiments published in Au et al., 2022, Current Biology and pooled the data with the earlier data for the results and updated total n's reported in Figure 3-5 and 3-6. The n's for the new data added to the earlier data are: for ZT 5: DmCRY: 7, AeCRY1: 4, AgCRY1: 9,

cry-null: 7; for ZT 11: DmCRY: 10, AeCRY1: 4, AgCRY1: 7, *cry-null*: 7; for ZT 17: DmCRY: 4, AeCRY1: 16, AgCRY1: 15, *cry-null*: 12; for ZT 23: DmCRY: 10, AeCRY1: 14, AgCRY1: 22, *cry-null*: 18.

3.2.4 Confocal Microscopy and Image Processing

For the data in Figures 3-5 and 3-6, brain samples were imaged with a Leica SP8 confocal microscope with 594 nm antibody fluorescence for TIM signal and 488 nm CRY-GFP signal. FIJI/ImageJ analysis software was utilized for quantification of ventral lateral neuronal. Maximum intensity projections were generated using the Z stack tool. Fluorescent quantification of TIM and CRY-GFP signal were obtained by marking regions-of-interest on LNv (small and large LNvs) soma identified by morphology and anatomical positioning within each brain sample. Fluorescent values for the total number of neurons in a brain are normalized to the background brain fluorescence, then measurements of all neurons from all brain samples are averaged together.

3.2.5 Light-Evoked Neuronal Electrophysiology

Previously established whole-cell current-clamp protocols from a previous study [3] were modified to run our light-evoked potential electrophysiology experiments. Adult male fly brains were dissected in external recording solution consisting of: 122mM NaCl, 3mM KCl, 1.8mM CaCl2, 0.8mM MgCl2, 5mM glucose, 10mM HEPES, 7.2 pH, and calibrated to an osmolarity of 250-255mOsm. The internal recording solution consists of: 102mM Kgluconate, 17mM NaCl, 0.085mM CaCl2, 1.7mM MgCl2 (hexahydrate), 8.5mM HEPES, 0.94mM EGTA, 7.2pH, and is calibrated to an osmolarity of 232-235mOsm. Custom multichannel LED source (Prizmatix/Stanford Photonics, Palo Alto, CA) fitted to the Olympus BX51 WI microscope was

used as the primary light source for our electrophysiology experiments. LED peak wavelengths are as follows: UV (365 nm), violet (405 nm), blue (450 nm), and red (635 nm), and all exposures were set to an intensity of 200 μW/cm² by use of a Newport 842-PE Power/Energy meter. Each LED was triggered on and off for each sweep with TTL pulses programmed by pClamp (Molecular Dynamics) data acquisition software. The light-evoked potential protocol is as follows: 50 seconds of dark for baseline recording, 5 seconds of colored-light stimulation, then 95 seconds of inter-pulse darkness for recovery back to baseline. The protocol repeats five times per recording. For analysis, sweeps are averaged, and baseline adjusted to pre-pulse signal, then low-pass noise filtered using Gaussian and Butterworth filters in the ClampFit 10 software (Molecular Dynamics). Our light-evoked potential protocol captures averaged light-evoked changes in membrane potential [1,3,91], thus providing a kinetically robust light-evoked potential.

3.2.6 Light Attraction/Avoidance Behavioral Assay

Standard LD light choice assays were conducted using behavioral protocols developed in previous studies [10,91]. The locomotor activity of individual flies was measured using the TriKinetics Locomotor Activity Monitoring System via dual infrared beam-crossing, recording total crosses in 1-min bins. Individual flies housed on glass tubes have a choice of exposure to a lighted side or in a dark side blocked by aluminum foil of the two infrared sensor tube. Percentage activity and statistics were measured using Microsoft Excel. Custom LED fixtures were built using Waveform Lighting blue and red LEDs with a narrow peak wavelength of 450 nm and 405 nm, respectively, and intensity-tuned to 10 μW/cm² and 400 μW/cm² for low and high intensity light exposures, respectively.

3.2.7 Quantification and Statistical Analysis

All reported values are represented as mean ± SEM. Values of n refer to the total number of experimental flies tested over all replicates of an experiment (minimum of three replicates). Firing frequency values are calculated as a ratio of spikes during the 5 seconds of lights on/average baseline firing rate binned in 10 second increments. Statistical tests were performed using Minitab, Matlab, and Microsoft Excel software. Statistical analysis began with performing an Anderson-Darling normality tests to determine normality of data. Variance was determined using F-tests for normally distributed data, then significance was determined using two-sample, one-tailed T-tests with alpha values of 0.5 before pairwise correction. Significance for non-normal data was determined by Mann-Whitney U-tests. Spike firing and membrane potential quantifications were performed using custom Matlab scripts and Clampfit software. Multi-comparison tests leading to Type I error/false positives were mitigated by a more stringent test of p-value adjustment based on false discovery rate (FDR [44,91]). A standard FDR threshold of 0.1 was then implemented in order to indicate significance as an expected proportion of false positives that is no greater than 10%.

3.3 Results

3.3.1 AgCRY1 and AeCRY1 expression is not sufficient to alter diurnal/nocturnal behavior or stop circadian rhythmicity

Diurnal *Aedes aegypti* (*Ae. aegypti*) and nocturnal *Anopheles gambiae* (*An. gambiae)* mosquitoes are anthropophilic mosquitoes that occupy opposite day/night temporal niches. To determine whether heterologous CRY1 expression might disrupt the circadian clock, we compared

circadian behavior in constant darkness (DD) in UAS-flies on a *cry-null* background expressing either *Drosophila* CRY (DmCRY), AeCRY1, AgCRY1 under the *crypGAL4-24* (drives expression in all cells that ordinarily express CRY [52]) versus negative control *cry-null* flies using two white light intensities of 1 lux and 400 lux. The expression of AgCRY1 is not sufficient to confer nocturnal activity at either 1 lux or 400 lux white light (Figure 3-1 and 3-4) in *Drosophila*, in contrast to the robust nocturnal behavior seen in Anopheles mosquitoes [19]. For low-intensity 1 lux LD entrainment, there are no significant differences in % rhythmicity between DmCRY, AeCRY1 and AgCRY1 expressing flies (Figure 3-1). In contrast, *cry-null* flies show significantly less % rhythmicity relative to DmCRY, AeCRY1 and AgCRY1 expressing flies (Figure 3-1). Similarly, at the higher-intensity 400 lux LD entrainment, there are no significant differences in % rhythmicity between DmCRY, AeCRY1 and AgCRY1 expressing flies, while again *cry-null* flies show significantly less % rhythmicity relative to DmCRY, AeCRY1 and AgCRY1 expressing flies (Figure 3-4). Thus, AgCRY1 nor AeCRY1 expression disrupts the circadian clock in *Drosophila*. Further analysis shows that AgCRY1 expressing flies show significantly longer period length (tau, τ) in constant darkness compared with DmCRY, AeCRY1 and *cry-null* following 1 lux and 400 lux light entrainment (Figure 3-2) and that *cry-null* flies show significantly shorter period length than DmCRY, AeCRY1 and AgCRY1 expressing flies following 1 lux and 400 lux light entrainment (Figure 3-2). Further, AgCRY1 expressing flies show significantly less morning anticipatory behavior and significantly greater evening anticipatory behavior compared with DmCRY, AeCRY1 and *cry-null* during 1 lux and 400 lux light entrainment (Figure 3-3). In an earlier paper, we also found that circadian clock function measured by free running behavior in constant darkness and morning anticipatory behavior are not well correlated [79]. Previous work from the Helfrich-Forster group concluded that eye photoreceptor inputs are primarily responsible

for modulating morning anticipation in the absence of a functional circadian clock [100]. However, the present results suggest that Cryptochromes may also modulate morning and evening anticipation, and perhaps this is not surprising that Cryptochromes from opposing temporal niches for diurnal versus nocturnal animals might drive differences in anticipatory behavior.

Upon photoactivation, DmCRY resets the circadian molecular clock by binding with the clock protein TIMELESS (TIM) and setting it for degradation [11,12,45]. The circadian clock cycles in anti-phase fashion comparing diurnal *Aedes* mosquitoes (PER levels in the s-LNv peak at ZT23) versus nocturnal *Anopheles* mosquitoes (PER levels in the s-LNv peak at ZT11 [19]). To determine if diurnal AeCRY1 or nocturnal AgCRY1 is sufficient to set the circadian clock to its peak timing of TIM protein expression, transgenic flies were entrained for at least 3 days of 12:12 hr Light: Dark (LD) and immunocytochemistry experiments were used to measure TIM levels at time points ZT5, ZT11, ZT17, and ZT23. Fluorescent TIM signals were quantified in the ventral lateral neuronal subgroup (LNvs) and showed peak signal at ZT23 and the lowest signals at ZT5 and ZT11 for control DmCRY, AeCRY1, and AgCRY1 expressing flies (Figures 3-5A-C). Negative control *cry-null* flies show a similar TIM expression pattern in the LNvs (Figure 3-5D). Fluorescent measurements of TIM signal during ZT17 are significantly different and are more than two-fold greater in flies expressing AeCRY1 than AgCRY1, suggesting diurnal AeCRY1 is less light sensitive than nocturnal AgCRY1. However, TIM signal at ZT5, ZT11, and ZT23 does not differ between AeCRY1 and AgCRY1 flies (summary of TIM measurements, Figure 3-5E). Transgenic expression of mosquito CRY1 in flies also includes N-terminal fusion of eGFP for protein expression verification. DmCRY expression measured by eGFP signal shows low expression during ZT5 and ZT11 with peak expression during ZT23 (Figure 3-6A). AeCRY1 expression is markedly higher than DmCRY, but exhibits a similar cycling pattern with ZT5 and

ZT11 showing the lowest protein levels, and ZT17 and ZT23 showing the highest protein levels (Figure 3-6B). AgCRY1 protein expression is consistently high during all time points (Figure 3-6C), but the levels are within an order of magnitude compared with DmCRY and AeCRY1 protein expression levels (summary of CRY-GFP measurements, Figure 3-6D). In summary, AeCRY1 and AgCRY1 expression in flies does not disrupt the circadian clock nor alter the timing of the TIM expression peak. Between genotype differences in absolute protein levels may be due to codon usage or differences in protein stability of different CRY proteins.

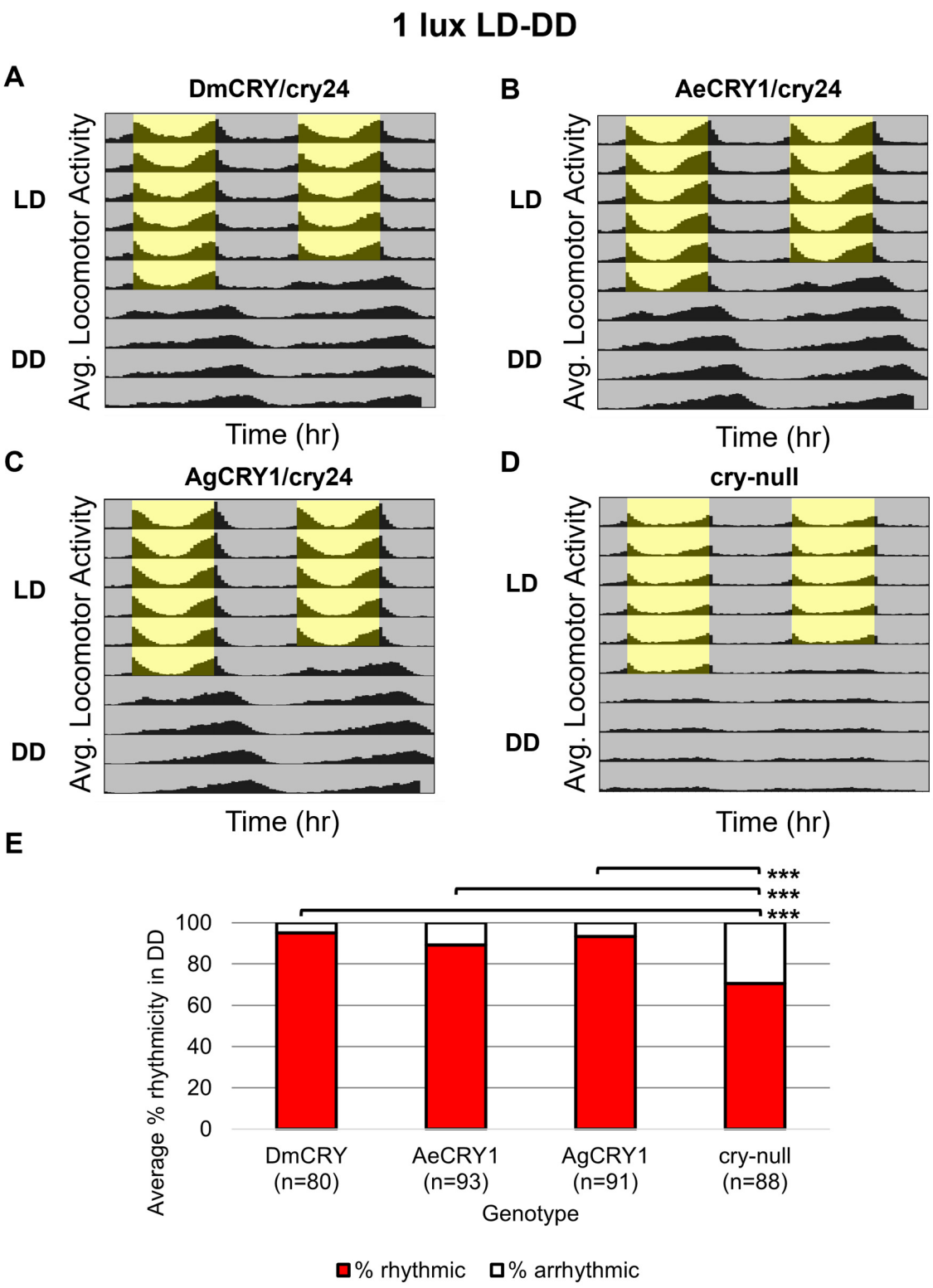
1 lux LD-DD
A
DmCRY/cry24
B
AeCRY1/cry24
C
AgCRY1/cry24
D
cry-null
LD
DD
Avg. Locomotor Activity
Time (hr)
E
***
***
***
Average % rhythmicity in DD
100
80
60
40
20
0
DmCRY
(n=80)
AeCRY1
(n=93)
AgCRY1
(n=91)
cry-null
(n=88)
Genotype
% rhythmic
% arrhythmic

Figure 3-1. AgCRY1, AeCRY1 expressing flies and control groups maintain high rhythmicity in constant dark conditions after entrainment in low 1 lux LD light

(A-D) Actogram plots containing 5 days of 12:12 hr LD entrainment in 1 lux white light conditions followed by 5 days of constant dark (DD) conditions for flies expressing: **(A)** DmCRY (n=80; $\tau_{avg,DD}\approx24.7$, $power_{avg,DD}\approx125.3$, $width_{avg,DD}\approx4.5$), **(B)** AeCRY1 (n=93; $\tau_{avg,DD}\approx24.8$, $power_{avg,DD}\approx150.6$, $width_{avg,DD}\approx5.0$), **(C)** AgCRY1 (n=91; $\tau_{avg,DD}\approx25.1$, $power_{avg,DD}\approx137.8$, $width_{avg,DD}\approx5.1$), **(D)** cry-null (n=88; $\tau_{avg,DD}\approx23.8$, $power_{avg,DD}\approx90.5$, $width_{avg,DD}\approx3.9$). **(E)** Quantification of fly rhythmicity (red) to arrhythmicity (white) in DD. Pairwise t-tests were used to determine significance: * $p \leq 0.1$, ** $p \leq 0.05$, ***$p \leq 0.01$**.**

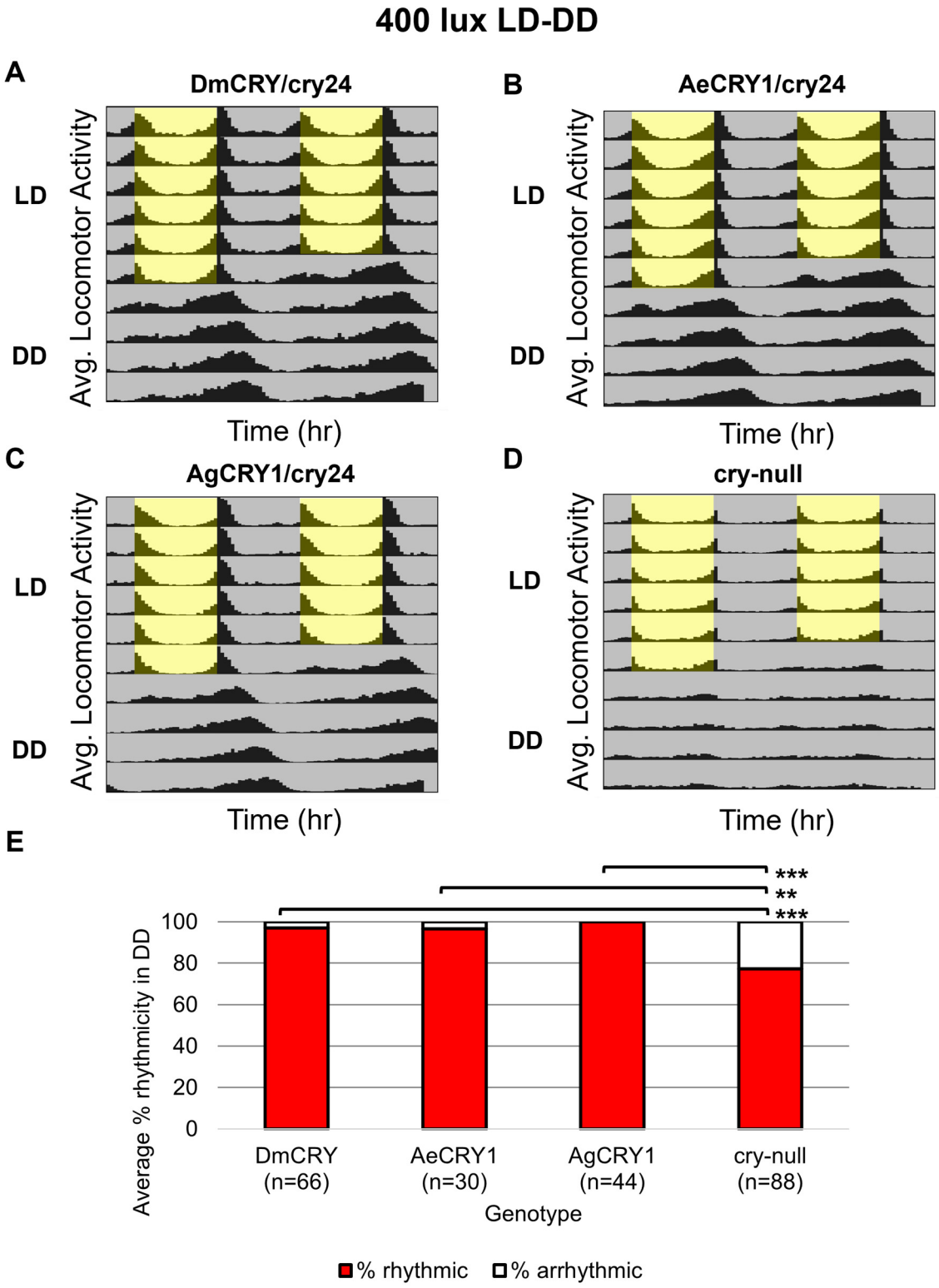
400 lux LD-DD
A
DmCRY/cry24
B
AeCRY1/cry24
C
AgCRY1/cry24
D
cry-null
LD
DD
Avg. Locomotor Activity
Time (hr)
E
Average % rhythmicity in DD
100
80
60
40
20
0
***
**
***
DmCRY
(n=66)
AeCRY1
(n=30)
AgCRY1
(n=44)
cry-null
(n=88)
Genotype
% rhythmic
% arrhythmic

Figure 3-2. AgCRY1, AeCRY1 expressing flies and control groups maintain high rhythmicity in constant dark conditions after entrainment in moderately high 400 lux LD light

(**A-D**) Actogram plots containing 5 days of 12:12 hr LD entrainment in 400 lux white light conditions followed by 5 days of constant dark (DD) conditions for flies expressing: (**A**) DmCRY (n=66; $\tau_{avg,DD}$≈24.7, $power_{avg,DD}$≈153.2, $width_{avg,DD}$≈4.9), (**B**) AeCRY1 (n=30; $\tau_{avg,DD}$≈24.6, $power_{avg,DD}$≈160.3, $width_{avg,DD}$≈5.0), (**C**) AgCRY1 (n=44; $\tau_{avg,DD}$≈25.4, $power_{avg,DD}$≈137.0, $width_{avg,DD}$≈4.9), (**D**) *cry-null* (n=88; $\tau_{avg,DD}$≈23.6, $power_{avg,DD}$≈84.5, $width_{avg,DD}$≈3.3). (**E**) Quantification of fly rhythmicity (red) to arrhythmicity (white) in DD. Pairwise t-tests were used to determine significance: * $p \leq 0.1$, ** $p \leq 0.05$, ***$p \leq 0.01$.

A

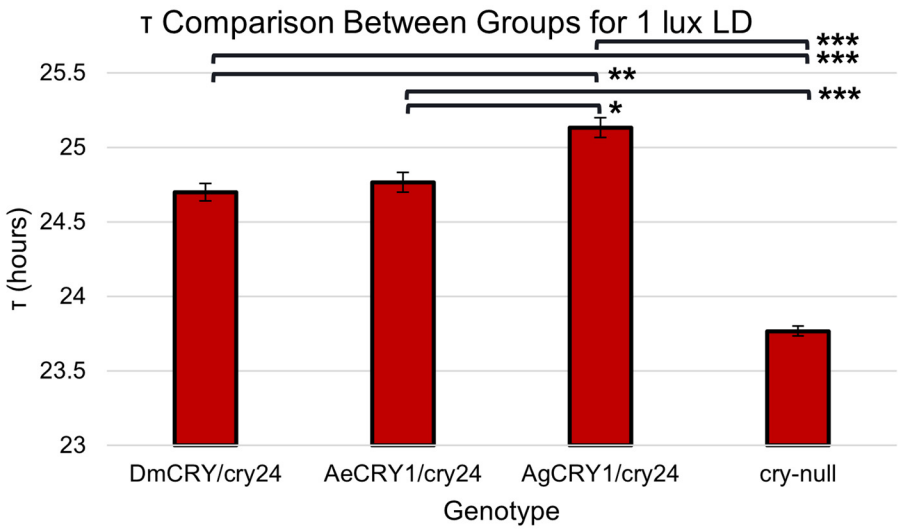

B

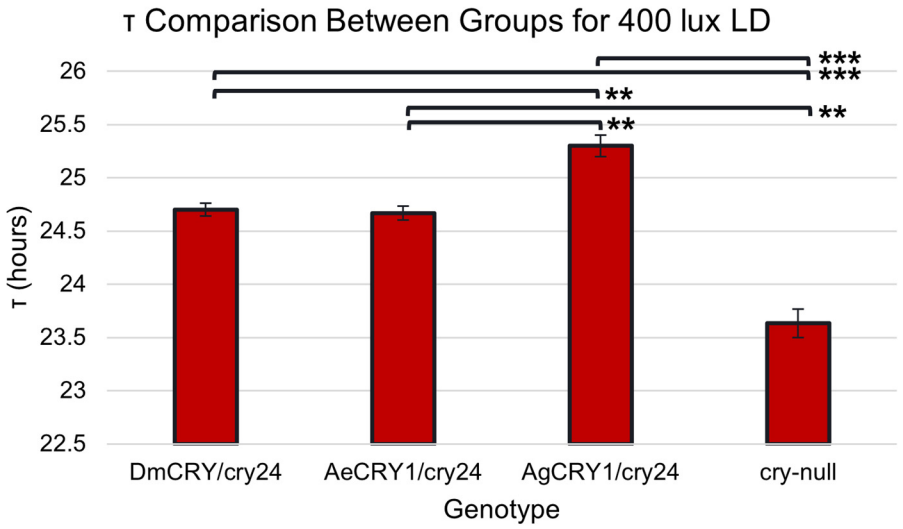

Figure 3-3. Comparison of period length during 1 lux and 400 lux LD entrainment

Average period length (tau, τ) over 5 days of LD entrainment for DmCRY, AeCRY1, AgCRY1, and *cry-null* groups are quantified for (**A**) 1 lux and (**B**) 400 lux light intensity. Pairwise t-tests were performed for statistical comparison. Data are represented as mean ± SEM. One significance symbol; $p \leq 0.05$, two significance symbols; $p \leq 0.005$, three significance symbols; $p \leq 0.001$.

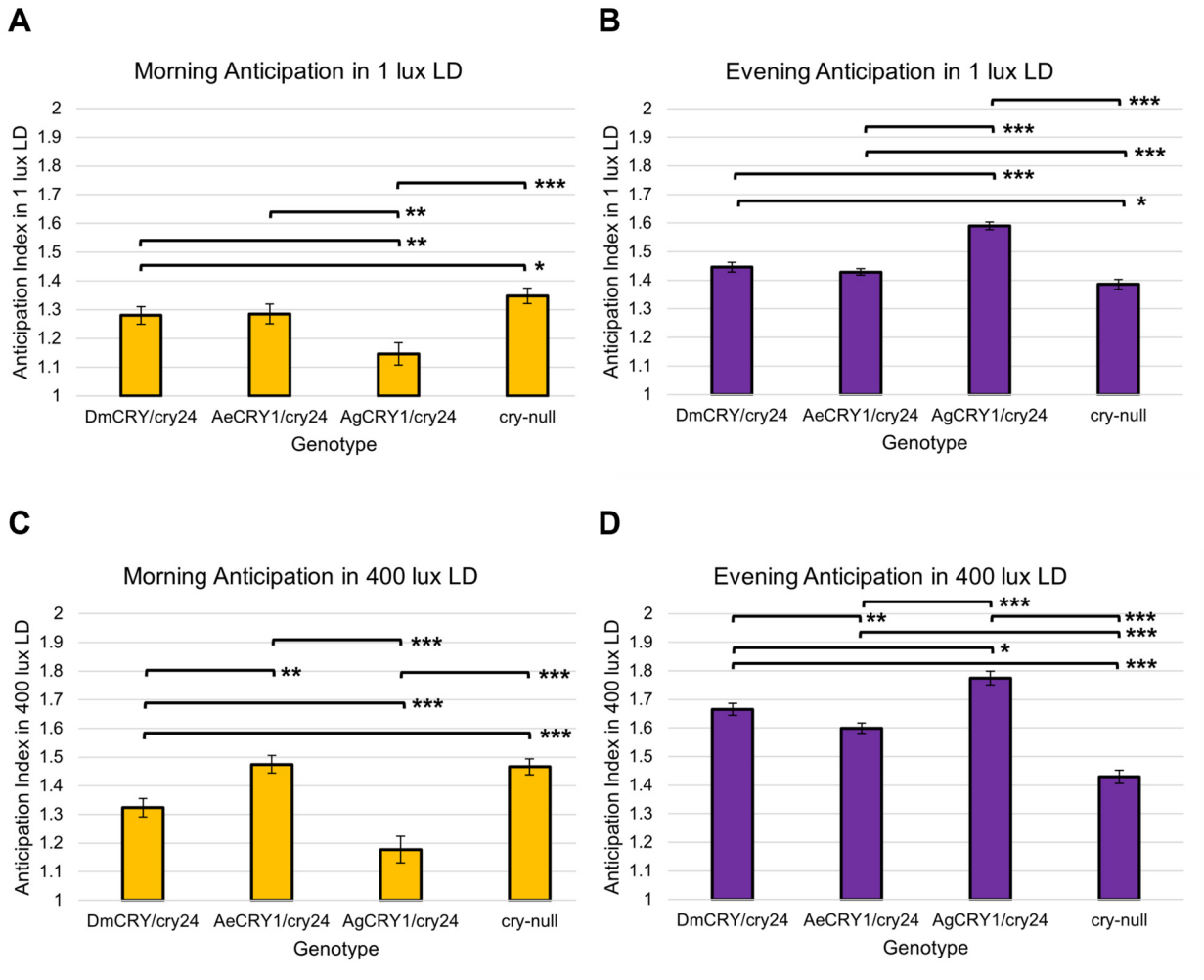

Figure 3-4. Morning and evening anticipatory indices for DmCRY, AeCRY1, AgCRY1, and *cry-null* at 1 lux and 400 lux LD

Quantification of morning and evening anticipation indices for (**A, B**) low 1 lux LD, and (**C, D**) moderately high 400 lux LD entrainment. (**A, C**) morning and (**B, D**) evening anticipation indices were measured as the ratio of average activity three hours before lights on or off to the average activity six hours before lights on or off, respectively. Pairwise t-tests were performed for statistical comparison. Data are represented as mean ± SEM. One significance symbol; $p \leq 0.05$, two significance symbols; $p \leq 0.005$, three significance symbols; $p \leq 0.001$.

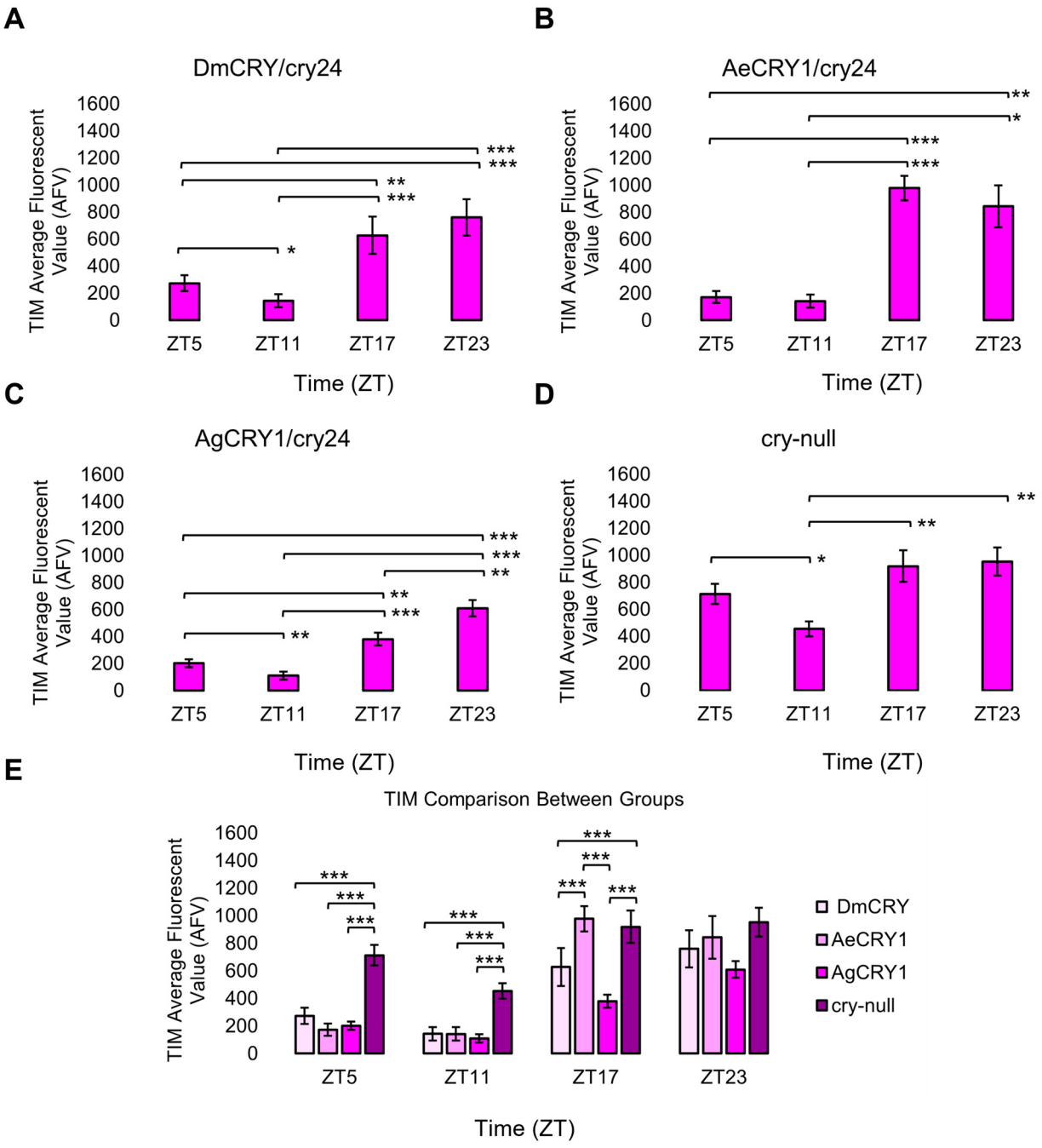
A
DmCRY/cry24
TIM Average Fluorescent Value (AFV)
1600
1400
1200
1000
800
600
400
200
0
ZT5
ZT11
ZT17
ZT23
Time (ZT)
B
AeCRY1/cry24
C
AgCRY1/cry24
D
cry-null
E
TIM Comparison Between Groups
DmCRY
AeCRY1
AgCRY1
cry-null

Figure 3-5. Transgenic mosquito CRY1 expression does not alter the overall pattern of cyclic TIM expression

Immunocytochemistry average fluorescent value of TIM expression over 12:12 hr LD at ZT5, 11, 17, and 23 timepoints in LNvs (small + large) expressing (**A**) DmCRY (ZT5, n=38; ZT11, n=26; ZT17, n=29; ZT23, n=33), (**B**) AeCRY1 (ZT5, n=15; ZT11, n=10; ZT17, n=26; ZT23, n=26), (**C**) AgCRY1 (ZT5, n=29; ZT11, n=27; ZT17, n=37; ZT23, n=44), and (**D**) negative control *cry-null* (ZT5, n=41; ZT11, n=26; ZT17, n=29; ZT23, n=52). Fluorescent quantification of TIM signal was obtained by marking regions-of-interest on LNv soma identified by morphology and anatomical positioning within each brain sample. Fluorescent values for the total number of neurons in a brain are normalized to the background brain fluorescence, then measurements of all neurons from all brain samples are averaged together. (**E**) Comparison summary between genotypes for each timepoint measurement of average TIM fluorescence. Mann-Whitney U-tests with FDR adjustment were performed for statistical comparison. Data are represented as mean ± SEM for. * $p \leq 0.1$, ** $p \leq 0.05$, ***$p \leq 0.01$.

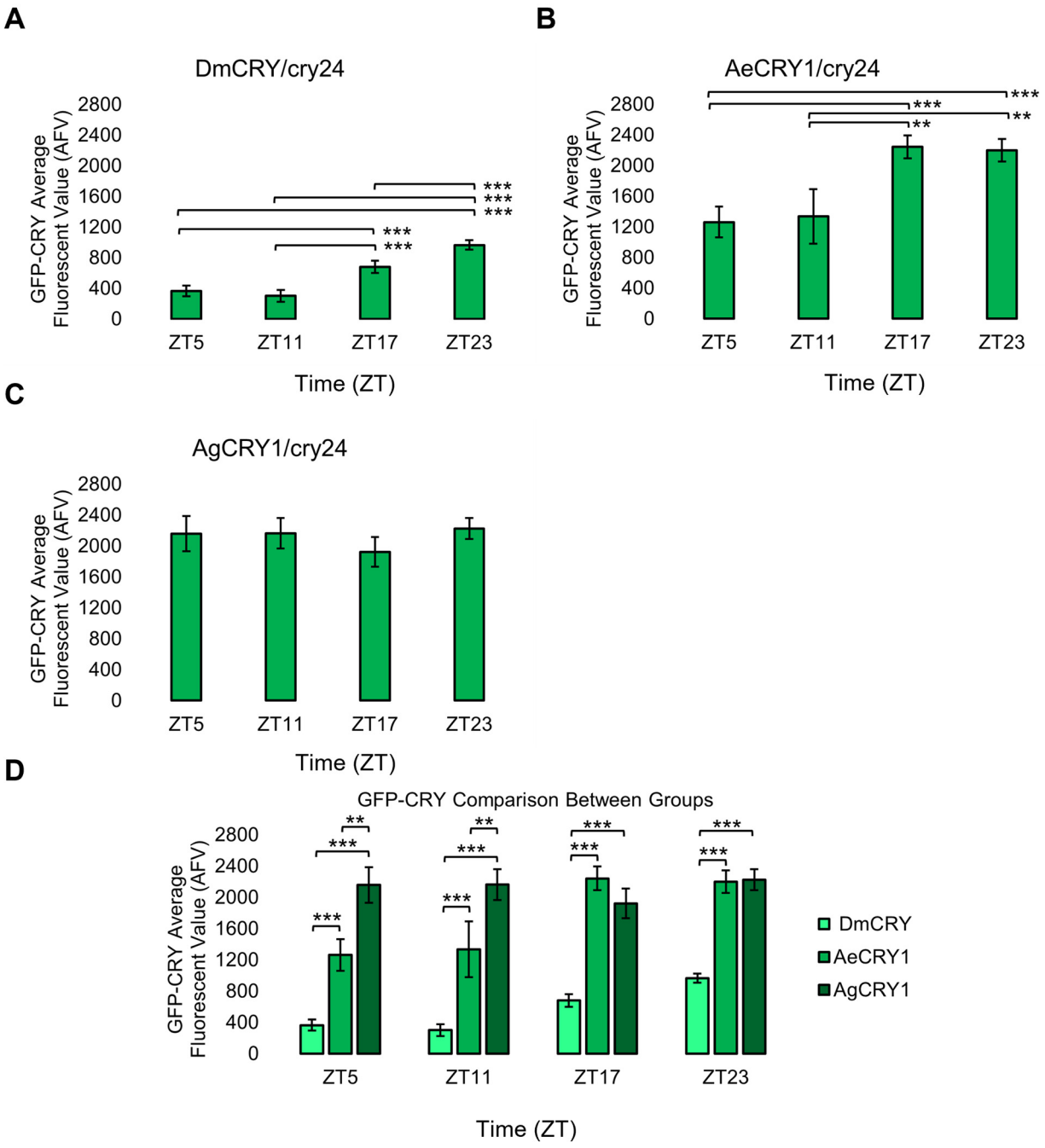
A
DmCRY/cry24
GFP-CRY Average Fluorescent Value (AFV)
2800
2400
2000
1600
1200
800
400
0
***
***
***
***
***
ZT5
ZT11
ZT17
ZT23
Time (ZT)
B
AeCRY1/cry24
GFP-CRY Average Fluorescent Value (AFV)
***
***
**
**
ZT5
ZT11
ZT17
ZT23
Time (ZT)
C
AgCRY1/cry24
GFP-CRY Average Fluorescent Value (AFV)
ZT5
ZT11
ZT17
ZT23
Time (ZT)
D
GFP-CRY Comparison Between Groups
GFP-CRY Average Fluorescent Value (AFV)
DmCRY
AeCRY1
AgCRY1
ZT5
ZT11
ZT17
ZT23
Time (ZT)

Figure 3-6. AeCRY1 and DmCRY shows lower protein levels during day and higher GFP-CRY during night, while AgCRY1 expression remains high throughout all timepoints

Immunocytochemistry average fluorescent value of GFP-CRY expression over 12:12 hr LD at ZT5, 11, 17, and 23 timepoints in LNvs (small + large) expressing (**A**) DmCRY (ZT5, n=38; ZT11, n=26; ZT17, n=29; ZT23, n=33), (**B**) AeCRY1 (ZT5, n=15; ZT11, n=10; ZT17, n=26; ZT23, n=26), and (**C**) AgCRY1 (ZT5, n=29; ZT11, n=27; ZT17, n=37; ZT23, n=44). Fluorescent quantification of GFP-CRY signal was obtained by marking regions-of-interest on LNv soma identified by morphology and anatomical positioning within each brain sample. Fluorescent values for the total number of neurons in a brain are normalized to the background brain fluorescence, then measurements of all neurons from all brain samples are averaged together. (**D**) Comparison summary between genotypes for each timepoint measurement of average GFP-CRY fluorescence. Mann-Whitney U-tests with FDR adjustment were performed for statistical comparison. Data are represented as mean ± SEM. * $p \leq 0.1$, ** $p \leq 0.05$, ***$p \leq 0.01$.

3.3.2 AgCRY1 and AeCRY1 mediate blue-light-evoked increases in electrophysiological action potential firing frequency

Drosophila ventral lateral neurons are circadian/arousal neurons that drive CRY-dependent acute electrophysiological light responses [1,3,6,10,89–91,101,102]. We expressed AeCRY1, AgCRY1, and control DmCRY in *cry-null* genetic background flies with the UAS/GAL4 expression system, then measured the light on/light off ratio of action potential firing frequency in response to 200 μW/cm² 450 nm blue-light from whole-cell patch-clamp recordings of l-LNvs in transgenic flies. For these experiments, we used the *crypGAL4-24* driver line that drives expression in all CRY neurons [52].

Positive control DmCRY expression driven by the *crypGAL4-24* line mediates robust and significant increases in action potential firing frequency (FF) in the l-LNvs in response to 200 μW/cm² blue-light (450 nm) relative to *cry-null* negative controls (Figure 3-7A, blue column versus grey column and mediates significant sustained increases in firing frequency in response to blue-light (Figure 3-7A). AeCRY1 driven by the *crypGAL4-24* line also shows significant increases in FF in the l-LNvs in response to 200 μW/cm² blue-light relative to *cry-null* negative

controls (Figure 3-7A, orange column versus grey column). However, after adjusting for false discovery rate (FDR), there is no significance difference observed between these two groups. This is unlike AgCRY1 driven by the *crypGAL4-24* line, which shows robust and significant increases in FF in the l-LNvs in response to 200 μW/cm² blue-light relative to *cry-null* negative controls (Figure 3-7, purple column versus grey column) even after adjusting for FDR, suggesting a greater blue light response for AgCRY1 compared to AeCRY1. Further, the AgCRY1 blue-light FF response does not significantly differ from the DmCRY blue-light FF response (purple column versus blue column, Figure 3-7A). Comparing the 200 μW/cm² blue-light-evoked FF ratio during stimulus and subsequent 10 second bins post-stimulus up to 40 seconds, AgCRY1 FF is significantly greater than AeCRY1 FF 30 seconds post-stimulus (Figure 3-7E), but again, does not show significance after FDR adjustment. The positive control DmCRY FF is significantly greater than the *cry-null* negative control FF during stimulus and at the 10 and 30 second bins (Figure 3-7B).

Previous work shows that light activated CRY mediates changes in membrane potential through the voltage gated potassium channel beta subunit and modulation of potassium channels [1,3,6,8,10,89,90,103]. To determine whether mosquito CRY expression alters LNv basal electrophysiological processes, we plotted basal l-LNv firing rates, basal resting membrane potential values and firing mode (tonic vs. burst firing) across the time of day of the recordings (Figure 3-8). The range of l-LNv firing rates and the average resting membrane potentials from the present set of whole-cell patch-clamp recordings for DmCRY expressing neurons are similar to previously reported values around -40mV (the mean is -37 mV, Figure 3-8B, D, F). Basal firing rates and resting membrane potentials for DmCRY expressing flies are significantly lower than *cry-null*, AeCRY1 and AgCRY1 expressing flies (Figure 3-8E, F). The majority of the l-LNv

recordings are from neurons during the day between ZT6-ZT12 and include a few recordings for the first few hours of night up until ZT16. None of the genotypes shows clear time of day differences in basal firing rate or membrane resting potential. However, these experiments were not designed to test time of day distributions as the present data cluster during midday. There are relatively few nighttime recordings and recordings from early morning and late night are not represented. Previous publications designed to test this question, including several of our own, show firing rates trending high at the beginning of day that tend to decrease at night [79,102,104–106]. Consistent with most earlier publications, we observe predominantly tonic action potential firing in l-LNv recordings [3,6,10,79,82,91,101,102,104–111]. Burst firing as the predominant firing mode in l-LNv has been reported by another group [81,112] however they do not systematically address firing mode as a function of time of day.

Light-evoked averaged potentials are more kinetically reliable than light onset and CRY mediated action potential firing [1,3,91]. The blue-light-evoked response of DmCRY relative to the *cry-null* negative control shows strong depolarization then a slowly tapering sustained response over the 10 seconds following light stimulus offset (Figure 3-9A) with a qualitatively similar response recorded from neurons expressing AeCRY1 relative to the *cry-null* negative control (Figure 3-9B). In contrast, the blue-light-evoked response of neurons expressing AgCRY1 relative to the *cry-null* negative control show sustained significant depolarization during lights on, followed by a very long sustained depolarization response that lasts tens of seconds (Figure 3-9C). The blue-light response of AgCRY1 relative to AeCRY1 exhibits a significantly longer and more sustained membrane depolarization event lasting for tens of seconds evoked by a five second pulse of 200 μW/cm² blue-light relative to the shorter-lasting AeCRY1 evoked blue-light potential (Figure 3-9D). The significantly higher AgCRY1 blue-light-evoked depolarization for most of the

duration of the evoked potential occurs after approximately 15 seconds post-stimulus relative to AeCRY1 (Figure 3-9D). These results, particularly the similar duration of the evoked potential blue-light response between AeCRY1 and DmCRY, suggest no direct relationship between CRY expression levels (Figure 3-5) and the magnitude of the physiological light response (Figures 3-6 – 3-8), confirming earlier findings concerning this [3,9,10,91]. The AgCRY1 blue-light-evoked potential is significantly greater than that for the *cry-null* negative control for almost the entire duration up to 40 seconds from the stimulus onset (Figure 3-9C), while the much weaker AeCRY1 evoked potential is only significantly higher than the *cry-null* negative control for the first few seconds following stimulus onset (Figure 3-9B), but after FDR adjustment, it does not show significant differences. AgCRY1 confers a more sustained light response than DmCRY (Figure 3-9A, C). Representative voltage traces showing light-evoked depolarization and increased action potential firing frequency in patch-clamp recordings of l-LNvs during the 5 seconds of blue-light stimuli and 60 seconds post-light stimulus for positive control DmCRY/cry24, AeCRY1/cry24, AgCRY1/cry24 and negative control *cry-null* flies are shown in Figure 3-10, where the blue bar indicates 5 seconds of 200 μW/cm² 450 nm blue-light stimulus.

As expected, there are no significant differences in light-evoked FF between all four CRY genotypes in response to 200 μW/cm² violet-light (405 nm) (Figure 3-11A), as there is a trough of the CRY action spectra around 405 nm and Rh7 and other opsin photoreceptors are activated in this range of the color spectra [2,7,9]. The depolarization magnitude and duration of DmCRY, AeCRY1, AgCRY1 and negative control *cry-null* responses to violet-light are similar and indistinguishable from *cry-null* and are at a lower magnitude of FF ratio and depolarization magnitude and duration relative to intensity matched blue-light stimuli (compare Figure 3-11 versus Figure 3-7). The violet-light-evoked increases in l-LNv firing frequency (Figure 3-11B-E)

and light-evoked depolarization (Figure 3-12) during and after the violet-light stimulus are weak and do not differ systematically between the different CRY genotypes. These results are consistent with earlier findings that CRY is not activated by violet-light and is consistent with earlier findings that Rh7 is the primary non-image forming visual violet-light photoreceptor in LNvs [2,7,9]. Representative voltage traces showing light-evoked depolarization and increased action potential firing frequency in patch-clamp recordings of l-LNvs during the 5 seconds of violet-light stimuli and 60 seconds post-light stimulus for positive control DmCRY/cry24, AeCRY1/cry24, AgCRY1/cry24 and negative control *cry-null* flies are shown in Figure 3-13, where the violet bar indicates 5 seconds of 200 $\mu W/cm^2$ 405 nm violet-light stimulus.

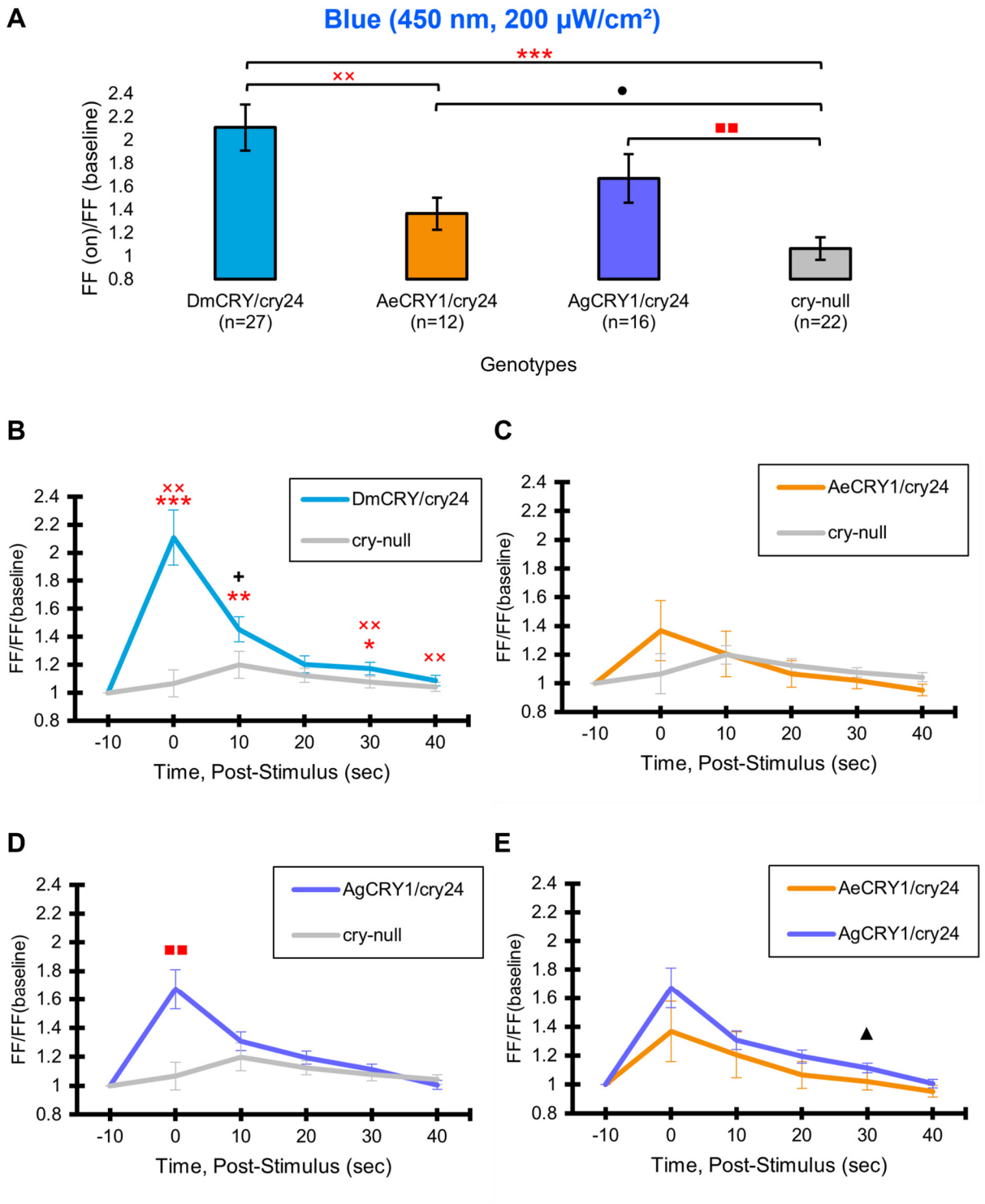
A
Blue (450 nm, 200 µW/cm²)
***
××
●
■■
FF (on)/FF (baseline)
2.4
2.2
2
1.8
1.6
1.4
1.2
1
0.8
DmCRY/cry24 (n=27)
AeCRY1/cry24 (n=12)
AgCRY1/cry24 (n=16)
cry-null (n=22)
Genotypes
B
××
***
+
**
××
*
××
DmCRY/cry24
cry-null
FF/FF(baseline)
-10
0
10
20
30
40
Time, Post-Stimulus (sec)
C
AeCRY1/cry24
cry-null
FF/FF(baseline)
Time, Post-Stimulus (sec)
D
■■
AgCRY1/cry24
cry-null
FF/FF(baseline)
Time, Post-Stimulus (sec)
E
AeCRY1/cry24
AgCRY1/cry24
▲
FF/FF(baseline)
Time, Post-Stimulus (sec)

Figure 3-7. AeCRY1 and AgCRY1 mediate electrophysiological responses to blue-light

Light-evoked (**A**) FF ratio comparison of blue-light (450 nm, 200 μW/cm²) excited l-LNvs expressing: DmCRY (blue, n=27) and negative control cry-null (grey, n=22), AeCRY1 (orange, n=12) and AgCRY1 (purple, n=16). Light-evoked (**B-E**) post-stimulus FF comparison of blue-light (450 nm, 200 μW/cm²) excited l-LNvs expressing: DmCRY (blue, n=27) and negative control cry-null (grey, n=22), AeCRY1 (orange, n=12) and AgCRY1 (purple, n=16). Traces represent the average last 60 seconds of each recording for (**B**) DmCRY vs. cry-null, (**C**) AeCRY1 vs. cry-null, (**D**) AgCRY1 vs. cry-null, and (**E**) AeCRY1 vs AgCRY1. Black + indicates two-sample t-test $p \leq 0.05$ between AgCRY1/cry24 and DmCRY/cry24. Black ▲ indicates two-sample t-test $p \leq 0.05$ between AgCRY1/cry24 and AeCRY1/cry24. Black ● indicates two-sample t-test $p \leq 0.05$ between AeCRY1/cry24 and cry-null. Red * indicates FDR adjusted $p \leq 0.1$ between DmCRY/cry24 and cry-null. Red x indicates $p \leq 0.1$ between AeCRY1/cry24 and DmCRY/cry24. Red ■ indicates FDR adjusted $p \leq 0.1$ between AgCRY1/cry24 and cry-null. Data are represented as mean ± SEM. For black significance symbols: One symbol; $p \leq 0.05$, two symbols; $p \leq 0.005$, three symbols; $p \leq 0.001$. For red significance symbols: One symbol; $p \leq 0.1$, two symbols; $p \leq 0.05$, three symbols; $p \leq 0.01$.

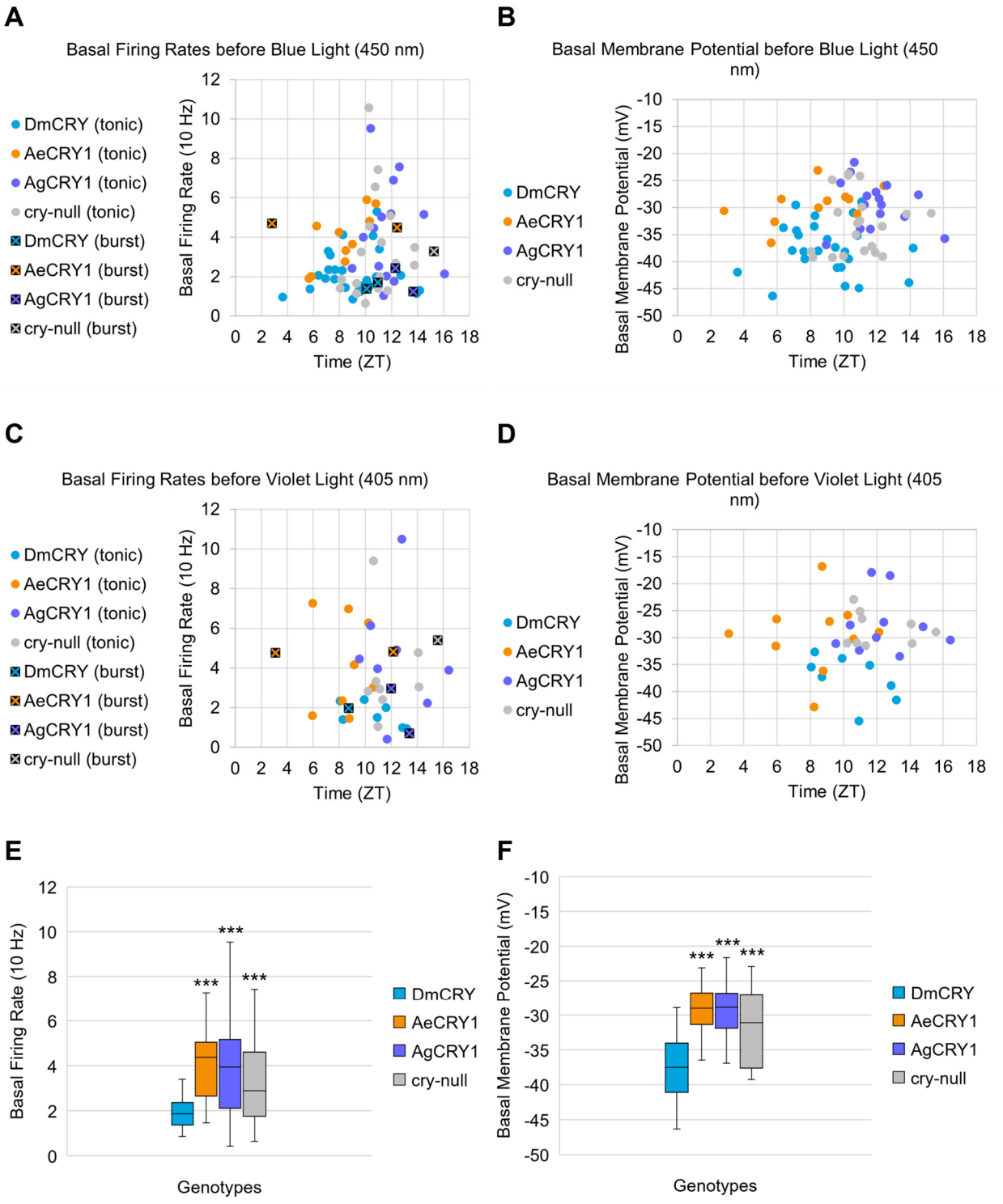
A
Basal Firing Rates before Blue Light (450 nm)
DmCRY (tonic)
AeCRY1 (tonic)
AgCRY1 (tonic)
cry-null (tonic)
DmCRY (burst)
AeCRY1 (burst)
AgCRY1 (burst)
cry-null (burst)
Basal Firing Rate (10 Hz)
Time (ZT)
B
Basal Membrane Potential before Blue Light (450 nm)
DmCRY
AeCRY1
AgCRY1
cry-null
Basal Membrane Potential (mV)
Time (ZT)
C
Basal Firing Rates before Violet Light (405 nm)
DmCRY (tonic)
AeCRY1 (tonic)
AgCRY1 (tonic)
cry-null (tonic)
DmCRY (burst)
AeCRY1 (burst)
AgCRY1 (burst)
cry-null (burst)
Basal Firing Rate (10 Hz)
Time (ZT)
D
Basal Membrane Potential before Violet Light (405 nm)
DmCRY
AeCRY1
AgCRY1
cry-null
Basal Membrane Potential (mV)
Time (ZT)
E
Basal Firing Rate (10 Hz)
***
***
***
DmCRY
AeCRY1
AgCRY1
cry-null
Genotypes
F
Basal Membrane Potential (mV)
***
***
***
DmCRY
AeCRY1
AgCRY1
cry-null
Genotypes

Figure 3-8. Basal firing rate and membrane potential are higher in all groups compared to the control DmCRY group and neither parameter exhibit time-of-day dependent effects

(**A**) Average basal firing rates and (**B**) average basal membrane potential before blue light stimulus plotted against the relative time-of-day of the recording for DmCRY (blue, n=27), AeCRY1 (orange, n=12), AgCRY1 (purple, n=16), and *cry-null* (grey, n=21). (**C**) Average basal firing rates and (**D**) average basal membrane potential before violet light stimulus plotted against the relative time-of-day of the recording for DmCRY (n=8), AeCRY1 (n=10), AgCRY1 (n=10), and cry-null (n=9). (**A, C**) Recordings that exhibit burst firing are denoted by a black square and cross for each respective genotype's color. (**E, F**) Box-and-whisker plot summary of the average (**E**) basal firing rate and (**F**) basal membrane potential for DmCRY ((n =35) total, n (ZT0-12) =30; n (ZT12-16) =5), AeCRY1 ((n=22) total, n (ZT0-12) =20; n (ZT12-16) =2), AgCRY1 ((n=26) total, n (ZT0-12) =14; n (ZT12-16) =12), and *cry-null* ((n=30) total, n (ZT0-12) =22; n (ZT12-16) =8). Median values are denoted by a solid black line within each box of the plot. Black * indicates FDR adjusted two-sample t-test $p \leq 0.01$ vs. DmCRY/cry24. Data are represented as a range of means in a sample set ± maximum and minimum values within the set. One significance symbol; $p \leq 0.1$, two significance symbols; $p \leq 0.05$, three significance symbols; $p \leq 0.01$.

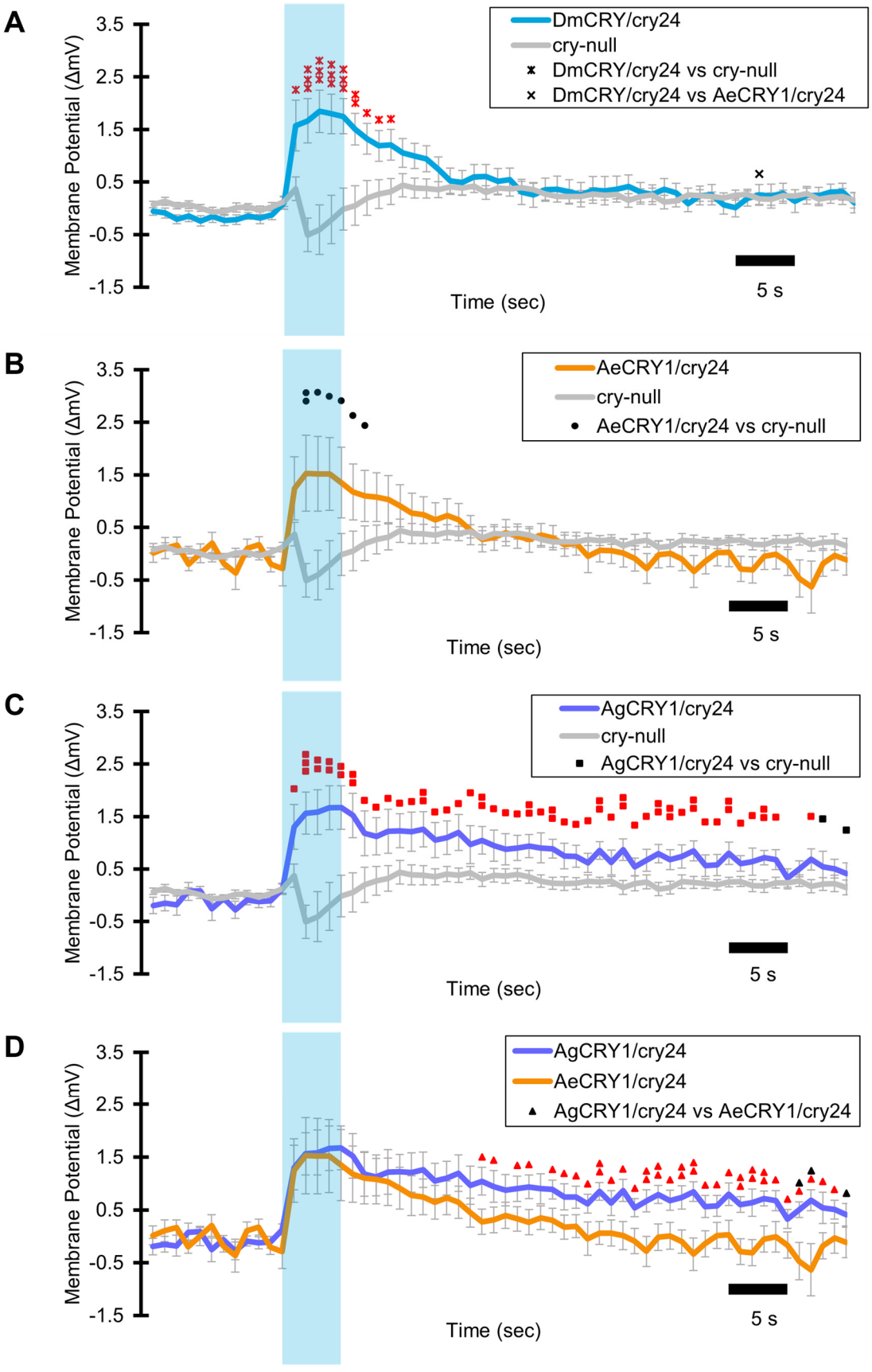
A
Membrane Potential (ΔmV)
3.5
2.5
1.5
0.5
-0.5
-1.5
DmCRY/cry24
cry-null
DmCRY/cry24 vs cry-null
DmCRY/cry24 vs AeCRY1/cry24
Time (sec)
5 s
B
Membrane Potential (ΔmV)
AeCRY1/cry24
cry-null
AeCRY1/cry24 vs cry-null
Time (sec)
5 s
C
Membrane Potential (ΔmV)
AgCRY1/cry24
cry-null
AgCRY1/cry24 vs cry-null
Time (sec)
5 s
D
Membrane Potential (ΔmV)
AgCRY1/cry24
AeCRY1/cry24
AgCRY1/cry24 vs AeCRY1/cry24
Time (sec)
5 s

Figure 3-9. AgCRY1 mediates significantly greater and sustained membrane depolarization in response to blue-light compared to AeCRY1

Light-evoked **(A-D)** membrane potential comparison of blue-light (450 nm, 200 µW/cm²) excited l-LNvs expressing: DmCRY (blue, n=27) and negative control *cry-null* (grey, n=22), AeCRY1 (orange, n=12) and AgCRY1 (purple, n=16). Blue bar on membrane potential plots indicates the timing of the 5 seconds of blue-light stimuli and black scale-bar indicates 5 seconds. Traces represent the average last 60 seconds of each recording for **(A)** DmCRY vs. *cry-null*, **(B)** AeCRY1 vs. *cry-null*, **(C)** AgCRY1 vs. *cry-null*, and **(D)** AeCRY1 vs AgCRY1. Black ● indicates two-sample t-test $p \leq 0.05$ between AeCRY1/cry24 and *cry-null*. Black + indicates two-sample t-test $p \leq 0.05$ between AgCRY1/cry24 and DmCRY/cry24. Black ▲ indicates two-sample t-test $p \leq 0.05$ between AgCRY1/cry24 and AeCRY1/cry24. Black **x** indicates two-sample t-test $p \leq 0.05$ between DmCRY/cry24 and AeCRY1/cry24. Black ■ indicates two-sample t-test $p \leq 0.05$ between AgCRY1/cry24 and *cry-null*. Black ▲ indicates two-sample t-test $p \leq 0.05$ between AgCRY1/cry24 and AeCRY1/cry24. Red * indicates FDR adjusted $p \leq 0.1$ between DmCRY/cry24 and *cry-null*. Red **x** indicates $p \leq 0.1$ between AeCRY1/cry24 and DmCRY/cry24. Red ■ indicates FDR adjusted $p \leq 0.1$ between AgCRY1/cry24 and *cry-null*. Red ▲ indicates FDR adjusted $p \leq 0.1$ between AgCRY1/cry24 and AeCRY1/cry24. Data are represented as mean ± SEM. For black significance symbols: One symbol; $p \leq 0.05$, two symbols; $p \leq 0.005$, three symbols; $p \leq 0.001$. For colored significance symbols: One symbol; $p \leq 0.1$, two symbols; $p \leq 0.05$, three symbols; $p \leq 0.01$.

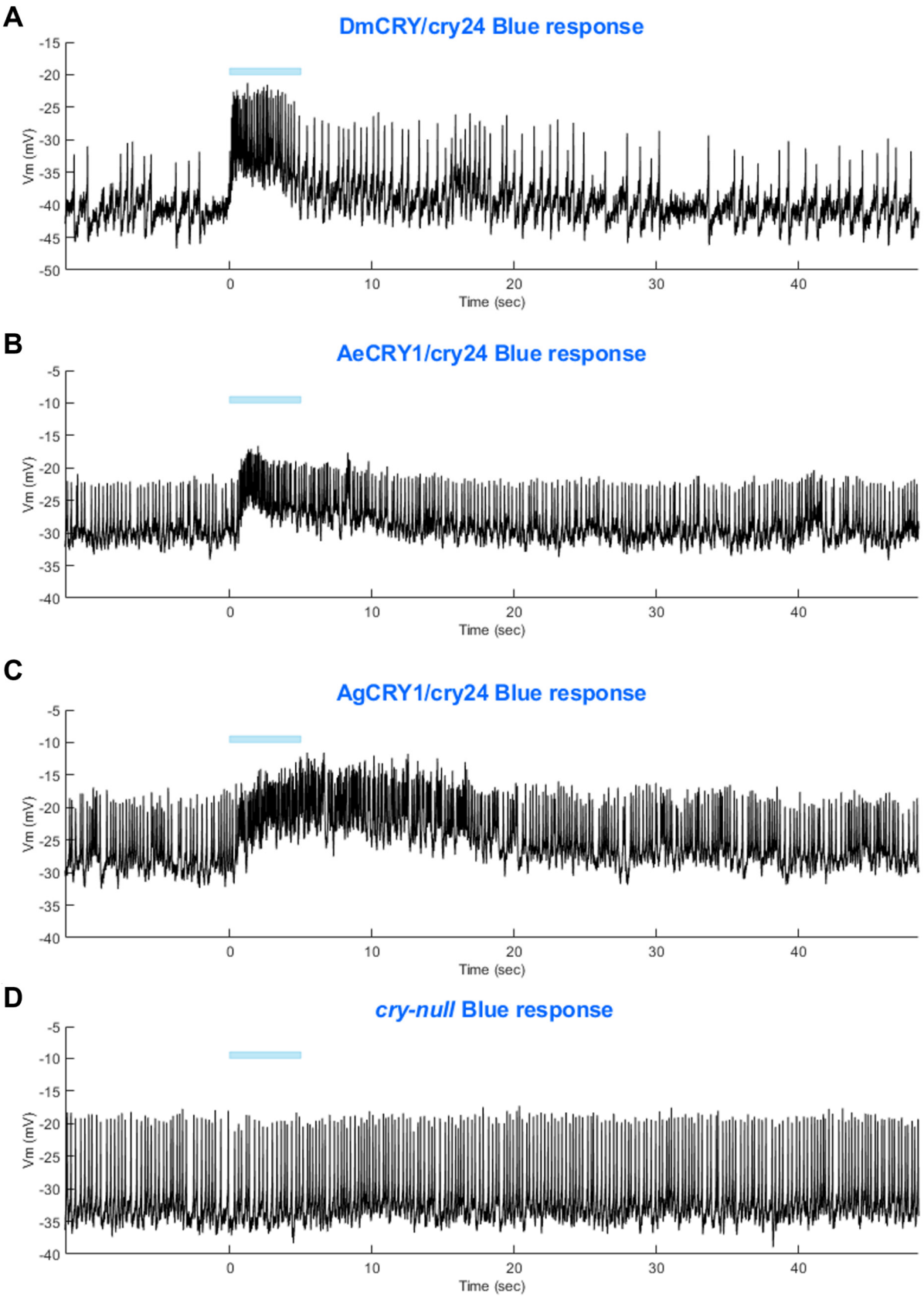
A
DmCRY/cry24 Blue response
Vm (mV)
Time (sec)
B
AeCRY1/cry24 Blue response
Vm (mV)
Time (sec)
C
AgCRY1/cry24 Blue response
Vm (mV)
Time (sec)
D
cry-null Blue response
Vm (mV)
Time (sec)

Figure 3-10. Representative voltage traces of l-LNvs electrophysiological responses to blue-light stimuli for all genotypes

Representative voltage traces of the last 60 seconds of a patch-clamp recording of l-LNvs subjected to 5 seconds of blue-light stimuli for **(A)** DmCRY/cry24, **(B)** AeCRY1/cry24, **(C)** AgCRY1/cry24, and **(D)** *cry-null* flies. Blue bar indicates 5 seconds of 200 μW/cm² blue-light stimulus.

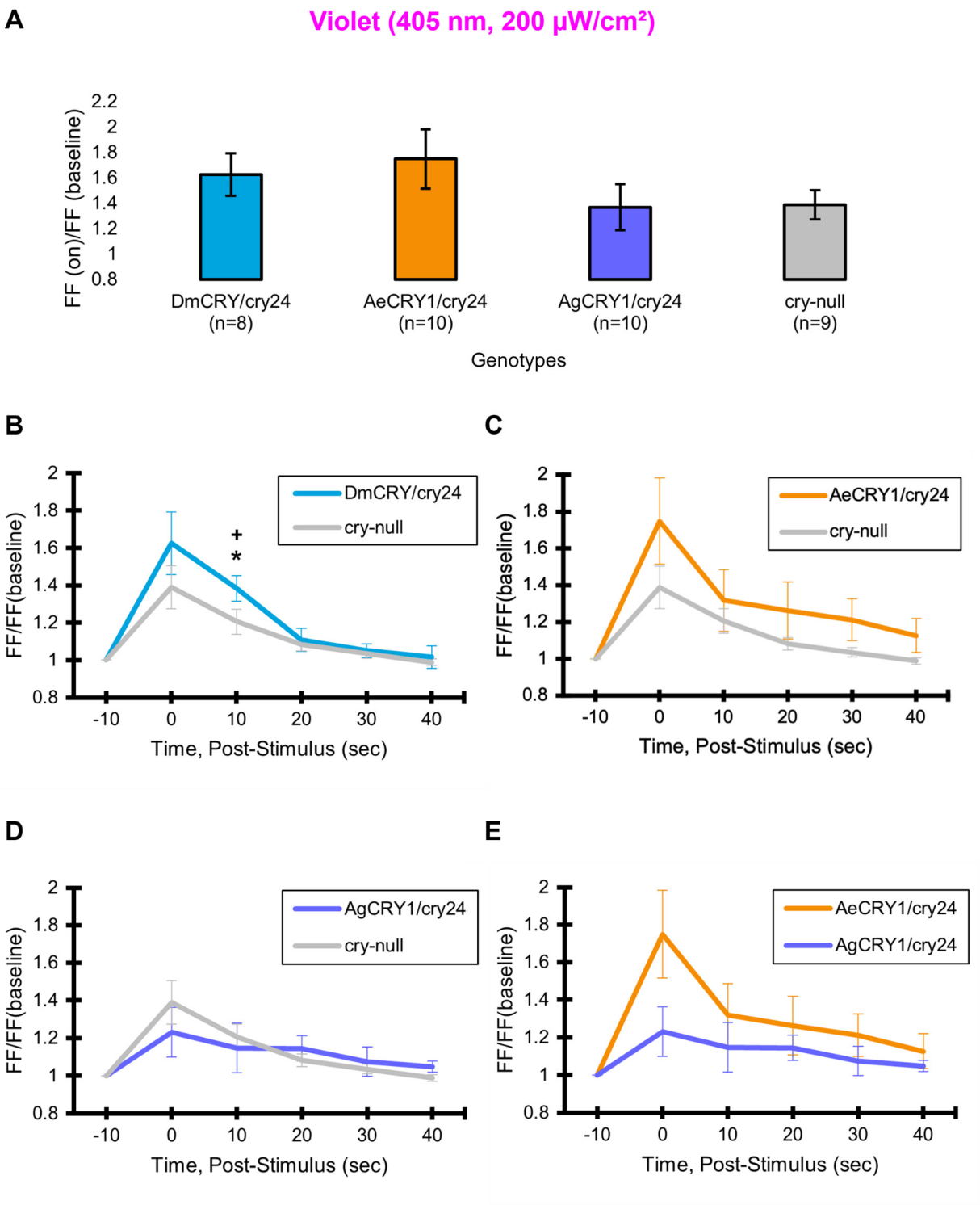
A
Violet (405 nm, 200 μW/cm²)
FF (on)/FF (baseline)
2.2
2
1.8
1.6
1.4
1.2
1
0.8
DmCRY/cry24 (n=8)
AeCRY1/cry24 (n=10)
AgCRY1/cry24 (n=10)
cry-null (n=9)
Genotypes
B
C
D
E
FF/FF(baseline)
Time, Post-Stimulus (sec)
-10
0
10
20
30
40
DmCRY/cry24
cry-null
AeCRY1/cry24
AgCRY1/cry24
+
*

Figure 3-11. AeCRY1 and AgCRY1 FF ratios shows weak responses to violet-light

Light-evoked (**A**) FF ratio comparison of violet-light (405 nm, 200 μW/cm²) excited l-LNvs expressing: DmCRY (blue, n=8) and negative control cry-null (grey, n=9), AeCRY1 (orange, n=10) and AgCRY1 (purple, n=10). Light-evoked (**B-E**) post-stimulus FF comparison of violet-light (405 nm, 200 μW/cm²) excited l-LNvs expressing: DmCRY (blue, n=8) and negative control cry-null (grey, n=9), AeCRY1 (orange, n=10) and AgCRY1 (purple, n=10). Traces represent the average last 60 seconds of each recording for (**B**) DmCRY vs. cry-null, (**C**) AeCRY1 vs. cry-null, (**D**) AgCRY1 vs. cry-null, and (**E**) AeCRY1 vs AgCRY1. Black * indicates two-sample t-test $p \leq 0.05$ between DmCRY/cry24 and cry-null. Black + indicates two-sample t-test $p \leq 0.05$ between AgCRY1/cry24 and DmCRY/cry24. Data are represented as mean ± SEM. For black significance symbols: One symbol; $p \leq 0.05$, two symbols; $p \leq 0.005$, three symbols; $p \leq 0.001$.

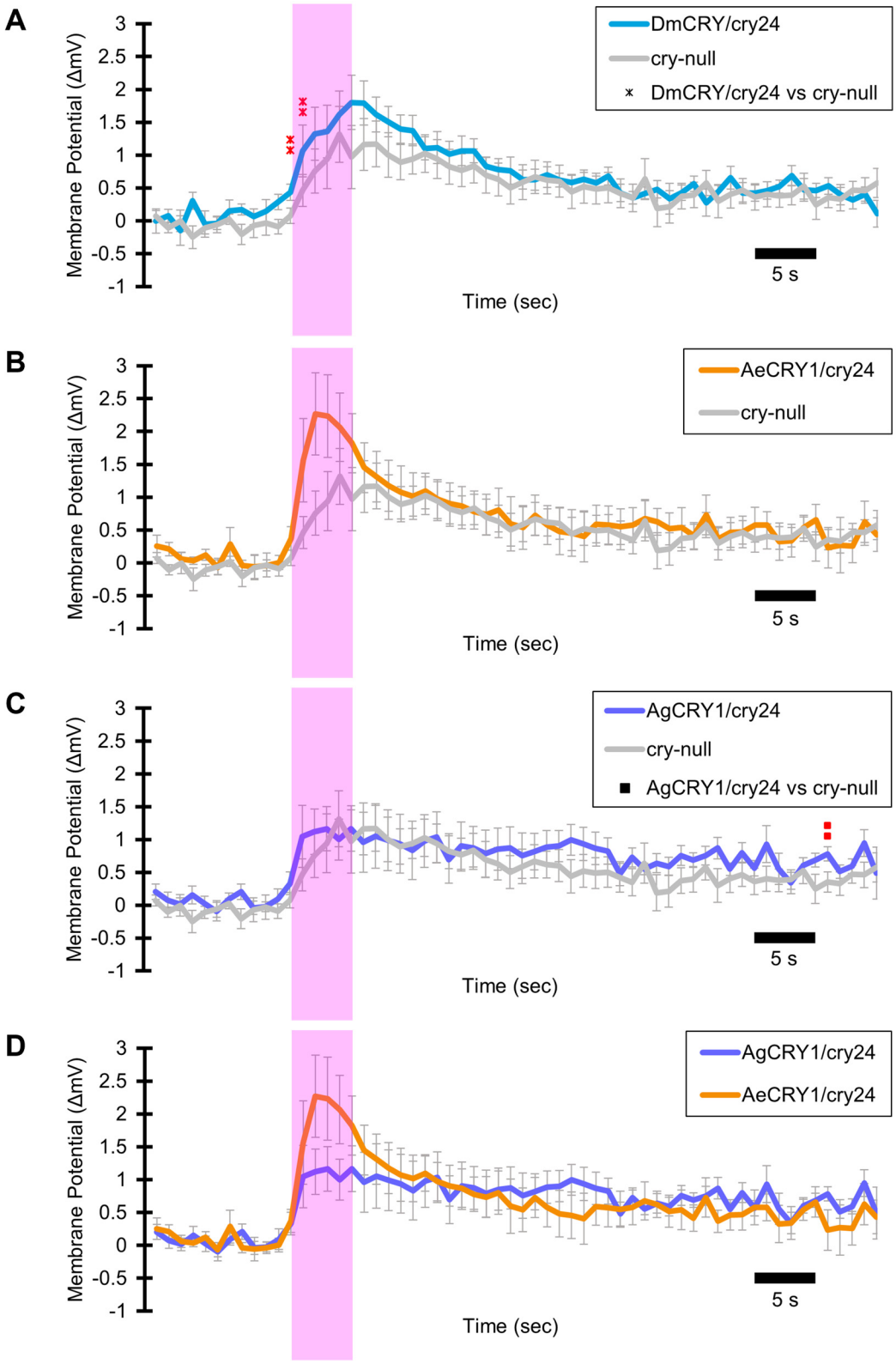
A
Membrane Potential (ΔmV)
3
2.5
2
1.5
1
0.5
0
-0.5
-1
DmCRY/cry24
cry-null
DmCRY/cry24 vs cry-null
5 s
Time (sec)
B
Membrane Potential (ΔmV)
AeCRY1/cry24
cry-null
5 s
Time (sec)
C
Membrane Potential (ΔmV)
AgCRY1/cry24
cry-null
AgCRY1/cry24 vs cry-null
5 s
Time (sec)
D
Membrane Potential (ΔmV)
AgCRY1/cry24
AeCRY1/cry24
5 s
Time (sec)

Figure 3-12. AeCRY1 and AgCRY1 RMP mediate weak membrane-evoked responses to violet-light

Light-evoked (**A-D**) membrane potential comparison of violet-light (405 nm, 200 µW/cm²) excited l-LNvs expressing: DmCRY (blue, n=8) and negative control cry-null (grey, n=9), AeCRY1 (orange, n=10) and AgCRY1 (purple, n=10). Violet bar on membrane potential plots indicates the timing of the 5 seconds of violet-light stimuli and black scale-bar indicates 5 seconds. Traces represent the average last 60 seconds of each recording for (**A**) DmCRY vs. cry-null, (**B**) AeCRY1 vs. cry-null, (**C**) AgCRY1 vs. cry-null, and (**D**) AeCRY1 vs AgCRY1. Red * indicates FDR adjusted $p \leq 0.1$ between DmCRY/cry24 and cry-null. Red x indicates FDR adjusted $p \leq 0.1$ between AeCRY1/cry24 and DmCRY/cry24. Red ■ indicates FDR adjusted $p \leq 0.1$ between AgCRY1/cry24 and cry-null. Data are represented as mean ± SEM. For red significance symbols: One symbol; $p \leq 0.1$, two symbols; $p \leq 0.05$, three symbols; $p \leq 0.01$.

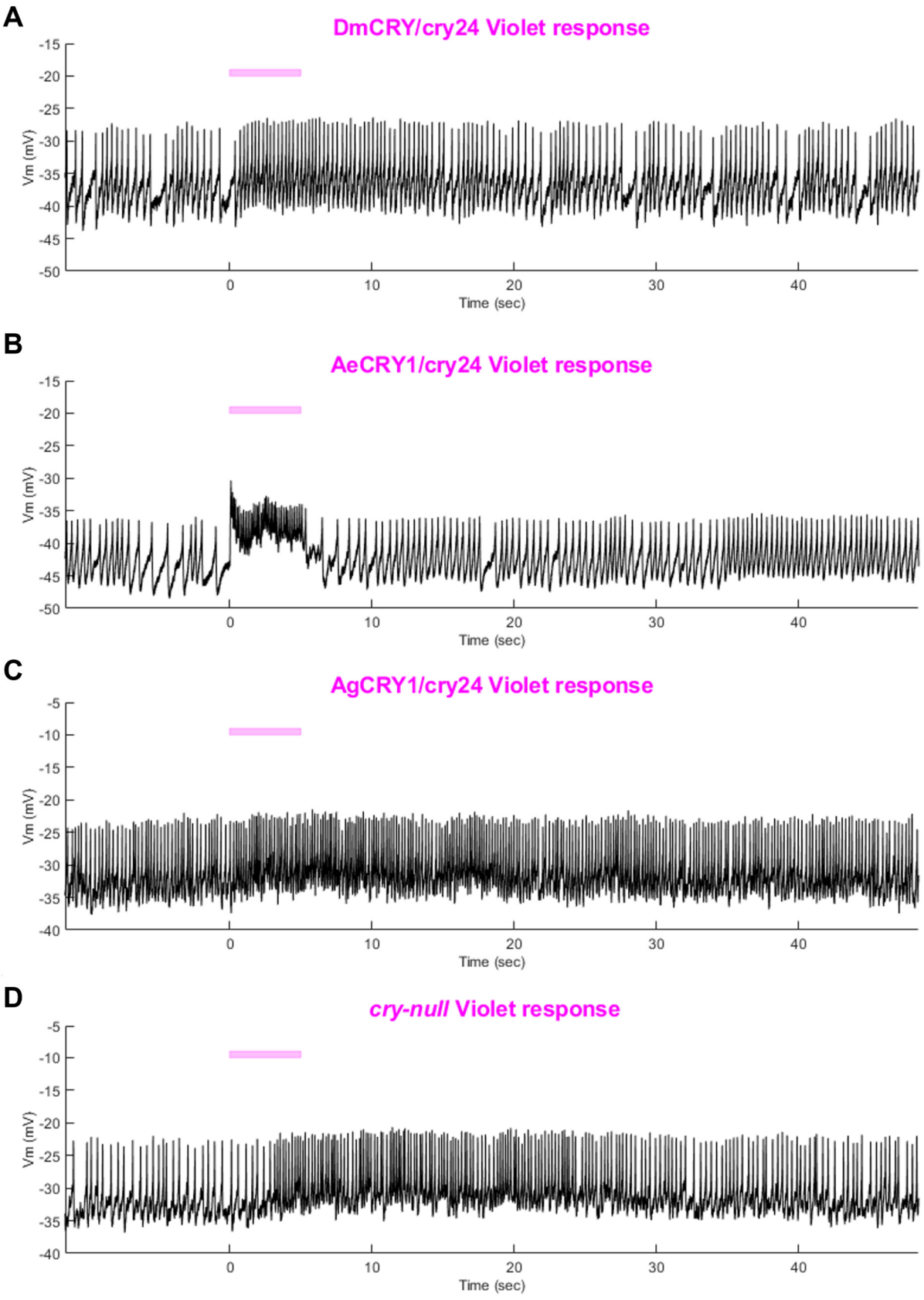
A
DmCRY/cry24 Violet response
Vm (mV)
Time (sec)
B
AeCRY1/cry24 Violet response
Vm (mV)
Time (sec)
C
AgCRY1/cry24 Violet response
Vm (mV)
Time (sec)
D
cry-null Violet response
Vm (mV)
Time (sec)

Figure 3-13. Representative voltage traces of l-LNvs electrophysiological response to violet light stimuli for all genotypes

Representative voltage traces of the last 60 seconds of a patch-clamp recording of l-LNvs subjected to 5 seconds of violet-light stimuli for **(A)** DmCRY/cry24, **(B)** AeCRY1/cry24, **(C)** AgCRY1/cry24, and **(D)** *cry-null* flies. Violet bar indicates 5 seconds of 200 μW/cm² violet-light stimulus.

3.3.3 Diurnal/nocturnal mosquito CRY1s confer species-specific and intensity-dependent behavioral attraction/avoidance responses to blue and violet-light

Diurnal mosquitoes are behaviorally attracted to short-wavelength light (UV, blue), while nocturnal mosquitoes behaviorally avoid short wavelength light [19]. CRY1 is a strong photoreceptor candidate to drive these species-specific attraction/avoidance behavioral light responses. In our recent study [91] testing transgenic *Drosophila* that express diurnal AeCRY1 or nocturnal AgCRY1 in a *cry-null* genetic background, we find that AeCRY1 expressing flies show strong photo-attraction behavioral responses to a wide intensity range (1-400 μW/cm²) of UV (365 nm) light. In contrast, nocturnal AgCRY1 expressing flies show discernable photo-attraction behavioral responses to UV light at very low intensities (1 μW/cm²) but show significant photo-avoidance behavioral responses to higher UV light intensities (at 10 μW/cm² and 400 μW/cm² of UV light). Here, we examine the role for CRY1s for conferring day- versus night-active mosquito species-specific light choice behaviors to other wavelengths by performing blue (450 nm) and violet (405 nm) light choice behavioral assays with flies expressing DmCRY, AgCRY1, AeCRY1 under the *crypGAL4-24* promoter at low (10 μW/cm²) and high (400 μW/cm²) light intensities using an environmental light choice preference test. At low intensity (10 μW/cm²) 450 nm blue-light, *cry-null* flies show significantly greater attraction to blue-light relative to all CRY expressing fly groups (Figure 3-14A-C). Flies expressing DmCRY, AgCRY1, or AeCRY1 show weak or no

behavioral attraction to low intensity blue-light (Figure 3-14 A-D). The average % activity of flies in the blue lit environment over the first 30 minutes shows no significant differences between flies expressing DmCRY, AeCRY1, or AgCRY1 (Figure 3-14E).

In contrast, at higher intensity 400 μW/cm² 450 nm blue-light, the genotypes behavioral light responses diverge: DmCRY expressing flies exhibit relatively neutral responses to the blue lit environment, showing moderate photo-attraction for 15 minutes of blue-light exposure, then moderate photo-avoidance to 400 μW/cm² 450 nm blue-light for the next 15 minutes (Figure 3-15A). AeCRY1 expressing flies show significantly greater behavioral attraction to high intensity blue-light relative to *cry-null* and AgCRY1 expressing flies at many time points (Figure 3-15B, D). AgCRY1 expressing flies exhibit the greatest significant light avoidance to the high-intensity blue-light exposed environment relative to other genotypes (Figures 3-15A-E). This is confirmed by average % activity plots for each CRY expressing genotype showing that AeCRY1 expressing flies have significantly greater activity in higher intensity blue-light than either AgCRY1 or DmCRY, and that AgCRY1 have significantly the least amount of activity in high intensity blue-light relative to AeCRY1 or DmCRY (Figure 3-15E).

At low intensity 405 nm violet-light (10 μW/cm²), DmCRY and AgCRY1 expressing flies both show behavioral photo-attraction to the low intensity violet lit environment (Figure 3-16A, C, D), while *cry-null* and AeCRY1 expressing flies show less behavioral photo-attraction to the violet lit environment (Figure 3-16B, D). The average % activity plots for each CRY expressing genotype shows AeCRY1 expressing flies show significantly the least behavioral activity in low intensity violet-light while DmCRY expressing flies show significantly the most behavioral activity in low intensity violet-light (Figure 3-16E). Control *cry-null* and DmCRY expressing flies

both behaviorally avoid high intensity violet-light (400 μW/cm², Figure 3-17A), except during the first 10 minutes of violet-light exposure for DmCRY expressing flies. The behavioral responses to high intensity violet-light are divergent between AgCRY1 and AeCRY1 expressing flies: AgCRY1 expressing flies behaviorally avoid high intensity violet-light while AeCRY1 expressing flies are behaviorally attracted to high intensity violet-light, consistent with the previously reported general attraction of *Ae. aegypti* mosquitoes to all visible light wavelengths (Figure 3-17A-E, also see results from a previous study [19]). The average % activity plots for each CRY expressing genotype shows that AeCRY1 expressing flies show significantly the greatest behavioral activity in high intensity violet-light while AgCRY1 expressing flies show significantly the least behavioral activity in high intensity violet-light (Figure 3-17E). Taken together for responses to varying intensities of violet-light, these complex behavioral effects may be due either to direct effects through mosquito CRY proteins or possibly due to unknown CRY interactions with the major violet-light sensor Rh7 that co-expresses in the LNv subgroups to mediate multi-photoreceptor inputs for light attraction/avoidance behavioral responses [2,8,9], or image forming photoreception in the eyes Altogether, these results indicate the blue and violet-light intensity-dependent light attraction/avoidance behaviors significantly diverge between AeCRY1 and AgCRY1 expressing flies and that these behavioral results are consistent with the distinct diurnal and nocturnal mosquito attraction/avoidance responses to short-wavelength light. Taken together, the data provides further support to our conclusions that CRY photoreceptors mediate species-specific physiological and behavioral light responses [19,91].

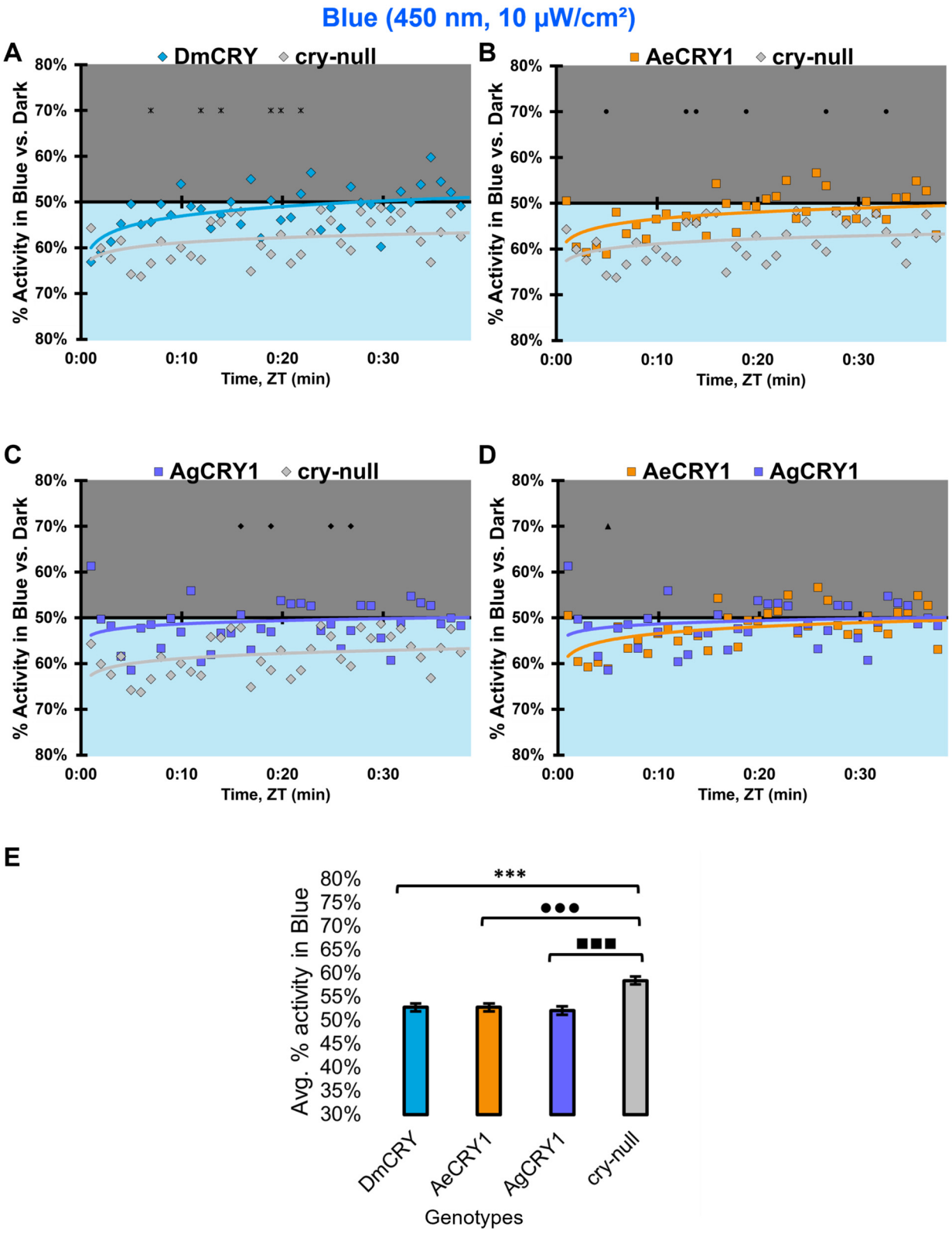
Blue (450 nm, 10 µW/cm²)
A
DmCRY
cry-null
B
AeCRY1
cry-null
C
AgCRY1
cry-null
D
AeCRY1
AgCRY1
% Activity in Blue vs. Dark
80%
70%
60%
50%
60%
70%
80%
0:00
0:10
0:20
0:30
Time, ZT (min)
E
Avg. % activity in Blue
80%
75%
70%
65%
60%
55%
50%
45%
40%
35%
30%
***
●●●
■■■
DmCRY
AeCRY1
AgCRY1
cry-null
Genotypes

Figure 3-14. All transgenic groups exhibit little or no behavioral attraction to low-intensity blue-light

(A-D) Blue attraction/avoidance behavior is measured by % activity in a dark shaded environment versus a low-intensity (10 μW/cm^2) blue-light-exposed environments (450 nm) during the light phase of a standard 12:12 hr LD cycle. Preference is calculated by percentage of activity in each environment over total activity for each time bin for **(A)** DmCRY (blue, n=53) vs. *cry-null* (red, n=53), **(B)** diurnal AeCRY1 (orange, n=46) vs. *cry-null*, **(C)** nocturnal AgCRY1 (purple, n=47) vs. *cry-null*, and **(D)** AeCRY1 vs. AgCRY1. All plots are shown from ZT0-30 min in 1-min bins. **(E)** Quantified mean % activity of flies in blue environment across the first 30 minutes for low-intensity blue-light environments. Black ***** indicates two-sample t-test $p \leq 0.05$ between DmCRY/cry24 and *cry-null*. Black ● indicates two-sample t-test $p \leq 0.05$ between AeCRY1/cry24 and *cry-null*. Black ■ indicates two-sample t-test $p \leq 0.05$ between AgCRY1/cry24 and *cry-null*. Black ▲ indicates two-sample t-test $p \leq 0.05$ between AgCRY1/cry24 and AeCRY1/cry24. Data are represented as mean ± SEM. One significance symbol; $p \leq 0.05$, two significance symbols; $p \leq 0.005$, three significance symbols; $p \leq 0.001$.

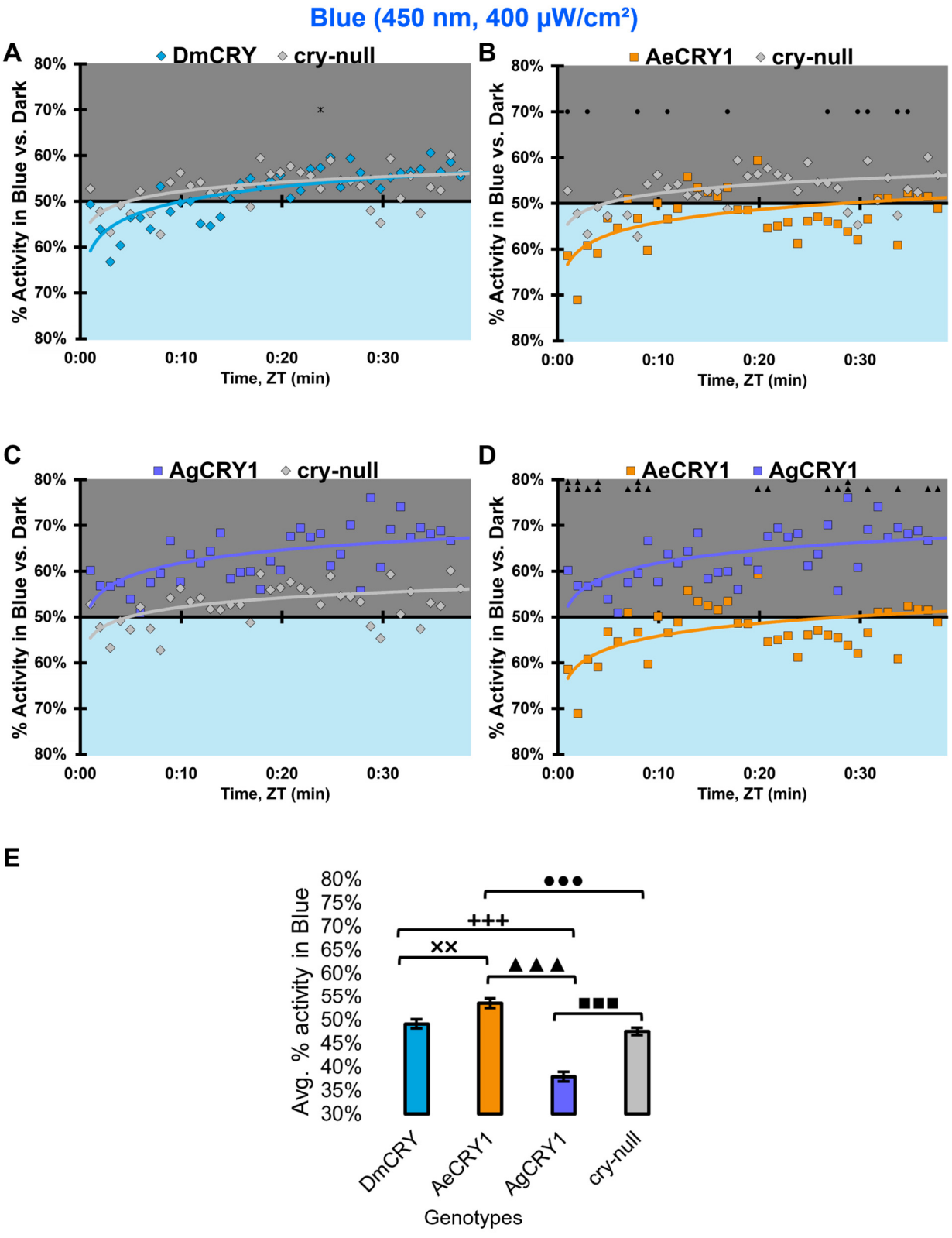
Blue (450 nm, 400 µW/cm²)
A
DmCRY
cry-null
B
AeCRY1
cry-null
C
AgCRY1
cry-null
D
AeCRY1
AgCRY1
% Activity in Blue vs. Dark
80%
70%
60%
50%
60%
70%
80%
0:00
0:10
0:20
0:30
Time, ZT (min)
E
Avg. % activity in Blue
80%
75%
70%
65%
60%
55%
50%
45%
40%
35%
30%
●●●
+++
××
▲▲▲
■■■
DmCRY
AeCRY1
AgCRY1
cry-null
Genotypes

Figure 3-15. AgCRY1 flies behaviorally avoid high-intensity blue-light

(A-D) Blue attraction/avoidance behavior is measured by % activity in a dark shaded environment versus a high-intensity (400 $\mu W/cm^2$) blue-light-exposed environments (450 nm) during the light phase of a standard 12:12 hr LD cycle. Preference is calculated by percentage of activity in each environment over total activity for each time bin for **(A)** DmCRY (blue, n=52) vs. *cry-null* (red, n=51), **(B)** diurnal AeCRY1 (orange, n=39) vs. *cry-null*, **(C)** nocturnal AgCRY1 (purple, n=46) vs. *cry-null*), and **(D)** AeCRY1 vs. AgCRY1. All plots are shown from ZT0-30 min in 1-min bins. **(E)** Quantified mean % activity of flies in blue environment across the first 30 minutes for high-intensity blue-light environments. Black ***** indicates two-sample t-test $p \leq 0.05$ between DmCRY/cry24 and *cry-null*. Black ● indicates two-sample t-test $p \leq 0.05$ between AeCRY1/cry24 and *cry-null*. Black ▲ indicates two-sample t-test $p \leq 0.05$ between AgCRY1/cry24 and AeCRY1/cry24. Black **+** indicates two-sample t-test $p \leq 0.05$ between AgCRY1/cry24 and DmCRY/cry24. Black **x** indicates two-sample t-test $p \leq 0.05$ between AeCRY1/cry24 and DmCRY/cry24. Data are represented as mean ± SEM. One significance symbol; $p \leq 0.05$, two significance symbols; $p \leq 0.005$, three significance symbols; $p \leq 0.001$.

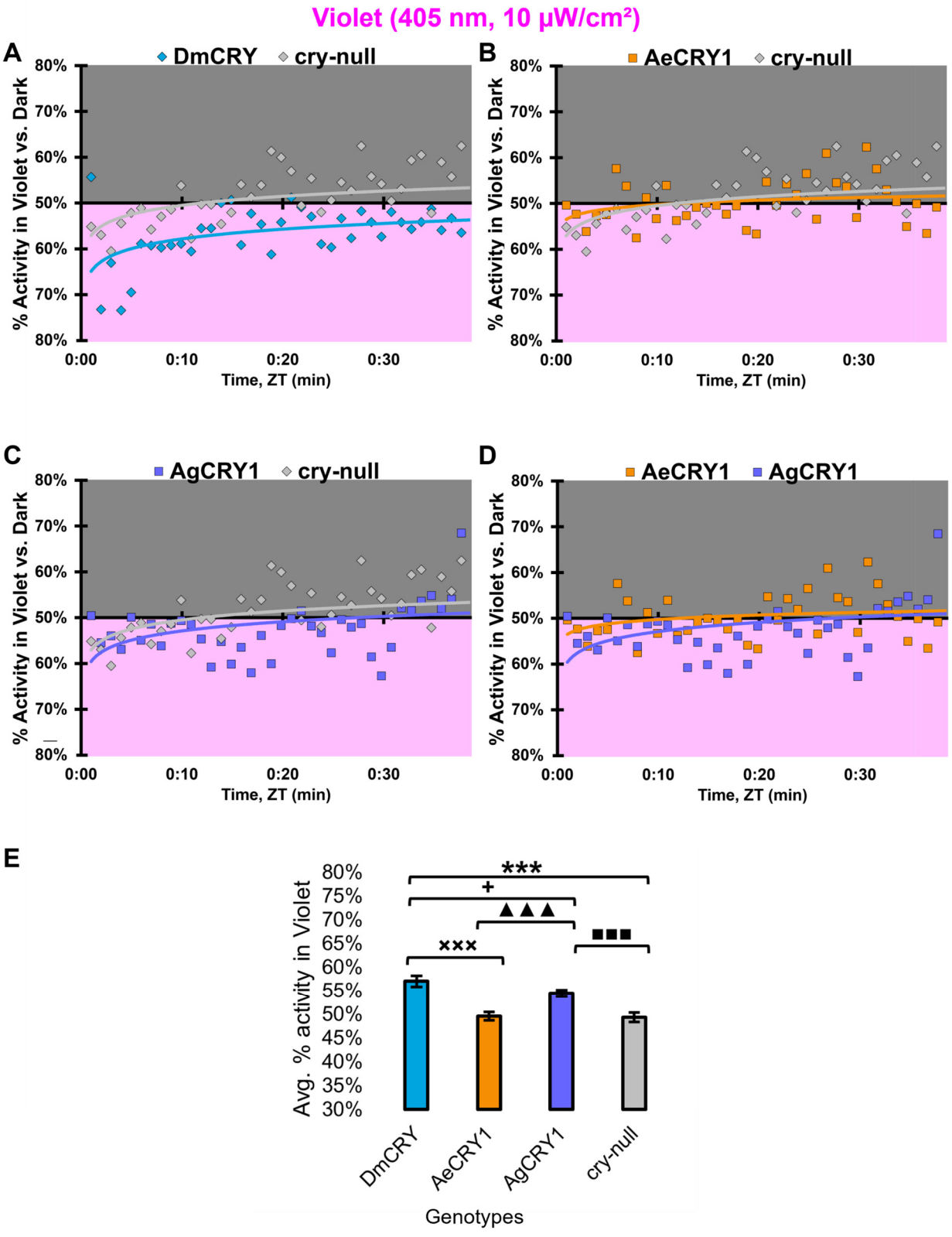
Violet (405 nm, 10 µW/cm²)
A
DmCRY
cry-null
B
AeCRY1
cry-null
C
AgCRY1
cry-null
D
AeCRY1
AgCRY1
% Activity in Violet vs. Dark
80%
70%
60%
50%
60%
70%
80%
0:00
0:10
0:20
0:30
Time, ZT (min)
E
Avg. % activity in Violet
80%
75%
70%
65%
60%
55%
50%
45%
40%
35%
30%
***
+
▲▲▲
■■■
×××
DmCRY
AeCRY1
AgCRY1
cry-null
Genotypes

Figure 3-16. All transgenic groups exhibit weak-moderate behavioral attraction to low-intensity violet-light

(A-D) Violet attraction/avoidance behavior is measured by % activity in a dark shaded environment versus a moderately low-intensity (10 μW/cm^2) violet-light-exposed environments (405 nm) during the light phase of a standard 12:12 hr LD cycle. Preference is calculated by percentage of activity in each environment over total activity for each time bin for **(A)** DmCRY (blue, n=43) vs. *cry-null* (red, n=42), **(B)** diurnal AeCRY1 (orange, n=35) vs. *cry-null*, **(C)** nocturnal AgCRY1 (purple, n=36) vs. *cry-null*, and **(D)** AeCRY1 vs. AgCRY1. All plots are shown from ZT0-30 min in 1-min bins. **(E)** Quantified mean % activity of flies in violet environment across the first 30 minutes for moderately low-intensity violet-light environments. Black + indicates two-sample t-test $p \leq 0.05$ between AgCRY1/cry24 and DmCRY/cry24. Black **x** indicates two-sample t-test $p \leq 0.05$ between AeCRY1/cry24 and DmCRY/cry24. Black ▲ indicates two-sample t-test $p \leq 0.05$ between AgCRY1/cry24 and AeCRY1/cry24. Data are represented as mean ± SEM. One significance symbol; $p \leq 0.05$, two significance symbols; $p \leq 0.005$, three significance symbols; $p \leq 0.001$.

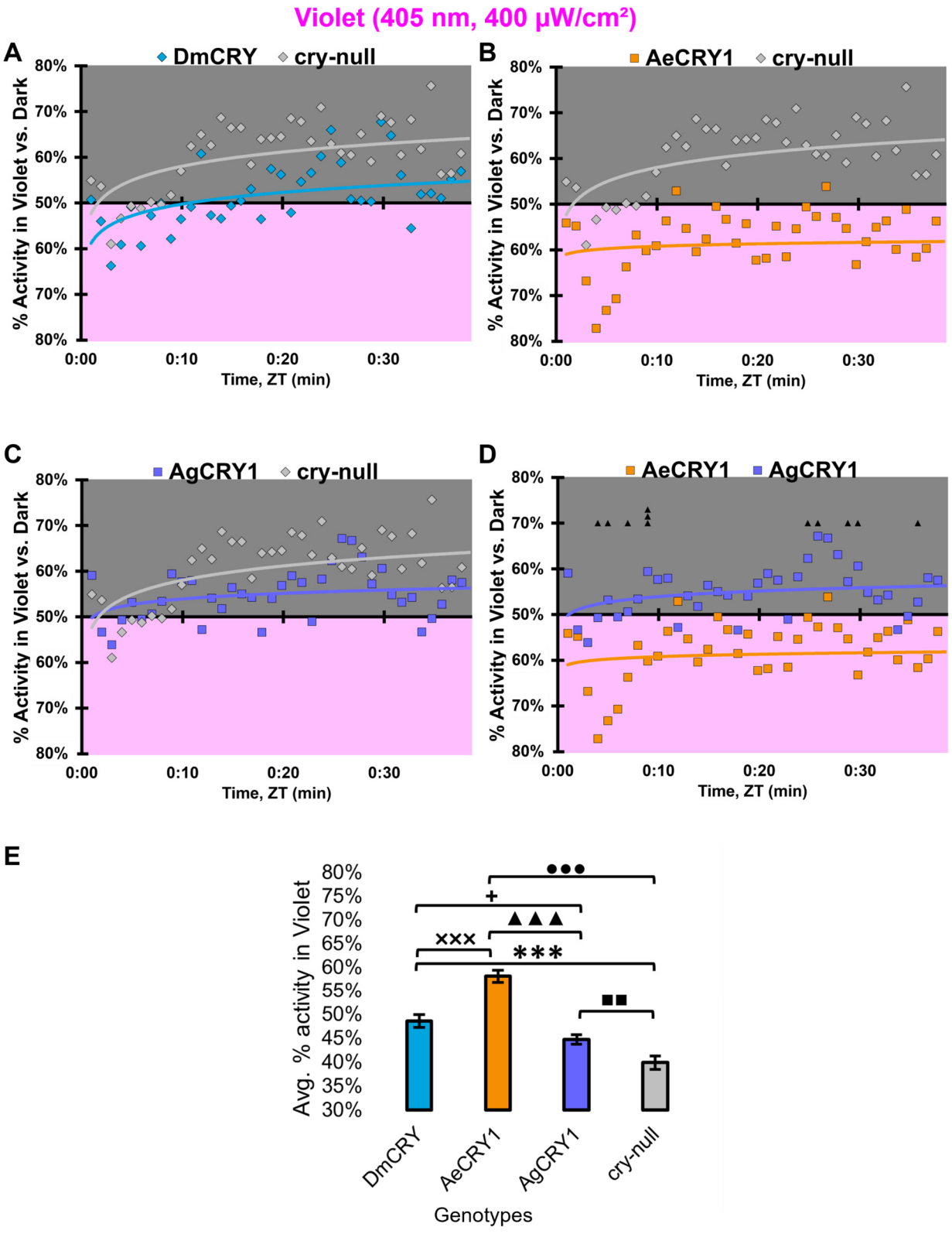
Violet (405 nm, 400 µW/cm²)
A
DmCRY
cry-null
B
AeCRY1
cry-null
C
AgCRY1
cry-null
D
AeCRY1
AgCRY1
% Activity in Violet vs. Dark
80%
70%
60%
50%
60%
70%
80%
0:00
0:10
0:20
0:30
Time, ZT (min)
E
Avg. % activity in Violet
80%
75%
70%
65%
60%
55%
50%
45%
40%
35%
30%
●●●
+
▲▲▲
×××
***
■■
DmCRY
AeCRY1
AgCRY1
cry-null
Genotypes

Figure 3-17. AeCRY1 flies exhibit behavioral attraction to high intensity violet-light

(A-D) Violet attraction/avoidance behavior is measured by % activity in a dark shaded environment versus a high-intensity (400 μW/cm^2) violet-light-exposed environments (405 nm) during the light phase of a standard 12:12 hr LD cycle. Preference is calculated by percentage of activity in each environment over total activity for each time bin for **(A)** DmCRY (blue, n=35) vs. *cry-null* (red, n=40), **(B)** diurnal AeCRY1 (orange, n=34) vs. *cry-null*, **(C)** nocturnal AgCRY1 (purple, n=40) vs. *cry-null*, and **(D)** AeCRY1 vs. AgCRY1. All plots are shown from ZT0-30 min in 1-min bins. **(E)** Quantified mean % activity of flies in violet environment across the first 30 minutes for high-intensity violet-light environments. Black ▲ indicates two-sample t-test $p \leq 0.05$ between AgCRY1/cry24 and AeCRY1/cry24. Black + indicates two-sample t-test $p \leq 0.05$ between AgCRY1/cry24 and DmCRY/cry24. Black **x** indicates two-sample t-test $p \leq 0.05$ between AeCRY1/cry24 and DmCRY/cry24. Data are represented as mean ± SEM. One significance symbol; $p \leq 0.05$, two significance symbols; $p \leq 0.005$, three significance symbols; $p \leq 0.001$.

3.4 Discussion

This work was motivated by our recent findings that diurnal *Ae. aegypti* mosquitoes and nocturnal *An. coluzzii* (gambiae sub-family) mosquitoes exhibit very different attraction/avoidance behavioral responses to different light spectra that vary by time of day; and that these light driven behaviors are modulated by CRY in mosquitoes [19]. We considered multiple hypotheses that might account for the distinct physiological light responses of diurnal and nocturnal mosquitoes and tested the simplest and most tractable hypothesis: informed by earlier work showing that *Drosophila* CRY codes for light avoidance responses to high intensity short wavelength light [8–10], we tested the hypothesis that there are species-specific differences in the CRY light responses between *Ae. aegypti* and *An. gambiae* -family mosquitoes, predicting that nocturnal *An. gambiae* CRY1 exhibits stronger electrophysiological and behavioral responses to blue-light than *Ae. aegypti* CRY1. For the present work, the comparison between blue and violet-light responses is logically dictated by the relative spectral absorbance profiles of two non-imaging forming

photoreceptors, CRY and Rh7 [2,7]. Rh7 exhibits a broad absorption spectrum that peaks in the violet range while the base state of CRY shows a trough in the violet range of the spectra.

We recently published a related study comparing the effects of expressing the light sensitive CRYs from *Ae. aegypti* (AeCRY1), *An. gambiae* (AgCRY1), and *Drosophila melanogaster* (DmCRY, a positive control in a *cry-null Drosophila melanogaster* genetic background) in a previous study [91]. While DmCRY is included as a positive control for the physiological assays, we acknowledge that DmCRY is a native protein in flies while mosquito CRYs are heterologously expressed. AeCRY1 is much less light sensitive than either AgCRY1 or DmCRY as shown by numerous physiological assays including partial behavioral rhythmicity seen in AeCRY1 expressing flies following constant light exposure [91] and herein. Remarkably, expression of nocturnal AgCRY1 confers low survival to constant white light exposure as does expression of AeCRY1 to a much lesser extent, which may contribute to enforcing species-specific time-of-day behavioral activity. In that study, we show that AgCRY1 mediates significantly stronger electrophysiological cell autonomous responses to 365 nm ultraviolet (UV) light relative to AeCRY1 [91]. Further, AgCRY1 expression mediates electrophysiological and behavioral sensitivity to 635 nm red-light while AeCRY1 does not, consistent with species-specific mosquito red-light responses [19,91]. AgCRY1 and DmCRY mediate intensity-dependent avoidance behavior to UV light at different light intensity thresholds, while AeCRY1 does not, thus mimicking mosquito and fly behaviors [91]. These findings along with the present findings showing physiological responses to blue and violet-light collectively highlight CRY as a key non-image forming visual photoreceptor that mediates physiological and behavioral light-responses in a species-specific fashion.

Several mechanisms mediate inter-protein signaling following CRY light activation. For CRY mediated clock resetting in *Drosophila*, there is clear evidence that light activation leads to conformational changes in the CRY c-terminal tail that signal to downstream proteins [87,93,113]. However, CRY mediated light-evoked increases in action potential firing rate is still observed in flies that express a C-terminal truncated form of CRY [1]. This response remains relatively poorly resolved as it has not yet been examined using evoked potential analysis of membrane depolarization, a method that shows greater kinetic details of light evoked electrophysiological responses [3,91]. The other CRY signaling mechanism involves inter-protein redox transfer for which the voltage-gated potassium beta subunit acts as a redox sensor and couple light activated CRY to changes in potassium channel activity [6,8–10,90]. CRY phototransduction is mediated by light-evoked changes in the FAD redox state from an oxidized base state that absorbs UV (365 nm peak) and blue-light (450 nm) peak to its FAD•- anionic semiquinone semi-reduced state that also absorbs UV [4,37,39,62,63]. Photoactivation of the CRY FAD•- anionic semiquinone semi-reduced state yields the FADH• neutral radical state [64] which absorbs a broad peak between 580 to 640 nm (yellow to red) and a sharper peak at 325 nm (UV). We have yet to explore CRY physiological light responses to 325 nm UV light. Red-light photoactivation of the CRY FADH• neutral radical state is best characterized in plant CRYs, but more recent work shows that insect CRYs are also physiologically activated by red-light. This indicates that the CRY FADH• neutral radical state occurs *in vivo* [3,39,91]. Most of the biophysical work done on the spectral absorbance properties of insect CRY proteins uses purified protein preparations. It appears that purified insect wild type CRYs do not absorb red-light when not in native cellular conditions [4,62,92–94]. It remains to be determined whether downstream signaling proteins like voltage-gated potassium subunits contribute further to species-specific differences in mosquito physiological light responses.

An alternative hypothesis for species-specific physiological light responses is based on comparative neuroanatomical analysis of diurnal *Ae. aegypti* mosquitoes and nocturnal *An. coluzzii* mosquitoes, differences in species-specific neural circuits, including PDF and PER expressing neurons may dictate attraction/avoidance behavioral light responses. Using antibodies against the well conserved PDF and PER proteins, which cross-react across a wide range of insect species, there are both similar and species-distinct features of PDF and PER expressing neural circuits of *Ae. aegypti* and *An. coluzzii* mosquitoes. PDF and PER proteins are co-expressed in the ventral lateral area in both *Ae. aegypti* and *An. coluzzii* mosquito female adult brains that can be identified as large- (l-LNvs) and small-ventral lateral neurons (s-LNvs) based on their morphological projections common to the very well characterized brains of *Drosophila melanogaster* and other insect species [19]. These include the large PDF+ neuronal arbors in the optic lobes that likely project from the l-LNvs and PDF+ dorsal projections to the putative dorsal neurons (DNs) that likely project from the s-LNvs for both mosquito species [19,114]. There are noteworthy differences between *Ae. aegypti* and *An. coluzzii* mosquito female adult brains for their PDF and PER neural circuits, notably that for *An. coluzzii*, PDF+ putative s-LNv dorsal projections continue medially to the pars intercerebralis (PI) region, a major neuroendocrine center in insect brains [115]. The PI region integrates feeding and circadian information in insulin-like peptide expressing PI neurons [116]. In contrast, this distinct s-LNv to PI neural projection is absent in *Ae. aegypti* mosquito female adult brains [19]. Another species-specific difference between *Ae. aegypti* and *An. coluzzii* mosquitoes is a midline crossing contralateral projection of PDF+ putative l-LNvs that is detected in *An. coluzzii* mosquito female adult brains, but is not detected in *Ae. aegypti* adult female brains [19]. There are entire neuronal groups that can be found in one mosquito species but not the other, notably ~5 PER+/PDF- neurons that are detected in the medial-anterior region of *Ae. aegypti* female brains

but are not seen in *An. coluzzii* mosquito female adult brains [19]. Reciprocally, there are ~7 PER+/PDF- neurons in the PI region in *An. coluzzii* that are not detected in *Ae. Aegypti* [19]. These similarities and differences in diurnal versus nocturnal mosquito PDF and PER expressing neural circuits are intriguing and while we cannot yet determine at present how much they may contribute to attraction/avoidance behavioral light responses; the results herein indicate that CRY1s themselves are sufficient to confer similar species-specific light responses observed in behaving mosquitoes. It would be interesting to express diurnal *Aedes* mosquito CRY1 in a nocturnal *Anopheles* mosquito and see how this transgenic mosquito behaves in response to different light wavelengths using the light attraction/avoidance assay, along with the reciprocal experiment of expressing nocturnal *Anopheles* CRY1 in diurnal *Aedes* mosquitoes.

These findings have interesting implications for evolutionary aspects of behavior and speciation. Many insects express two forms of CRY: light sensitive CRY1s and light insensitive CRY2s which act as transcriptional repressors [56]. The evolutionary divergence between CRY1s and CRY2s appear to have occurred prior to the Cambrian radiation as multiple *cry* genes are found in sponges, an early metazoan that precedes the evolution of animal opsins [117]. Different mosquito species have evolved distinct circadian timing of behaviors according to their temporal/ecological niches, including diurnal (*Ae. aegypti*) and nocturnal (*An. coluzzii*). Numerous mosquito species-specific behaviors change with time-of-day, including flight activity, mating, oviposition, and biting [21,22]. Such behaviors enforce speciation [118]. Due to their large impact on health and ecology, more work on the basis of diurnality/nocturnality, behavioral timing and how species-specific niches are enforced in mosquitoes is merited.

Reprinted with permission from:

Au, D. D. *et al.* Nocturnal mosquito Cryptochrome 1 mediates greater electrophysiological and behavioral responses to blue light relative to diurnal mosquito Cryptochrome 1. *Front. Neurosci.* **16**, 1042508 (2022).

CHAPTER 4: *Drosophila* photoreceptor systems converge in arousal neurons as a possible coincidence detector

4.1 Introduction

Light provides sensory cues to many animals for navigating their environment. In insects like *Drosophila*, short-wavelength light has robust effects on visual behaviors, such as circadian entrainment, phototaxis, sleep/wake, and arousal that are mediated in part by non-image forming mechanisms based on two deep-brain photopigments: Cryptochrome (CRY) and Rhodopsin 7 (Rh7) [2,6,8–10,12,13,77,119–121]. CRY is a light-sensitive photopigment that was initially identified in flies based on its role in light entraining fly circadian rhythm. CRY binds to TIMELESS (TIM) and PERIOD (PER) clock protein heteromultimeric complexes. Light-activated conformational changes of CRY's C-terminal tail initiates a degradation cascade of co-complexed clock protein TIM and PER, thus calibrating/resetting the transcription-translation loop circadian clock [45,88,122]. CRY photoactivation also depends on electron transfer between multiple tryptophan residues embedded within the structure that result in photoreduction of CRY's chromophore, flavin adenine dinucleotide (FAD) [3–5,37,38,94,123]. CRY photoactivation also evokes robust increases in neuronal electrical excitability via redox coupled interactions with voltage-gated potassium channel beta subunits (Kvβ) Hyperkinetic (Hk) [1,6,10]. Rh7 is a spectrally broad bistable photopigment with an absorbance peak around violet (~400 nm) light couples to the Gq/PLC signaling pathway [2,7]. Both CRY and Rh7 are highly expressed in many of the neurons of the circadian/arousal neural circuit [1,2,13,40,41,77,78], including the lateral ventral neurons (LNvs), which use light input to tune many physiological and behavioral processes of the fly as noted above [6,13–15,79–84]. Flies and other insects

also navigate their environments using six external rhodopsin photoreceptors found in the compound eyes, the Hofbauer-Buchner (HB) eyelet, and the ocelli that contribute to image-forming and non-image forming visual processes. Together, six rhodopsin photopigments, Rhodopsin 1-6 (Rh1-6), mediate a broad range of spectral sensitivity from UV to red (~300-630 nm) light [124–128]. CRY and Rh7 are also expressed in these external photoreceptor structures, where they may play a role in modulating visual sensitivity gain control. Previous work shows that circadian photoreception and light attraction/avoidance behaviors are coordinately regulated by all three cell-autonomous photoreceptive pathways (CRY, Rh7, external photoreceptors), which input to the LNvs, and provide functional redundancy for these important behaviors [2,8,9,11–13,78,100,129–137].

Most of the LNv light-activated arousal neurons express the circadian neuropeptide pigment-dispersing factor (PDF) and can be further categorized as small and large (s-LNvs and l-LNvs, respectively) that are each uniquely capable of transmitting light information that contribute to endogenous circadian timekeeping or wakefulness/arousal. Light-activated s-LNvs trigger the release of PDF to entrain Dorsal neurons (DNs), Lateral Dorsal neurons (LNds), and other circadian pacemaker neurons, while l-LNvs receive inputs from CRY, Rh7, or the external photoreceptors to trigger PDF release in the accessory medulla (aME) to signal light information to s-LNvs, LNds, and other clock neurons [137–143]. Additionally, l-LNvs exhibit both rapid and long-lasting excitatory electrophysiological events upon short-wavelength light exposure as marked by an increase in firing frequency (FF) and membrane depolarization lasting 10s of seconds from stimulus onset [1,3,6,10,102]. This phenomenon is thought to be driven primarily by the CRY/Hk and Rh7 photoreceptor systems. However, l-LNvs also exhibit acute responses to red light (~635 nm) that, albeit weaker, persist in a *cry-null* system [3,91]. In terms of l-LNv photoexcitability, this suggests a possible input contribution from red-sensitive rhodopsin photopigments (Rh1 and Rh6)

from the external photoreceptor structures or direct effects mediated by CRY and/or Rh7. While circadian photoentrainment is primarily modulated by CRY, flies are still able to entrain to Light:Dark (LD) cycles in a CRY-independent manner, also suggesting that light inputs to LNvs and the rest of the clock circuitry is mediated by external opsin-based photoreceptor structures and/or Rh7. Further evidence suggests that different properties of light (intensity, exposure timing, spectral composition) recruit different photoreceptors for photoentrainment [144] and light attraction/avoidance behaviors [9]. Anatomically, external photoreceptor structures project either directly into the aME or indirectly via lamina monopolar cells that project to the aME [145]. It has been proposed that the aME acts as a central hub for parallel light input circuits from the external photoreceptor system to the clock circuit for photoentrainment [111], but the extent of how all three photoreceptor systems functionally contribute to light evoked neuronal photoexcitation and behavioral arousal remain largely unknown.

Here, we comprehensively explore the functional contributions of the light input pathways from the three distinct external and internal photoreceptor systems that activate LNvs electrical excitability and the relative contributions of these three distinct photoreceptor systems to the fly's arousal responses to UV, violet, blue, and red light stimuli. We employ the light-evoked whole-cell current clamp electrophysiology assay to measure l-LNvs responses to intensity matched UV, violet, blue, and red light, comparing control versus fly mutants that lack photoreceptor inputs *gl60j*, *cry-null*, *rh7-null*, and double mutant *gl60j-cry-null* flies. In a parallel set of studies, we use a light-pulse arousal assay to measure behavioral responses to intensity matched UV, violet, blue, and red light, measuring light-triggered wakefulness from sleep for controls and each fly mutant at two different levels of light intensity. We find that all photoreceptor systems functionally integrate in l-LNvs to enable light-evoked electrophysiological excitability. We find similarly that

all light input channels contribute to arousal behavioral responses to light. Identifying a functional connection between each of the fly photoreceptor systems strengthens an emerging model that insect image-forming and non-image forming visual processes work together in a coordinate fashion to mediate complex light-evoked behaviors.

4.2 Materials and Methods

4.2.1 Experimental Animals

Our experimental flies were allowed ad libitum access to a standard food media consisting of yeast, cornmeal, and agar at 25±1 ºC and 40-60% relative humidity in 12:12 hr Light:Dark cycles during behavioral experiments. All flies used in the experiments are 3 to 4-day post-eclosion adult male flies. We obtained our *rh7-null*, *gl60j*, and *gl60j-cry-null* mutant flies through a prior collaboration with Craig Montell of UC Santa Barbara, and *cry-null* mutant flies from Amita Seghal of University of Pennsylvania. Once obtained, we crossed each photoreceptor mutant with a *pdfGAL4-p12c* driver line to drive expression of GFP in all PDF+ neurons in order to visualize l-LNvs for patch-clamp electrophysiology. The *p12c* mutation was previously developed in our lab to mark GAL4 protein expression with GFP. Large lateral ventral neurons were identified by size, morphology, and anatomical positioning. Our wild-type control is the *pdfGAL4-p12c* driver line.

4.2.2 Light-Evoked Neuronal Electrophysiology

We adapted our light-evoked potential electrophysiology assays established in a previous study [3] to measure adult male fly brain's large lateral ventral neuronal responses to various light stimuli. Flies are dissected in an external recording solution comprised of the following components: 122 mM NaCl, 3 mM KCl, 1.8 mM CaCl2, 0.8 mM MgCl2, 5 mM glucose, 10 mM HEPES, and calibrated to a pH of 7.2±.02 and osmolarity of 250-255 mOsm. The internal recording solution is comprised of the following components: 102 mM Kgluconate, 17 mM NaCl, 0.085 mM CaCl2, 1.7 mM MgCl2 (hexahydrate), 8.5 mM HEPES, 0.94 mM EGTA, and is calibrated to a pH of 7.2±.02 and osmolarity of 232-235 mOsm. Our custom multichannel LED source (Prizmatix/Stanford Photonics, Palo Alto, CA) is fitted onto an Olympus BX51 WI microscope and was used as our primary light source for light-evoked potential recordings. The LED are tuned to the following wavelengths of color: UV (365 nm), violet (405 nm), blue (450 nm), and red (635 nm), and all exposures were set to an intensity of 200 μW/cm² by use of a Newport 842-PE Power/Energy meter. Transistor-Transistor-Logic (TTL) triggered LEDs programmed by the data acquisition software, pClamp (Molecular Dynamics), enabled rapid on/off light stimuli with the following protocol: 50 seconds of dark for baseline recording, 5 seconds of colored-light stimulation, then 95 seconds of inter-pulse darkness for firing frequency and membrane potential baseline recovery. We measure five continuously repeated sweeps per recording to allow for greater statistical confidence in our measurements, which are analyzed as follows: firing frequency is determined by counting spikes per 10 second interval per 100 second sweep, then calculated as a firing frequency ratio by the average number of spikes during lights on over the average number of spikes per 10 second interval pre-light stimulus. These ratios are averaged across the five repeated sweeps per recording for all samples of the same light-stimulus

in the genotype set. This custom light-evoked potential protocol allows greater measurements for kinetically robust light-evoked effects in our samples.

4.2.3 Light-Pulse Arousal Behavioral Assay

Standard LD light pulse arousal assays were conducted from previously established and adapted protocols [10]. The locomotor activity of individual flies was measured using the TriKinetics Locomotor Activity Monitoring System via infrared beam-crossing, recording total crosses in 1-min bins. Percentage activity and statistics were measured using Microsoft Excel. Custom LED fixtures were built using Waveform Lighting blue, violet, UV, and red LEDs with a narrow peak wavelength of 450 nm, 405 nm, 365 nm, and 635 nm respectively, and intensity-tuned to 10 $\mu W/cm^2$ and 400 $\mu W/cm^2$ for low and high intensity light exposures, respectively.

4.2.4 Quantification and Statistical Analysis

All reported values are represented as mean ± SEM. Values of n refer to the total number of experimental flies tested over all replicates of an experiment (minimum of three replicates). Firing frequency values are calculated as a ratio of spikes during the 5 seconds of lights on/average baseline firing rate binned in 10 second increments. Statistical tests were performed using Minitab, Matlab, and Microsoft Excel software. Statistical analysis began with performing an Anderson-Darling normality tests to determine normality of data. Variance was determined using F-tests for normally distributed data, then significance was determined using two-sample, one-tailed T-tests with alpha values of 0.5 before pairwise correction. Significance for non-normal data was determined by Mann-Whitney U-tests. Spike firing quantifications were performed using custom Matlab scripts and Clampfit software. Multi-comparison tests leading to Type I error/false

positives were mitigated by p-value adjustment based on false discovery rate (FDR [44]). A standard FDR threshold of 0.1 was then implemented in order to indicate significance as an expected proportion of false positives that is no greater than 10%.

4.3 Results

4.3.1 Light excitation of arousal neurons to short-wavelength light relies on input coincident of multiple photoreceptor systems

Physiological and anatomical evidence indicates the convergence of multiple photoreceptor channels on the LNvs [2,9,11–13,78,111,129–131,135,137,144,145]. CRY light activation is based successive redox reduction of its flavin adenine dinucleotide (FAD) starting at a base oxidized state with two absorption peaks corresponding to ultraviolet (UV, 365 nm) and blue (450 nm) light [37,62,63]. Higher reduction states of CRY confer light-evoked excitation by red light (635 nm) due to spectral absorption peak shifts. Light evoked redox transfer reactions mediated by FAD in CRY are transduced to changes in membrane potential and neuronal excitability through voltage gated potassium channel beta subunit, Hyperkinetic [1,6,10,102]. Rh7 exhibits a very broad absorption that peaks at violet light (405 nm) [2,120]. In order to test the relative contributions of different photoreceptor systems on l-LNv photoexcitability to short-wavelength light, we performed whole-cell current-clamp electrophysiology using 200 μW/cm² of UV (365 nm), violet (405 nm), and blue (450 nm) LED light. To test the contribution of each photoreceptor system to circadian/arousal neuronal photoexcitability to these short wavelengths, we measured the electrophysiological light responses of l-LNvs as a ratio of action potential firing frequency (FF)

during lights on/lights off, comparing control wild-type *p12c* with recordings of genetic knockouts *cry-null*, *rh7-null*, total external photoreceptor knockout *gl60j*, and a double-mutant *gl60j-cry-null* photoreceptor mutant flies using the whole-cell patch-clamp electrophysiology configuration. Recordings were performed on l-LNvs from each photoreceptor knockout group with 50 seconds of dark, 5 second exposures of 200 μW/cm² LED light for each wavelength of light, and 95 seconds of dark inter-pulse intervals in order to measure post-stimulus decay back to baseline. Each recording trace was repeated 5 times and FF ratios are reported as an average of all traces of all recordings for each group of parameters.

200 μW/cm² UV (365 nm) LED light evokes a robust 1.6-fold FF increase in recordings of *p12c* control l-LNvs (Figure 4-1A blue column). As expected, intensity matched UV light electrophysiological responses of l-LNvs are significantly attenuated in neurons recorded from *cry-null* fly brains (Figure 4-1A, blue column vs. green column) as 365 nm corresponds to one of the principal spectral absorption peaks for the base oxidized state of CRY. Intensity matched UV light electrophysiological responses of l-LNvs also are significantly attenuated to a similar degree in neurons recorded from *gl60j* and *rh7-null* fly brains (Figure 4-1A, blue column vs. red column and violet column, respectively). This indicates that opsin-based phototransduction in eyes/external photoreceptors and cell autonomously expressed Rh7 also contribute to the l-LNv electrophysiological responses to UV light. The UV photoresponse of control *p12c* that expresses both CRY and Rh-7 is not significantly different from the double mutant *gl60j-cry-null* (Figure 4-1A, blue column vs. yellow column). This may be due to the relatively high variance of double mutant *gl60j-cry-null* recordings. Short term light exposure evokes long term subsequent increases in neuronal excitation in LNvs [1,3,6,10]. In order to measure any lasting photoexcitatory effects post-stimulus, FF ratios for each knockout mutant are reported as 10 second intervals for 50 seconds

post-stimulus: FF(10 seconds post-stimulus)/FF(baseline), FF(20 seconds post-stimulus)/FF(baseline), FF(30 seconds post-stimulus)/FF(baseline), FF(40 seconds post-stimulus)/FF(baseline), and FF(50 seconds post-stimulus)/FF(baseline). There are no significant increases in FF ratio post-stimulus when comparing *p12c* versus any of the knockout mutants (Figure 4-1B-E).

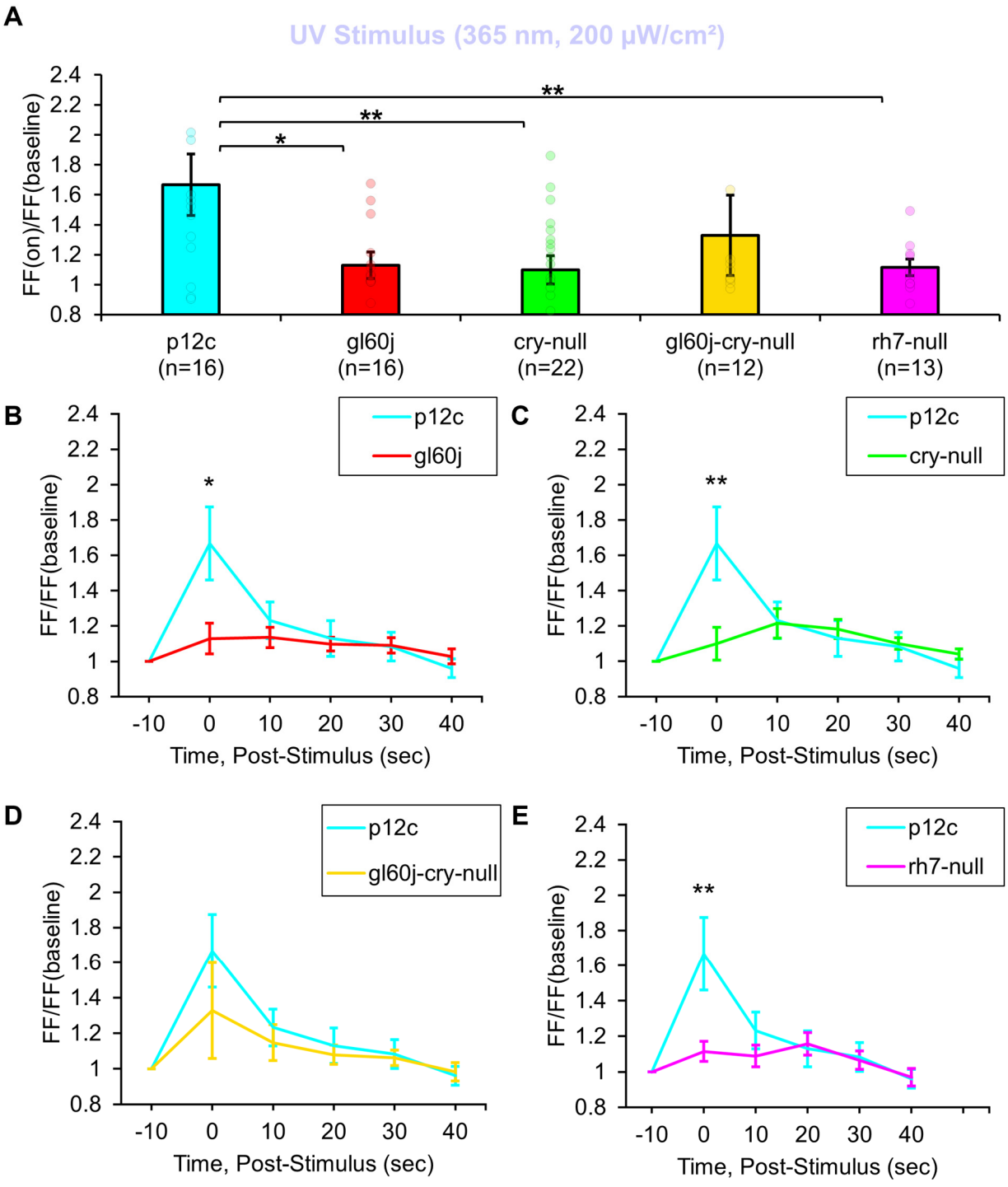
A
UV Stimulus (365 nm, 200 µW/cm²)
FF(on)/FF(baseline)
2.4
2.2
2
1.8
1.6
1.4
1.2
1
0.8
*
**
**
p12c
(n=16)
gl60j
(n=16)
cry-null
(n=22)
gl60j-cry-null
(n=12)
rh7-null
(n=13)
B
p12c
gl60j
FF/FF(baseline)
*
-10
0
10
20
30
40
Time, Post-Stimulus (sec)
C
p12c
cry-null
FF/FF(baseline)
**
Time, Post-Stimulus (sec)
D
p12c
gl60j-cry-null
FF/FF(baseline)
Time, Post-Stimulus (sec)
E
p12c
rh7-null
FF/FF(baseline)
**
Time, Post-Stimulus (sec)

Figure 4-1. All photoreceptor mutants except *gl60j-cry-null show* an attenuated UV light firing frequency (FF) compared to native expressed *Drosophila* CRY

(A) Firing frequency response of p12c (blue column, n=16) versus gl60j (red column, n=16), cry-null (green column, n=22), gl60j-cry-null (yellow column, n=12), and rh7-null (violet column, n=13) with 5 second UV (365 nm, 200 μW/cm²) light stimulus. Post-stimulus FF response in 10 minute bins for (B) p12c (blue trace) vs gl60j (red trace), (C) p12c vs cry-null (green trace), (D) p12c vs gl60j-cry-null (yellow trace), and (E) p12c vs rh7-null (violet trace). Data are plotted as average ± SEM. Pairwise comparison was analyzed using two-sample t-test with FDR adjustment. p*<0.1, p**<0.05, p***<.01.

200 μW/cm² of violet (405 nm) LED light evokes 1.8-fold increases in FF in control *p12c* l-LNvs Figure 4-2A, blue column). In contrast, intensity matched l-LNv violet light responses in FF are significantly attenuated in l-LNv recordings of *gl60j*, *rh7-null*, and double mutant *gl60j-cry-null* neurons (Figure 4-2A, blue column vs. red column, violet column, and yellow column, respectively). Unsurprisingly, *cry-null* violet light responses in FF are not significantly different from control as there is an absorption trough at 405 nm for CRY, but *cry-null* violet light responses are significantly higher compared to the *gl60j-cry-null* response (Figure 4-2A, green column vs. yellow column, respectively). Comparing the *gl60j* versus the double mutant *gl60j-cry-null* recordings of violet evoked changes in FF, this result suggests the l-LNvs responsiveness to violet light depends entirely on external and cell autonomous opsin-based photoreceptors. In comparison to control *p12c*, the post-stimulus FF ratio for violet light shows significant increases up to 10 seconds post-stimulus for *gl60j* and *gl60j-cry-null* responses (Figures 4-2B, D, respectively), and up to 20 seconds for *rh7-null* responses (Figure 4-2E).

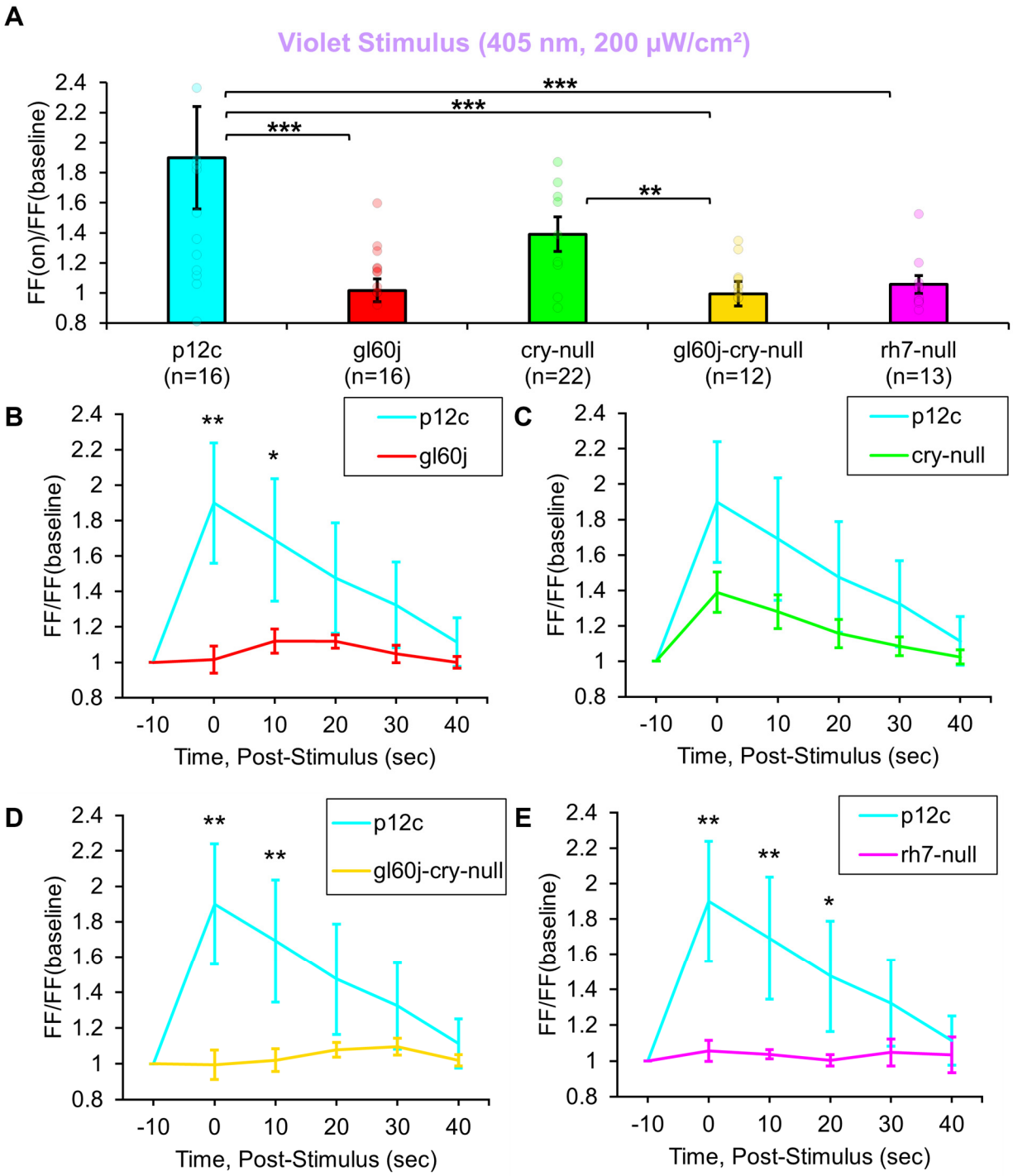
A
Violet Stimulus (405 nm, 200 μW/cm²)
FF(on)/FF(baseline)
***
***
***
**
p12c (n=16)
gl60j (n=16)
cry-null (n=22)
gl60j-cry-null (n=12)
rh7-null (n=13)
B
p12c
gl60j
FF/FF(baseline)
Time, Post-Stimulus (sec)
C
p12c
cry-null
FF/FF(baseline)
Time, Post-Stimulus (sec)
D
p12c
gl60j-cry-null
FF/FF(baseline)
Time, Post-Stimulus (sec)
E
p12c
rh7-null
FF/FF(baseline)
Time, Post-Stimulus (sec)

Figure 4-2. All photoreceptor mutants except *cry-null* show an attenuated violet light FF compared to native expressed *Drosophila* CRY

(A) Firing frequency response of p12c (blue column, n=16) versus gl60j (red column, n=16), cry-null (green column, n=22), gl60j-cry-null (yellow column, n=12), and rh7-null (violet column, n=13) with 5 second violet (405 nm, 200 μW/cm²) light stimulus. Post-stimulus FF response in 10 minute bins for (B) p12c (blue trace) vs gl60j (red trace), (C) p12c vs cry-null (green trace), (D) p12c vs gl60j-cry-null (yellow trace), and (E) p12c vs rh7-null (violet trace). Data are plotted as average ± SEM. Pairwise comparison was analyzed using two-sample t-test with FDR adjustment. p*<0.1, p**<0.05, p***<.01.

Natively expressed CRY control *p12c* l-LNvs are robustly excited by blue light exposure, showing an almost a 2-fold increase in FF (Figure 4-3A, blue column), similar to results reported previously. Compared to *p12c* controls, the genetic absence of other photoreceptors/ phototransducers including the *gl60j* mutation or *rh7-null* results in a significant attenuation of l-LNv responsiveness to blue light (Figure 4-3A, blue column vs. red column and violet column, respectively). Mutant *cry-null* show a significantly more attenuated response, as we have demonstrated previously (Figure 4-3A, blue column vs. green column). The double-mutant *gl60j-cry-null* exhibits the greatest attenuation of l-LNv responsiveness to blue light (Figure 4-3A, yellow column) suggesting a compounding effect from loss of photoreception from both systems. Blue light-responses are also long-lasting for the *p12c* control group compared to *gl60j* and *cry-null*, with *p12c* having a sustained FF ratio increase lasting up to 20 seconds post-stimulus (Figures 4-3B, 4-3C, respectively). In comparison to *rh7-null* and the double mutant *gl60j-cry-null*, the control blue light response persists for even longer, up to 30 seconds post-stimulus (Figures 4-3D, E, respectively).

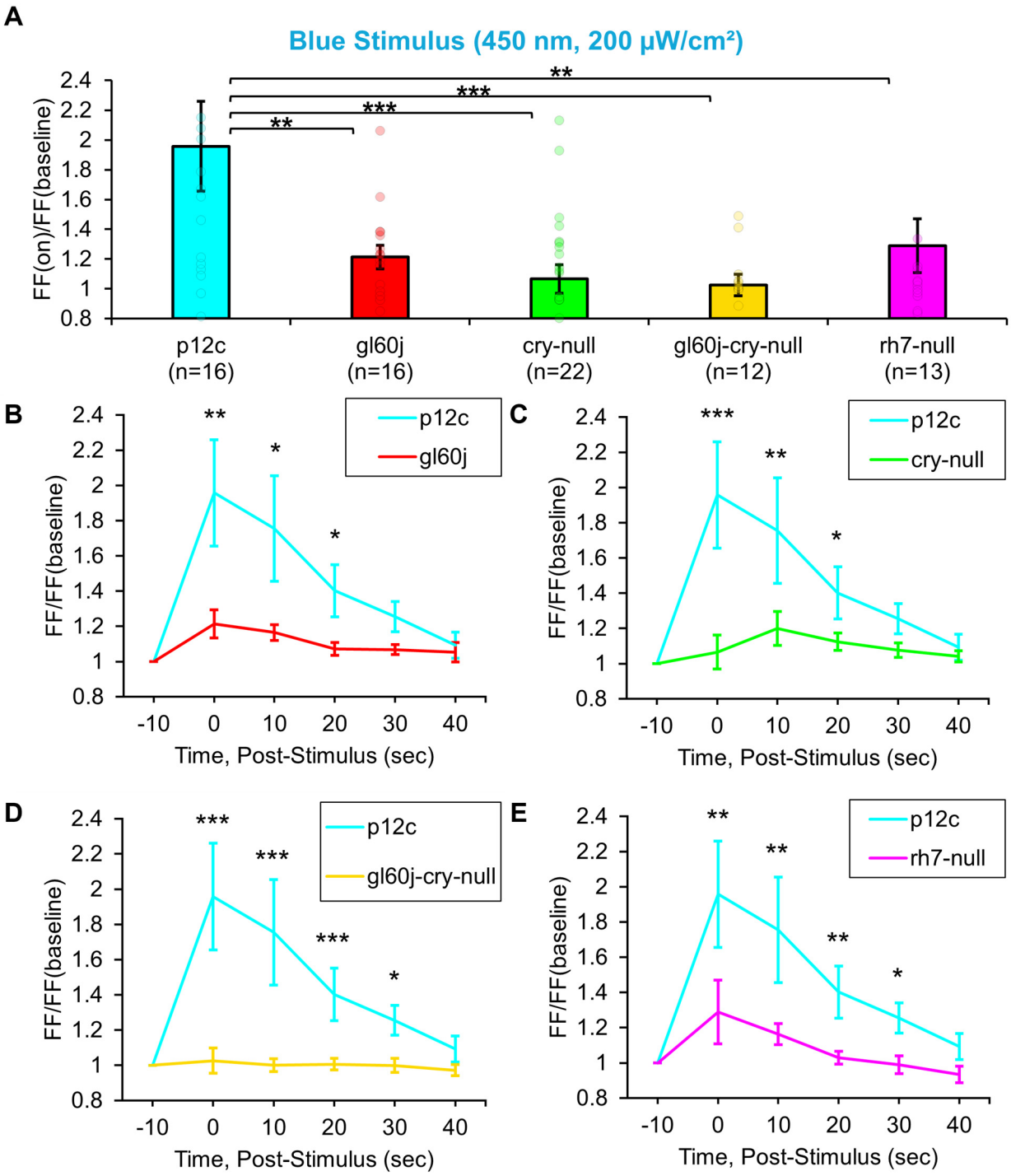
A
Blue Stimulus (450 nm, 200 μW/cm²)
FF(on)/FF(baseline)
p12c (n=16)
gl60j (n=16)
cry-null (n=22)
gl60j-cry-null (n=12)
rh7-null (n=13)
B
C
D
E
FF/FF(baseline)
Time, Post-Stimulus (sec)
p12c
gl60j
cry-null
gl60j-cry-null
rh7-null

Figure 4-3. All photoreceptor mutants show an attenuated blue light FF compared to native expressed *Drosophila* CRY

(A) Firing frequency response of p12c (blue column, n=16) versus gl60j (red column, n=16), cry-null (green column, n=22), gl60j-cry-null (yellow column, n=12), and rh7-null (violet column, n=13) with 5 second blue (450 nm, 200 μW/cm²) light stimulus. Post-stimulus FF response in 10 minute bins for (B) p12c (blue trace) vs gl60j (red trace), (C) p12c vs cry-null (green trace), (D) p12c vs gl60j-cry-null (yellow trace), and (E) p12c vs rh7-null (violet trace). Data are plotted as average ± SEM. Pairwise comparison was analyzed using two-sample t-test with FDR adjustment. p*<0.1, p**<0.05, p***<.01.

4.3.2 External photoreceptors and cryptochrome dually contribute to mediate red light excitability in primary arousal neurons

Multiple lines of evidence show that CRY also mediates acute red light responsiveness as measured by l-LNv electrophysiology [3,91]. These surprising results suggest that CRY can be sufficiently reduced to reach long-wavelength light absorption *in vivo*. The only other known candidates for red light sensing in flies occur via red sensitive opsin-based photoreceptors expressed in the compound eyes including Rhodopsin 1 and Rhodopsin 6. Anatomical and physiological evidence suggest circumstantially that external photoreceptor systems directly input light information to the circadian/arousal neural circuits. Internally expressed Rh7 does contribute violet (405 nm) light sensing to l-LNvs, yet Rh7's contribution to l-LNv input to other wavelengths of light is largely unexplored. 200 μW/cm² red light exposure evokes small but measurable acute increases in action potential FF in control *p12c* l-LNvs. In contrast, attenuated responses are measured in double knockout *gl60j-cry-null* l-LNvs (Figure 4-4A, blue column vs. yellow column). Red light evoked increases in FF quickly return to baseline firing within 10 seconds post-stimulus, indicating that l-LNv electrophysiological responses to red light are acute rather

than long-lasting (Figure 4-4D, blue trace vs. yellow trace). Post-red stimulus plots for *gl60j*, *cry-null*, and *rh7-null* mutant groups show no significant differences in comparison to the *p12c* control (Figures 4-4B, C, E).

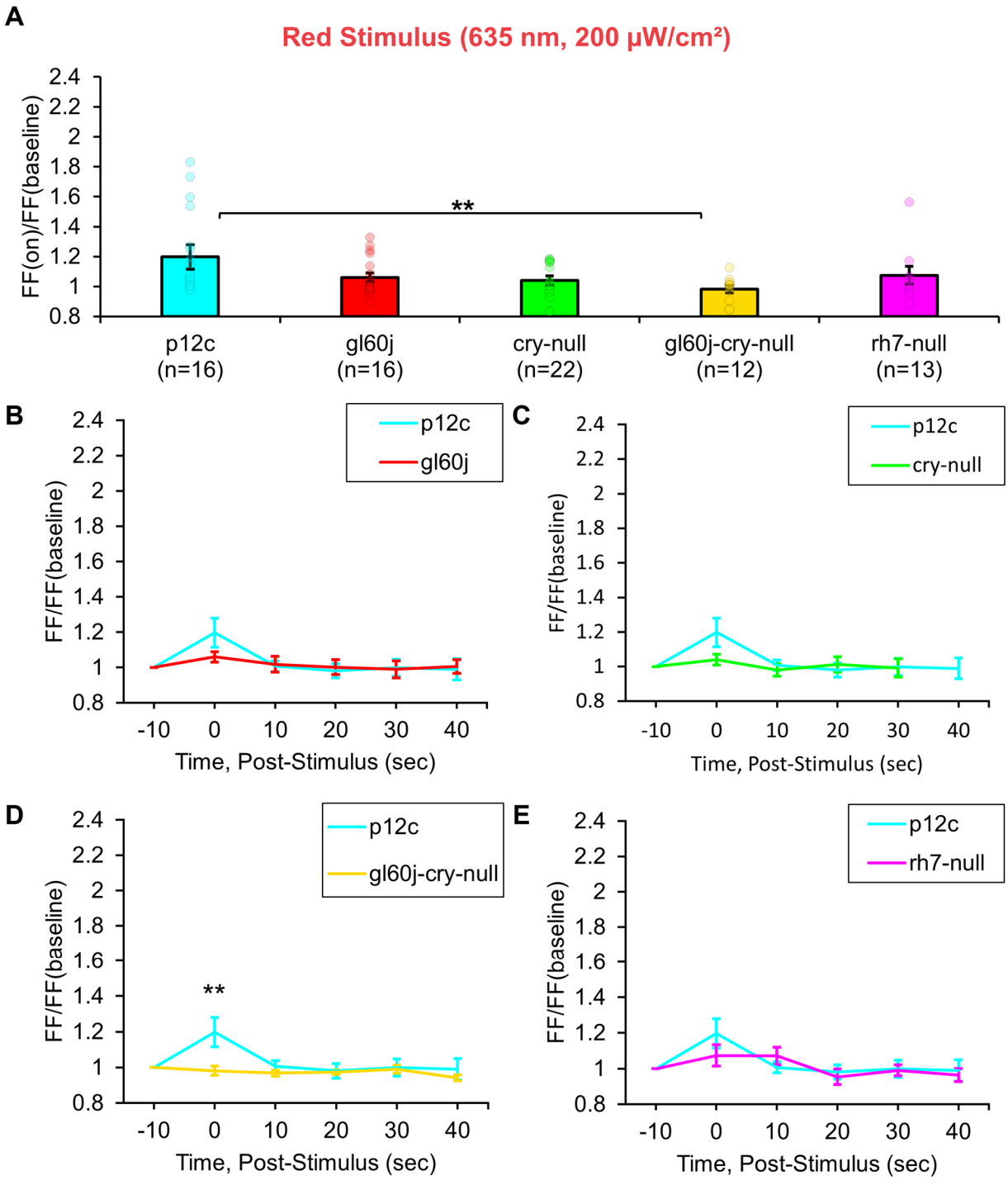
A
Red Stimulus (635 nm, 200 µW/cm²)
FF(on)/FF(baseline)
2.4
2.2
2
1.8
1.6
1.4
1.2
1
0.8
**
p12c (n=16)
gl60j (n=16)
cry-null (n=22)
gl60j-cry-null (n=12)
rh7-null (n=13)
B
p12c
gl60j
FF/FF(baseline)
-10
0
10
20
30
40
Time, Post-Stimulus (sec)
C
p12c
cry-null
FF/FF(baseline)
Time, Post-Stimulus (sec)
D
p12c
gl60j-cry-null
**
FF/FF(baseline)
Time, Post-Stimulus (sec)
E
p12c
rh7-null
FF/FF(baseline)
Time, Post-Stimulus (sec)

Figure 4-4. *gl60j-cry-null* photoreceptor mutants show an attenuated red light FF compared to native expressed *Drosophila* CRY

(A) Firing frequency response of p12c (blue column, n=16) versus gl60j (red column, n=16), cry-null (green column, n=22), gl60j-cry-null (yellow column, n=12), and rh7-null (violet column, n=13) with 5 second red (635 nm, 200 μW/cm²) light stimulus. Post-stimulus FF response in 10 minute bins for (B) p12c (blue trace) vs gl60j (red trace), (C) p12c vs cry-null (green trace), (D) p12c vs gl60j-cry-null (yellow trace), and (E) p12c vs rh7-null (violet trace). Data are plotted as average ± SEM. Pairwise comparison was analyzed using two-sample t-test with FDR adjustment. p*<0.1, p**<0.05, p***<.01.

4.3.3 Light responses recorded from l-LNvs show no apparent time-of-day differences

Representative voltage traces with a 5 sec baseline in dark, during the 5 sec of 200 μW/cm² red, blue, violet, or UV light stimulation, and 50 sec post-stimuli show the increase in FF and duration of sustained excitation for *p12c* (Figure 4-5, blue traces), *gl60j* (Figure 4-6, red traces), *cry-null* (Figure 4-7, green traces), *gl60j-cry-null* (Figure 4-8, yellow traces), and *rh7-null* (Figure 4-9, violet traces). The colored bars indicate onset of 5 sec of 200 μW/cm² lights on and off during each recording. Most of the individual l-LNv recordings reveal predominately tonic action potential firing pattern, consistent with most other reports [3,10,79,82,91,101,102,104–111,146].

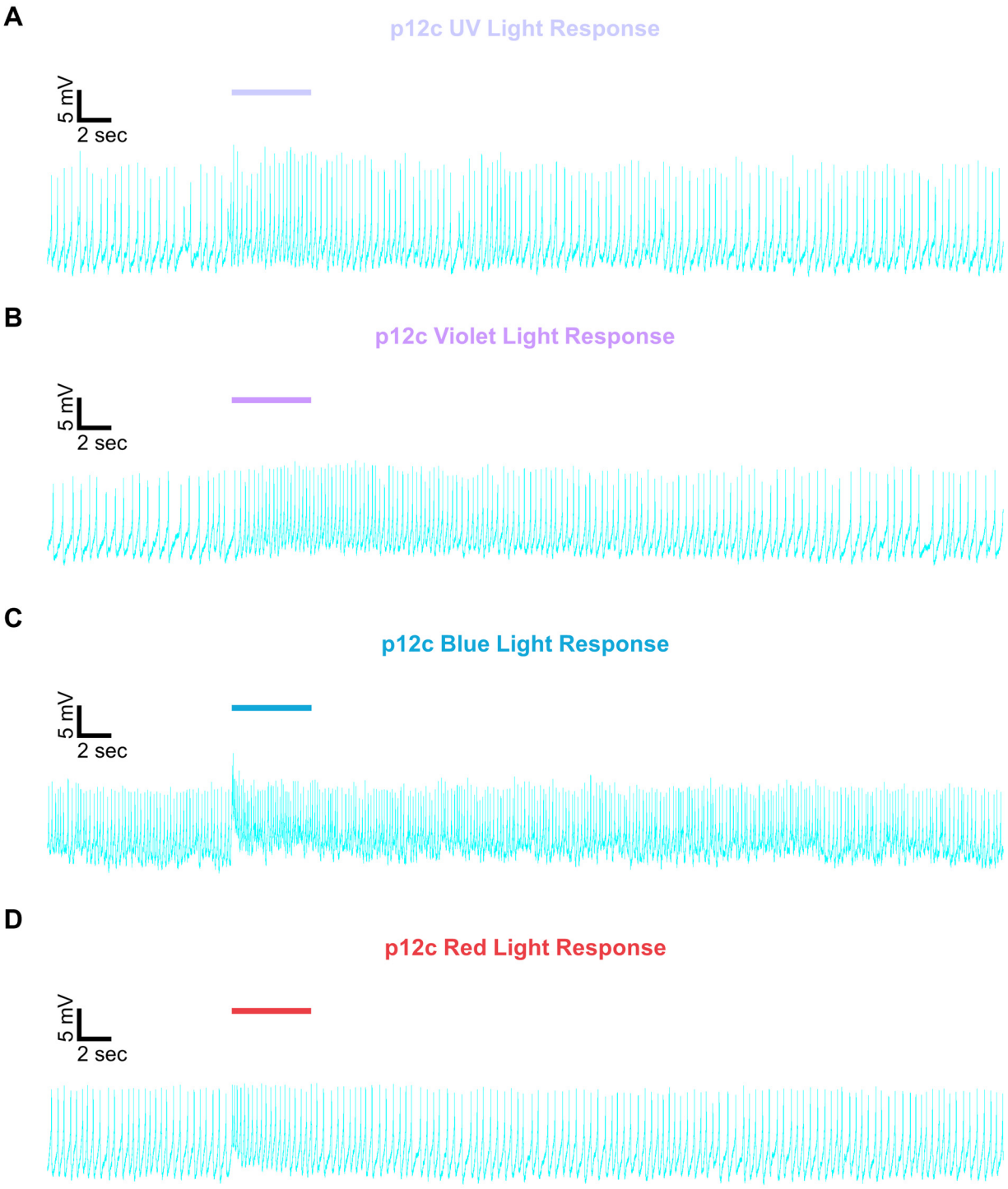
A
p12c UV Light Response
5 mV
2 sec
B
p12c Violet Light Response
5 mV
2 sec
C
p12c Blue Light Response
5 mV
2 sec
D
p12c Red Light Response
5 mV
2 sec

Figure 4-5. Representative voltage traces of l-LNvs electrophysiological responses to UV, violet, blue, and red light stimulus for native expressed *Drosophila* CRY

Representative voltage traces of the last 60 seconds of a patch-clamp recording of l-LNvs subjected to 5 seconds of (A) UV, (B) violet, (C) blue, and (D) red light stimulus for natively expressed Drosophila CRY, p12c (blue traces). Colored bars indicate 5 seconds of 200 μW/cm² light stimulus. Vertical scale bars represent 5 mV and horizontal scale bars represent 2 sec.

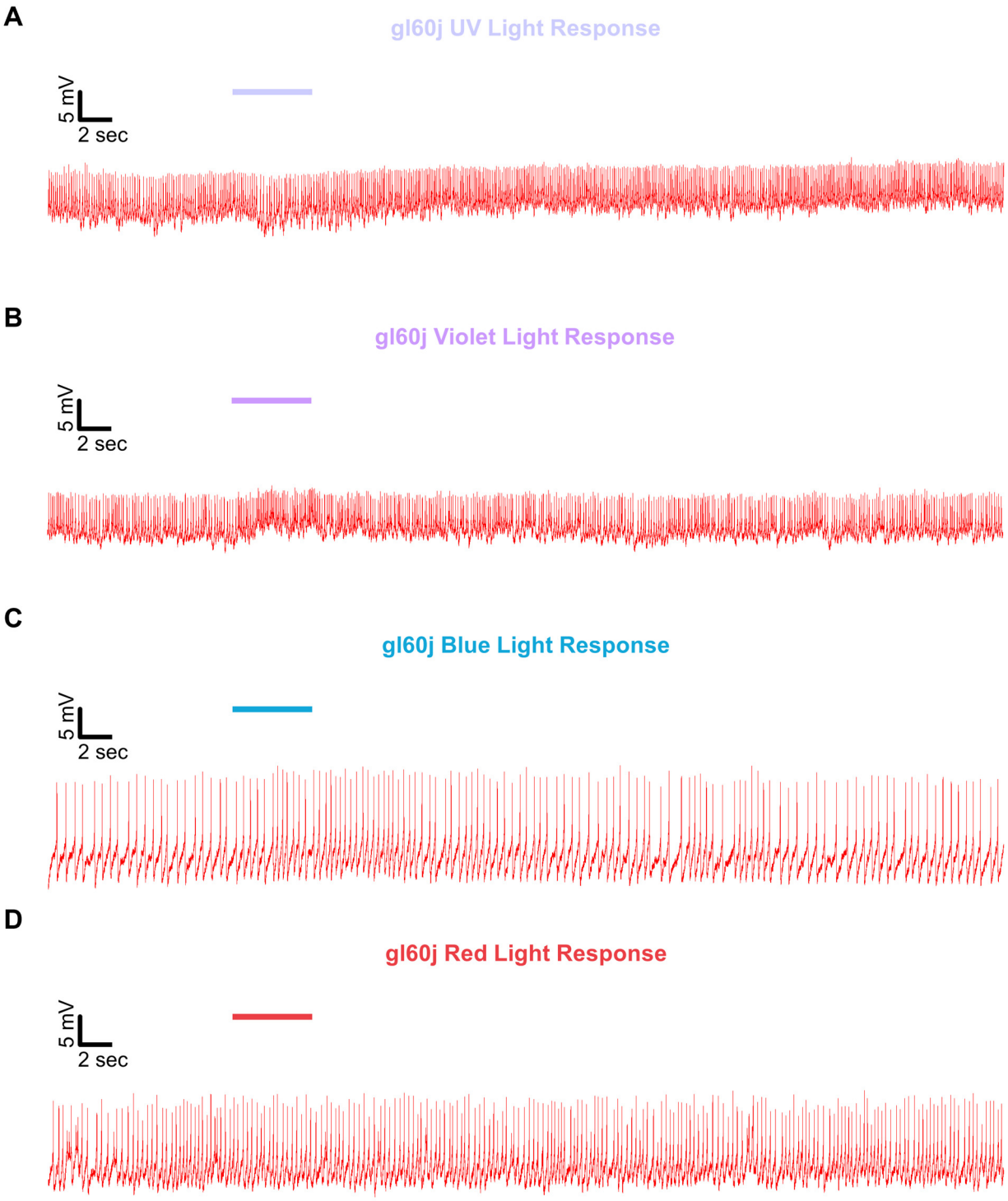
A
gl60j UV Light Response
5 mV
2 sec
B
gl60j Violet Light Response
5 mV
2 sec
C
gl60j Blue Light Response
5 mV
2 sec
D
gl60j Red Light Response
5 mV
2 sec

Figure 4-6. Representative voltage traces of l-LNvs electrophysiological responses to UV, violet, blue, and red light stimulus for *gl60j*

Representative voltage traces of the last 60 seconds of a patch-clamp recording of l-LNvs subjected to 5 seconds of (A) UV, (B) violet, (C) blue, and (D) red light stimulus for gl60j flies (red traces). Colored bars indicate 5 seconds of 200 μW/cm² light stimulus. Vertical scale bars represent 5 mV and horizontal scale bars represent 2 sec.

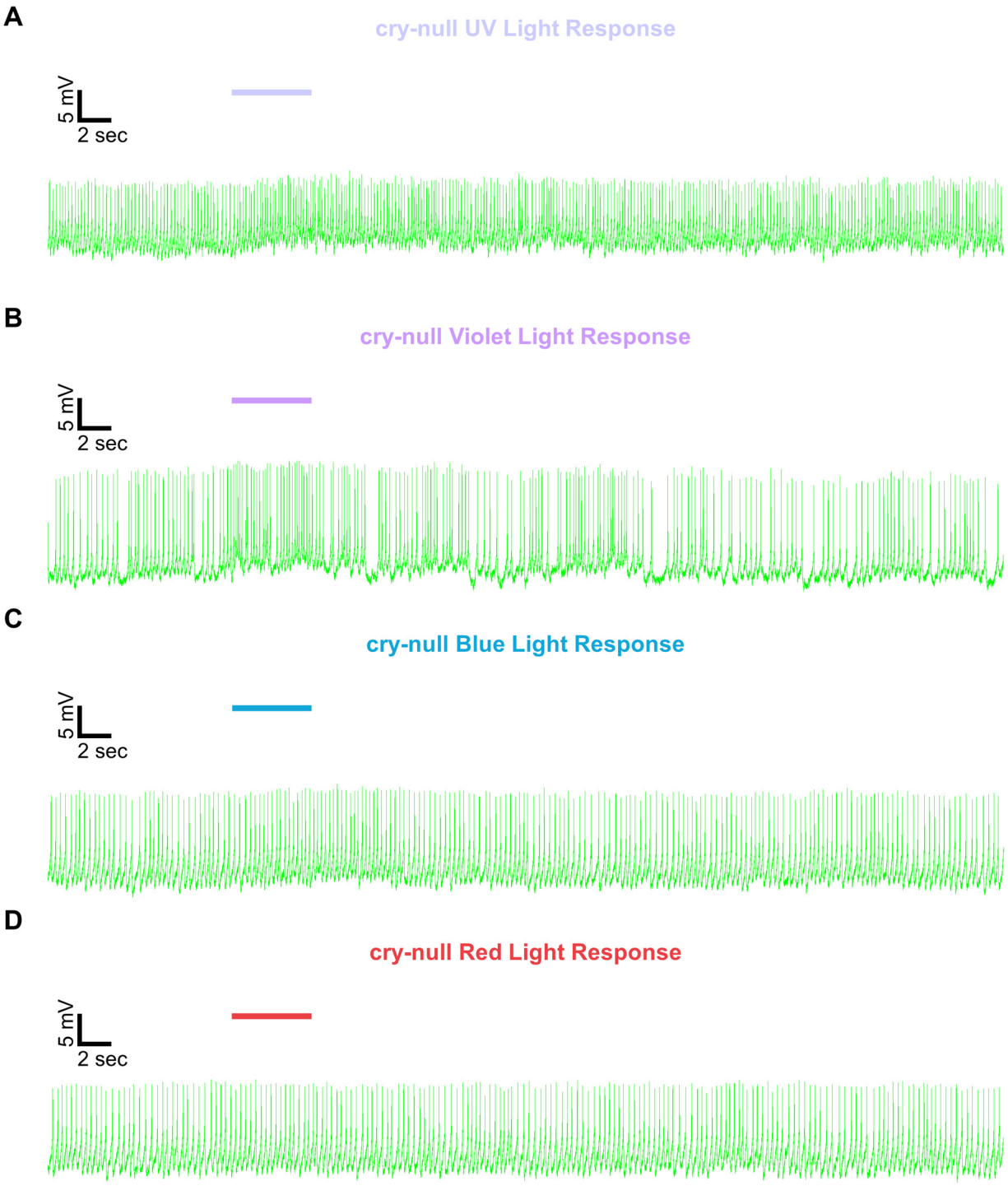
A
cry-null UV Light Response
5 mV
2 sec
B
cry-null Violet Light Response
5 mV
2 sec
C
cry-null Blue Light Response
5 mV
2 sec
D
cry-null Red Light Response
5 mV
2 sec

Figure 4-7. Representative voltage traces of l-LNvs electrophysiological responses to UV, violet, blue, and red light stimulus for *cry-null*

Representative voltage traces of the last 60 seconds of a patch-clamp recording of l-LNvs subjected to 5 seconds of (A) UV, (B) violet, (C) blue, and (D) red light stimulus for cry-null flies (green traces). Colored bars indicate 5 seconds of 200 μW/cm² light stimulus. Vertical scale bars represent 5 mV and horizontal scale bars represent 2 sec.

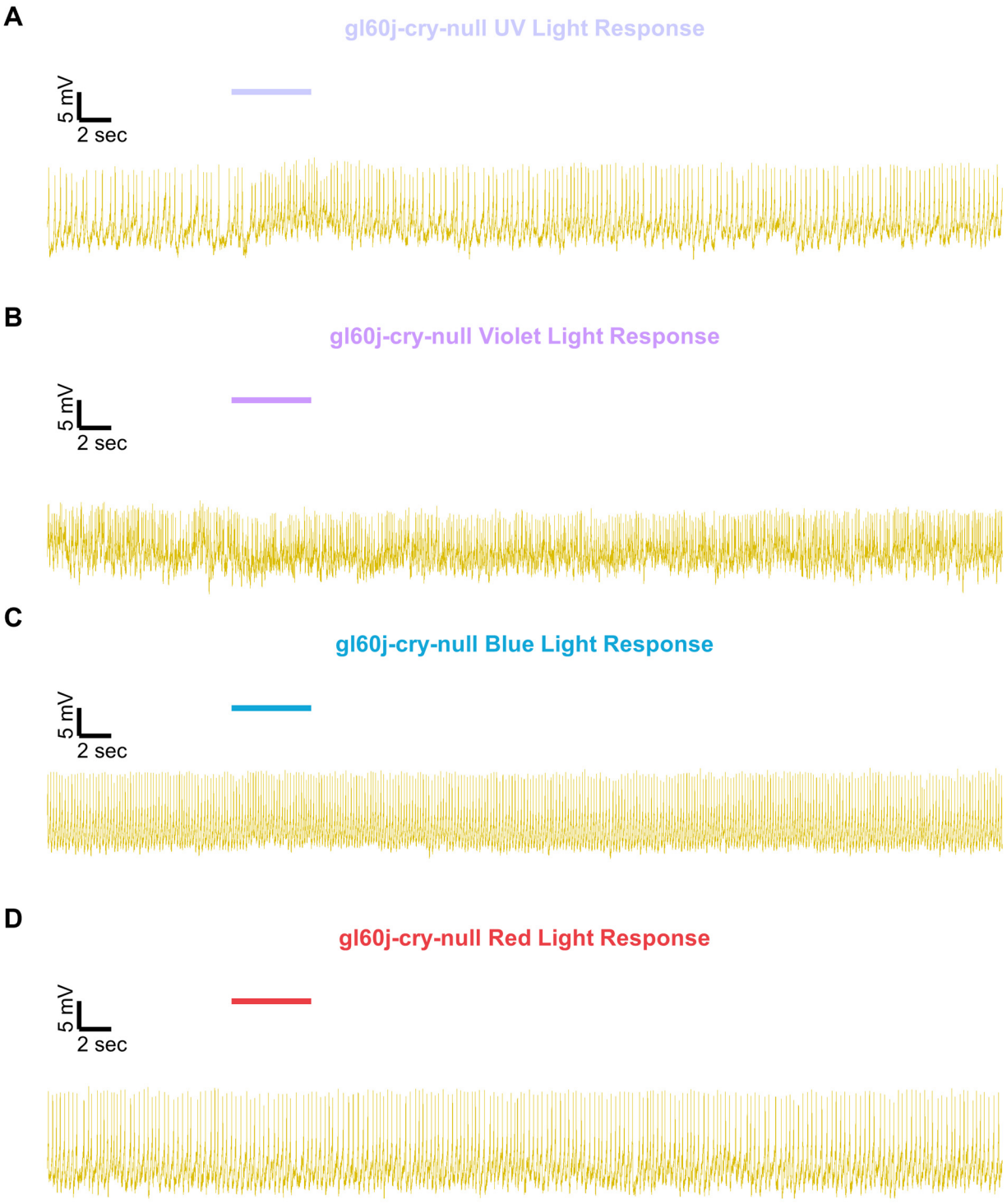
A
gl60j-cry-null UV Light Response
5 mV
2 sec
B
gl60j-cry-null Violet Light Response
5 mV
2 sec
C
gl60j-cry-null Blue Light Response
5 mV
2 sec
D
gl60j-cry-null Red Light Response
5 mV
2 sec

Figure 4-8. Representative voltage traces of l-LNvs electrophysiological responses to UV, violet, blue, and red light stimulus for *gl60j-cry-null*

Representative voltage traces of the last 60 seconds of a patch-clamp recording of l-LNvs subjected to 5 seconds of (A) UV, (B) violet, (C) blue, and (D) red light stimulus for gl60j-cry-null flies (yellow traces). Colored bars indicate 5 seconds of 200 μW/cm² light stimulus. Vertical scale bars represent 5 mV and horizontal scale bars represent 2 sec.

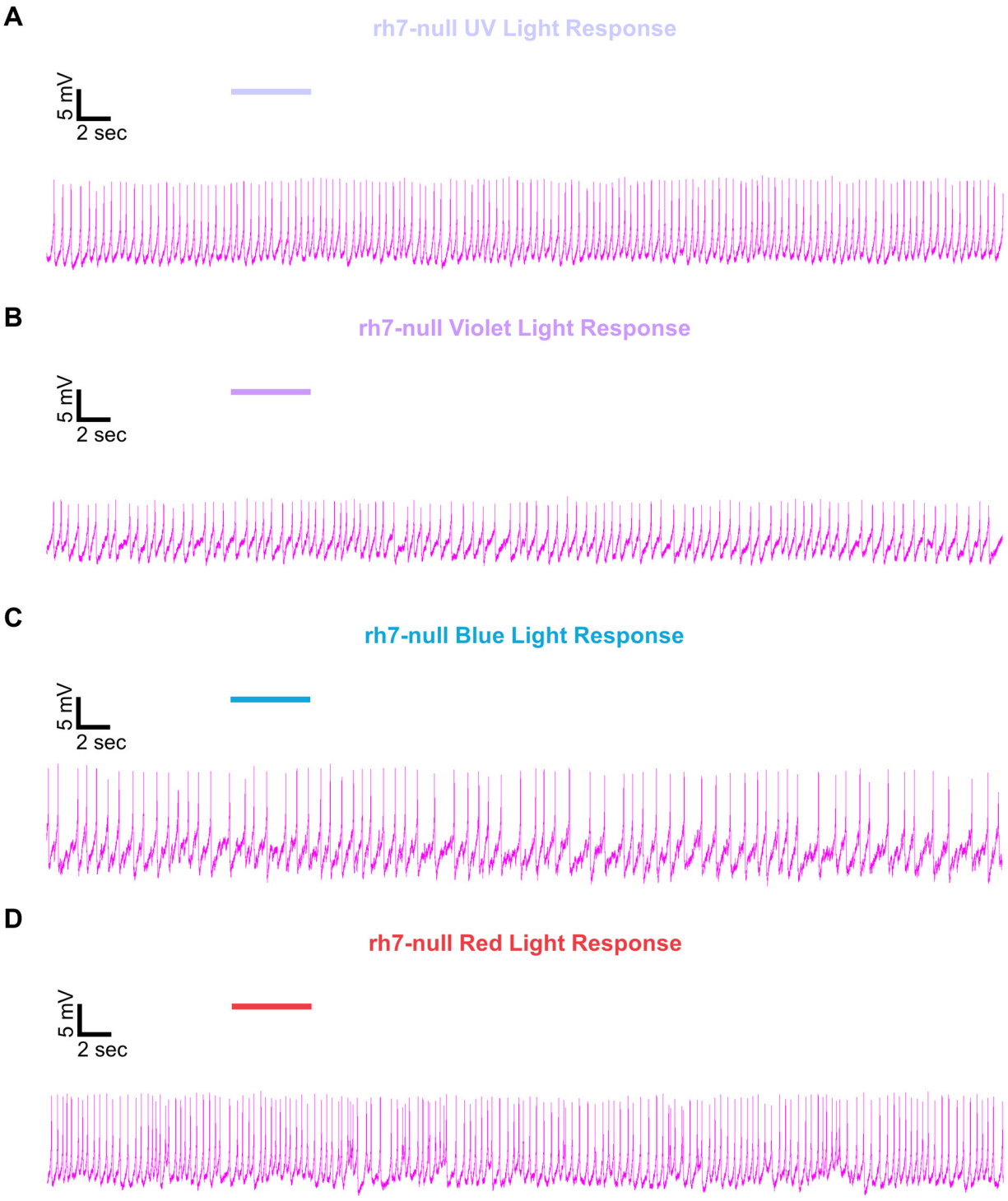
A
rh7-null UV Light Response
5 mV
2 sec
B
rh7-null Violet Light Response
5 mV
2 sec
C
rh7-null Blue Light Response
5 mV
2 sec
D
rh7-null Red Light Response
5 mV
2 sec

Figure 4-9. Representative voltage traces of l-LNvs electrophysiological responses to UV, violet, blue, and red light stimulus for *rh7-null*

Representative voltage traces of the last 60 seconds of a patch-clamp recording of l-LNvs subjected to 5 seconds of (A) UV, (B) violet, (C) blue, and (D) red light stimulus for rh7-null flies (violet traces). Colored bars indicate 5 seconds of 200 μW/cm² light stimulus. Vertical scale bars represent 5 mV and horizontal scale bars represent 2 sec.

To determine if the absence of CRY or the internal and external Rhodopsin photoreceptors alters the basal FF of l-LNvs, we plotted basal firing rates across the time of day of the recordings (Figure 4-10). Scatter plots for the *p12c* control and all photoreceptor mutants pre-exposed to UV, violet, blue, or red light (Figure 4-10A-D, respectively) show no discernable correlation to time-of-day of the recording and FF baseline. However, average FF baseline for each group plotted as a box and whisker plot shows significantly lower baseline FF for *gl60j* and *rh7-null* mutants compared to the control *p12c* (Figure 4-10E, approximately 30 Hz for *p12c*, blue box vs. 21 Hz for *gl60j*, red box and 20 Hz for *rh7-null*, violet box). The double knockout *gl60j-cry-null* had a significantly higher FF baseline than *gl60j* (Figure 4-10E, yellow box vs. red box) but recordings from this genotype tend to be more unstable as indicated by the wide range of measured FF. Similarly, *cry-null* baseline FF is significantly higher than *rh7-null* baseline FF (Figure 4-10E, green box vs. violet box). These results indicate removal of any opsin-based photoreceptor system results in a decrease in l-LNv baseline FF and thus opsin-based photoreceptors may be necessary for baseline circadian/arousal neuronal firing.

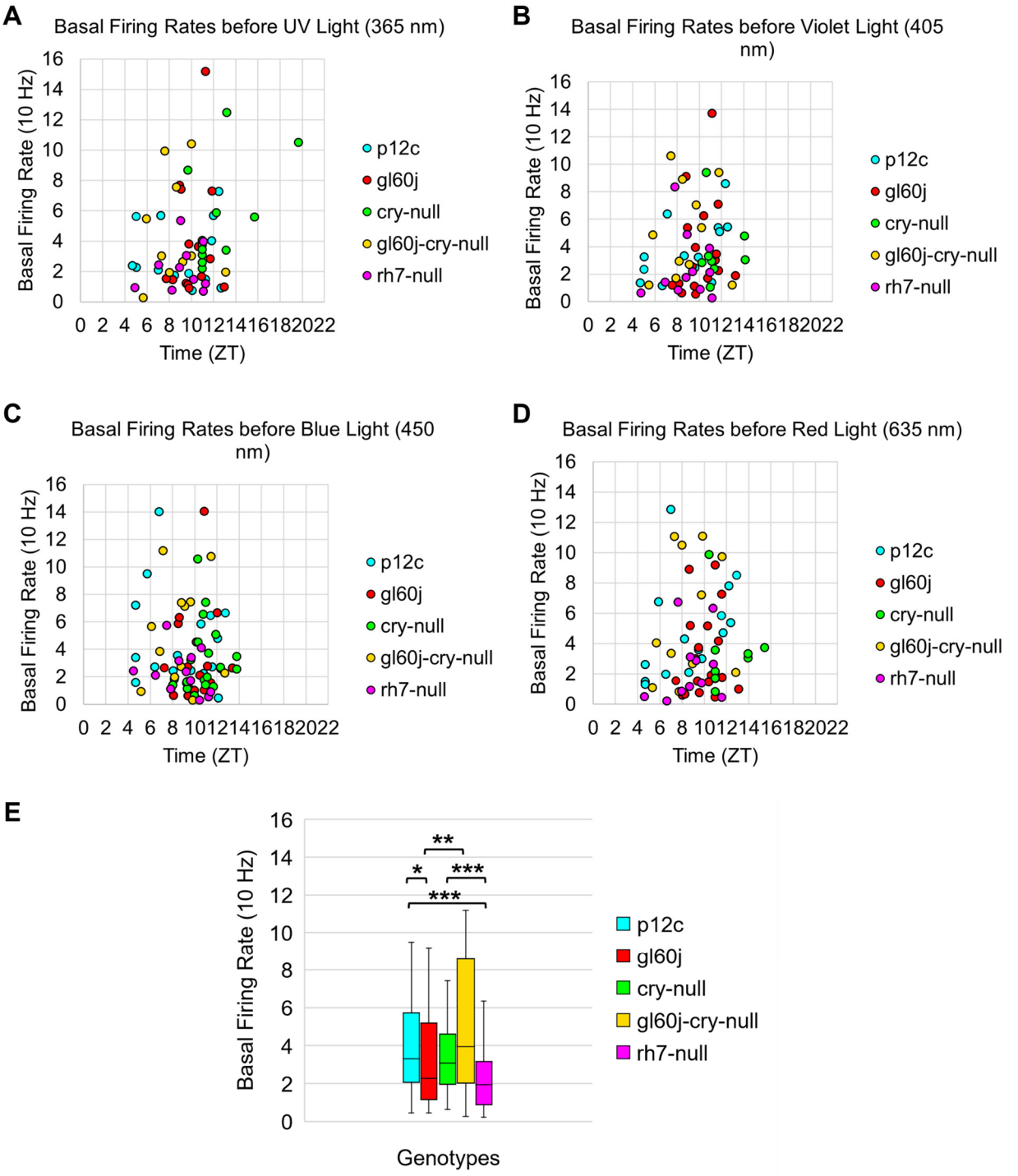
A
Basal Firing Rates before UV Light (365 nm)
Basal Firing Rate (10 Hz)
Time (ZT)
p12c
gl60j
cry-null
gl60j-cry-null
rh7-null
B
Basal Firing Rates before Violet Light (405 nm)
C
Basal Firing Rates before Blue Light (450 nm)
D
Basal Firing Rates before Red Light (635 nm)
E
Genotypes
*
**
***
***

Figure 4-10. Basal firing rates are not equivalent across groups and there is no time-of-day dependent effect

Average basal firing rates of p12c (blue), gl60j (red), cry-null (green), gl60j-cry-null (yellow), and rh7-null (violet) before (A) UV, (B) violet, (C) blue, and (D) red light stimulus plotted against the relative time-of-day of each recording. (E) Box-and-whisker plot summary of the average basal firing rate for p12c ((n =35) total, n (ZT0-12) =30; n (ZT12-16) =5), gl60j ((n=22) total, n (ZT0-12) =20; n (ZT12-16) =2), cry-null ((n=26) total, n (ZT0-12) =14; n (ZT12-16) =12), gl60j-cry-null ((n=30) total, n (ZT0-12) =22; n (ZT12-16) =8), and rh7-null ((n=30) total, n (ZT0-12) =22; n (ZT12-16) =8). Median values are denoted by a solid black line within each box of the plot. Black * indicates FDR adjusted two-sample t-test $p \leq 0.01$ vs. p12c. Data are represented as a range of means in a sample set ± maximum and minimum values within the set. One significance symbol; $p \leq 0.1$, two significance symbols; $p \leq 0.05$, three significance symbols; $p \leq 0.01$.

4.3.4 Photoreceptor mutant fly light-evoked arousal responses during sleep are significantly attenuated but not abolished, similar to the l-LNvs photoexcitatory defects

Non-imaging forming vision in flies is primarily mediated by CRY and Rh7 photoreceptors expressed in the LNv subset of circadian/arousal neurons are responsible for acute light-mediated behaviors such as arousal as well as circadian entrainment. Fly light evoked arousal responses occur over a range of wavelengths from 365 – 635 nm and vary with intensity. Though primarily short-wavelength photodetectors, CRY and Rh7 may also exhibit sensitivities reaching longer wavelength orange-red colored light. External photoreceptors in the compound eyes, ocelli, and Hofbauer-Buchner eyelet of flies express a wide range of opsin-based photoreceptors that further equip the fly with image-forming visual photoreception spanning the UV and visible light spectrum. Visual neural circuits downstream of external photoreceptors appear to synapse in the accessory medulla in the fly brain in close proximity to LNv circadian/arousal neurons and appear to integrate with CRY and Rh7 non-image forming visual mechanisms to modulate circadian entrainment to light and phototaxis/photoavoidance [78,133,147]. Whether these external

photoreceptors contribute excitatory light color-specific information to mediate behavioral arousal responses remains unclear. We measured the acute behavioral responses of *p12c* control flies and photoreceptor mutant flies (*gl60j*, *cry-null*, double mutant *gl60j-cry-null*, and *rh7-null*) to three 5-min pulses of low (10 μW/cm²) or high (400 μW/cm²) red (635 nm), blue (450 nm), violet (405 nm), or UV (365 nm) LED light during subjective nighttime at time points ZT18, ZT19, and ZT20 for three consecutive nights. Scatter plots show the average % of flies that awaken across the three days of experiment per each light-pulse with responses from the first, second, and third pulses spanning each cluster from left, middle, and right, respectively. Average fly arousal responses do not significantly differ between consecutive nights of experiment.

An average of nearly 85% of control *p12c* flies are aroused from sleep in response to low (10 μW/cm²) intensity UV light (Figure 4-11A, light blue points). All photoreceptor mutants except *cry-null* exhibit significantly lower arousal responses to low intensity UV light pulses relative to *p12c* controls (Figure 4-11A), suggesting that the light intensity threshold for CRY activation is higher than that for opsins. The double mutant *gl60j-cry-null* shows the greatest response attenuation of light evoked arousal to low intensity UV light pulses compared to all other genotypes (Figure 4-11A, light yellow points). Notably, *gl60j-cry-nulls* do not show significantly attenuated response in l-LNv photoexcitability to UV light at 20 fold higher light stimulus intensity (Figures 4-1A, D), suggesting possible additional UV sensing mechanisms for fly arousal. All photoreceptor mutants except *cry-null* exhibit a loss of arousal sensitivity compared to *p12c* in response to higher intensity UV light pulses (Figure 4-11B). However, both *gl60j* and *gl60j-cry-null* flies show significantly attenuated higher intensity UV light arousal responses (Figure 4-11B, dark red points and dark yellow points, respectively) and double mutant *gl60j-cry-null* flies show significantly attenuated higher intensity UV light arousal responses relative to *gl60j* alone,

indicating that CRY does contribute to UV light evoked arousal. Mutant *rh7-null* flies show the greatest degree of attenuation of higher intensity UV light arousal responses (Figure 4-11B, dark violet points and dark yellow points, respectively) and show significantly attenuated arousal responses to higher intensity UV light relative to *gl60j* (Figure 4-11B, dark violet points versus red points), *cry-null* (Figure 4-11B, dark violet points versus green points), and *gl60j-cry-null* (Figure 4-11B, dark violet points versus yellow points), underscoring the importance of Rh7 for UV light evoked arousal for this light intensity. This result is consistent with reports that Rh7 is a bistable broad range photopigment and is activated in the UV range [2,7].

A

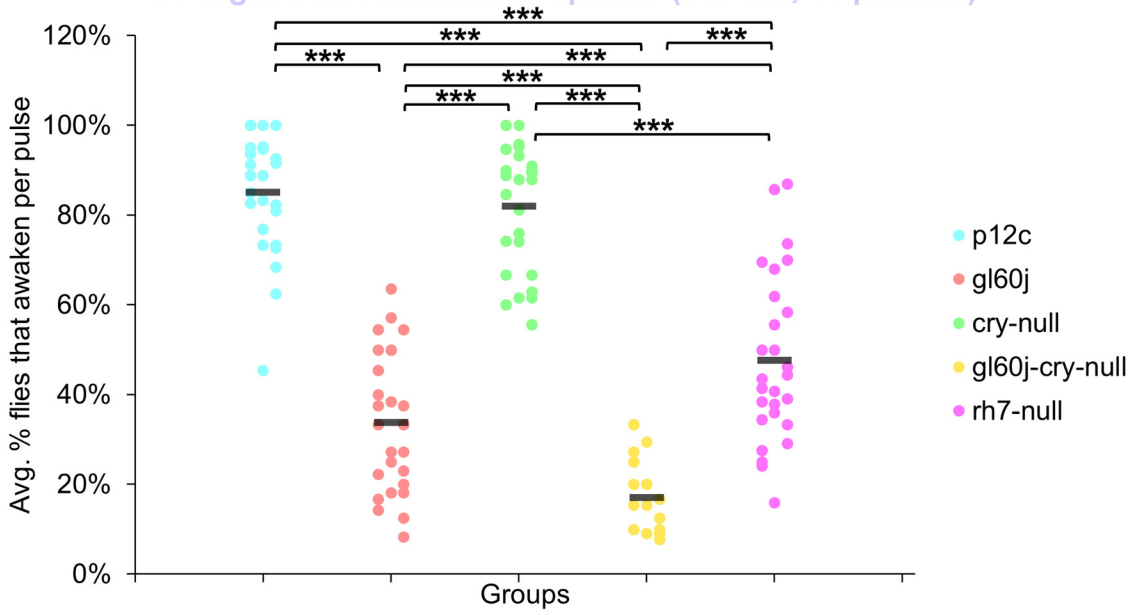
UV Light-Pulse Arousal Response (365 nm, 10 µW/cm²)
Avg. % flies that awaken per pulse
120%
100%
80%
60%
40%
20%
0%
Groups
***
p12c
gl60j
cry-null
gl60j-cry-null
rh7-null

B

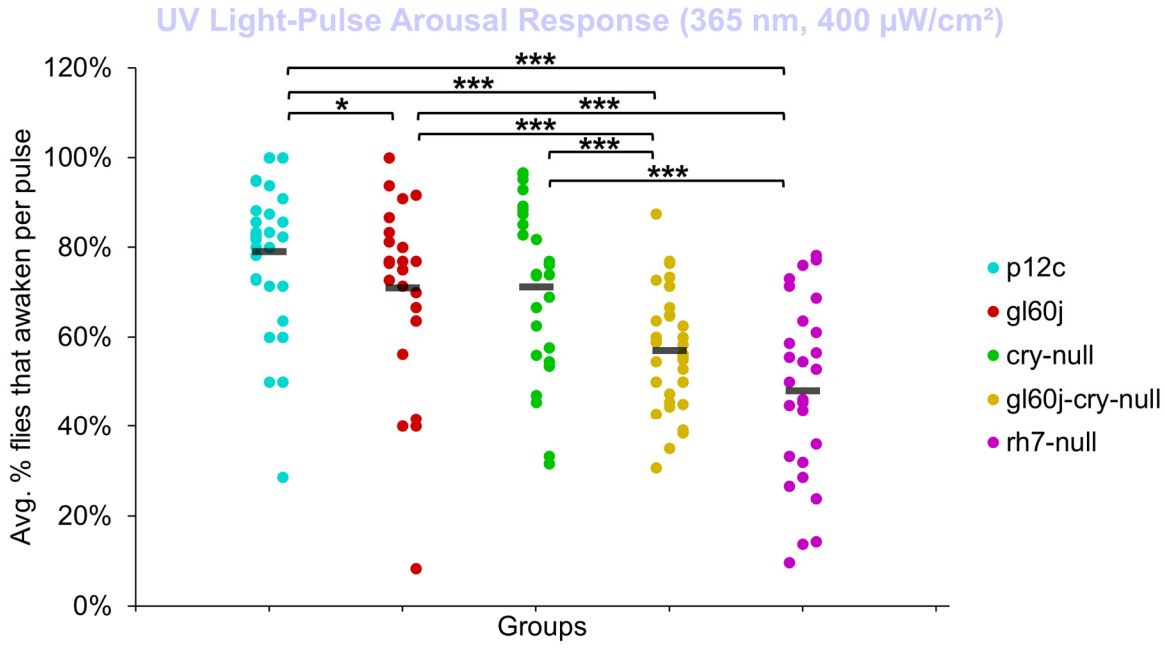
UV Light-Pulse Arousal Response (365 nm, 400 µW/cm²)
Avg. % flies that awaken per pulse
120%
100%
80%
60%
40%
20%
0%
Groups
*
***
p12c
gl60j
cry-null
gl60j-cry-null
rh7-null

Figure 4-11. Low and high intensity UV light pulse arousal behavior is significantly attenuated in all photoreceptor mutants except *cry-null* compared to the control p12c

Three 5 min pulses of UV light were applied to flies during subjective nighttime (ZT18, ZT19, ZT20) for three days after 12:12 hr LD entrainment to measure the arousal response of p12c (blue), gl60j (red), cry-null (green), gl60j-cry-null (yellow), and rh7-null (violet) flies for (A) low (10 μW/cm²) and (B) high (400 μW/cm²) light intensity. Scatter plots are grouped by average % of flies that awaken across the three days of light-pulse arousal experiment and separated as pulse 1 (left points for each group), pulse 2 (middle points for each group), and pulse 3 (right points for each group). Black bars indicate total average % flies that awaken across the three days and three pulses of light. Pairwise comparison was analyzed using two-sample t-test with FDR adjustment. p*<0.1, p**<0.05, p***<.01.

An average of approximately 85% of control *p12c* flies are aroused from sleep in response to low (10 μW/cm²) intensity violet light (Figure 4-12A, light blue points). Low intensity violet light pulses evoke significantly lower arousal responses for all photoreceptor mutants compared to *p12c*, with *gl60j* and *gl60j-cry-null* showing the greatest attenuation of violet light evoked arousal (Figure 4-12A). Not surprisingly, *cry-null* alone shows the least attenuation of violet light evoked arousal as no redox state of CRY exhibits high absorption in the violet range of the spectra. Loss of Rh7 results in significant attenuation of the low intensity violet light response, but significantly less so relative to either *gl60j* or *gl60j-cry-null*. For high intensity violet light pulses, all photoreceptor mutants except *cry-null* flies show significantly attenuated arousal responses (Figure 4-12B), suggesting that the lack of CRY activation by violet light may mediate spectral differentiation for short-wavelength light arousal responses. Arousal of *rh7-null* flies is most significantly attenuated in response to high intensity violet light pulses (Figure 4-12B, dark violet points).

A

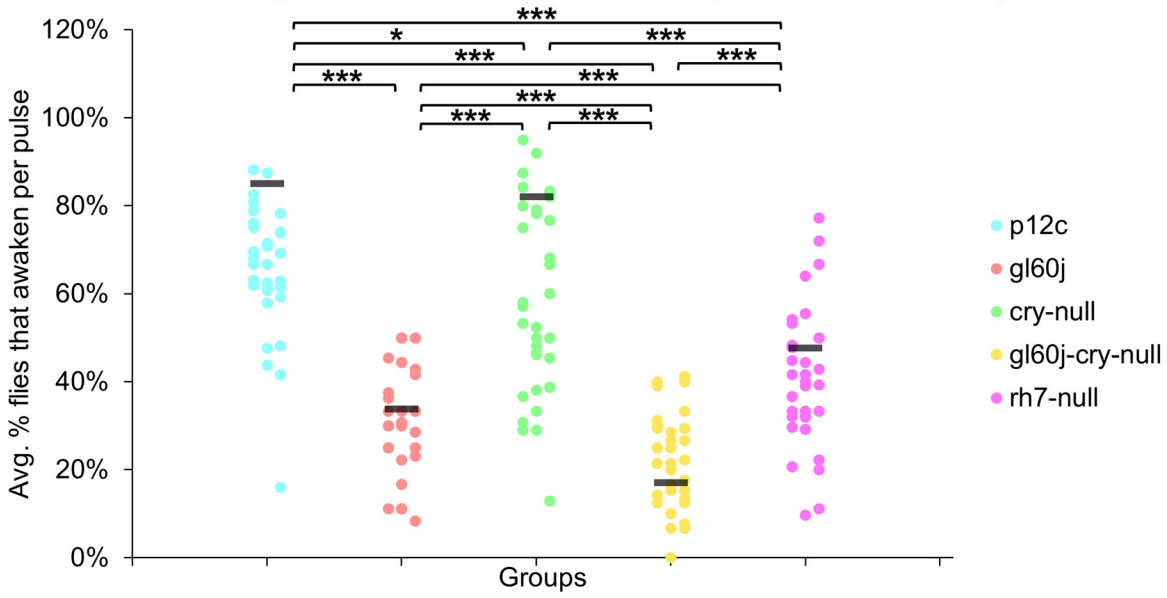
Violet Light-Pulse Arousal Response (405 nm, 10 µW/cm²)
Avg. % flies that awaken per pulse
120%
100%
80%
60%
40%
20%
0%
Groups
p12c
gl60j
cry-null
gl60j-cry-null
rh7-null

B

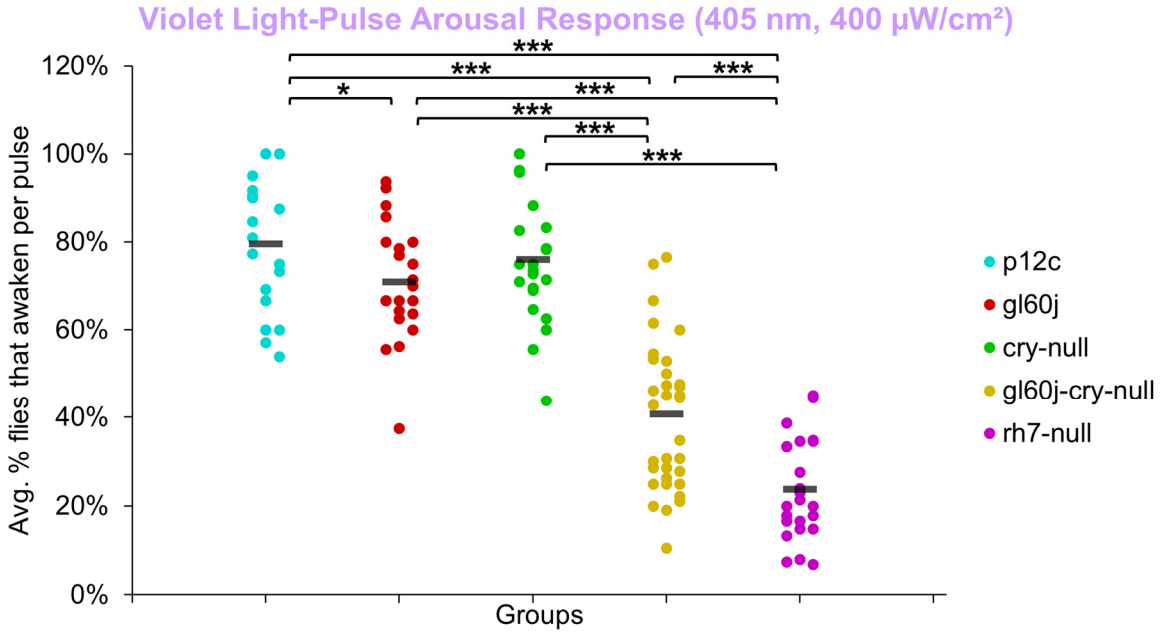
Violet Light-Pulse Arousal Response (405 nm, 400 µW/cm²)
Avg. % flies that awaken per pulse
120%
100%
80%
60%
40%
20%
0%
Groups
p12c
gl60j
cry-null
gl60j-cry-null
rh7-null

Figure 4-12. Violet light pulse arousal behavior is significantly attenuated in flies lacking Rh7 or external photoreceptors with low and high intensity light compared to the control p12c

Three 5 min pulses of violet light were applied to flies during subjective nighttime (ZT18, ZT19, ZT20) for three days after 12:12 hr LD entrainment to measure the arousal response of p12c (blue), gl60j (red), cry-null (green), gl60j-cry-null (yellow), and rh7-null (violet) flies for (A) low (10 μW/cm²) and (B) high (400 μW/cm²) light intensity. Scatter plots are grouped by average % of flies that awaken across the three days of light-pulse arousal experiment and separated as pulse 1 (left points for each group), pulse 2 (middle points for each group), and pulse 3 (right points for each group). Black bars indicate total average % flies that awaken across the three days and three pulses of light. Pairwise comparison was analyzed using two-sample t-test with FDR adjustment. p*<0.1, p**<0.05, p***<.01.

On average, approximately 65% of *p12c* control flies are aroused in response to low intensity blue light while approximately 75% are aroused in response to high intensity blue light (Figure 4-13A, B). All photoreceptor mutants exhibit significantly attenuated arousal responses compared to *p12c* control flies for both low and high intensity blue light (Figures 4-13A, B). The trends for the degree of attenuation of blue light evoked arousal responses are very similar to those measured for l-LNv blue light evoked electrophysiological action potential firing (Figure 4-3). Both low and high intensity blue light evoked arousal responses show *rh7-null* flies have the most attenuated response (Figure 4-13A, light violet points; Figure 4-13B, dark violet points). Interestingly, compared to *gl60j* and *gl60j-cry-null* flies, *cry-null* flies exhibit significantly less arousal response attenuation to low intensity blue light pulses (Figure 4-13A, light green points) but significantly greater attenuation responses to high intensity blue light pulses (Figure 4-13B, dark green points) which may reflect higher threshold for CRY blue light activation relative to the blue light activation threshold for opsins.

A

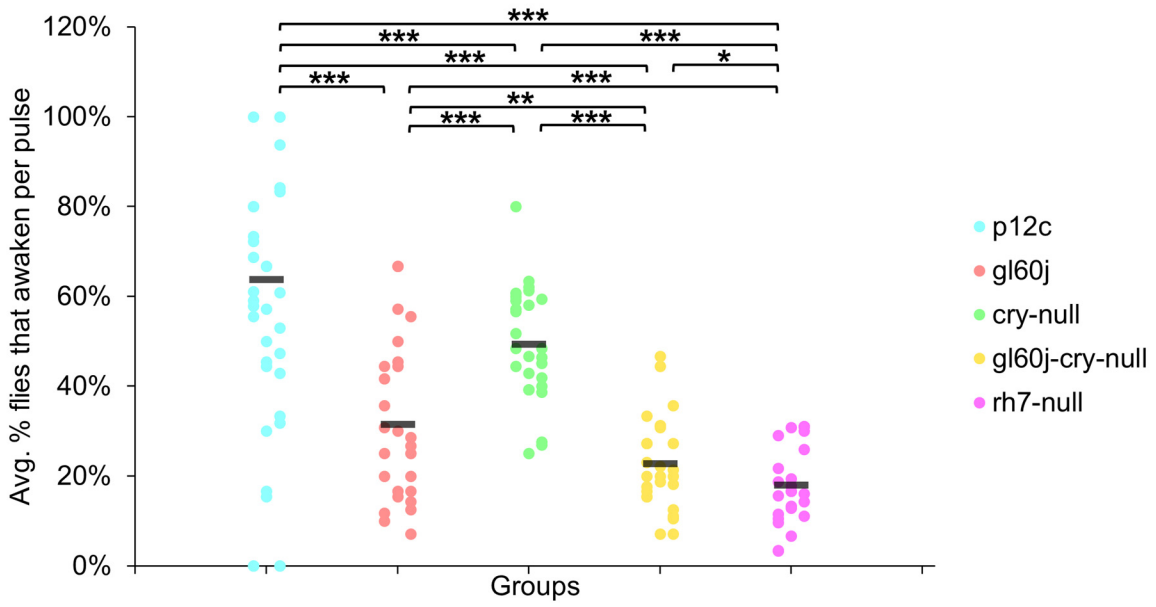
Blue Light-Pulse Arousal Response (450 nm, 10 µW/cm²)
Avg. % flies that awaken per pulse
120%
100%
80%
60%
40%
20%
0%
Groups
p12c
gl60j
cry-null
gl60j-cry-null
rh7-null

B

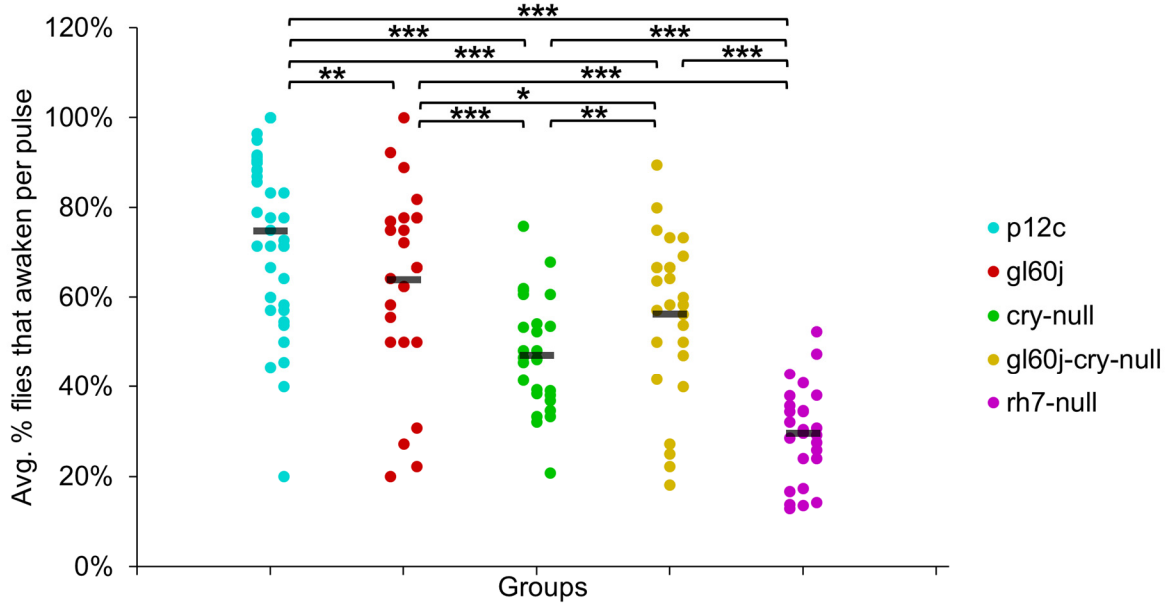
Blue Light-Pulse Arousal Response (450 nm, 400 µW/cm²)
Avg. % flies that awaken per pulse
120%
100%
80%
60%
40%
20%
0%
Groups
p12c
gl60j
cry-null
gl60j-cry-null
rh7-null

Figure 4-13. Low and high intensity blue light pulse arousal behavior is significantly attenuated in all photoreceptor mutants compared to the control p12c

Three 5 min pulses of blue light were applied to flies during subjective nighttime (ZT18, ZT19, ZT20) for three days after 12:12 hr LD entrainment to measure the arousal response of p12c (blue), gl60j (red), cry-null (green), gl60j-cry-null (yellow), and rh7-null (violet) flies for (A) low (10 μW/cm²) and (B) high (400 μW/cm²) light intensity. Scatter plots are grouped by average % of flies that awaken across the three days of light-pulse arousal experiment and separated as pulse 1 (left points for each group), pulse 2 (middle points for each group), and pulse 3 (right points for each group). Black bars indicate total average % flies that awaken across the three days and three pulses of light. Pairwise comparison was analyzed using two-sample t-test with FDR adjustment. p*<0.1, p**<0.05, p***<.01.

On average, approximately 70% of *p12c* control flies are aroused in response to low intensity red light while less than 40% are aroused in response to high intensity red light (Figure 4-14A, B). Significantly fewer *gl60j*, *cry-null*, and *gl60j-cry-null* flies are aroused in response to low intensity red light relative to control (Figure 4-14A, light blue points vs. light red points, light green points, and light yellow points, respectively). Compared to *p12c* control flies, *rh7-null* flies do not significantly differ for low intensity red light pulse arousal responsiveness (Figures 4-14A, light blue points vs. light violet points). As the low intensity red light responses compared between *cry-null* and *gl60j-cry-null* flies do not significantly differ, external opsin-based photoreceptors appear to be the primary mediators of low intensity red light pulse arousal. High intensity red light evoked arousal response measurements further supports this (Figure 4-14B), as only *gl60j* (dark red points) and *gl60j-cry-null* (dark yellow points) flies are significantly less responsive compared to *p12c* controls (dark blue points).

A

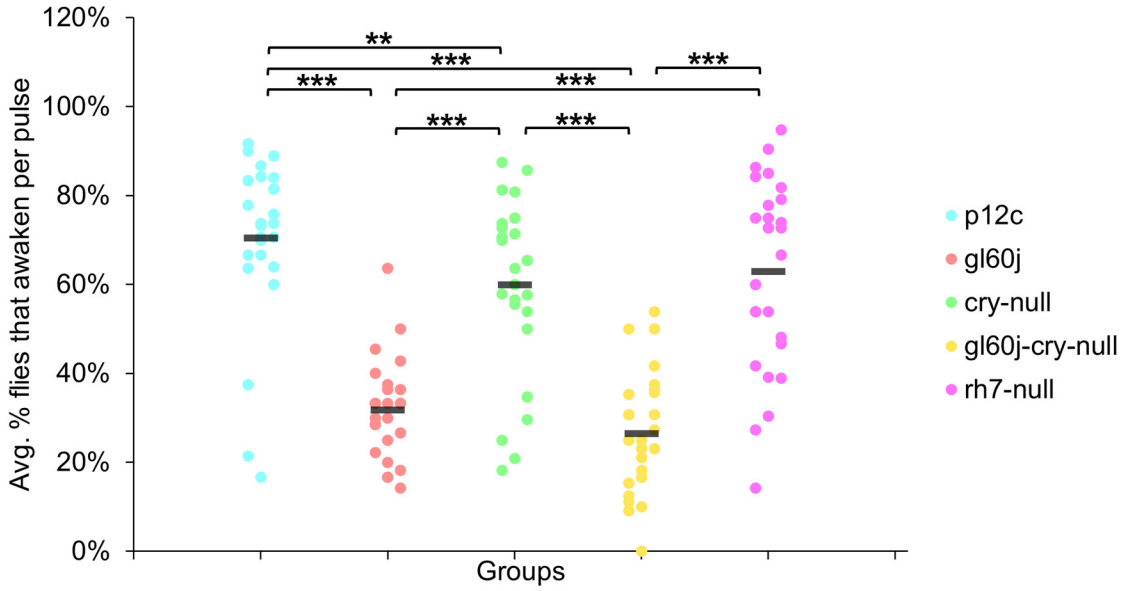
Red Light-Pulse Arousal Response (635 nm, 10 µW/cm²)
Avg. % flies that awaken per pulse
120%
100%
80%
60%
40%
20%
0%
Groups
**
***
***
***
***
***
***
p12c
gl60j
cry-null
gl60j-cry-null
rh7-null

B

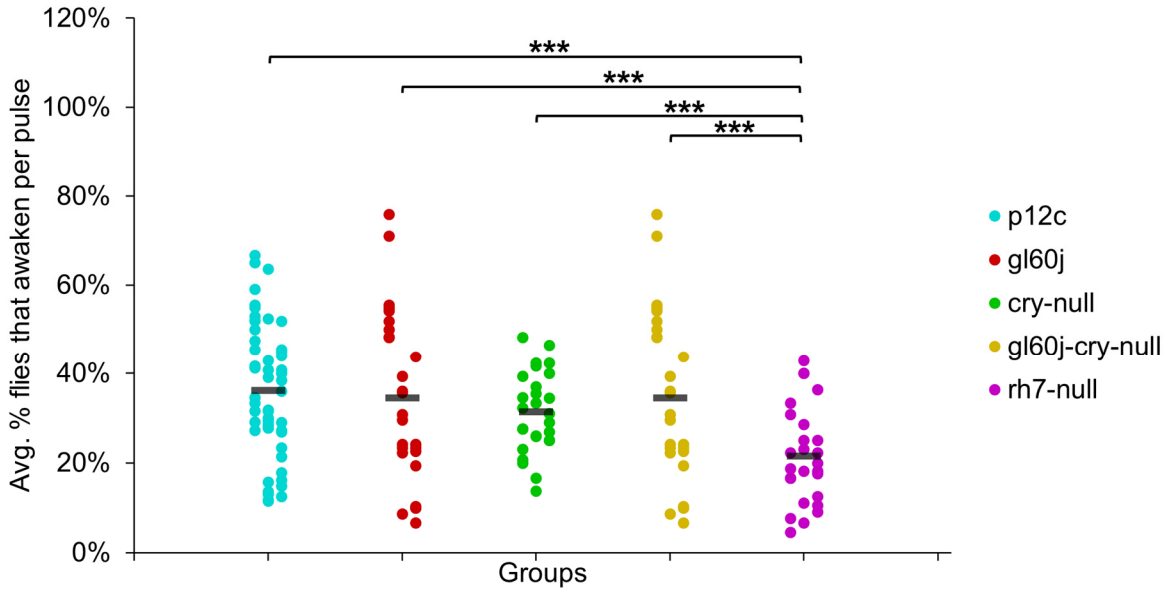
Red Light-Pulse Arousal Response (635 nm, 400 µW/cm²)
Avg. % flies that awaken per pulse
120%
100%
80%
60%
40%
20%
0%
Groups
***
***
***
***
p12c
gl60j
cry-null
gl60j-cry-null
rh7-null

Figure 4-14. Red light pulse arousal behavior is significantly attenuated in flies lacking external photoreceptors at low and high light intensity compared to the control p12c

Three 5 min pulses of red light were applied to flies during subjective nighttime (ZT18, ZT19, ZT20) for three days after 12:12 hr LD entrainment to measure the arousal response of p12c (blue), gl60j (red), cry-null (green), gl60j-cry-null (yellow), and rh7-null (violet) flies for (A) low (10 μW/cm²) and (B) high (400 μW/cm²) light intensity. Scatter plots are grouped by average % of flies that awaken across the three days of light-pulse arousal experiment and separated as pulse 1 (left points for each group), pulse 2 (middle points for each group), and pulse 3 (right points for each group). Black bars indicate total average % flies that awaken across the three days and three pulses of light. Pairwise comparison was analyzed using two-sample t-test with FDR adjustment. p*<0.1, p**<0.05, p***<.01.

The overall trend indicates that intensity matched short wavelength light more effectively arouses flies from sleep than long wavelength light. Curiously, for red light, significantly fewer flies are aroused by the higher intensity condition (Figure 4-15), while for blue light, significantly more flies respond to the higher intensity condition, except *cry-null* flies, which are effectively aroused for both intensity conditions (Figure 4-15). Violet light pulses also showed a similar trend, with all photoreceptor groups except *rh7-null* flies having an increase in arousal responsiveness to high intensity compared to low intensity violet light, while *rh7-null* flies significantly respond less to the high intensity condition compared to the low light intensity condition (Figure 4-15). Taken altogether, these results provide strong evidence of a multifaceted photoreceptor convergence system that inputs mechanistically distinct different channels of photic information to arousal neurons that correspond to different spectral wavelengths and different intensity-dependent light activation thresholds. Removal of any one of these photoreceptor systems results in a significant loss of l-LNv photoexcitability or downstream behavioral arousal, with partial remaining functionality indicating robustness through redundancy.

A

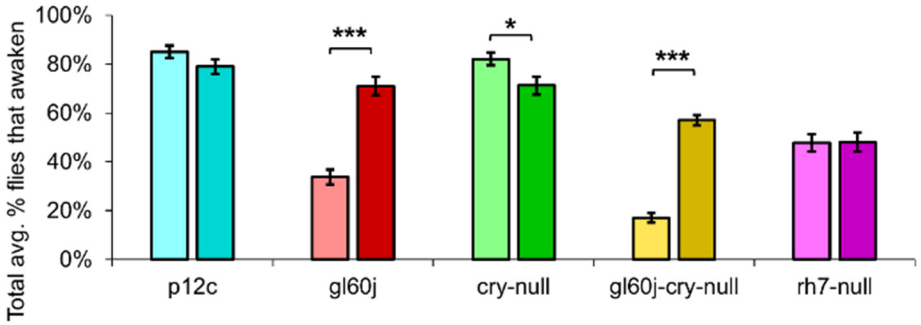
UV Light-Pulse Arousal Response (365 nm, 10 vs. 400 µW/cm²)
Total avg. % flies that awaken
100%
80%
60%
40%
20%
0%
***
*
***
p12c
gl60j
cry-null
gl60j-cry-null
rh7-null

B

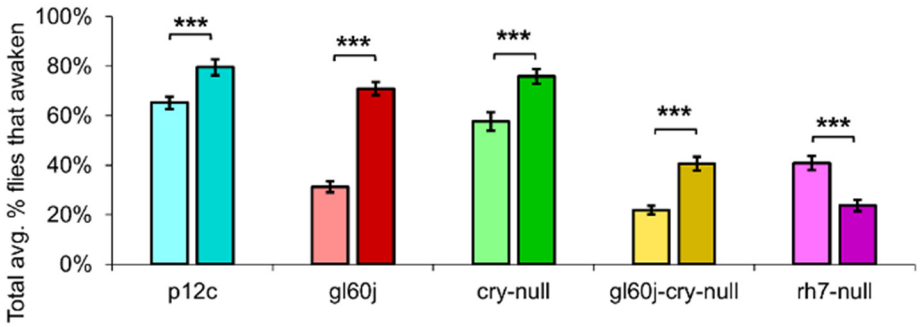
Violet Light-Pulse Arousal Response (405 nm, 10 vs. 400 µW/cm²)
Total avg. % flies that awaken
100%
80%
60%
40%
20%
0%
***
***
***
***
***
p12c
gl60j
cry-null
gl60j-cry-null
rh7-null

C

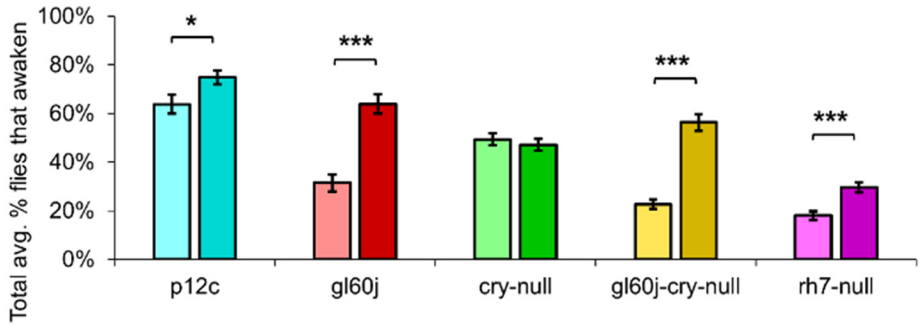
Blue Light-Pulse Arousal Response (450 nm, 10 vs. 400 µW/cm²)
Total avg. % flies that awaken
100%
80%
60%
40%
20%
0%
*
***
***
***
p12c
gl60j
cry-null
gl60j-cry-null
rh7-null

D

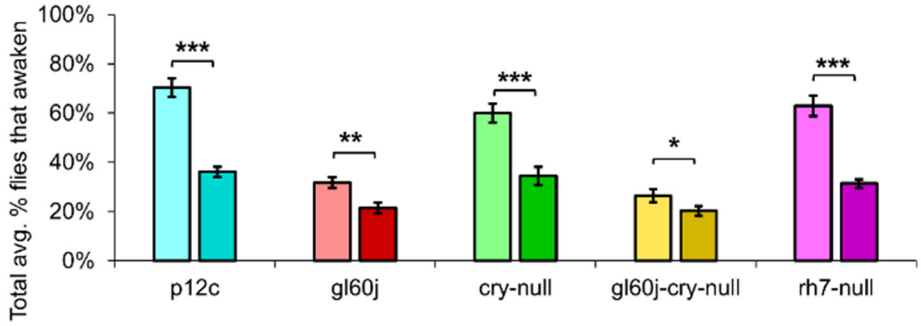
Red Light-Pulse Arousal Response (635 nm, 10 vs. 400 µW/cm²)
Total avg. % flies that awaken
100%
80%
60%
40%
20%
0%
***
**
***
*
***
p12c
gl60j
cry-null
gl60j-cry-null
rh7-null

Figure 4-15. Pairwise summary comparison of light-pulse arousal between low and high intensity light

Light intensity comparison of total average % arousal response across 3 days and 3 pulses of light for p12c (lighter blue column, left, 10 μW/cm²; darker blue column, right, 400 μW/cm²), gl60j (light red, left, 10 μW/cm²; dark red column, right, 400 μW/cm²), cry-null (light green, left, 10 μW/cm²; dark green column, right, 400 μW/cm²), gl60j-cry-null (light yellow, left, 10 μW/cm²; dark yellow column, right, 400 μW/cm²), and rh7-null (light violet, left, 10 μW/cm²; dark violet column, right, 400 μW/cm²) flies for (A) UV, (B) violet, (C) blue, and (D) red light stimulus. Pairwise comparison was analyzed using two-sample t-test. p*<0.05, p**<0.005, p***<.001.

4.4 Discussion

Insects use a variety of sensory modalities to navigate their environments, including image forming and non-image forming vision. Remarkably, multiple critical light-driven behaviors are mediated through the clock gene expressing neural circuit in flies. In addition to regulating circadian behavior, this circuit also contributes to light activated behavioral arousal and phototaxis/photoavoidance light choice behavior. The circuit localization of these functions suggest that these light evoked behaviors may be modulated by time of day. The integration of multiple photosensory inputs for behavioral responses to light suggests the importance of functional redundancy as well as higher level processing of complex light spectral and intensity features. Circadian photoentrainment is mediated through a combination of external rhodopsin photoreceptors in the eyes and HB eyelets, as well as deep-brain photopigments CRY and Rh7 [2,11–13,77,78,100,121,129–137]. These mechanistically distinct photoreceptors detect differences in light intensity, spectral composition, and exposure time. The rich multiplicity of photosensory inputs suggests that these different input channels work together in a coordinated fashion, and likely extract sensory cues to determine precise time of day information. Such a system would allow

further tuning of the circadian clock to respond to complex light cues that vary according to time of day, weather and season, particularly in the morning [142,148–156]. Other sensory modalities, such as temperature sensing also provide further cues. Similarly, light choice behavior, expressed as phototaxis versus photoavoidance, also relies on the combination of external rhodopsin photoreceptors in the eyes and HB eyelets and the deep-brain neuronal photopigments CRY and Rh7 [8–10,33,35,36,157]. Recent work shows that light choice behavior varies by time of day and that the LNvs are a point of convergence for multiple light input channels that modulate light choice behavior [9]. The LNvs, particularly the l-LNv also serve as light activated arousal neurons that are embedded within the circadian neural circuit [14,15,102,158,159]. Yet how LNv circadian/arousal neurons functionally integrate different photic inputs to behavioral light arousal responses remained incompletely understood. Based on this set of earlier findings, we were motivated to measure the relative input contributions to l-LNv light evoked electrical excitation and behavioral arousal.

Short wavelength light evoked electrical excitation of the l-LNvs is mediated through all three photoreceptor systems. Our previous work has shown that upon blue and UV exposure of l-LNvs, CRY-mediated phototransduction increases in membrane electrical activity via the potassium channel subunit Hyperkinetic (HK), an NADH binding redox-sensor [6,160,161]. Using light-evoked electrophysiological assays that measure light evoked increases in action potential firing frequency in positive control *w;pdfGAL4-p12c;+* flies, we record robust increases in FF following 5 second exposures of UV, blue, and violet light stimuli. By comparison, significantly attenuated short wavelength light responses relative to control are recorded most of the mutant photoreceptor knockout flies that lack either all external opsin-based photoreceptors (*gl60j*), or CRY (*cry-null*), Rh7 (*rh7-null*), and the double mutant *gl60j-cry-null.* Blue light stimulation

evokes highly sustained FF increases for >20 seconds before returning to baseline in controls. Blue light evoked sustained FF rates are significantly attenuated in each of mutant knockouts, showing that all three photosystems are critical for blue light sustained action potential firing rates. Violet light also evokes sustained action potential FF increases in controls, persisting for >10 seconds, which are significantly attenuated in the mutant knockouts of photopigments that code for violet-sensitive rhodopsin-based phototransduction inputs (*gl60j*, *rh7-null*, and *gl60j-cry-null*). These results are consistent with previous findings that indicate CRY and Rh7 as the predominant blue and violet light internal photosensors, respectively, and show that external opsin driven photoreceptors also contribute additive/converging effects for blue and violet light sensing by the l-LNv. UV light exposure evokes significant, but less robust sustained increases in FF (<10 seconds) in controls, which more rapidly return to baseline FF after the cessation of light. These results indicate that the duration of l-LNv firing following lights off may code for spectral composition of light inputs. Interestingly, UV light FF increases of the double knockout *gl60j-cry-null* does not significantly differ from the control. This may be a result of unknown inhibitory interactions occurring between the different light input channels converging on the l-LNvs. Rh7's photosensitivity to UV light in the absence of CRY and external rhodopsin mediated photic input may be greater.

In contrast to short wavelength light, red light evokes relatively weak but still measurable excitation in the l-LNvs. Furthermore, the short wavelength sustained light evoked responses recorded in the l-LNv are not observed for red light responses. Surprisingly, red photoexcitation of the l-LNvs is dually regulated by CRY and external photoreceptors as shown by the significant attenuation of red light evoked action potential firing in neurons double knockout *gl60j-cry-null* flies compared with controls. Earlier work also shows that red light evokes minimal FF changes

during the red light pulse that are not as sustained as light evoked action potential post-stimulus probability of firing increases evoked by short wavelength light [3,91]. Further, l-LNv red light excitability has been found to attenuate with treatment with an FAD functional inhibitor, Diphenyleneiodnium (DPI), with *cry-null* mutants, or with a partial loss-of-function CRY point mutant that disrupts FAD photoreduction [3]. In our most recent study, we transgenically expressed CRY1 from a nocturnal mosquito species, *Anopheles gambiae*, in a *cry-null Drosophila* background and found those l-LNvs exhibit an even greater electrophysiological sensitivity to red light [91]. Although spectral absorption analysis of CRY's FAD at oxidized and anionic semiquinone reduced states exhibit peak sensitivity primarily around blue and UV wavelengths, red wavelength sensitivity could occur if CRY expresses a biologically active neutral semiquinone $FADH^{\bullet}$ state. Altogether, external rhodopsins and CRY dually contribute to the l-LNv red light excitability in the present study, with previous work also supporting red light-excitatory CRY as an input to l-LNvs based on higher reduced states of FAD cycles. Additional experiments are required to dissect the exact external photoreceptive elements that provide red light signaling to l-LNvs, though Rh1 and Rh6 are likely candidates as they exhibit partial red light sensitivity and are expressed in photoreceptor cells that either directly or indirectly input to l-LNvs [81,137].

We show representative firing records for each genotype tested and for each of the four light spectra employed in this study (UV, violet, blue and red). Consistent with most earlier publications, for our recordings, we observe predominantly tonic action potential firing in l-LNv recordings [3,6,10,79,82,91,101,102,104–111,146]. Burst firing as the predominant firing mode in l-LNv has been reported by another group [81,112]. It remains unclear why different groups see different firing patterns in l-LNv recordings. Based on anatomical location of the l-LNvs embedded within the circadian neural circuit, we considered the possibility that light evoked excitation of the l-LNvs is

circadian regulated. However, we find no significant time-of-day effects for the l-LNv electrical light responses we recorded.

The l-LNvs contribute to different light regulated behaviors of the fly, including circadian behavior, light choice attraction/avoidance behavior and arousal behavior [6,8–10,13]. CRY is the primary circadian photopigment in *Drosophila melanogaster* yet is not required to maintain light-dark entrainment, since the fly clock has been shown to directly entrain by inputs from Rhodopsins in each of the external photoreceptor systems: compound eyes, HB eyelets, and ocelli [132]. Specifically, Rh1, Rh3, Rh4, and Rh6 mediate low-intensity light re-entrainment properties of the clock [136], while Rh5 mediates medium and high intensity light re-entrainment, though this may occur via a non-PLC phototransduction pathway [162,163]. It is thought that Rh6 expressing photoreceptor cells in the eyes converge all inputs from the outer and inner receptor cells in order to mediate circadian entrainment [135,163,164], though the precise anatomical characterization to clock neurons from these photoreceptor cells remains elusive. However, even with the removal of CRY and all externally expressed rhodopsins, flies were observed to still respond and entrain to light, leading to the discovery of internally expressed Rhodopsin 7, which was found to also contribute to circadian light entrainment via pacemaker neurons of the fly circadian neural circuit [2]. Only true "circadian blind" flies exist if all three photoreceptor pathways are removed.

Light choice attraction/avoidance behavior is mediated by multiple photic inputs from the eyes, CRY, and Rh7 [3,8,10,26,31,52–54,56]. Each of these photic input channels have distinct features based on light intensity, spectral composition, and light exposure time. Specifically, acute (minutes) high-intensity (400 $\mu W/cm^2$) and low-intensity (10 $\mu W/cm^2$) UV light attraction is primarily mediated by external rhodopsin photopigments while long-lasting (tens of seconds) high-

intensity (400 μW/cm²) UV light avoidance is primarily mediated by internal CRY and Rh7 photopigments.

In our present study, we provide evidence of multiple photic input integration for light arousal behavior. UV light-pulses show a significant attenuation in the arousal response of all Rhodopsin-based phototransduction mutants (*gl60j*, *rh7-null*, and *gl60j-cry-null*) relative to controls for both low and high intensity lighting conditions, but not in *cry-null* mutant flies. Thus, fly arousal to UV light pulses is apparently opsin-dependent and CRY-independent. Unsurprisingly, violet light-pulses indicate the violet light-sensitive rhodopsins in the eyes and Rh7 as functional violet photosensors for violet light evoked arousal behavior. CRY appears to have a minor contribution for low-intensity violet light evoked arousal responses. Similarly, blue light evoked arousal responses depend on CRY and all rhodopsin photopigments (external and Rh7) for both low and high intensity blue light evoked arousal responses. These results suggest that functional redundancy is achieved by neutral integration of all three channels of photic input for blue light evoked arousal responses, while Rh7 activation may provide gain modulation for UV light evoked arousal responses. The average % of flies that awaken from low-intensity red light pulses is significantly attenuated relative to control with both the single knockout mutants *gl60j* and *cry-null*, as well as the double knockout mutants *gl60j-cry-null*. This finding closely matches the electrophysiological results for l-LNv electrophysiological recordings made from double knockout *gl60j-cry-null* flies. Surprisingly, with high-intensity red light pulses, the overall average % of flies that awaken are lower for all groups, and only *rh7-null* flies show significantly attenuated red light evoked arousal responses. This was a surprising observation that we believe suggests two possibilities: 1) the arousal neural circuit may have a detection threshold for red light that our 400 μW/cm² high-intensity red stimulus exceeds, and 2) Rh7 has the highest intensity

detection threshold amongst the three photoreceptor systems, but still requires input from external rhodopsins and CRY to enable a proper red light pulse arousal response.

There is a strong relationship between circadian neuronal electrical activity and clock cycling [43,165,166]. There are only a handful of publications that measure clock protein cycling at high temporal-spatial resolution [99,167,168], and only a subset of those show the effects of 12h:12h light:dark cycles on the clock [99,167]. For clock driven behaviors, CRYPTOCHROME (CRY) is the primary circadian photoreceptor and mediates clock disruption by constant light, while eye light input is redundant to CRY [99,129]. PER and TIM oscillations are highly synchronous across all major circadian neuronal subgroups in unshifted light schedules for 11 days. PER entry into the nucleus precedes TIM by about three hours late at night [99,167]. 3hr light phase delays followed several days later by 3hr light phase advances significantly dampens PER oscillator synchrony and rhythmicity in most circadian neurons during and after exposure. LNv clock protein oscillations are the first to desynchronize and the last to resynchronize following such light shifts, while the dorsal neuron group-3 (DN3s) within the circadian circuit increase their within-group synchrony in response to phase delay/phase advance light shifts. In vivo, alternating light shifts transiently disrupt sleep stability, and learning and memory processes, temporally coinciding with circuit desynchrony. The role of light shifts and subsequent clock circuit desynchrony is yet to be explored for other light evoked behaviors including light choice behavior and light evoked arousal.

Insect photobehaviors are evoked by many parameters of light, including intensity, spectral composition, and exposure time. Circadian photoentrainment and light attraction/avoidance behaviors function through the integration of multiple photic inputs. We provide additional evidence of a functional integration between these multiple sensory systems that converge input

in l-LNvs to mediate neuronal photoexcitation and behavioral light arousal. Understanding how such complex light-evoked behaviors may allow us to target specific photoreceptor systems for more effective behavioral manipulations, which would lead a promising direction towards novel insect vector-control strategies.

CHAPTER 5: Light-evoked membrane excitability of fly primary arousal neurons are mediated by convergent pathways from multiple photoreceptor systems

5.1 Introduction

Photoreception provides a powerful sensory system that allow animals to adapt and navigate different environments. Multiple photoreceptor systems contribute to photoentrainment, sleep/wake behaviors, attraction/avoidance to light and more, all converging on the ventral lateral neuronal (LNv) subset within the circadian circuit in insects. Short-wavelength light is particularly effective for mediating visual functions including circadian photo entrainment, phototaxis, sleep, and arousal. Two non-image forming mechanisms that operate cell autonomously in LNvs are based on two brain photopigments: Cryptochrome (CRY) and Rhodopsin 7 (Rh7) [2,6,8–10,12,77,102,119–121]. CRY is a photosensor initially characterized for its role in light resetting the circadian molecular clock [45,88,122]. More recently, it was discovered that CRY phototransduction mediates increase the neuronal electrical excitability of circadian/arousal neurons. These neurons tune certain physiological and behavioral responses according to different intensities, spectrum, and timing of light inputs [6,13–15,79,80,82–84,169].

CRY relies on its flavin adenine dinucleotide (FAD) chromophore for phototransduction, a process that involves successive redox reduction reactions that depend on stepwise electron transfer between several tryptophan residues embedded within the structure [3–5,38,94,123]. From a base oxidized FAD state with roughly equal absorption peaks for ultraviolet light (UV, 365 nm) and blue light (450 nm), light evokes a reduced anionic semiquinone $FAD^{\bullet -}$ state with a primary absorption peak for UV light (365 nm) [16,17,64], then to a higher reduced neutral semiquinone

FADH state that exhibits a short wavelength spectral absorption peak around 340 nm along with a broad longer wavelength absorption with peaks corresponding to green light (510 nm), yellow light (580 nm) and red light (635 nm). Light-activated CRY redox reactions are transduced into changes in neuronal membrane potential and electrical excitability via intermolecular redox transfer the voltage-gated potassium channel beta subunits (Kvβ) Hyperkinetic (Hk) redox sensor [1,10,13,102]. Rh7 absorption is broad, with a peak at violet (405 nm) [2,120] and Rh7 signaling relies on the Gq/PLC signaling pathway [2,7]. In addition to these internal photopigments, insects like *Drosophila* also express six rhodopsin photopigments found in the compound eyes, the Hofbauer-Buchner (HB) eyelet, and the ocelli. These external photoreceptor systems relying on these six opsins mediate a broad spectral range spanning from UV to red (~300-630 nm) light [124–128]. There is growing evidence showing that complex light-evoked behaviors, including circadian photoentrainment, arousal and photo attraction/avoidance are mediated by these three distinct photoreceptor systems [2,8,9,11–13,78,129,131–137,170,171].

Most of the LNv light-activated arousal neurons express the circadian neuropeptide pigment-dispersing factor (PDF) and can be further categorized as small and large (s-LNvs and l-LNvs, respectively) that are each uniquely capable of transmitting light information that contribute to endogenous circadian timekeeping or wakefulness/arousal. Large LNvs (l-LNvs) are the fly primary arousal neuronal subgroup that have been found to respond rapidly to short-wavelength light with sustained membrane depolarization responses lasting 10s of second after light exposure [1,3,6,10]. Additional studies show that l-LNv acute responses to red light (~635 nm) attenuated in neurons recorded from *cry-null* flies [3,146], thus adding CRY as another photoreceptor system capable of transmitting red light input to the l-LNvs along with light driven synaptic inputs downstream from light activation of red light sensitive Rh1 and Rh6

photopigments expressed in external photoreceptor structures. Additional evidence shows circadian photoentrainment is modulated by CRY, external opsin-based photoreceptor structures and Rh7, which tune to differing intensities, exposure times, and spectrum of light for photoentrainment [144], and even attraction/avoidance to light [9]. Anatomical and physiological evidence suggests direct or indirect projections from external photoreceptors, particularly the HB-eyelet to LNv groups via an accessory medulla (aME) region, which receives projections from external photoreceptor structures and lamina monopolar cells [111,131,132,145,170]. The mutant *gl60j* lacks all external photoreceptor inputs.

How these multiple photoreceptor systems converge functionally on l-LNvs to mediate changes in electrical excitability in response to different colors of light remains largely unexplored. We find that multiple photoreceptor systems do indeed exhibit integration. Identifying functional convergence between multiple photoreceptor systems in the fly strengthen our understanding of how insect image-forming and non-image forming visual processes to mediate complex light-evoked behaviors.

5.2 Materials and Methods

5.2.1 Experimental Animals

The flies we raise for experiments are given a standard food media consisting of yeast, cornmeal, and agar at 25±1 ºC. We use 3 to 4-day post-eclosion adult male flies. The baseline mutations of *rh7-null*, *gl60j*, and *gl60j-cry-null* mutant flies were obtained from collaborators Craig Montell of UC Santa Barbara, and *cry-null* mutant flies from Amita Seghal of University of

Pennsylvania. In order to visualize the arousal neurons of interest for electrophysiological experiments, we crossed each photoreceptor mutant with a *pdfGAL4-p12c* driver line. This cross schematic takes advantage of our previously engineered *p12c* mutation that tags GAL4 expression with GFP. We relied on cell size, morphological characteristics, and anatomical location to identity and patch-clamp large lateral ventral neurons.

5.2.2 Light-Evoked Neuronal Electrophysiology

We employ previously established light-evoked potential electrophysiology assays from [3] to measure the fly large lateral ventral neuronal responses to light stimuli. Adult male flies are selected after 3 to 4-days post-eclosion, then are dissected in a chilled external recording solution of 122 mM NaCl, 3 mM KCl, 1.8 mM CaCl2, 0.8 mM MgCl2, 5 mM glucose, 10 mM HEPES, calibrated to a pH of 7.2±.02 and osmolarity of 250-255 mOsm. A patch recording pipette is filled with an internal recording solution of 102 mM Kgluconate, 17 mM NaCl, 0.085 mM CaCl2, 1.7 mM MgCl2 (hexahydrate), 8.5 mM HEPES, 0.94 mM EGTA, and is calibrated to a pH of 7.2±.02 and osmolarity of 232-235 mOsm, then patched onto the large lateral ventral neurons for recording. We use a custom modified multichannel LED source developed by Prizmatix/Stanford Photonics based in Palo Alto, CA, which is is fitted onto our Olympus BX51 WI microscope. Each LED from the multichannel source is tuned to specific wavelengths of color: UV (365 nm), violet (405 nm), blue (450 nm), and red (635 nm). Using a Newport 842-PE Power/Energy meter, we set all LED exposures to an intensity of 200±20 $\mu W/cm^2$. Using pClamp (Molecular Dynamics) software, we program 50 seconds of dark for baseline recording, followed by 5 seconds of colored-light stimulation, then 95 seconds of inter-pulse darkness in order to measure the kinetics of membrane depolarization after light excitation. This protocol repeats continuously over five sweeps per

recording and the resulting traces analyzed using Clampfit (Molecular Dynamics) software. Analysis consists of averaging all sweeps and traces of an experimental group then applying a 3 Hz Gaussian filter, then a 1 Hz butterworth filter, and baseline normalized to 0. We report the membrane potential data from our lateral ventral neurons as the average last 60 seconds of all recordings in a given group.

5.2.3 Quantification and Statistical Analysis

All values are presented as mean ± SEM. We report the total number of recordings as n replicates of an experiment, with a minimum of three replicates per color per genotype. We use statistical tests and methods from Minitab, Matlab, and Microsoft Excel software to analyze our data sets. We determine normality of our datasets using Anderson-Darling normality tests, followed by F-tests to determine variance of normally distributed data, and two-sample, one-tailed T-tests to determine significance between groups with an alpha of 0.5. For non-normal data, we use Mann-Whitney U-tests to determine significance between groups. We use false discovery rate (FDR [44]) to mitigate the accumulation of Type I error/false positives after repeat multi-group comparisons. As a result, we adjust the alpha to 0.1 in order to indicate significance as an expected proportion of false positives that is no greater than 10%.

5.3 Results

5.3.1 Coincident inputs from three photoreceptor systems enables complex UV light-evoked responses in membrane excitability of arousal neurons

Opsin-based photoreceptor systems from the external environment (compound eyes, ocelli, HB eyelets) converge on primary circadian/arousal LNv neurons that dually express CRY and Rh7, indicating a convergence of photic inputs [2,9,11–13,78,111,129–131,135,137,144,145]. To test the relative contributions of multiple phototransduction systems that converge on the l-LNv leading to changes in membrane excitability to light, we employed our light-evoked potential electrophysiology assay [3,91,146,174] by testing photoreceptor mutants *gl60j, cry-null, rh7-null*, and double mutant *gl60j-cry-null* flies. We compared l-LNv membrane depolarization responses for each mutant after repeat 5 second exposures of 200 μW/cm² UV, violet, blue, or red light stimuli, reporting the electrophysiological light-evoked potential responses of l-LNvs as a 60 second average traces of membrane potential containing recordings 10 seconds before stimulus, 5 seconds during stimulus, and 45 seconds post stimulus. Traces are filtered and normalized in order to accurately compare control wild-type *p12c* recordings with recordings from genetic knockouts *cry-null*, *rh7-null*, total external photoreceptor knockout *gl60j*, and a double-mutant *gl60j-cry-null* photoreceptor mutant.

Five seconds of 200 μW/cm² UV (365 nm) LED light evokes a robust membrane depolarization event with the native CRY expressing *p12c* control l-LNvs (Figure 5-1A-D, light blue traces). The depolarization event persists for the duration of the UV light stimulus, then returns to baseline membrane potential after approximately 5 seconds after the cessation of light. For *gl60j* mutants, the response is not significantly different from the *p12c* control, but there is a noticeable delay in membrane depolarization (Figure 5-1A, red trace). As expected, excitation of

cry-null l-LNvs with an intensity matched UV light stimulus significantly reduce the depolarization response (Figure 5-1B, green trace) as CRY's FAD exhibits a spectral absorption peak around 365 nm. The double mutant *gl60j-cry-null* exhibits both an attenuated depolarization response at the initial onset of UV light stimulus, and a delayed in membrane depolarization (Figure 5-1C, yellow trace). The *rh7-null* mutation shows a flattened response during and after UV light stimulus (Figure 5-1D, violet trace). For the *gl60j*, *cry-null*, and *gl60j-cry-null* depolarization responses, it is preceded with a slight hyperpolarization event that is absent with the *rh7-null* response. These results indicate that the eyes/external rhodopsin photoreceptors and cell autonomously expressed CRY and Rh7 all contribute to the l-LNv light-evoked potential responses to UV light.

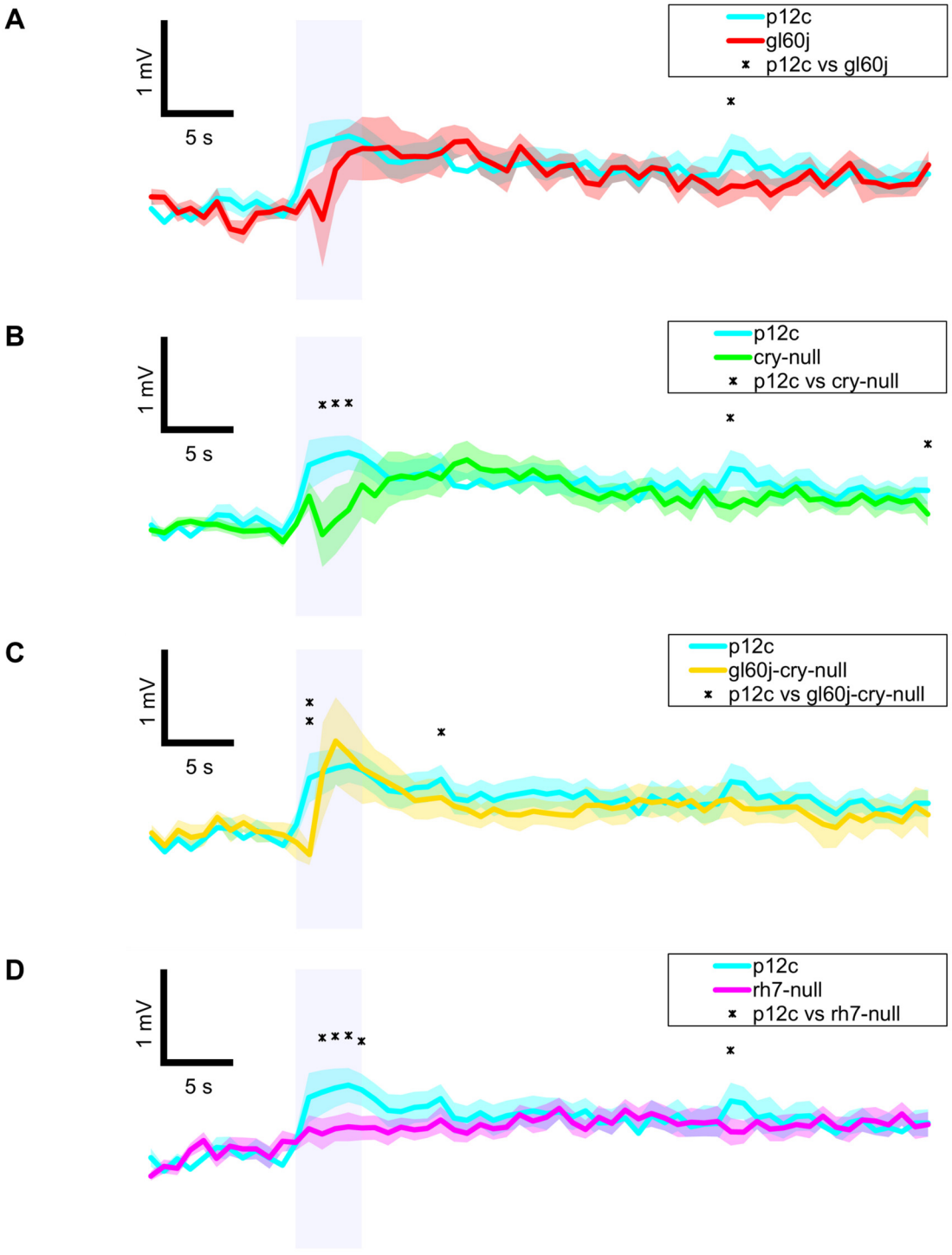
A
1 mV
5 s
p12c
gl60j
p12c vs gl60j
B
1 mV
5 s
p12c
cry-null
p12c vs cry-null
C
1 mV
5 s
p12c
gl60j-cry-null
p12c vs gl60j-cry-null
D
1 mV
5 s
p12c
rh7-null
p12c vs rh7-null

Figure 5-1. All photoreceptor mutants except *gl60j* mutants show an attenuated UV light response during stimulus compared to native expressed *Drosophila* CRY

Membrane depolarization response of *p12c* (blue trace, n=16) versus (A) *gl60j* (red trace, n=16), (B) *cry-null* (green trace, n=22), (C) *gl60j-cry-null* (yellow trace, n=12), and (D) *rh7-null* (violet trace, n=13) with UV (365 nm, 200 μW/cm²) light stimulus. Purple bar indicates 5 seconds of UV light stimulus. Data are plotted as average ± SEM. Pairwise comparison was analyzed using two-sample t-test with FDR adjustment. p*<0.1, p**<0.05, p***<.01.

5.3.2 Violet light-evoked responses do not depend on CRY phototransduction

Violet light sensing input to the l-LNvs has been shown to predominantly rely on Rh7 phototransduction, but it is not well explored how other violet sensitive rhodopsins expressed in the external environment contribute to the membrane excitability of these neurons. In order to test CRY and other photoreceptor contributions to l-LNv membrane excitability to violet light, we repeated our light-evoked electrophysiology protocol with a violet light stimulus. Five seconds of 200 μW/cm² of violet (405 nm) LED light evokes an almost 1 mV depolarization response that persists for 30-40 seconds post-stimulus before returning to baseline for native CRY expressing control *p12c* l-LNvs (Figure 5-2A-D, light blue traces). In contrast, *gl60j* l-LNvs show a significantly attenuated response to intensity matched violet light stimulus compared to the *p12c* control (Figure 5-2A, red trace). Unsurprisingly, the violet light-evoked response of *cry-null* flies do not significantly differ (Figure 5-2B, green trace) as the spectral absorption of CRY's FAD does not peak around 405 nm. The double mutant *gl60j-cry-null* violet light response is also significantly attenuated compared to the *p12c* control for the first 25 seconds after stimulus onset (Figure 5-2C, yellow trace), but exhibits an even lesser depolarized response compared to that of the single *gl60j* mutant violet light response. The gradual membrane depolarization after 25

seconds may be a result of unstable resting membrane potentials for this mutation. Similarly, the *rh7-null* response to violet light is also significantly attenuated for almost the entire duration of the *p12c* response (Figure 5-2D, violet trace). Both *gl60j* and *gl60j-cry-null* violet light depolarization responses are yet again preceded by a hyperpolarization event during violet light stimulus (Figure 5-2A and 5-2C, respectively) with a noticeable absence with the *cry-null* and *rh7-null* responses (Figure 5-2B and 5-2D, respectively). Taken together, these results indicate the violet light-mediated responses in l-LNvs occur primarily through convergent rhodopsin-based signals, especially that of the internal violet photosensor, Rh7, and possibly external violet sensitive Rh1, Rh2, Rh4, Rh5, and Rh6.

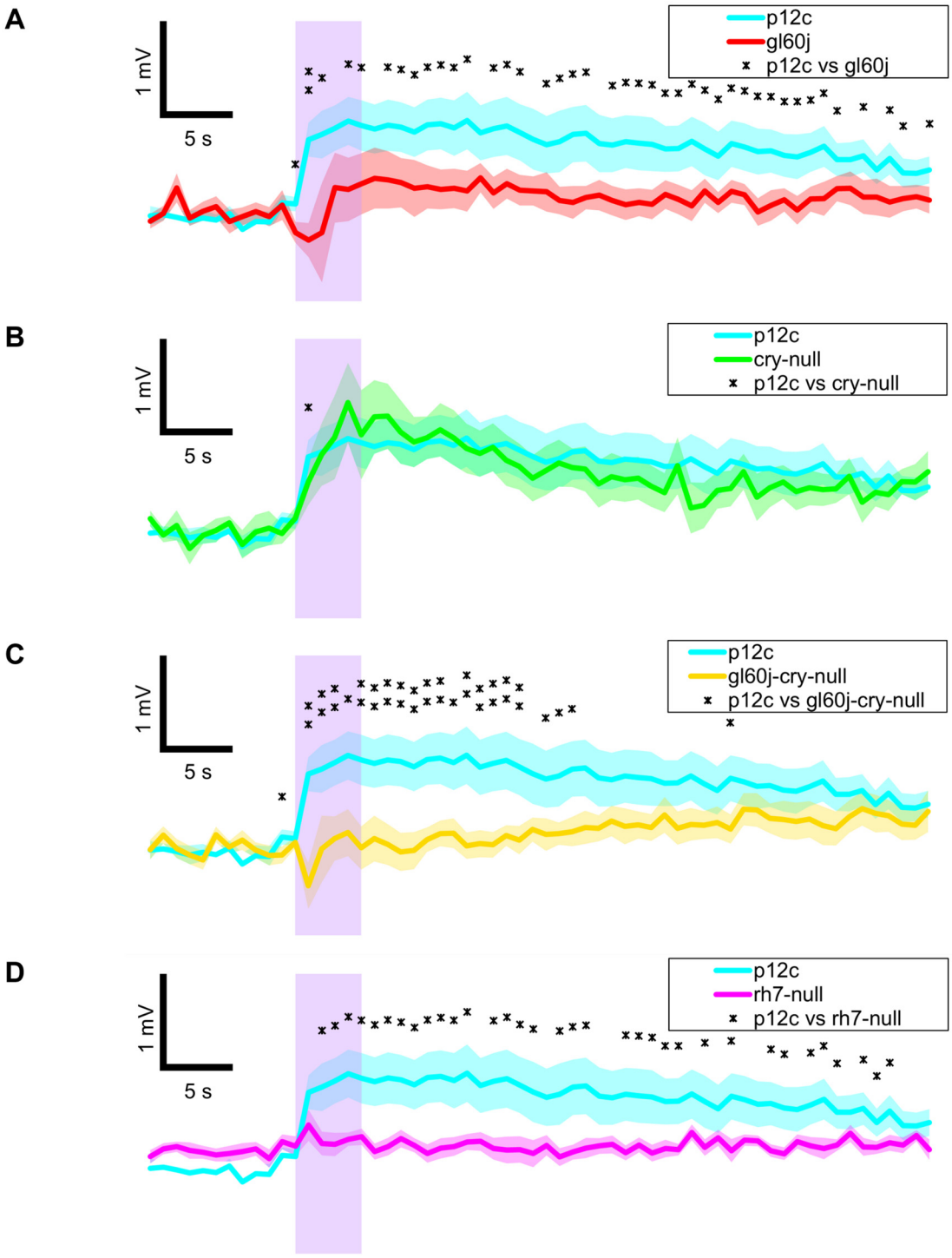
A
1 mV
5 s
p12c
gl60j
p12c vs gl60j
B
1 mV
5 s
p12c
cry-null
p12c vs cry-null
C
1 mV
5 s
p12c
gl60j-cry-null
p12c vs gl60j-cry-null
D
1 mV
5 s
p12c
rh7-null
p12c vs rh7-null

Figure 5-2. All photoreceptor mutants except *cry-null* show a long-lasting attenuated violet light response compared to native expressed *Drosophila* CRY

Membrane depolarization response of *p12c* (blue trace, n=16) versus (A) *gl60j* (red trace, n=16), (B) *cry-null* (green trace, n=22), (C) *gl60j-cry-null* (yellow trace, n=12), and (D) *rh7-null* (violet trace, n=13) with violet (405 nm, 200 μW/cm²) light stimulus. Violet bar indicates 5 seconds of violet light stimulus. Data are plotted as average ± SEM. Pairwise comparison was analyzed using two-sample t-test with FDR adjustment. p*<0.1, p**<0.05, p***<.01.

5.3.3 All photoreceptor systems converge input to mediate blue light-evoked arousal neuronal membrane excitability

CRY is the primary blue light photosensor in the fly circadian neural circuit, yet anatomical and physiological evidence circumstantially indicate external photoreceptor systems also input light information. Blue light input to the l-LNvs has remained largely unexplored, thus we readapt our light-evoked electrophysiology protocol to emit blue light stimulus to test our photoreceptor mutants targeting other potential inputs to the l-LNvs. Five seconds of 200 μW/cm² of blue (450 nm) LED light evokes an approximate 1 mV depolarization response that sustains for approximately 10 seconds after light onset then gradually decays back to baseline while still remaining depolarized for an additional 30-40 seconds for native CRY expressing control *p12c* l-LNvs (Figure 5-3A-D, light blue traces). The *gl60j* mutant response to blue light is significantly attenuated at the initial onset of light and during the post-stimulus depolarization decay to baseline (Figure 5-3A, red trace). Unsurprisingly, the *cry-null* depolarization response to blue light is largely attenuated during and after stimulus and even exhibits a sharp depolarization spike followed by hyperpolarization during stimulus (Figure 5-3B, green trace), which corroborates our previous *cry-null* recordings to blue light. The hyperpolarized response may be due to rhodopsin

contribution to the l-LNvs, which is a common characteristic of rhodopsin-based to mediate hyperpolarized phototransduction responses. The double mutant *gl60j-cry-null* has the most significantly attenuated response to blue light stimulation but doesn't noticeably exhibit hyperpolarization like the single *cry-null* response does (Figure 5-3C, yellow trace vs. Figure 5-3B, respectively), thus supporting the idea that rhodopsins in the absence of CRY mediate a hyperpolarized blue light response in l-LNvs. Additional support can be seen with the *rh7-null* blue light response, which is also significantly attenuated compared to the *p12c* control, yet also does not exhibit a hyperpolarized response to blue light (Figure 5-3D, violet trace). These results support blue light sensing in l-LNvs is mediated through all three photoreceptor systems, with a primarily rhodopsin-based hyperpolarization response to blue light that is otherwise not observed in other short-wavelength lights tested.

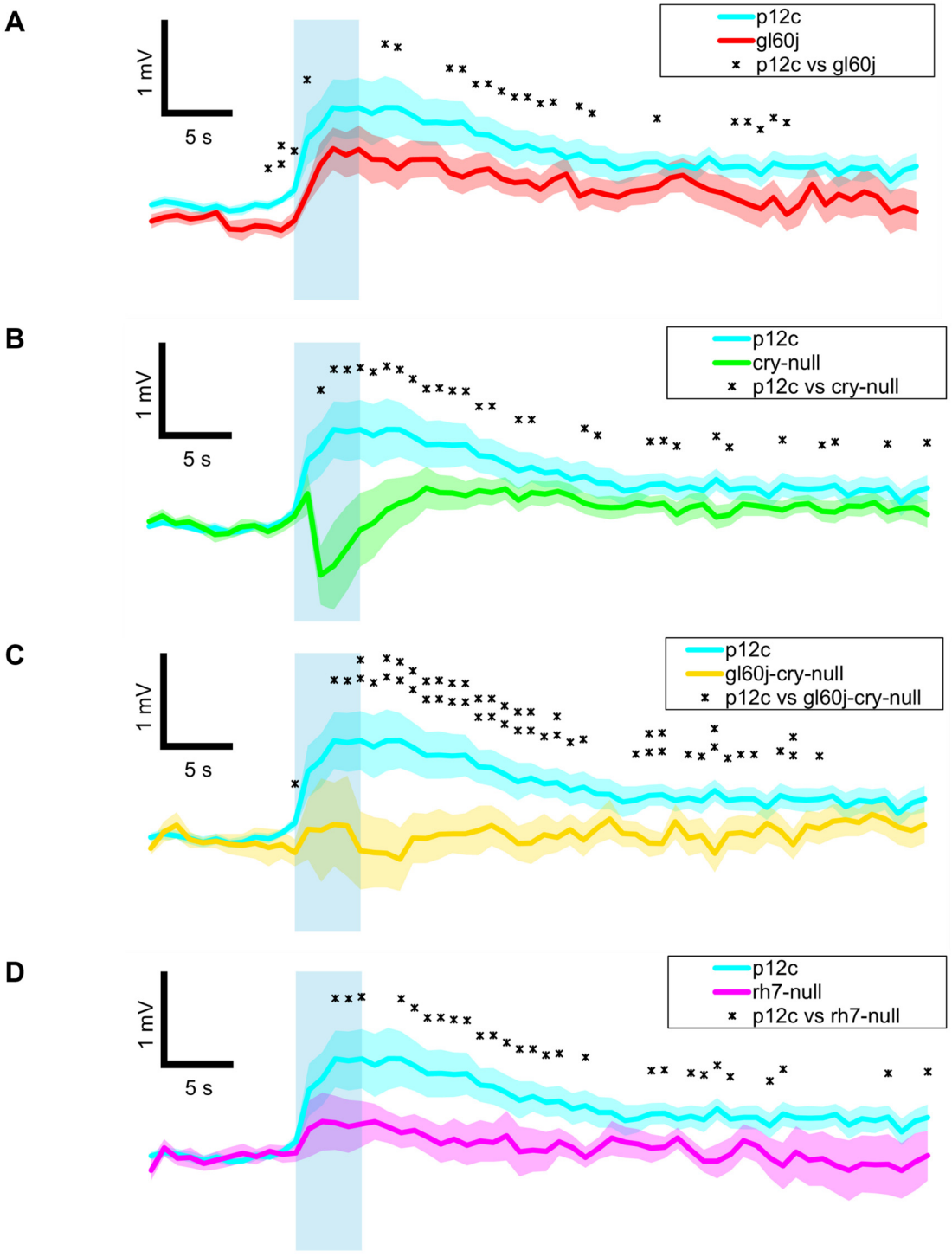
A
1 mV
5 s
p12c
gl60j
p12c vs gl60j
B
1 mV
5 s
p12c
cry-null
p12c vs cry-null
C
1 mV
5 s
p12c
gl60j-cry-null
p12c vs gl60j-cry-null
D
1 mV
5 s
p12c
rh7-null
p12c vs rh7-null

Figure 5-3. All photoreceptor mutants show an attenuated blue light response compared to native *Drosophila* CRY

Membrane depolarization response of *p12c* (blue trace, n=16) versus (A) *gl60j* (red trace, n=16), (B) *cry-null* (green trace, n=22), (C) *gl60j-cry-null* (yellow trace, n=12), and (D) *rh7-null* (violet trace, n=13) with blue (450 nm, 200 μW/cm²) light stimulus. Blue bar indicates 5 seconds of blue light stimulus. Data are plotted as average ± SEM. Pairwise comparison was analyzed using two-sample t-test with FDR adjustment. p*<0.1, p**<0.05, p***<.01.

5.3.4 All mutants attenuate the acute red light-evoked membrane excitability, but CRY may also contribute longer-lasting effects

Red light excitability in l-LNvs have been explored previously [3,91]. One explanation for these surprising results could involve CRY's FAD reaching higher states of photoreduction that reach longer-wavelength sensitivities. Other explanation could rely on red light sensitive rhodopsins in the fly compound eyes, which include Rhodopsin 1 and Rhodopsin 6. Projections from these external systems, as well as physiological evidence suggest that LNvs may also receive photic input from external photoreceptors. We test the idea of red light membrane excitability from multiple photoreceptors more in depth here. Much like our previous reports, five seconds of 200 μW/cm² of red (635 nm) LED light also exhibit a small and acute depolarization response for our control p12c group (Figure 5-4A-D, blue traces). The depolarization response does not sustain as it quickly reaches baseline membrane potential at the offset of red light. Removal of all external photoreceptors, including red light sensitive Rh1 and Rh6, with the *gl60j* mutation yields a significant loss of red light excitability in l-LNvs (Figure 5-4A, red trace). Surprisingly, the *cry-null* mutation also exhibits a significantly attenuated response to red light during stimulus, while also showing a significant difference to the post-stimulus *p12c* membrane potential for approximately 10 seconds immediately after stimulus and for another 10-15 seconds twenty

seconds after stimulus (Figure 5-4B, green trace). The double mutant *gl60j-cry-null* shows a very similar attenuation to the single mutant *gl60j* red light response, with depolarization attenuation primarily during red light stimulus (Figure 5-4C, yellow trace). The *rh7-null* mutation exhibits the least attenuated red light response and thus may only minimally contribute to signaling red light excitability to l-LNvs (Figure 5-4D, violet trace).

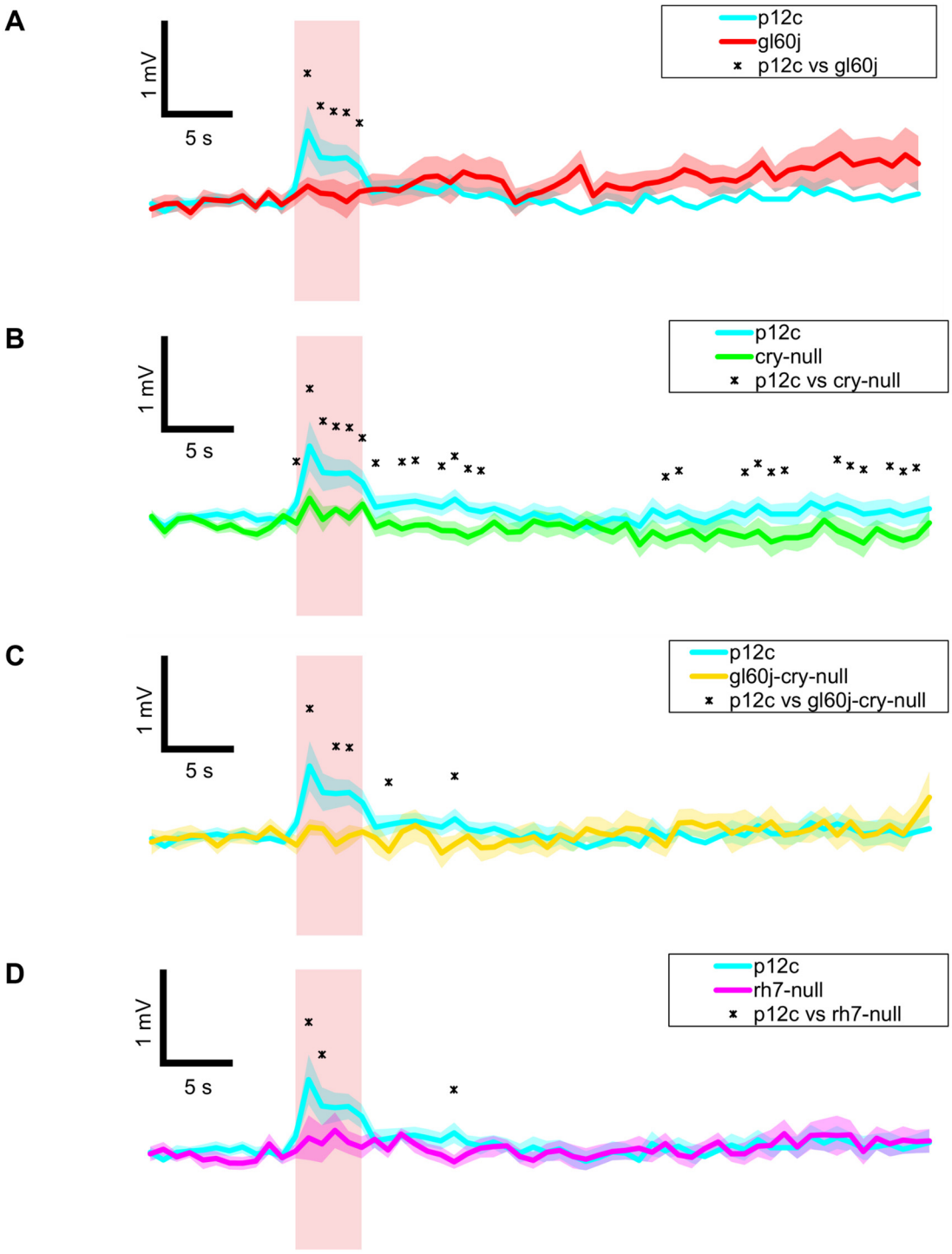
A
1 mV
5 s
p12c
gl60j
p12c vs gl60j
B
1 mV
5 s
p12c
cry-null
p12c vs cry-null
C
1 mV
5 s
p12c
gl60j-cry-null
p12c vs gl60j-cry-null
D
1 mV
5 s
p12c
rh7-null
p12c vs rh7-null

Figure 5-4. All photoreceptor mutants show an attenuated red light response during stimulus compared to native expressed *Drosophila* CRY

Membrane depolarization response of *p12c* (blue trace, n=16) versus (A) *gl60j* (red trace, n=16), (B) *cry-null* (green trace, n=22), (C) *gl60j-cry-null* (yellow trace, n=12), and (D) *rh7-null* (violet trace, n=13) with red (635 nm, 200 μW/cm²) light stimulus. Red bar indicates 5 seconds of red light stimulus. Data are plotted as average ± SEM. Pairwise comparison was analyzed using two-sample t-test with FDR adjustment. p*<0.1, p**<0.05, p***<.01.

5.3.5 Light responses recorded from l-LNvs show no apparent time-of-day differences

Light-evoked electrophysiological recordings on the individual l-LNv primarily result in tonic action potential firing patterns, consistent with most other reports [1,3,6,10,79,82,91,101,102,104–111,146]. To determine if the absence of CRY or the internal and external Rhodopsin photoreceptors alters the basal membrane potential (MP) of l-LNvs, we plotted basal MP values across the time of day of the recordings (Figure 5-5). Scatter plots for the *p12c* control and all photoreceptor mutants pre-exposed to UV, violet, blue, or red light (Figure 5-5A-D, respectively) show no discernable correlation to time-of-day of the recording and baseline MP. However, average baseline MP for each group plotted as a box and whisker plot shows significantly higher baseline MP for *gl60j-cry-null* over *gl60j* mutants (Figure 5-5E, yellow box vs red box, respectively). The median values of the double knockout *gl60j-cry-null* is notably higher than the rest of the groups, indicating an unstable baseline MP, but all other groups are otherwise equivalent. These results indicate removal of both CRY and external photoreceptor systems could destabilize the baseline MP of l-LNv and thus may be necessary for baseline circadian/arousal neuronal membrane responses to light.

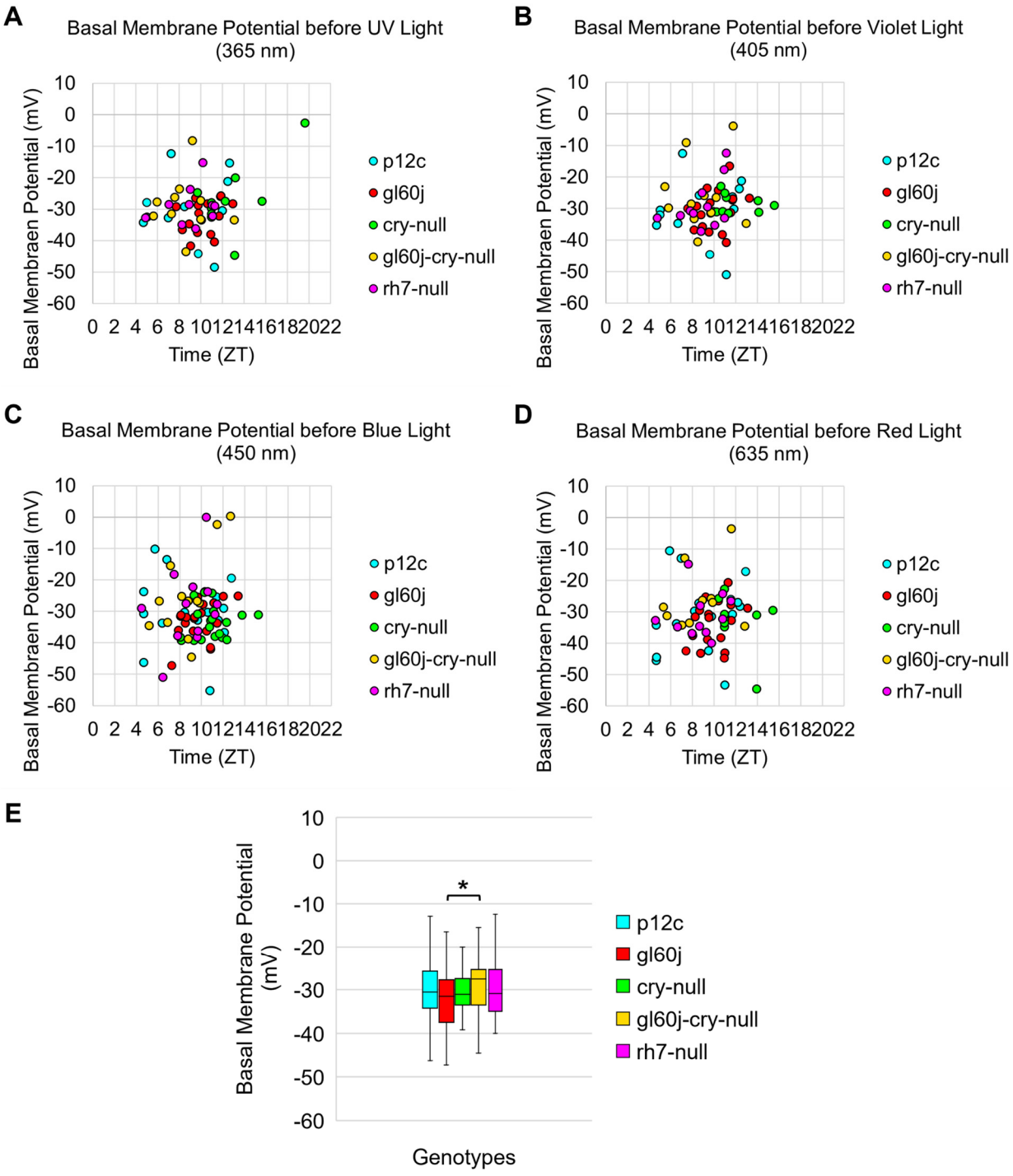
A
Basal Membrane Potential before UV Light
(365 nm)
Basal Membraen Potential (mV)
10
0
-10
-20
-30
-40
-50
-60
0 2 4 6 8 10 12 14 16 18 20 22
Time (ZT)
p12c
gl60j
cry-null
gl60j-cry-null
rh7-null
B
Basal Membrane Potential before Violet Light
(405 nm)
Basal Membraen Potential (mV)
Time (ZT)
p12c
gl60j
cry-null
gl60j-cry-null
rh7-null
C
Basal Membrane Potential before Blue Light
(450 nm)
Basal Membraen Potential (mV)
Time (ZT)
p12c
gl60j
cry-null
gl60j-cry-null
rh7-null
D
Basal Membrane Potential before Red Light
(635 nm)
Basal Membraen Potential (mV)
Time (ZT)
p12c
gl60j
cry-null
gl60j-cry-null
rh7-null
E
Basal Membrane Potential
(mV)
10
0
-10
-20
-30
-40
-50
-60
*
Genotypes
p12c
gl60j
cry-null
gl60j-cry-null
rh7-null

Figure 5-5. Basal membrane potential is most unstable with *gl60j-cry-null* but are otherwise equivalent in all other groups and there is no time-of-day dependent effect

Average basal membrane potential of *p12c* (blue), *gl60j* (red), *cry-null* (green), *gl60j-cry-null* (yellow), and *rh7-null* (violet) before (A) red, (B) blue, (C) violet, and (D) UV light stimulus plotted against the relative time-of-day of each recording. (E) Box-and-whisker plot summary of the average basal membrane potential for *p12c* ((n =35) total, n (ZT0-12) =30; n (ZT12-16) =5), *gl60j* ((n=22) total, n (ZT0-12) =20; n (ZT12-16) =2), *cry-null* ((n=26) total, n (ZT0-12) =14; n (ZT12-16) =12), *gl60j-cry-null* ((n=30) total, n (ZT0-12) =22; n (ZT12-16) =8), and *rh7-null* ((n=30) total, n (ZT0-12) =22; n (ZT12-16) =8). Median values are denoted by a solid black line within each box of the plot. Black * indicates FDR adjusted two-sample t-test $p \leq 0.01$ vs. *p12c*. Data are represented as a range of means in a sample set ± maximum and minimum values within the set. One significance symbol; $p \leq 0.1$, two significance symbols; $p \leq 0.05$, three significance symbols; $p \leq 0.01$.

5.4 Discussion

Drosophila transduce a wide range of sensory cues to detect changes in the environment, many of which drive photosensory stimulation for image forming and non-image forming visual behaviors. Many of these light-based behaviors are mediated through the circadian molecular clock and circadian neural circuit. Large ventral lateral neurons are a key subgroup of this circuit because they provide excitatory responses to light that signal to other neuronal subgroups. We propose a multi-photosensory system integration in the l-LNvs that contribute to the excitatory light responses to short-wavelength light, as well as red light. Previous studies have shown that circadian photoentrainment is mediated through a multi-photosensory system, including external rhodopsin in extraretinal systems, as well as internally expressed CRY and Rh7 in the circadian circuit [2,11–13,77,78,100,121,129–137]. These photoreceptor systems rely on different mechanism of phototransduction that differences in light intensity, spectral composition, and exposure time. The many broad range of photosensory inputs requires multiple different input channels that

coordinated in order to transduce photo sensory cues that help determine precise time of day information. This system would help explain how the circadian clock is able to respond to variations in daily, season, and even weather-dependent light stimuli [142,148–156]. The photoelectrical contribution of multi-photosensory systems has remained largely unexplored, thus we were motivated to address the potential integration of several photic inputs to the l-LNvs that provide excitatory responses to short wavelength light, as well as red light.

UV, violet, blue, and red light-evoked membrane depolarization of l-LNvs is mediated through multiple photoreceptor systems. We have previously shown that CRY is largely responsible for blue and UV light-evoked l-LNv responses via a redox-based interaction with Hyperkinetic [6,160,161]. We extended these findings in the present study by adapting our light-evoked electrophysiological assay to measure the membrane depolarization during and after 5 seconds of light stimulation of positive control *w;pdfGAL4-p12c;+* flies compared against photoreceptor mutants that selectively remove different photoreceptor systems, including all external opsin-based photoreceptors (*gl60j*), CRY (*cry-null*), Rh7 (*rh7-null*), or a double mutant *gl60j-cry-null.* UV light stimulation shows an attenuated membrane depolarization for all mutant groups against the control *p12c* group. These results indicate that the eyes/external rhodopsin photoreceptors and cell autonomously expressed CRY and Rh7 all contribute to the l-LNv light-evoked potential response to UV light. Violet light stimulation relies on more rhodopsin-based phototransduction processes, as evidenced by a non-attenuated *cry-null* response to violet light, while all other mutants are significantly attenuated. These results indicate the violet light-mediated responses in l-LNvs occur primarily through convergent rhodopsin-based signals, especially that of the internal violet photosensory, Rh7, and possibly external violet sensitive Rh1, Rh2, Rh4, Rh5, and Rh6. Blue light stimulation of *p12c* l-LNvs results in large (>1 mV) and long-lasting (>30 seconds) of

membrane depolarization that are overall significantly attenuated with all mutant groups. The double mutant *gl60j-cry-null* has the greatest attenuation and suggests a compounding attenuation that reflects the single *gl60j* and *cry-null* responses to blue light. These results support blue light sensing in l-LNvs is mediated through all three photoreceptor systems, with a primarily rhodopsin-based hyperpolarization response to blue light that is otherwise not observed in other short-wavelength lights tested. These results are consistent with previous findings that indicate CRY and Rh7 as the predominant blue and violet light internal photosensors, respectively, and show that external opsin driven photoreceptors also contribute additive/converging effects for blue and violet light sensing by the l-LNv. Interestingly, longer wavelength red light evokes acute but measurable membrane depolarization responses in the l-LNvs. Each of the photoreceptor mutants also exhibit an attenuated response to red light during stimulus, with CRY appearing to have persistent post-stimulus effects as well. This may be due to resting membrane potential stability, however. As a result, much like short-wavelength excitatory effects, red light also relies on multiple photosensory systems in order to evoke l-LNv depolarization responses, thus further supporting an integration between multiple inputs to provide a wide range of photosensory transduction. These results parallel a separate study that showed red light evokes minimal actional potential firing frequencies responses during red light pulses [3,91]. CRY is perhaps the most surprising contributor of red light, since it is not well known to be sensitive to larger-wavelengths of light, yet l-LNv red light excitatory effects have been found to diminish after treatment with an FAD functional inhibitor, Diphenyleneiodnium (DPI) [3]. As well, cross-species CRY1 from a nocturnal mosquito species, *Anopheles gambiae*, exhibits an even greater response to red light when expressed in a transgenic *cry-null Drosophila* background [91]. A possible explanation for CRY-mediated red light sensitivity could occur if CRY expresses a biologically active neutral semiquinone $FADH^{\bullet}$ state. Though,

there this idea will require additional experiments to dissect the exact mechanism of CRY phototransduction at higher reduced states that enable red light signaling to l-LNvs. As for rhodopsin-based red light phototransduction, Rh1 and Rh6 are likely candidates as they are red light sensitive project from extraretinal structures directly or indirectly to l-LNvs via the central hub aME [81,137]. We also show that for our recordings, we observe predominantly tonic action potential firing in l-LNv recordings [3,6,10,79,82,91,101,102,104–111,146]. Burst firing occurs sporadically but has been reported as the predominant firing mode in l-LNvs by other groups [81,112].

We also tested the possibility that light evoked excitation of the l-LNvs is circadian regulated but find no correlatory evidence to suggest significant time-of-day effects for the l-LNv membrane depolarization response to light. In this study, we show that l-LNv membrane depolarization responses to various light stimuli require inputs from multiple photoreceptor systems. These results add functional support to the growing body of evidence that neurons in the circadian/arousal neural circuit receive photic inputs from the eyes, as well as CRY and Rh7 to mediate circadian photoentrainment, light attraction/avoidance behaviors, sleep/arousal, and more. This work could help us better understand how complex light-based behaviors tune different photosensory cues that we can then manipulate to produce stronger behavioral responses. This would lead to an exciting future towards insect vector-control strategies.

CHAPTER 6: Conclusion and Final Remarks

Non-image forming vision comprises one of the two core visual mechanisms that allow animals to detect changes in light to be able to navigate their environments. In insects like *Drosophila melanogaster*, behavioral responses that arise from non-image forming visual phototransduction processes include circadian photoentrainment, sleep/arousal, light attraction and avoidance, and more. Recent discoveries of internally expressed Cryptochrome (CRY) and Rhodopsin 7 (Rh7) in the circadian/arousal neural circuit of flies show directly photoexcitable effects to short-wavelength light that are marked by both an increase of action potential propagation as well as membrane depolarization. These photoexcitatory effects in the primary arousal neurons (large lateral ventral neurons (l-LNvs)) also influence fly behavioral responsiveness to light. However, additional parameters of light, such as longer wavelengths of light, exposure timing, and intensity, are not well understood on how they influence non-image forming visual behaviors in flies and other insects like mosquitos, and thus is the central focus of this dissertation. The long-standing goal of the Holmes Lab is to better understand the integrative photoreceptor framework that drives non-image forming behaviors in insects, specifically to manipulate the behavioral responses of harmful insects. Such insects include the infamous mosquito disease vectors, with the goal of using light as a potent yet environmentally friendly control mechanisms as an alternative to toxic pesticides. In order to determine CRY mediated non-image forming visual processes across species, I examined the electrophysiological and behavioral light responsiveness of CRY1s from a nocturnal and diurnal mosquito species transgenically expressed using an “empty neuron” system in the circadian/arousal circuit of flies. I also determined the contribution that classical image-forming visual photoreceptors in the eyes

have on l-LNvs phototransduction by measuring the electrophysiological and behavioral responses of several photoreceptor mutants exposed to several wavelengths of light.

In CHAPTER 2 of this dissertation, I examined cross-species CRY1 to extend our understanding that CRY is a short-wavelength light-sensitive photoreceptor expressed in a subset of circadian neurons and eyes in *Drosophila* that regulates light-evoked circadian clock resetting. Further, I show that acutely, light evokes rapid electrical excitation of the ventral lateral subset of circadian neurons and confers circadian-modulated avoidance behavioral responses to short-wavelength light from these cross-species CRY1s. Recent work shows dramatically different avoidance versus attraction behavioral responses to short-wavelength light in day-active versus night-active mosquitoes and that these behavioral responses are attenuated by CRY protein degradation by constant light exposure in mosquitoes. To determine whether CRY1s mediate species-specific coding for behavioral and electrophysiological light responses, I used an ‘‘empty neuron’’ approach and transgenically expressed diurnal Aedes aegypti (AeCRY1) versus nocturnal Anopheles gambiae (AgCRY1) in a *cry-null Drosophila* background. I found that AeCRY1 is much less light sensitive than either AgCRY1 or DmCRY as shown by partial behavioral rhythmicity following constant light exposure. Remarkably, expression of nocturnal AgCRY1 confers low survival to constant white light as does expression of AeCRY1 to a lesser extent. AgCRY1 mediates significantly stronger electrophysiological cell-autonomous responses to 365 nm ultraviolet (UV) light relative to AeCRY1. I also found that AgCRY1 expression mediates electrophysiological sensitivity to 635 nm red light, whereas AeCRY1 does not, consistent with species-specific mosquito red light responses. Further, AgCRY1 and DmCRY mediate intensity-dependent avoidance behavior to UV light at different light intensity thresholds, whereas AeCRY1 does not, thus mimicking mosquito and fly behaviors. These

findings highlight CRY as a key non-image-forming visual photoreceptor that mediates physiological and behavioral light responses in a species-specific fashion.

In CHAPTER 3 of this dissertation, I build on the findings from our recent work that Nocturnal *Anopheles* mosquitoes exhibit strong behavioral avoidance to blue-light while diurnal Aedes mosquitoes are behaviorally attracted to blue-light and a wide range of other wavelengths of light. To determine the molecular mechanism of these effects, I expressed light-sensing *Anopheles gambiae* (AgCRY1) and *Aedes aegypti* (AeCRY1) Cryptochrome 1 (CRY) genes under a *crypGAL4-24* driver line in a mutant *Drosophila* genetic background lacking native functional CRY, then tested behavioral and electrophysiological effects of mosquito CRY expression relative to positive and negative CRY control conditions. I found that neither mosquito CRY stops the circadian clock as shown by robust circadian behavioral rhythmicity in constant darkness in flies expressing either AgCRY1 or AeCRY1. I also found that AgCRY1 and AeCRY1 both mediate acute increases in large ventral lateral neuronal firing rate evoked by 450 nm blue-light, corresponding to CRY's peak absorbance in its base state, indicating that both mosquito CRYs are functional, however, AgCRY1 mediates significantly stronger sustained electrophysiological light-evoked depolarization in response to blue-light relative to AeCRY1. In contrast, neither AgCRY1 nor AeCRY1 expression mediates measurable increases in large ventral lateral neuronal firing rates in response to 405 nm violet-light, the peak of the Rhodopsin-7 photoreceptor that is co-expressed in the large lateral ventral neurons. These results are consistent with the known action spectra of type 1 CRYs and lack of response in cry-null controls. AgCRY1 and AeCRY1 expressing flies show behavioral attraction to low intensity blue-light, but AgCRY1 expressing flies show behavioral avoidance to higher intensity blue-light. These results show that nocturnal and diurnal mosquito Cryptochrome 1 proteins mediate

differential physiological and behavioral responses to blue light that are consistent with species-specific mosquito behavior.

In CHAPTER 4 of this dissertation, I explored the photosensitive properties of lateral ventral neurons (LNvs) in the fly circadian neural circuit and how they receive input to mediate behaviors other than clock resetting, including light-activated acute arousal. Converging sensory inputs often confer functional redundancy. The LNvs have three distinct light input pathways: 1) cell autonomously expressed Cryptochrome (CRY), 2) Rhodopsin-7 (Rh7), and 3) synaptic inputs from the eyes and other external photoreceptors that express opsins and CRY. I explored the relative photoelectrical and behavioral input contributions of these three photoreceptor systems to determine their functional impact in flies. Patch-clamp electrophysiology measuring light evoked firing frequency was performed on large LNvs (l-LNvs) in response to UV (365 nm), violet (405 nm), blue (450 nm), or red (635 nm) LED light stimulation, testing controls versus mutants that lack photoreceptor inputs *gl60j, cry-null, rh7-null,* and double mutant *gl60j-cry-null* flies. For UV, violet, and blue short wavelength light inputs, all photoreceptor mutants show significantly attenuated action. Potential firing frequency (FF) responses measured in the l-LNv except for the double mutant *gl60j-cry-null* flies in response to UV light. In contrast, red light firing frequency responses are on significantly attenuated in double mutant *gl60j-cry-null* flies. We used a light-pulse arousal assay to compare behavioral responses to UV, violet, blue, and red light of control and light input mutants, measuring the awakening arousal response of flies during subjective nighttime at two different intensities to capture potential threshold differences (10 μw/cm² and 400 μw/cm²). The light arousal behavioral results are similar to the electrophysiological results, showing significant attenuation of behavioral light responses for mutants. Compared to control. These results show that the different LNv convergent

photoreceptor systems are integrated and together confer functional redundancy for light evoked behavioral arousal.

In CHAPTER 5 of this dissertation, I explore the photopigments Cryptochrome (CRY) and Rhodopsin-7 (Rh7) that are expressed in a small number of central brain neurons and how they mediate light-evoked electrical excitation of the ventral lateral subset in the circadian/arousal neural circuit along with functional input from the eyes. I explored the photoelectrical input contributions of these three photoreceptor systems to determine their functional convergence on the large ventral lateral neurons (l-LNvs) in flies using patch-clamp electrophysiology along with UV (365 nm), violet (405 nm), blue (450 nm), and red (635 nm) LED light stimulation, testing control versus *gl60j, cry-null, rh7-null*, and *gl60j-cry-null* mutants. Based on comparative subtractive analysis of light evoked potentials recorded in controls and mutants, CRY and external photoreceptors underlie prolonged light evoked depolarization responses for short wavelengths UV, violet and blue, while for these wavelengths, Rh7 mediates initial transient hyperpolarization followed by long lasting depolarization. In terms of magnitude, CRY and Rh7 contribute the greatest light-excitatory membrane depolarization in response to UV light. I also show that external rhodopsins and Rh7 both mediate violet light-induced membrane excitability, with almost no contribution from CRY. Further, I found that CRY is the primary blue light photosensor, external photoreceptors and Rh7 also contribute to light evoked changes in membrane potential, including a compounded defect seen in the double mutant *gl60j-cry-null*. Red light evoked electrical responses in the l-LNvs is mediated by all photoreceptor systems. These results show that convergent photoreceptor input to the LNvs mediate a complex

sequence of excitatory and inhibitory responses to light in flies for non-image forming visual processes.

To test my hypothesis that CRY and other photoreceptor systems converge photic input to the circadian/arousal circuit of flies and mosquitos in order to mediate specific light-based behavioral responses, I employed a series of electrophysiological assays on the l-LNvs of transgenic flies expressing mosquito CRY1 and photoreceptor knockout mutants. I demonstrated mosquito CRY1s confer photoexcitability in response to a wide range of spectral parameters, and these CRY-mediated phototransduction processes strongly regulate light attraction and avoidance to different wavelengths of light in a species-specific and intensity dependent manner. Furthermore, I demonstrated multiple photoreceptor systems converge in l-LNvs to confer photoexcitable effects reminiscent of a coincidence detector system, with CRY serving as the predominant short-wavelength photoreceptor, and rhodopsin-based photopigments as the primary red photoreceptors. My work shows that non-image forming vision in flies and mosquitos rely on a complex series of photoreceptor systems that each influence behavioral responses to light. This idea can be explored further if we can identify an altered light response of CRY by a multi-color photo-switching light response mechanism. This concept relies on recent studies that suggest multiple mechanisms may exist that utilize electron transfer pathways to facilitate FAD conversion to its anionic radical state, FAD^{-}. Also, accumulation of reactive oxygen species (ROS) may play a large role in CRY signaling upon FAD photoreduction.

The future of light-based disease vector control is one step closer to becoming a reality with the completion of my work here that shows how light can be a powerful cue to driving complex insect behaviors.

REFERENCES

1. Fogle, K. J., Parson, K. G., Dahm, N. A. & Holmes, T. C. CRYPTOCHROME Is a Blue-Light Sensor That Regulates Neuronal Firing Rate. *Science* **331**, 1409–1413 (2011).
2. Ni, J. D., Baik, L. S., Holmes, T. C. & Montell, C. A rhodopsin in the brain functions in circadian photoentrainment in Drosophila. *Nature* **545**, 340–344 (2017).
3. Baik, L. S. *et al.* Distinct mechanisms of *Drosophila* CRYPTOCHROME-mediated light-evoked membrane depolarization and in vivo clock resetting. *Proc. Natl. Acad. Sci.* **116**, 23339–23344 (2019).
4. Lin, C., Top, D., Manahan, C. C., Young, M. W. & Crane, B. R. Circadian clock activity of cryptochrome relies on tryptophan-mediated photoreduction. *Proc. Natl. Acad. Sci.* **115**, 3822–3827 (2018).
5. Zoltowski, B. D. *et al.* Structure of full-length Drosophila cryptochrome. *Nature* **480**, 396–399 (2011).
6. Fogle, K. J. *et al.* CRYPTOCHROME-mediated phototransduction by modulation of the potassium ion channel β-subunit redox sensor. *Proc. Natl. Acad. Sci.* **112**, 2245–2250 (2015).
7. Sakai, K. *et al.* Drosophila melanogaster rhodopsin Rh7 is a UV-to-visible light sensor with an extraordinarily broad absorption spectrum. *Sci. Rep.* **7**, 7349 (2017).
8. Baik, L. S., Recinos, Y., Chevez, J. A. & Holmes, T. C. Circadian modulation of light-evoked avoidance/attraction behavior in Drosophila. *PLOS ONE* **13**, e0201927 (2018).
9. Baik, L. S., Recinos, Y., Chevez, J. A., Au, D. D. & Holmes, T. C. Multiple Phototransduction Inputs Integrate to Mediate UV Light–evoked Avoidance/Attraction Behavior in *Drosophila*. *J. Biol. Rhythms* **34**, 391–400 (2019).

10. Baik, L. S. *et al.* CRYPTOCHROME mediates behavioral executive choice in response to UV light. *Proc. Natl. Acad. Sci.* **114**, 776–781 (2017).

11. Emery, P., So, W. V., Kaneko, M., Hall, J. C. & Rosbash, M. CRY, a Drosophila Clock and Light-Regulated Cryptochrome, Is a Major Contributor to Circadian Rhythm Resetting and Photosensitivity. *Cell* **95**, 669–679 (1998).

12. Stanewsky, R. *et al.* The cryb Mutation Identifies Cryptochrome as a Circadian Photoreceptor in Drosophila. *Cell* **95**, 681–692 (1998).

13. Sheeba, V. *et al.* Large Ventral Lateral Neurons Modulate Arousal and Sleep in Drosophila. *Curr. Biol.* **18**, 1537–1545 (2008).

14. Parisky, K. M. *et al.* PDF Cells Are a GABA-Responsive Wake-Promoting Component of the Drosophila Sleep Circuit. *Neuron* **60**, 672–682 (2008).

15. Shang, Y., Griffith, L. C. & Rosbash, M. Light-arousal and circadian photoreception circuits intersect at the large PDF cells of the Drosophila brain. *Proc. Natl. Acad. Sci.* **105**, 19587–19594 (2008).

16. Ahmad, M. Photocycle and signaling mechanisms of plant cryptochromes. *Curr. Opin. Plant Biol.* **33**, 108–115 (2016).

17. Arthaut, L.-D. *et al.* Blue-light induced accumulation of reactive oxygen species is a consequence of the Drosophila cryptochrome photocycle. *PLOS ONE* **12**, e0171836 (2017).

18. Wang, J., Du, X., Pan, W., Wang, X. & Wu, W. Photoactivation of the cryptochrome/photolyase superfamily. *J. Photochem. Photobiol. C Photochem. Rev.* **22**, 84–102 (2015).

19. Baik, L. S. *et al.* Circadian Regulation of Light-Evoked Attraction and Avoidance Behaviors in Daytime- versus Nighttime-Biting Mosquitoes. *Curr. Biol.* **30**, 3252-3259.e3 (2020).

20. Whitfield, J. Portrait of a serial killer. *Nature* news021001-6 (2002) doi:10.1038/news021001-6.

21. Bidlingmayer, W. L. How mosquitoes see traps: role of visual responses. *J. Am. Mosq. Control Assoc.* **10**, 272–279 (1994).

22. Ditzen, M., Pellegrino, M. & Vosshall, L. B. Insect Odorant Receptors Are Molecular Targets of the Insect Repellent DEET. *Science* **319**, 1838–1842 (2008).

23. Lazzari, C. R. Chapter 1 Orientation Towards Hosts in Haematophagous Insects. in *Advances in Insect Physiology* vol. 37 1–58 (Elsevier, 2009).

24. McMeniman, C. J., Corfas, R. A., Matthews, B. J., Ritchie, S. A. & Vosshall, L. B. Multimodal Integration of Carbon Dioxide and Other Sensory Cues Drives Mosquito Attraction to Humans. *Cell* **156**, 1060–1071 (2014).

25. Raji, J. I. & DeGennaro, M. Genetic analysis of mosquito detection of humans. *Curr. Opin. Insect Sci.* **20**, 34–38 (2017).

26. Alonso San Alberto, D. *et al.* The olfactory gating of visual preferences to human skin and visible spectra in mosquitoes. *Nat. Commun.* **13**, 555 (2022).

27. Blondell, J. Epidemiology of pesticide poisonings in the United States, with special reference to occupational cases. *Occup. Med. Phila. Pa* **12**, 209–220 (1997).

28. Garey, J. & Wolff, M. S. Estrogenic and Antiprogestagenic Activities of Pyrethroid Insecticides. *Biochem. Biophys. Res. Commun.* **251**, 855–859 (1998).

29. Hemingway, J. & Ranson, H. Insecticide Resistance in Insect Vectors of Human Disease. *Annu. Rev. Entomol.* **45**, 371–391 (2000).

30. Garbe, D. S. *et al.* Context-specific comparison of sleep acquisition systems in *Drosophila*. *Biol. Open* **4**, 1558–1568 (2015).

31. Keene, A. C. *et al.* Distinct Visual Pathways Mediate Drosophila Larval Light Avoidance and Circadian Clock Entrainment. *J. Neurosci.* **31**, 6527–6534 (2011).

32. Klarsfeld, A., Picot, M., Vias, C., Chelot, E. & Rouyer, F. Identifying Specific Light Inputs for Each Subgroup of Brain Clock Neurons in Drosophila Larvae. *J. Neurosci.* **31**, 17406–17415 (2011).

33. Miller, G. V., Hansen, K. N. & Stark, W. S. Phototaxis in Drosophila: R1–6 input and interaction among ocellar and compound eye receptors. *J. Insect Physiol.* **27**, 813–819 (1981).

34. Keene, A. C. *et al.* Distinct Visual Pathways Mediate Drosophila Larval Light Avoidance and Circadian Clock Entrainment. *J. Neurosci.* **31**, 6527–6534 (2011).

35. Gao, S. *et al.* The Neural Substrate of Spectral Preference in Drosophila. *Neuron* **60**, 328–342 (2008).

36. Yamaguchi, S., Desplan, C. & Heisenberg, M. Contribution of photoreceptor subtypes to spectral wavelength preference in Drosophila. *Proc. Natl. Acad. Sci.* **107**, 5634–5639 (2010).

37. Hoang, N. *et al.* Human and Drosophila Cryptochromes Are Light Activated by Flavin Photoreduction in Living Cells. *PLoS Biol.* **6**, e160 (2008).

38. Levy, C. *et al.* Updated structure of Drosophila cryptochrome. *Nature* **495**, E3–E4 (2013).

39. Öztürk, N., Song, S.-H., Selby, C. P. & Sancar, A. Animal Type 1 Cryptochromes. *J. Biol. Chem.* **283**, 3256–3263 (2008).

40. Benito, J., Houl, J. H., Roman, G. W. & Hardin, P. E. The Blue-Light Photoreceptor CRYPTOCHROME Is Expressed in a Subset of Circadian Oscillator Neurons in the *Drosophila* CNS. *J. Biol. Rhythms* **23**, 296–307 (2008).

41. Yoshii, T., Todo, T., Wülbeck, C., Stanewsky, R. & Helfrich-Förster, C. Cryptochrome is present in the compound eyes and a subset ofDrosophila's clock neurons. *J. Comp. Neurol.* **508**, 952–966 (2008).

42. Chiu, J. C., Low, K. H., Pike, D. H., Yildirim, E. & Edery, I. Assaying Locomotor Activity to Study Circadian Rhythms and Sleep Parameters in Drosophila. *J. Vis. Exp.* 2157 (2010) doi:10.3791/2157.

43. Nitabach, M. N., Blau, J. & Holmes, T. C. Electrical Silencing of Drosophila Pacemaker Neurons Stops the Free-Running Circadian Clock. *Cell* **109**, 485–495 (2002).

44. Benjamini, Y. & Hochberg, Y. Controlling the False Discovery Rate: A Practical and Powerful Approach to Multiple Testing. *J. R. Stat. Soc. Ser. B Methodol.* **57**, 289–300 (1995).

45. Koh, K., Zheng, X. & Sehgal, A. JETLAG Resets the *Drosophila* Circadian Clock by Promoting Light-Induced Degradation of TIMELESS. *Science* **312**, 1809–1812 (2006).

46. Petersen, G., Hall, J. C. & Rosbash, M. The period gene of Drosophila carries species-specific behavioral instructions. *EMBO J.* **7**, 3939–3947 (1988).

47. Wheeler, D. A. *et al.* Molecular Transfer of a Species-specific Behavior from *Drosophila simulans* to *Drosophila melanogaster*. *Science* **251**, 1082–1085 (1991).

48. Tauber, E., Roe, H., Costa, R., Hennessy, J. M. & Kyriacou, C. P. Temporal Mating Isolation Driven by a Behavioral Gene in Drosophila. *Curr. Biol.* **13**, 140–145 (2003).

49. Dobritsa, A. A., van der Goes van Naters, W., Warr, C. G., Steinbrecht, R. A. & Carlson, J. R. Integrating the Molecular and Cellular Basis of Odor Coding in the Drosophila Antenna. *Neuron* **37**, 827–841 (2003).

50. Hallem, E. A., Ho, M. G. & Carlson, J. R. The Molecular Basis of Odor Coding in the Drosophila Antenna. *Cell* **117**, 965–979 (2004).

51. Helfrich-Förster, C. Robust circadian rhythmicity of Drosophila melanogaster requires the presence of lateral neurons: a brain-behavioral study of disconnected mutants. *J. Comp. Physiol. [A]* **182**, 435–453 (1998).

52. Zhao, J. *et al.* Drosophila Clock Can Generate Ectopic Circadian Clocks. *Cell* **113**, 755–766 (2003).

53. Dolezelova, E., Dolezel, D. & Hall, J. C. Rhythm Defects Caused by Newly Engineered Null Mutations in Drosophila's *cryptochrome* Gene. *Genetics* **177**, 329–345 (2007).

54. Rakshit, K. & Giebultowicz, J. M. *Cryptochrome* restores dampened circadian rhythms and promotes healthspan in aging *Drosophila*. *Aging Cell* **12**, 752–762 (2013).

55. Zhu, H., Yuan, Q., Froy, O., Casselman, A. & Reppert, S. M. The two CRYs of the butterfly. *Curr. Biol.* **15**, R953–R954 (2005).

56. Yuan, Q., Metterville, D., Briscoe, A. D. & Reppert, S. M. Insect Cryptochromes: Gene Duplication and Loss Define Diverse Ways to Construct Insect Circadian Clocks. *Mol. Biol. Evol.* **24**, 948–955 (2007).

57. Chandler, J. A., Hill, M. N. & Highton, R. B. The use of light traps for long-term surveillance of mosquitoes of epidemiological importance on the Kano Plain, Kenya. *East Afr. Med. J.* **53**, 596–600 (1976).

58. Doukas, D. & Payne, C. C. The use of ultraviolet-blocking films in insect pest management in the UK; effects on naturally occurring arthropod pest and natural enemy populations in a protected cucumber crop. *Ann. Appl. Biol.* **151**, 221–231 (2007).

59. Grant, G. G., Carmichael, A. G., Smith, C. N. & Brown, A. W. A. Autochemosterilization of the Southern House Mosquito by Means of a Modified Light Trap12. *J. Econ. Entomol.* **63**, 648–650 (1970).

60. Jawara, M. *et al.* Field Testing of Different Chemical Combinations as Odour Baits for Trapping Wild Mosquitoes in The Gambia. *PLoS ONE* **6**, e19676 (2011).

61. Pickens, L. G. Relative Attractiveness of Paired BL and BLB Fluorescent Bulbs for House and Stable Flies (Diptera: Muscidae). *J. Econ. Entomol.* **82**, 535–538 (1989).

62. Berndt, A. *et al.* A Novel Photoreaction Mechanism for the Circadian Blue Light Photoreceptor Drosophila Cryptochrome. *J. Biol. Chem.* **282**, 13011–13021 (2007).

63. Bouly, J.-P. *et al.* Cryptochrome Blue Light Photoreceptors Are Activated through Interconversion of Flavin Redox States. *J. Biol. Chem.* **282**, 9383–9391 (2007).

64. Liu, B., Liu, H., Zhong, D. & Lin, C. Searching for a photocycle of the cryptochrome photoreceptors. *Curr. Opin. Plant Biol.* **13**, 578–586 (2010).

65. Coombe, P. E. Visual behaviour of the greenhouse whitefly, Trialeurodes vaporariorum. *Physiol. Entomol.* **7**, 243–251 (1982).

66. Green, C. H. & Cosens, D. Spectral responses of the tsetse fly, Glossina morsitans morsitans. *J. Insect Physiol.* **29**, 795–800 (1983).

67. Sumba, L. A. *et al.* Daily oviposition patterns of the African malaria mosquito Anopheles gambiae Giles (Diptera: Culicidae) on different types of aqueous substrates. *J. Circadian Rhythms* **2**, 6 (2004).

68. Das, S. & Dimopoulos, G. Molecular analysis of photic inhibition of blood-feeding in Anopheles gambiae. *BMC Physiol.* **8**, 23 (2008).

69. Rund, S. S. C., Lee, S. J., Bush, B. R. & Duffield, G. E. Strain- and sex-specific differences in daily flight activity and the circadian clock of Anopheles gambiae mosquitoes. *J. Insect Physiol.* **58**, 1609–1619 (2012).

70. Sawadogo, S. P. *et al.* Differences in timing of mating swarms in sympatric populations of Anopheles coluzzii and Anopheles gambiae s.s. (formerly An. gambiae M and S molecular forms) in Burkina Faso, West Africa. *Parasit. Vectors* **6**, 275 (2013).

71. Tokushima, Y. *et al.* Broadband Photoreceptors Are Involved in Violet Light Preference in the Parasitoid Fly Exorista Japonica. *PLOS ONE* **11**, e0160441 (2016).

72. Knop, E. *et al.* Artificial light at night as a new threat to pollination. *Nature* **548**, 206–209 (2017).

73. Sheppard, A. D. *et al.* Light manipulation of mosquito behaviour: acute and sustained photic suppression of biting activity in the Anopheles gambiae malaria mosquito. *Parasit. Vectors* **10**, 255 (2017).

74. Farnesi, L. C., Barbosa, C. S., Araripe, L. O. & Bruno, R. V. The influence of a light and dark cycle on the egg laying activity of Aedes aegypti (Linnaeus, 1762) (Diptera: Culicidae). *Mem. Inst. Oswaldo Cruz* **113**, (2018).

75. Kistenpfennig, C. *et al.* A Tug-of-War between Cryptochrome and the Visual System Allows the Adaptation of Evening Activity to Long Photoperiods in *Drosophila melanogaster*. *J. Biol. Rhythms* **33**, 24–34 (2018).

76. Lazopulo, S., Lazopulo, A., Baker, J. D. & Syed, S. Daytime colour preference in Drosophila depends on the circadian clock and TRP channels. *Nature* **574**, 108–111 (2019).

77. Emery, P. *et al.* Drosophila CRY Is a Deep Brain Circadian Photoreceptor. *Neuron* **26**, 493–504 (2000).

78. Klarsfeld, A. Novel Features of Cryptochrome-Mediated Photoreception in the Brain Circadian Clock of Drosophila. *J. Neurosci.* **24**, 1468–1477 (2004).

79. Sheeba, V., Fogle, K. J. & Holmes, T. C. Persistence of Morning Anticipation Behavior and High Amplitude Morning Startle Response Following Functional Loss of Small Ventral Lateral Neurons in Drosophila. *PLoS ONE* **5**, e11628 (2010).

80. Liu, S. *et al.* WIDE AWAKE mediates the circadian timing of sleep onset. *Neuron* **82**, 151–166 (2014).

81. Muraro, N. I. & Ceriani, M. F. Acetylcholine from Visual Circuits Modulates the Activity of Arousal Neurons in Drosophila. *J. Neurosci.* **35**, 16315–16327 (2015).

82. Buhl, E. *et al.* Quasimodo mediates daily and acute light effects on *Drosophila* clock neuron excitability. *Proc. Natl. Acad. Sci.* **113**, 13486–13491 (2016).

83. Potdar, S. & Sheeba, V. Wakefulness Is Promoted during Day Time by PDFR Signalling to Dopaminergic Neurons in Drosophila melanogaster. *eNeuro* **5**, ENEURO.0129-18.2018 (2018).

84. Chaturvedi, R., Stork, T., Yuan, C., Freeman, M. R. & Emery, P. Astrocytic GABA transporter controls sleep by modulating GABAergic signaling in Drosophila circadian neurons. *Curr. Biol. CB* **32**, 1895-1908.e5 (2022).

85. Gegear, R. J., Foley, L. E., Casselman, A. & Reppert, S. M. Animal cryptochromes mediate magnetoreception by an unconventional photochemical mechanism. *Nature* **463**, 804–807 (2010).

86. Damulewicz, M. & Mazzotta, G. M. One Actor, Multiple Roles: The Performances of Cryptochrome in Drosophila. *Front. Physiol.* **11**, 99 (2020).

87. Busza, A., Emery-Le, M., Rosbash, M. & Emery, P. Roles of the two Drosophila CRYPTOCHROME structural domains in circadian photoreception. *Science* **304**, 1503–1506 (2004).

88. Peschel, N., Chen, K. F., Szabo, G. & Stanewsky, R. Light-Dependent Interactions between the Drosophila Circadian Clock Factors Cryptochrome, Jetlag, and Timeless. *Curr. Biol.* **19**, 241–247 (2009).

89. Giachello, C. N. G., Scrutton, N. S., Jones, A. R. & Baines, R. A. Magnetic Fields Modulate Blue-Light-Dependent Regulation of Neuronal Firing by Cryptochrome. *J. Neurosci. Off. J. Soc. Neurosci.* **36**, 10742–10749 (2016).

90. Hong, G., Pachter, R. & Ritz, T. Coupling Drosophila melanogaster Cryptochrome Light Activation and Oxidation of the Kvβ Subunit Hyperkinetic NADPH Cofactor. *J. Phys. Chem. B* **122**, 6503–6510 (2018).

91. Au, D. D. *et al.* Mosquito cryptochromes expressed in Drosophila confer species-specific behavioral light responses. *Curr. Biol.* S0960982222011228 (2022) doi:10.1016/j.cub.2022.07.021.

92. Ozturk, N., Selby, C. P., Zhong, D. & Sancar, A. Mechanism of Photosignaling by Drosophila Cryptochrome. *J. Biol. Chem.* **289**, 4634–4642 (2014).

93. Ozturk, N., Selby, C. P., Annayev, Y., Zhong, D. & Sancar, A. Reaction mechanism of Drosophila cryptochrome. *Proc. Natl. Acad. Sci.* **108**, 516–521 (2011).

94. Vaidya, A. T. *et al.* Flavin reduction activates Drosophila cryptochrome. *Proc. Natl. Acad. Sci.* **110**, 20455–20460 (2013).

95. Lin, C., Schneps, C. M., Chandrasekaran, S., Ganguly, A. & Crane, B. R. Mechanistic insight into light-dependent recognition of Timeless by Drosophila Cryptochrome. *Struct. Lond. Engl. 1993* **30**, 851-861.e5 (2022).

96. Chandrasekaran, S. *et al.* Tuning flavin environment to detect and control light-induced conformational switching in Drosophila cryptochrome. *Commun. Biol.* **4**, 249 (2021).

97. Jones, M. D. R., Hill, M. & Hope, A. M. The Circadian Flight Activity of the Mosquito, *Anopheles Gambiae* : Phase Setting by the Light Regime. *J. Exp. Biol.* **47**, 503–511 (1967).

98. Taylor, B. & Jones, M. D. R. The Circadian Rhythm of Flight Activity in the Mosquito *Aedes Aegypti* (L.): The Phase-Setting Effects of Light-On and Light-Off. *J. Exp. Biol.* **51**, 59–70 (1969).

99. Nave, C. *et al.* Weekend Light Shifts Evoke Persistent *Drosophila* Circadian Neural Network Desynchrony. *J. Neurosci.* **41**, 5173–5189 (2021).

100. Schlichting, M., Grebler, R., Menegazzi, P. & Helfrich-Förster, C. Twilight Dominates Over Moonlight in Adjusting *Drosophila* 's Activity Pattern. *J. Biol. Rhythms* **30**, 117–128 (2015).

101. Holmes, T., Sheeba, V., Mizrak, D., Rubovszky, B. & Dahdal, D. Circuit-breaking and behavioral analysis by molecular genetic manipulation of neural activity in Drosophila. *Invertebr. Neurobiol. Eds G North R Greenspan Cold Spring Harb. NY Cold Spring Harb. Press* **49**, 19–52 (2007).

102. Sheeba, V., Gu, H., Sharma, V. K., O'Dowd, D. K. & Holmes, T. C. Circadian- and Light-Dependent Regulation of Resting Membrane Potential and Spontaneous Action Potential Firing of *Drosophila* Circadian Pacemaker Neurons. *J. Neurophysiol.* **99**, 976–988 (2008).

103. Tabuchi, M., Coates, K. E., Bautista, O. B. & Zukowski, L. H. Light/Clock Influences Membrane Potential Dynamics to Regulate Sleep States. *Front. Neurol.* **12**, 625369 (2021).

104. Cao, G. & Nitabach, M. N. Circadian Control of Membrane Excitability in Drosophila melanogaster Lateral Ventral Clock Neurons. *J. Neurosci.* **28**, 6493–6501 (2008).

105. Flourakis, M. *et al.* A Conserved Bicycle Model for Circadian Clock Control of Membrane Excitability. *Cell* **162**, 836–848 (2015).

106. Smith, P., Buhl, E., Tsaneva-Atanasova, K. & Hodge, J. J. L. Shaw and Shal voltage-gated potassium channels mediate circadian changes in Drosophila clock neuron excitability. *J. Physiol.* **597**, 5707–5722 (2019).

107. McCarthy, E. V. *et al.* Synchronized bilateral synaptic inputs to Drosophila melanogaster neuropeptidergic rest/arousal neurons. *J. Neurosci. Off. J. Soc. Neurosci.* **31**, 8181–8193 (2011).

108. Seluzicki, A. *et al.* Dual PDF Signaling Pathways Reset Clocks Via TIMELESS and Acutely Excite Target Neurons to Control Circadian Behavior. *PLoS Biol.* **12**, e1001810 (2014).

109. Flourakis, M. & Allada, R. Patch-Clamp Electrophysiology in Drosophila Circadian Pacemaker Neurons. in *Methods in Enzymology* vol. 552 23–44 (Elsevier, 2015).

110. Buhl, E., Higham, J. P. & Hodge, J. J. L. Alzheimer's disease-associated tau alters Drosophila circadian activity, sleep and clock neuron electrophysiology. *Neurobiol. Dis.* **130**, 104507 (2019).

111. Li, M.-T. *et al.* Hub-organized parallel circuits of central circadian pacemaker neurons for visual photoentrainment in Drosophila. *Nat. Commun.* **9**, 4247 (2018).

112. Fernandez-Chiappe, F. *et al.* High-Frequency Neuronal Bursting is Essential for Circadian and Sleep Behaviors in Drosophila. *J. Neurosci. Off. J. Soc. Neurosci.* **41**, 689–710 (2021).

113. Dissel, S. *et al.* A constitutively active cryptochrome in Drosophila melanogaster. *Nat. Neurosci.* **7**, 834–840 (2004).

114. Renn, S. C. P., Park, J. H., Rosbash, M., Hall, J. C. & Taghert, P. H. A pdf Neuropeptide Gene Mutation and Ablation of PDF Neurons Each Cause Severe Abnormalities of Behavioral Circadian Rhythms in Drosophila. *Cell* **99**, 791–802 (1999).

115. de Velasco, B. *et al.* Specification and development of the pars intercerebralis and pars lateralis, neuroendocrine command centers in the Drosophila brain. *Dev. Biol.* **302**, 309–323 (2007).

116. Barber, A. F., Erion, R., Holmes, T. C. & Sehgal, A. Circadian and feeding cues integrate to drive rhythms of physiology in *Drosophila* insulin-producing cells. *Genes Dev.* **30**, 2596–2606 (2016).

117. Rivera, A. S. *et al.* Gene duplication and the origins of morphological complexity in pancrustacean eyes, a genomic approach. *BMC Evol. Biol.* **10**, 123 (2010).

118. Wilson, E. O. Some central problems of sociobiology. *Soc. Sci. Inf.* **14**, 5–18 (1975).

119. Kumar, S., Chen, D. & Sehgal, A. Dopamine acts through Cryptochrome to promote acute arousal in Drosophila. *Genes Dev.* **26**, 1224–1234 (2012).

120. Kistenpfennig, C. *et al.* A New Rhodopsin Influences Light-dependent Daily Activity Patterns of Fruit Flies. *J. Biol. Rhythms* **32**, 406–422 (2017).

121. Senthilan, P. R., Grebler, R., Reinhard, N., Rieger, D. & Helfrich-Förster, C. Role of Rhodopsins as Circadian Photoreceptors in the Drosophila melanogaster. *Biology* **8**, 6 (2019).

122. Ceriani, M. F. *et al.* Light-Dependent Sequestration of TIMELESS by CRYPTOCHROME. *Science* **285**, 553–556 (1999).

123. Czarna, A. *et al.* Structures of Drosophila Cryptochrome and Mouse Cryptochrome1 Provide Insight into Circadian Function. *Cell* **153**, 1394–1405 (2013).

124. Kirschfeld, K., Franceschini, N. & Minke, B. Evidence for a sensitising pigment in fly photoreceptors. *Nature* **269**, 386–390 (1977).

125. Kirschfeld, K., Feiler, R. & Franceschini, N. A photostable pigment within the rhabdomere of fly photoreceptors no. 7. *J. Comp. Physiol. A* **125**, 275–284 (1978).

126. Feiler, R. *et al.* Ectopic expression of ultraviolet-rhodopsins in the blue photoreceptor cells of Drosophila: visual physiology and photochemistry of transgenic animals. *J. Neurosci.* **12**, 3862–3868 (1992).

127. Salcedo, E. *et al.* Blue- and Green-Absorbing Visual Pigments of *Drosophila* : Ectopic Expression and Physiological Characterization of the R8 Photoreceptor Cell-Specific Rh5 and Rh6 Rhodopsins. *J. Neurosci.* **19**, 10716–10726 (1999).

128. Sharkey, C. R., Blanco, J., Leibowitz, M. M., Pinto-Benito, D. & Wardill, T. J. The spectral sensitivity of Drosophila photoreceptors. *Sci. Rep.* **10**, 18242 (2020).

129. Helfrich-Förster, C., Winter, C., Hofbauer, A., Hall, J. C. & Stanewsky, R. The Circadian Clock of Fruit Flies Is Blind after Elimination of All Known Photoreceptors. *Neuron* **30**, 249–261 (2001).

130. Helfrich-Förster, C. *et al.* The Extraretinal Eyelet of *Drosophila* : Development, Ultrastructure, and Putative Circadian Function. *J. Neurosci.* **22**, 9255–9266 (2002).

131. Malpel, S., Klarsfeld, A. & Rouyer, F. Larval optic nerve and adult extra-retinal photoreceptors sequentially associate with clock neurons during *Drosophila* brain development. *Development* **129**, 1443–1453 (2002).

132. Rieger, D., Stanewsky, R. & Helfrich-Förster, C. Cryptochrome, Compound Eyes, Hofbauer-Buchner Eyelets, and Ocelli Play Different Roles in the Entrainment and Masking Pathway of the Locomotor Activity Rhythm in the Fruit Fly Drosophila Melanogaster. *J. Biol. Rhythms* **18**, 377–391 (2003).

133. Veleri, S., Rieger, D., Helfrich-Förster, C. & Stanewsky, R. Hofbauer-Buchner Eyelet Affects Circadian Photosensitivity and Coordinates TIM and PER Expression in *Drosophila* Clock Neurons. *J. Biol. Rhythms* **22**, 29–42 (2007).

134. Kistenpfennig, C., Hirsh, J., Yoshii, T. & Helfrich-Förster, C. Phase-Shifting the Fruit Fly Clock without Cryptochrome. *J. Biol. Rhythms* **27**, 117–125 (2012).

135. Schlichting, M., Grebler, R., Peschel, N., Yoshii, T. & Helfrich-Förster, C. Moonlight Detection by *Drosophila* 's Endogenous Clock Depends on Multiple Photopigments in the Compound Eyes. *J. Biol. Rhythms* **29**, 75–86 (2014).

136. Saint-Charles, A. *et al.* Four of the six *Drosophila* rhodopsin-expressing photoreceptors can mediate circadian entrainment in low light: Rhodopsin-Dependent Clock Synchronization. *J. Comp. Neurol.* **524**, 2828–2844 (2016).

137. Schlichting, M. *et al.* A Neural Network Underlying Circadian Entrainment and Photoperiodic Adjustment of Sleep and Activity in Drosophila. *J. Neurosci.* **36**, 9084–9096 (2016).

138. Helfrich-Förster, C. *et al.* The Lateral and Dorsal Neurons of *Drosophila melanogaster:* New Insights about Their Morphology and Function. *Cold Spring Harb. Symp. Quant. Biol.* **72**, 517–525 (2007).

139. Cusumano, P. *et al.* PDF-modulated visual inputs and cryptochrome define diurnal behavior in Drosophila. *Nat. Neurosci.* **12**, 1431–1437 (2009).

140. Yoshii, T., Vanin, S., Costa, R. & Helfrich-Förster, C. Synergic Entrainment of *Drosophila's* Circadian Clock by Light and Temperature. *J. Biol. Rhythms* **24**, 452–464 (2009).

141. Yoshii, T., Hermann-Luibl, C. & Helfrich-Förster, C. Circadian light-input pathways in *Drosophila*. *Commun. Integr. Biol.* **9**, e1102805 (2016).

142. Guo, F., Cerullo, I., Chen, X. & Rosbash, M. PDF neuron firing phase-shifts key circadian activity neurons in Drosophila. *eLife* **3**, e02780 (2014).

143. Eck, S., Helfrich-Förster, C. & Rieger, D. The Timed Depolarization of Morning and Evening Oscillators Phase Shifts the Circadian Clock of *Drosophila*. *J. Biol. Rhythms* **31**, 428–442 (2016).

144. Chatterjee, A. *et al.* Reconfiguration of a Multi-oscillator Network by Light in the Drosophila Circadian Clock. *Curr. Biol.* **28**, 2007-2017.e4 (2018).

145. Behnia, R. & Desplan, C. Visual circuits in flies: beginning to see the whole picture. *Curr. Opin. Neurobiol.* **34**, 125–132 (2015).

146. Au, D. D. *et al.* Nocturnal mosquito Cryptochrome 1 mediates greater electrophysiological and behavioral responses to blue light relative to diurnal mosquito Cryptochrome 1. *Front. Neurosci.* **16**, 1042508 (2022).

147. Helfrich-Förster, C. Light input pathways to the circadian clock of insects with an emphasis on the fruit fly Drosophila melanogaster. *J. Comp. Physiol. A* **206**, 259–272 (2020).

148. Majercak, J., Sidote, D., Hardin, P. E. & Edery, I. How a Circadian Clock Adapts to Seasonal Decreases in Temperature and Day Length. *Neuron* **24**, 219–230 (1999).

149. Chen, W.-F., Majercak, J. & Edery, I. Clock-Gated Photic Stimulation of Timeless Expression at Cold Temperatures and Seasonal Adaptation in Drosophila. *J. Biol. Rhythms* **21**, 256–271 (2006).

150. Bachleitner, W., Kempinger, L., Wülbeck, C., Rieger, D. & Helfrich-Förster, C. Moonlight shifts the endogenous clock of *Drosophila melanogaster*. *Proc. Natl. Acad. Sci.* **104**, 3538–3543 (2007).

151. Boothroyd, C. E., Wijnen, H., Naef, F., Saez, L. & Young, M. W. Integration of Light and Temperature in the Regulation of Circadian Gene Expression in Drosophila. *PLoS Genet.* **3**, e54 (2007).

152. Picot, M., Cusumano, P., Klarsfeld, A., Ueda, R. & Rouyer, F. Light activates output from evening neurons and inhibits output from morning neurons in the Drosophila circadian clock. *PLoS Biol.* **5**, e315 (2007).

153. Stoleru, D. *et al.* The Drosophila Circadian Network Is a Seasonal Timer. *Cell* **129**, 207–219 (2007).

154. Vanin, S. *et al.* Unexpected features of Drosophila circadian behavioural rhythms under natural conditions. *Nature* **484**, 371–375 (2012).

155. Green, E. W. *et al. Drosophila* circadian rhythms in seminatural environments: Summer afternoon component is not an artifact and requires TrpA1 channels. *Proc. Natl. Acad. Sci.* **112**, 8702–8707 (2015).

156. Breda, C., Rosato, E. & Kyriacou, C. P. Norpa Signalling and the Seasonal Circadian Locomotor Phenotype in Drosophila. *Biology* **9**, 130 (2020).

157. Heisenberg, M. & Buchner, E. The r**?**le of retinula cell types in visual behavior ofDrosophila melanogaster. *J. Comp. Physiol. A* **117**, 127–162 (1977).

158. Chung, B. Y., Kilman, V. L., Keath, J. R., Pitman, J. L. & Allada, R. The GABAA Receptor RDL Acts in Peptidergic PDF Neurons to Promote Sleep in Drosophila. *Curr. Biol.* **19**, 386–390 (2009).

159. Kilman, V. L., Zhang, L., Meissner, R.-A., Burg, E. & Allada, R. Perturbing Dynamin Reveals Potent Effects on the Drosophila Circadian Clock. *PLoS ONE* **4**, e5235 (2009).

160. Weng, J., Cao, Y., Moss, N. & Zhou, M. Modulation of Voltage-dependent Shaker Family Potassium Channels by an Aldo-Keto Reductase*. *J. Biol. Chem.* **281**, 15194–15200 (2006).

161. Pan, Y., Weng, J., Cao, Y., Bhosle, R. C. & Zhou, M. Functional Coupling between the Kv1.1 Channel and Aldoketoreductase Kvβ1. *J. Biol. Chem.* **283**, 8634–8642 (2008).

162. Szular, J. *et al. Rhodopsin 5* – and *Rhodopsin 6* –Mediated Clock Synchronization in *Drosophila melanogaster* Is Independent of Retinal Phospholipase C-β Signaling. *J. Biol. Rhythms* **27**, 25–36 (2012).

163. Ogueta, M., Hardie, R. C. & Stanewsky, R. Non-canonical Phototransduction Mediates Synchronization of the Drosophila melanogaster Circadian Clock and Retinal Light Responses. *Curr. Biol.* **28**, 1725-1735.e3 (2018).

164. Alejevski, F. *et al.* The HisCl1 histamine receptor acts in photoreceptors to synchronize Drosophila behavioral rhythms with light-dark cycles. *Nat. Commun.* **10**, 252 (2019).

165. Nitabach, M. N., Sheeba, V., Vera, D. A., Blau, J. & Holmes, T. C. Membrane electrical excitability is necessary for the free-running larvalDrosophila circadian clock. *J. Neurobiol.* **62**, 1–13 (2005).

166. Nitabach, M. N. Electrical Hyperexcitation of Lateral Ventral Pacemaker Neurons Desynchronizes Downstream Circadian Oscillators in the Fly Circadian Circuit and Induces Multiple Behavioral Periods. *J. Neurosci.* **26**, 479–489 (2006).

167. Shafer, O. T., Rosbash, M. & Truman, J. W. Sequential nuclear accumulation of the clock proteins period and timeless in the pacemaker neurons of Drosophila melanogaster. *J. Neurosci. Off. J. Soc. Neurosci.* **22**, 5946–5954 (2002).

168. Roberts, L. *et al.* Light Evokes Rapid Circadian Network Oscillator Desynchrony Followed by Gradual Phase Retuning of Synchrony. *Curr. Biol.* **25**, 858–867 (2015).

169. Muraro, N. I. & Ceriani, M. F. Acetylcholine from Visual Circuits Modulates the Activity of Arousal Neurons in Drosophila. *J. Neurosci. Off. J. Soc. Neurosci.* **35**, 16315–16327 (2015).

170. Helfrich-Förster, C. *et al.* The Extraretinal Eyelet of *Drosophila* : Development, Ultrastructure, and Putative Circadian Function. *J. Neurosci.* **22**, 9255–9266 (2002).

171. Schlichting, M., Menegazzi, P. & Helfrich-Förster, C. Normal vision can compensate for the loss of the circadian clock. *Proc. R. Soc. B Biol. Sci.* **282**, 20151846 (2015).

172. Helfrich-Förster, C., Winter, C., Hofbauer, A., Hall, J. C. & Stanewsky, R. The Circadian Clock of Fruit Flies Is Blind after Elimination of All Known Photoreceptors. *Neuron* **30**, 249–261 (2001).

173. Klarsfeld, A. Novel Features of Cryptochrome-Mediated Photoreception in the Brain Circadian Clock of Drosophila. *J. Neurosci.* **24**, 1468–1477 (2004).

174. Fogle, K. J., Parson, K. G., Dahm, N. A. & Holmes, T. C. CRYPTOCHROME Is a Blue-Light Sensor That Regulates Neuronal Firing Rate. *Science* **331**, 1409–1413 (2011).